



Monteverde, Tiziana (2017) *Investigating the function and regulation of NUA1 and its role in non-small cell lung cancer*. PhD thesis.

<https://theses.gla.ac.uk/8701/>

Copyright and moral rights for this work are retained by the author

A copy can be downloaded for personal non-commercial research or study, without prior permission or charge

This work cannot be reproduced or quoted extensively from without first obtaining permission in writing from the author

The content must not be changed in any way or sold commercially in any format or medium without the formal permission of the author

When referring to this work, full bibliographic details including the author, title, awarding institution and date of the thesis must be given

Enlighten: Theses

<https://theses.gla.ac.uk/>
research-enlighten@glasgow.ac.uk



University
of Glasgow

**Investigating the function and regulation of
NUAK1 and its role in Non-small cell lung
cancer**

Tiziana Monteverde

MSc

Submitted in fulfilment of the requirements for the Degree
of Doctor of Philosophy

Institute of Cancer Sciences
College of Medical, Veterinary and Life Sciences
University of Glasgow
September 2017



CANCER
RESEARCH
UK

BEATSON
INSTITUTE

Abstract

The AMPK-related kinase NUA1 has been implicated in the regulation of a spectrum of biological processes such as cell proliferation, metabolism, cell adhesion and migration. As deregulation of such processes plays an important role in cancer, NUA1 targeting has been suggested as a promising therapeutic strategy. In addition, higher NUA1 expression has been correlated with more advanced tumour stages and poor prognosis in multiple cancer types, indicating that its targeting could be clinically relevant. However, manipulation of NUA1 for therapeutic purposes is still restricted by our limited knowledge of its regulation and function.

Therefore, the work presented in this thesis aimed to further explore the NUA1 signalling network, with particular focus on a more comprehensive understanding of the previously described synthetic lethal interaction between NUA1 and MYC.

The tumour suppressor LKB1 is considered as the master upstream regulator of the AMPK-related kinases, including NUA1. Our analysis performed in HeLa cells, which are characterized by LKB1 deficiency and high levels of MYC, revealed that NUA1 activity was maintained by an alternative pathway involving Ca^{2+} -dependent activation of PKC α . Ca^{2+} /PKC α -dependent activation of NUA1 supported the engagement of the Raptor-mTORC1 metabolic checkpoint to protect cells from MYC-driven cell death. Indeed, we have revealed that MYC selects for this pathway via amplification of Ca^{2+} signalling, which involves increased activation of PKC.

MYC upregulation in Non-small cell lung cancer (NSCLC) is frequently observed due to oncogenic activation of upstream signalling pathways that promote MYC stability, e.g. by RAS activation. Therefore, in light of the synthetic lethal interaction between NUA1 and MYC but also aware of the emblematic tumour suppressor role of LKB1 in lung tumorigenesis, we sought to investigate the role of NUA1 in a pre-clinical model of NSCLC driven by mutant KRas. Interestingly, NUA1 did not replicate the tumour suppressive function of LKB1, while Nuak1 deletion decreased tumour angiogenesis and delayed tumour progression, which was reflected by an increased overall survival.

Finally, as we investigated the molecular mechanisms of progression of KRas mutant-driven NSCLC, we uncovered the upregulation of the ERBB network in association with the tumorigenic process. Inhibition of ERBB receptors cooperated with MEK inhibition in enhancing overall survival, proposing a novel therapeutic relevance for multi-ERBB inhibitors.

Taken together our data have provided a more comprehensive understanding of NIAK1 signalling network and have proposed new targets that could be exploited for therapeutic purposes in lung cancer and potentially in many other tumour types.

Table of Contents

ABSTRACT	2
TABLE OF CONTENTS	4
LIST OF TABLES.....	9
LIST OF FIGURES.....	10
ABBREVIATIONS.....	13
ACKNOWLEDGMENTS.....	17
AUTHOR'S DECLARATION	18
CHAPTER 1 - INTRODUCTION	19
1.1 AMPK, THE MASTER ENERGY SENSOR.....	19
1.1.1 Structure and expression of AMPK.....	19
1.1.2 Nucleotide-dependent activation of AMPK	22
1.1.3 Pharmacological activation of AMPK	23
1.1.4 Upstream kinases of AMPK.....	24
1.1.5 Metabolic implications of AMPK activity.....	25
1.1.5.1 Regulation of protein synthesis	26
1.1.5.2 Regulation of glucose and lipid metabolism	29
1.1.5.3 Regulation of mitochondria biogenesis and autophagy.....	30
1.1.6 Role of AMPK in the regulation of proliferation	31
1.1.7 Role of AMPK in cancer	31
1.2 AMPK RELATED KINASES.....	33
1.2.1 Activation modalities of ARKs	35
1.2.2 Regulation of ARKs by upstream kinases.....	36
1.3 NUA1	38
1.3.1 Structure and expression profile of NUA1.....	38
1.3.2 Upstream kinases regulating NUA1.....	38
1.3.3 Lesson on NUA1's physiological role from in vivo studies.....	39
1.3.4 Additional biological roles of NUA1	41
1.3.4.1 Migration and Invasion	41
1.3.4.2 Cell adhesion	42
1.3.4.3 Cell proliferation and senescence	43

1.3.4.4 Metabolic homeostasis	44
1.3.5 Clinical relevance for NUA1	45
1.3.6 Exploiting the synthetic lethal interaction between NUA1 and MYC in cancer therapy	47
1.4 LUNG CANCER	48
1.4.1 Heterogeneity of lung cancer	48
1.4.2 Molecular profiling of NSCLC	52
1.4.2.1 EGFR and the ERBB signalling network	53
1.4.2.2 RAS signalling	54
1.4.3 Targeted therapies for NSCLC	58
1.5 PHD OBJECTIVES	60
CHAPTER 2 - MATERIALS AND METHODS	62
2.1 MATERIALS	62
2.1.1 Chemicals	62
2.1.2 Kits	63
2.1.3 Solutions	64
2.1.4 Primary Antibodies	64
2.1.5 Secondary Antibodies	66
2.1.6 siRNA	66
2.1.7 shRNA	67
2.1.8 Primers	67
2.1.9 Acrylamide gels	68
2.1.10 Drugs	68
2.2 METHODS	69
2.2.1 Cell Culture	69
2.2.1.1 Tumour Cells	69
2.2.1.2 Primary mouse embryonic fibroblasts	69
2.2.1.3 Cryopreservation and resuscitation of cells	70
2.2.2 Plasmid transfection	71
2.2.3 siRNA transfection	71
2.2.4 RNA extraction and Quantitative Real-Time PCR	72
2.2.4.1 RNA extraction	72
2.2.4.2 cDNA synthesis	72
2.2.4.3 qPCR primers design and analysis	73
2.2.4.4 Quantitative Real-Time PCR	73
2.2.5 Immunoprecipitation and immunoblotting	74

2.2.5.1 Immunoprecipitation.....	74
2.2.5.2 Preparation of whole cell proteins extracts.....	74
2.2.5.3 SDS-PAGE.....	74
2.2.5.4 Western Blotting.....	75
2.2.6 Cell death analysis.....	75
2.2.7 Determination of protein synthesis rates.....	76
2.2.8 Animals.....	76
2.2.8.1 Mouse Models.....	76
2.2.8.2 Breeding and Maintenance.....	76
2.2.8.3 Intranasal instillation of Adenovirus.....	77
2.2.8.4 Administration of drugs.....	78
2.2.8.5 <i>In vivo</i> imaging.....	78
2.2.8.6 Tissue collection.....	78
2.2.8.7 Protein isolations from lung tumours.....	79
2.2.9 Histology.....	79
2.2.9.1 Immunohistochemistry.....	79
2.2.9.2 TUNEL staining.....	81
2.2.10 Tumour burden quantification and Immunohistochemistry scoring..	82
2.2.11 Laser-Capture Microdissection and RNA-SEQ analysis.....	83
2.2.12 Statistical analysis.....	84

CHAPTER 3 - INVESTIGATING THE ROLE OF NUAKE1 IN CELL SURVIVAL UNDER METABOLIC STRESS.....	85
3.1 INTRODUCTION.....	85
3.2 RESULTS.....	88
3.2.1 NUAKE1 does not regulate AMPK subunits nor basal activity.....	88
3.2.2 NUAKE1 is specifically required for Ca ²⁺ -mediated activation of AMPK	89
3.2.3 NUAKE1 is activated by Ca ²⁺ signalling by an LKB1-independent pathway.....	91
3.2.4 CaMKK β does not mediate Ca ²⁺ -induced activation of NUAKE1.....	92
3.2.5 Both NUAKE1 and NUAKE2 phosphorylate MYPT1 ^{S445} in response to increased intracellular Ca ²⁺	94
3.2.6 MYC modulates activation of PKC.....	96
3.2.7 PKC α mediates NUAKE1 activation by Ca ²⁺ signalling.....	97
3.2.8 PKC α regulates NUAKE1 protein levels.....	100
3.2.9 NUAKE1 and NUAKE2 reside in two distinct pathways for the regulation of MYPT1 ^{S445} phosphorylation in response to Ca ²⁺ signalling.....	102

3.2.10 The PKC α -NUAK1 pathway supports viability of MYC overexpressing cells.....	103
3.2.11 The PKC α -NUAK1 pathway regulates activation of mTORC1 via Raptor	106
3.3 DISCUSSION	111
CHAPTER 4 - INVESTIGATION OF NUAK1 ROLE IN LUNG TUMORIGENESIS.....	118
4.1 INTRODUCTION	118
4.1.1 Mouse models	119
4.2 RESULTS	120
4.2.1 KRas-mutant lung tumours develop as adenocarcinoma even in the absence of Nuak1	120
4.2.2 Deletion of Nuak1 does not affect the cell of origin of KRas-mutant lung adenocarcinoma.....	123
4.2.3 Nuak1 deletion does not affect KRas-driven tumorigenic process ...	125
4.2.4 Characterization of Nuak1 deletion in KRas ^{G12D} /MYC lung adenocarcinoma	126
4.2.5 MYC overexpression is not synthetically lethal with Nuak1 deletion in KRas-driven NSCLC.....	129
4.2.6 Upregulation of the PI3K/AKT pathway in Nuak1 deleted lung tumours	130
4.2.7 Deletion of Nuak1 does not sensitize lung tumours to mTORC1 inhibition.....	132
4.2.8 Deletion of Nuak1 confers a survival advantage to KRas ^{G12D} /MYC mice	135
4.3 DISCUSSION	136
CHAPTER 5 - THE ROLE OF THE ERBB NETWORK IN SUPPORTING KRAS MUTANT LUNG ADENOCARCINOMA	141
5.1 INTRODUCTION	141
5.1.1 Mouse models	142
5.2 RESULTS	143
5.2.1 Upregulation of the ERBB network during progression of KRas mutant lung adenocarcinoma.....	143
5.2.2 KRas ^{G12D} /MYC lung tumours are sensitive to ERBB inhibition	145
5.2.3 Inhibition of the ERBB receptors impairs KRas-driven tumorigenesis	147

5.2.4 ERBB blockade enhances therapeutic impact of MEK inhibition in KRas mutant lung adenocarcinoma	148
5.3 DISCUSSION	153
CHAPTER 6 - FINAL DISCUSSION	158
REFERENCES.....	164

List of Tables

Table 1. 1 - Histological types and subtypes of NSCLC.....	51
Table 2. 1 - Chemicals and Suppliers.....	63
Table 2. 2 - Kits	63
Table 2. 3 - Recipes of solutions	64
Table 2. 4 - Primary antibodies	66
Table 2. 5 - Secondary antibodies	66
Table 2. 6 - siRNA used for RNA interference experiments.....	66
Table 2. 7 - shRNA used for RNA interference experiments.....	67
Table 2. 8 - qPCR primer sequences.....	67
Table 2. 9 - Acrylamide gels composition.....	68
Table 2. 10 - Drugs and Suppliers.....	68
Table 2. 11 - Cycling conditions for qPCR reaction.....	73
Table 2. 12 - Primary antibodies used for Immunohistochemistry.....	81
Table 5. 1- Overexpression of genes belonging to the ERBB network in phospho- ERK ^{high} tumour regions.	144

List of Figures

Figure 1. 1 - Domain structure of AMPK subunits.	21
Figure 1. 2 - Signal pathways regulated by AMPK.	26
Figure 1. 3 - The mTORC1 signalling pathway.	28
Figure 1. 4 - Dendrogram of the AMPK related kinases.	34
Figure 1. 5 - ARKs sequence homology of the kinase domain.	36
Figure 1. 6 - Mechanism of regulation of cell adhesion by NUAK1.	43
Figure 1. 7 - NUAK1 gene alteration frequency in human cancer.	46
Figure 1. 8 - Histogenesis and molecular markers of Adenocarcinoma and Squamous cell carcinoma.	50
Figure 1. 9 - The ERBB signalling network.	54
Figure 1. 10 - Downstream targets of RAS.	56
Figure 3. 1 - NUAK1 is not required for the maintenance of AMPK subunits.	88
Figure 3. 2 - NUAK1 is not required for the maintenance of AMPK basal activity.	89
Figure 3. 3 - AMPK response to increase in intracellular Ca ²⁺ is impaired by NUAK1 inhibition.	90
Figure 3. 4 - NUAK1 is still required for AMPK response to increase in intracellular Ca ²⁺ in the absence of LKB1.	91
Figure 3. 5 - NUAK1 is active and can be modulated in LKB1-null cells.	92
Figure 3. 6 - CaMKKB is not an upstream kinase for NUAK1.	93
Figure 3. 7 - Modulation of intracellular Ca ²⁺ levels impacts on NUAK1 activation.	94
Figure 3. 8 - Simultaneous depletion of NUAK1 and NUAK2 abrogates modulation of phospho-MYPT1 ^{S445} in response to calcium.	95
Figure 3. 9 - Overexpression of MYC induces upregulation of components of the Ca ²⁺ signalling pathway.	97
Figure 3. 10 - Inhibition of PKC impairs MYPT1 ^{S445} phosphorylation.	98
Figure 3. 11 - PKC α and not PKC β_1 regulates downstream phosphorylation of MYPT1 ^{S445}	99
Figure 3. 12 - Phosphorylation of NUAK1 is decreased by PKC inhibition.	100
Figure 3. 13 - PKC α depletion induces NUAK1 degradation.	101

Figure 3. 14 - PKC α and NUAK2 co-depletion further decreases phospho-MYPT1 ^{S445} levels.	102
Figure 3. 15 - NUAK1 inhibition and depletion is lethal in HeLa cells.	103
Figure 3. 16 - Cell death induced by NUAK1 inhibition is rescued by MYC downregulation.	104
Figure 3. 17 - PKC α depletion and inhibition is lethal in HeLa cells.	105
Figure 3. 18 - Dynamic Ca ²⁺ -dependent modulation of mTORC1.	106
Figure 3. 19 - PKC α and NUAK1 depletion impairs Raptor inhibition at basal levels and in response to AMPK stimulation.	108
Figure 3. 20 - NUAK1 downregulation increases protein translation.	109
Figure 3. 21 - mTORC1 inhibition rescues cell death induced by PKC α or NUAK1 depletion.	110
Figure 3. 22 - NUAK1 regulates Raptor ^{S792} phosphorylation in the absence of AMPK.	111
Figure 3. 23 - Proposed model for the MYC-PKC α -NUAK1 signalling pathway.	117
Figure 4. 1 - Schematic representation of conditional <i>lsl-KRas</i> ^{G12D} and <i>lsl-KRas</i> ^{G12D} ; <i>Nuak1</i> ^{F/F} mouse model.	120
Figure 4. 2 - <i>KRas</i> ^{G12D} / <i>Nuak1</i> ^{F/F} mice develop only lung adenocarcinoma.	122
Figure 4. 3 - <i>Nuak1</i> deletion does not affect the histogenesis of <i>KRas</i> ^{G12D} lung adenocarcinoma.	124
Figure 4. 4 - <i>Nuak1</i> deletion does not affect <i>KRas</i> ^{G12D} -driven lung tumorigenesis.	125
Figure 4. 5 - Moderate overexpression of MYC accelerate <i>KRas</i> ^{G12D} -driven lung cancer.	126
Figure 4. 6 - Histological examintaion of KM and KMN tumours.	128
Figure 4. 7 - Deletion of <i>Nuak1</i> does not affect growth of <i>KRas</i> /MYC lung tumours.	129
Figure 4. 8 - <i>Nuak1</i> deletion decreases signalling through ERK.	131
Figure 4. 9 - <i>Nuak1</i> deletion results in increased AKT phosphorylation in lung tumours.	132
Figure 4. 10 - <i>Nuak1</i> deletion results in increased phosphorylation of 4E-BP1.	133
Figure 4. 11 - <i>Nuak1</i> deletion does not sensitize tumours to mTORC1 inhibition.	134
Figure 4. 12 - <i>Nuak1</i> deletion affects tumour blood vessels.	135

Figure 4. 13 - Nuak1 deletion enhances survival of KRas ^{G12D} /MYC lung tumours-bearing mice.....	136
Figure 5. 1 - Schematic representation of the lsl-KRas ^{G12D} /R26-lsl-MYC/Hprt-lsl-Irfp mouse model.	142
Figure 5. 2 - ERBB receptors are active in KRas ^{G12D} /MYC lung adenomas.	145
Figure 5. 3 - ERBB inhibition induces growth arrest and cell death in KM lung tumours.	146
Figure 5. 4 - Neratinib but not Erlotinib treatment reduces lung tumour burden of KM mice.....	148
Figure 5. 5 - Neratinib treatment does not increase the overall survival of KM mice.	149
Figure 5. 6 - Combination of ERBB and MEK inhibition more efficiently induces cell death in KRas mutant human lung cancer cell lines.	150
Figure 5. 7 - iRFP signal detection identified impaired growth of lung tumours treated with Neratinib in combination with Trametinib.	151
Figure 5. 8 - Combination of Neratinib with Trametinib enhances survival of KM mice.	152
Figure 5. 9 - Simultaneous inhibition of the ERBB receptors and MEK impacts on AKT activation.....	153

Abbreviations

4-OHT	4-Hydroxytamoxifen
4E-BP1	Eukaryotic translation initiation factor 4E-binding protein 1
AAH	Atypical adenomatous hyperplasia
ACC	Acetyl-CoA Carboxylase
ADAM	A Disintegrin and Metalloprotease
ADP	Adenosine diphosphate
AID	Auto-inhibitory domain
AMARA	Synthetic peptide, AMARAASAAALARRR
AMP	Adenosine monophosphate
AMPK	AMP-activated protein kinase
ARK	AMPK-related kinases
ATM	Ataxia-telangiectasia mutated
ATP	Adenosine triphosphate
BCA	Bicinchoninic acid
BrdU	Bromodeoxyuridine
BRSK	Brain-specific kinases
BSA	Bovine serum albumin
CaMKK	Calcium/calmodulin-dependent protein kinase kinase
cAMP	Cyclic adenosine monophosphate
CBM	Carbohydrate binding module
CBS	Cystathionine β -synthase
CC10	Clara Cell 10
CoA	Coenzyme A
CTD	C-terminal domain
DAG	Diacylglycerol
DEPTOR	DEP Domain Containing MTOR Interacting Protein
DMEM	Dulbecco's Modified Eagle Medium
DMSO	Dimethyl sulfoxide
DNA	Deoxyribonucleic acid

eEF2K	Eukaryotic elongation factor-2 kinase
EGFR	Epidermal growth factor receptor
EH	Epithelial hyperplasia of the bronchioles
EIF4E	Eukaryotic translation initiation factor 4E
EMT	Epithelial-to-mesenchymal transition
ER	Estrogen receptor
ERK	Extracellular signal-regulated kinase
FACS	Fluorescence activated cell sorting
FBS	Foetal Bovine Serum
FFPE	Formalin-fixed paraffin-embedded
FT	Farnesyltransferase
g	Relative centrifugal force
GBD	Glycogen-binding domain
GDP	Guanosine diphosphate
GEM	Genetically engineered mouse
GGT	Geranylgeranyltransferase
GLUT	Glucose transporter
GS	Glycogen synthase
GSK-3β	Glycogen synthase kinase-3 β
GTP	Guanosine triphosphate
H&E	Haematoxylin & Eosin
HCl	Hydrochloric acid
HRP	Horseradish peroxidase
IDT	Integrated DNA Technology
IGF	Insulin-like growth factor
IHC	Immunohistochemistry
IP2	Inositol bisphosphate
IP3	Inositol trisphosphate
KD	Kinase domain
KRT	Keratin
LATS	Large tumour suppressor
MAPK	Mitogen-activated protein kinase

MAPKK	Mitogen-activated protein kinase kinase
MAPKKK	Mitogen-activated protein kinase kinase kinase
MARCKS	Myristoylated alanine-rich C-kinase substrate
MARK	Microtubule affinity-regulating kinase
MEF	Mouse Embryonic Fibroblast
MELK	Maternal embryonic leucine zipper kinase
MEM	Minimum Essential Media
MFF	Mitochondrial fission factor
MLC	Myosin regulatory light chain
MMP	Matrix metalloproteinases
MO25	Mouse protein 25
MOI	Multiplicity of infection
mTOR	Mechanistic Target of rapamycin
mTORC	mTOR complex
MYPT1	Myosin phosphatase targeting 1
NDR	Nuclear Dbf2-Related Kinase
NGS	Normal goat serum
NSCLC	Non-small cell lung cancer
NT	Non-targeting control
NUAK	Nua (novel) kinase
PBS	Phosphate-buffered saline
PBS/T	Phosphate-buffered saline with Tween
PCR	Polymerase chain reaction
PFK-2	6-phosphofructo-2-kinase
PI3K	Phosphoinositide 3-kinase
PKC	Protein kinase C
PLK1	Polo like kinase 1
PP1	Protein Phosphatase 1
PRAS40	Proline-rich Akt substrate of 40 kDa
Raptor	Regulatory-associated protein of mTOR
Rheb	RAS homologue enriched in brain
RIM	Regulatory subunit-interacting motif

RNA	Ribonucleic acid
rpm	Revolutions per minute
SCC	Squamous cell carcinoma
SCLC	Small cell lung cancer
SD	Standard Deviation
SDS	Sodium dodecyl sulfate
SEM	Standard error of the mean
SIK	Salt-inducible kinases
SNF1	Sucrose non-fermenting protein 1
SPC	Surfactant protein C
STRAD	STE20-related adaptor protein
TAK1	Transforming growth factor- β activated kinase-1
TBC1D1	TBC1 domain family member 1
TBS	Tris-buffered saline
TBS/T	Tris-buffered saline with Tween
TdT	Terminal deoxynucleotidyl transferase
TK	Tyrosine Kinase
TKI	Tyrosine kinase inhibitor
TSC	Tuberous sclerosis complex
TXNIP	Thioredoxin-interacting protein

Acknowledgments

I would like to express my gratitude to my supervisor Daniel Murphy for giving me the opportunity to work in his group and for his precious guidance over the years. I am also thankful to all the members of M10, past and present, for their support, advice and for creating a great working environment. Thanks also to Björn, Allan and Nat for their feedbacks during the writing process, and to Jacqueline for her support and encouragement over the years. Nat has been a great mentor and friend from the very first day, always available for constructive discussions but also for a laugh together that helped during tough times.

Words cannot describe the important role that my work-wife, Jennifer, has played throughout my adventure in Scotland; with her sparkingly personality and kind heart she has always been there for me. Thanks to Alessandra, Dominika and Christin for the great time we had together, our therapeutic chats over coffee and drinks and for sharing with me the pain and the joy of this PhD. My wish is that our friendship will last in time and space.

I am grateful to my family for always believing in me and supporting my decisions; despite the distance, my heart will always be next to theirs.

Thanks to Nicolas, without him by my side I would have not made it this far. His love gave me the strength during this journey and I will always be grateful for his willingness to follow me to Scotland and make everything possible.

Author's Declaration

I declare that, except where explicit reference is made to the contribution of others, this dissertation is the result of my own work and has not been submitted for any other degree at the University of Glasgow or any other institution.

Tiziana Monteverde

Chapter 1 – Introduction

The Novel (Nua) kinase family 1 (NUAK1, also known as ARK5), is a serine/threonine kinase identified as the fifth AMPK-related kinase (ARK) (Suzuki et al., 2003a). The biological function of NUAK1 has not been extensively studied but multiple experimental evidence has suggested a role for NUAK1 in a broad variety of processes ranging from metabolism to cell adhesion, migration and neuronal axon branching. Although the information obtained so far places NUAK1 as a potential target in cancer therapy, additional studies are required to fully explore and understand its roles. On the other hand, a large number of investigations have been carried out on the function and activity of AMPK, which provided the molecular basis for the understanding of the roles of other AMPK-related kinases, such as NUAK1. Therefore, in this chapter an overview of AMPK and the AMPK-related kinases is given before discussing in more detail the function and regulation of NUAK1. Lung cancer is also discussed, as the mechanisms of progression and the involvement of NUAK1 in lung tumorigenesis have been investigated as part of this thesis.

1.1 AMPK, the master energy sensor

1.1.1 Structure and expression of AMPK

The AMP-activated protein kinase (AMPK) is a threonine/serine kinase with a fundamental role in the maintenance of energy homeostasis. The key function exerted by AMPK is to act as a sensor of cellular energetic levels and to rebalance them when energetic stress occurs. It is conserved across most eukaryotes, with one of the exception represented by the intracellular parasite *Encephalitozoon cuniculi*, and exists as a heterotrimeric complex composed by an α catalytic subunit and two regulatory subunits, β and γ . The existence of multiple isoforms for each subunit further increases the level of complexity of AMPK. Specifically, the genes *PRKAA1* and *PRKAA2* encode for two isoforms of the catalytic subunit, $\alpha1$ and $\alpha2$, respectively; two and three isoforms for the β and γ regulatory subunits are encoded by *PRKAB1*, *PRKAB2* and *PRKAG1*, *PRKAG2* and *PRKAG3*, respectively.

Several studies have been carried out in the recent years to characterize the structure of AMPK. Starting from the identification of the crystal structure of isolated domains and fragments of the heterotrimeric complex (Chen et al., 2009; Townley and Shapiro, 2007), more recent studies have obtained data on full-length complexes (Li et al., 2015b; Xiao et al., 2013), contributing with precious information to the function of the kinase. The α subunit is formed by an N-terminal kinase domain (KD), which possesses catalytic activity and that contains a conserved threonine in the activation loop (Thr172) that can be phosphorylated resulting in full activation of the kinase. The kinase domain is then followed by an auto-inhibitory domain (AID) and by the α regulatory subunit-interacting motifs (RIMs), which has been shown to be important for allosteric activation (Chen et al., 2009). Located at the C-terminus of the α subunit, the subunit-interacting domain mediates the interaction with the β regulatory subunit (Fig. 1.1).

The β subunits are characterized by a glycogen-binding domain (GBD) that allows binding of the complex to glycogen and β -cyclodextrin (Polekhina et al., 2005) and by a C-terminal domain (CTD) for interaction with α -CTD. Finally, the structure of three γ subunits slightly differ from each other because the $\gamma 2$ and $\gamma 3$ subunits contain an N-terminal extension that is missing in $\gamma 1$. The γ isoforms, which form complexes with the β subunits through β -strands interactions (Xiao et al., 2007), comprise four tandem repeats of a cystathionine β synthase motifs (CBS1-4). A pair of CBS motifs forms the Bateman domain, which can bind two adenine nucleotides (Fig. 1.1). In particular, AMP is permanently bound to site-4 and appears not exchangeable as soaking of ATP into AMPK crystals did not displace AMP from site 4 (Xiao et al., 2007). Site-2 remains constantly unoccupied whereas site-1 and site-3 are the two exchangeable sites in which ATP, ADP and AMP bind in a competitive manner. Binding of adenine nucleotides at site-1 is at least 30-fold stronger than at the site-3 (Xiao et al., 2011).

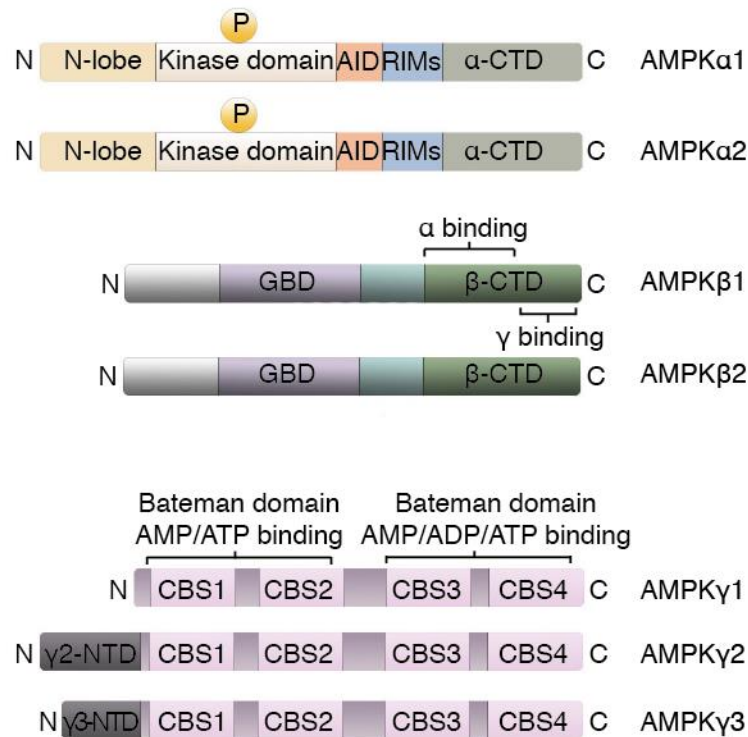


Figure 1. 1 – Domain structure of AMPK subunits.

Schematic representation of the domain organization of the catalytic (α 1, α 2) and regulatory (β 1, β 2, γ 1, γ 2, γ 3) subunits of AMPK. AID, autoinhibitory domain; RIMs, regulatory subunit-interacting motifs; CTD, C-terminal domain; GBD, glycogen binding domain; NTD, N-terminal domain; CBS, cystathionine B synthase motifs. Adapted from (Salt and Hardie, 2017).

Different combinations of the multiple isoforms can give rise to twelve distinctive holo-AMPK complexes and their expression levels differ across tissue types. Specifically, AMPK α 1, AMPK β 1, AMPK γ 1 and AMPK γ 2 are widely expressed whereas expression of AMPK α 2 and AMPK β 2 is dominant in the skeletal and cardiac muscle, but lower levels can be found in many other tissue; expression of AMPK γ 3 appears to be limited to skeletal and cardiac muscle.

A further level of complexity is given by the dynamic localization of AMPK in various cell compartments. It has been previously described that AMPK can shuttle between the cytoplasm and the nucleus (Kodiha et al., 2007), but Miyamoto and colleagues, by using a FRET-based biosensor for detection of AMPK activity, were additionally able to show a differential modulation of AMPK

activation and subcellular localization in response to stimuli like 2-Deoxyglucose or glucose starvation (Miyamoto et al., 2015).

1.1.2 Nucleotide-dependent activation of AMPK

As the key regulator of the cellular energetic status, AMPK can sense changes in ATP, ADP and AMP levels. During energetic stress, induced i.e. by nutrient or oxygen deprivation, an increased use of ATP, which represents the “energy currency molecule” of the cell, would lead to energetic imbalance characterized by increased ADP:ATP and AMP:ATP ratios. Binding of adenine nucleotide to the γ subunit of AMPK, commonly referred to as canonical activation, can regulate the activity of the AMPK complex by three mechanisms. Firstly, binding of AMP, but not ADP, can induce allosteric activation of various folds depending on the type of the γ isoform comprised in the complex (Cheung et al., 2000). Secondly, binding of AMP or ADP can promote phosphorylation at Thr172 by upstream kinases, such as LKB1 or CaMKK β , which represents the most important event for full activation. However, the mechanism still remains controversial, with some experimental evidence supporting a role of CaMKK β in phosphorylation of AMPK in response to ADP and AMP (Oakhill et al., 2011), whereas other studies have highlighted that AMP can induce phosphorylation through LKB1 and not CaMKK β (Gowans et al., 2013). In addition, myristoylation of the β subunit was reported to be necessary for phosphorylation at Thr172 in response to AMP binding, as loss of the post-translational modification resulted in a reduction of the phosphorylation levels (Oakhill et al., 2010). Finally, binding of either AMP or ADP can induce a conformational change that protects the Thr172 site in the α catalytic subunit from dephosphorylation by phosphatases (Gowans et al., 2013; Xiao et al., 2011), with a more potent effect exerted by binding of AMP in comparison to ADP (Ross et al., 2016). Binding of ATP instead of ADP or AMP can inhibit all the three mechanisms of activation.

1.1.3 Pharmacological activation of AMPK

As a consequence of energetic stress, changes in adenine nucleotide ratios can finely tune the activation of AMPK. However, many other xenobiotics and natural compounds have been found to induce AMPK activity. Natural products such as Resveratrol (polyphenol compound found in grapes), or other plant extracts such as Berberine and Curcumine can activate AMPK and were utilised since ancient times as part of herbal remedies (Kim et al., 2009; Lee et al., 2006; Park et al., 2007). In addition, synthetic compounds such as Metformin, extensively used for the treatment of type II diabetes, and phenformin have also been described for their ability to induce AMPK. Although some of those compounds, like Resveratrol, phenformin and Berberine are mitochondrial poisons that interfere with ATP generation (Owen et al., 2000; Turner et al., 2008; Zheng and Ramirez, 2000), thereby activating AMPK by increasing the ADP or AMP levels, other drugs have revealed novel and AMP/ADP-independent mechanisms of activation. For example, Salicylate, which is the active metabolite of aspirin and a natural molecule found in many flowering plants, has been shown to directly induce AMPK activation. Similarly to AMP Salicylate is inducing allosteric activation and inhibits dephosphorylation of Thr172, but without affecting the AMP and ADP levels and interacting with a different site compared to the adenine nucleotides (Hawley et al., 2012). Furthermore, a synthetic compound member of the thienopyridone family and named A-769962 was identified during a screening of over 700,000 compounds for its ability to directly activate AMPK (Cool et al., 2006). Particularly, A-769662 was found to activate AMPK with a similar mechanism to Salicylate, without affecting the levels and the binding of AMP to the γ subunit of AMPK (Goransson et al., 2007; Sanders et al., 2007). Interestingly, both the synthetic and natural activators were found to require a wild-type AMPK β 1 subunit for their function. Mutation of the Ser108 residue to Alanine in the β 1 subunit was shown to abolish the activation by both agents, suggesting an overlap of their site of action (Hawley et al., 2012).

1.1.4 Upstream kinases of AMPK

The Thr172 was identified as the major site for phosphorylation in AMPK (Hawley et al., 1996), which results in more than 100-fold activation (Suter et al., 2006). In the long search for the upstream kinase of AMPK, the yeast enzymes Tos3p, Pak1p and Elm1p were initially identified as being required for the *in vivo* function but also *in vitro* phosphorylation of Snf1, the yeast homologue of AMPK (Hong et al., 2003). In addition, Tos3p was found in the same study to phosphorylate AMPK *in vitro*. The similarity of Tos3p, Pak1p and Elm1p to the mammalian Liver Kinase B1 (LKB1) led to the important identification of the latter as the major upstream kinase for AMPK (Hong et al., 2003; Woods et al., 2003). Following studies have revealed that the activity of LKB1 was enhanced when in complex with two other proteins, STRAD and MO25 (Boudeau et al., 2003), and that the same complex could activate AMPK (Hawley et al., 2003).

The yeast activators of Snf1 displayed a similarity to the mammalian family of Ca^{2+} /Calmodulin-dependent kinases CaMKK, suggesting that alternative upstream kinases to LKB1 could take part in AMPK activation. Indeed, despite the initial underestimation of CaMKK as a potential alternative upstream kinase for AMPK, further studies have compellingly established the role of CaMKK in the activation of AMPK through phosphorylation at Thr172. Particularly, Carling's group demonstrated that AMPK can be activated in cells lacking LKB1, such as HeLa cells, corroborating the theory of the existence of additional upstream kinases. Moreover, treatment of HeLa cells with STO-609, a pharmacological inhibitor of CaMKK, strikingly reduced the basal levels of AMPK activity as well as its response to multiple activators. Further experiments in the same study proved that agents that cause an increase in intracellular Ca^{2+} levels, such as Ionomycin, could induce activation of AMPK and established that the CaMKK β isoform, rather than the α isoform, is the main regulator of AMPK in cells lacking LKB1 (Woods et al., 2005). Corroborating the findings of Woods and colleagues, additional studies published in the same year also highlighted the Calcium/CaMKK β dependent activation of AMPK (Hawley et al., 2005; Hurley et al., 2005). Overall, the studies provided compelling evidence on CaMKK β being an alternative upstream kinase for AMPK and revealed a novel and Calcium-dependent mechanism of regulation.

A third kinase has been suggested to play a role in the activation of AMPK. Some reports have suggested that the Transforming growth factor- β -activated kinase (TAK1) can phosphorylate and activate AMPK (Momcilovic et al., 2006; Xie et al., 2006). In addition, further investigations have suggested a reciprocal regulation between TAK1 and AMPK, as AMPK α 1 was shown to induce TAK1 with a role in inflammatory processes (Kim et al., 2012b). However, the physiological implications of AMPK activation by TAK1 are not clear yet.

1.1.5 Metabolic implications of AMPK activity

As the pivotal regulator of energy homeostasis, a fundamental function of AMPK in restoring the energetic levels is to activate intracellular catabolic pathways intent to produce energy while inhibiting energy consuming processes (Fig. 1.2). Over time, several downstream targets of AMPK have been identified, ranging from enzymes and kinases to transcription factors. AMPK, through the modulation of many targets, can regulate major cellular metabolic processes, such as protein synthesis, glucose and lipid metabolism, mitochondrial biogenesis and autophagy to orchestrate the energy production and consumption of cells, specifically under stress conditions.

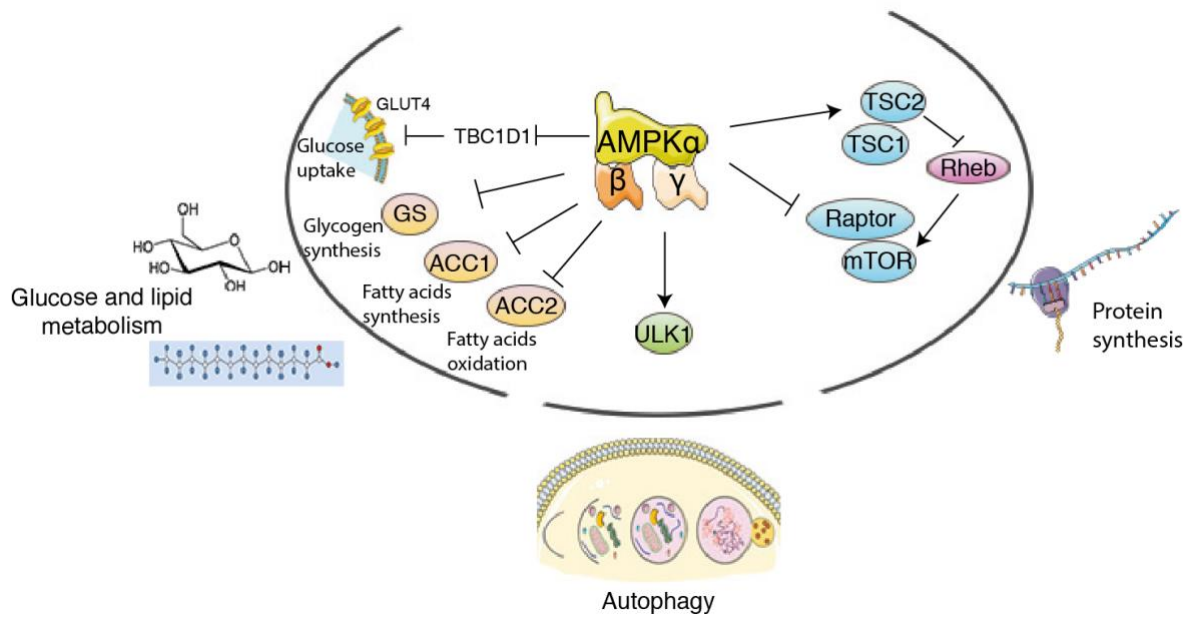


Figure 1. 2 – Signal pathways regulated by AMPK.

AMPK can regulate several downstream targets to inhibit anabolic pathways in favour of catabolic processes. Phosphorylation of TBC1D1 (TBC1 domain family member 1) promotes membrane translocation of the glucose transporter GLUT4 and glucose uptake; phosphorylation and inhibition of Glycogen synthase (GS) inhibits glycogen synthesis; Phosphorylation and inhibition of ACC1 and ACC2 (Acetyl CoA carboxylase) impairs fatty acids biosynthesis and promotes fatty oxidation, respectively; Phosphorylation of ULK1 (Unc-51 Like Autophagy Activating Kinase 1) contributes to autophagy induction; inhibition of protein synthesis is achieved by AMPK-mediated inhibition of Raptor and induction of Tuberin (TSC2, Tuberous Sclerosis 2). Only some of the targets and pathways are represented in this image generated using items from Servier Medical Art.

1.1.5.1 Regulation of protein synthesis

AMPK has been established as an important negative regulator of the mechanistic target of rapamycin (mTOR) complex 1 (mTORC1) (Fig. 1.3). mTOR acts as a coordinator of signals from nutrients and growth factors to regulate cell growth and proliferation. mTOR is the catalytic subunit of two distinct complexes that differ in their components but also for their substrates and regulation: mTORC1 and mTORC2. mTORC1 is a multi-protein complex formed by mTOR, Raptor (regulatory protein associated with mTOR), mLST8 (mammalian lethal with Sec13 protein 8, also known as GβL) and two inhibitory subunits, namely PRAS40 and DEPTOR. mTORC1 regulates multiple processes, such as

protein synthesis, lipid and glucose metabolism and autophagy. mTORC1 is activated by Rheb on the surface of the lysosomes but active mTOR has also been detected in other cellular compartments, such as nucleus and cytoplasm (Betz and Hall, 2013; Manifava et al., 2016).

Regarding the regulation of protein synthesis, two important effectors are located downstream of mTORC1: p70S6 Kinase 1 (S6K1) and eIF4E Binding Protein (4E-BP1) (Fig. 1.3). Phosphorylation and consequent activation of S6K promotes mRNA translation. 4E-BP1 negatively regulates 5'-cap-dependent mRNA translation by binding the eukaryotic translation initiation factor 4E (eIF4E). Hyperphosphorylation of 4E-BP1 by mTORC1 induces the release of the eIF4E factor and stimulation of 5'-cap-dependent mRNA translation.

Interestingly, AMPK was shown to target multiple components of the mTORC1 pathway. In particular, AMPK activation by nutrient starvation resulted in the induction of TSC2, a negative regulator of mTORC1, through phosphorylation of Thr1227 and Ser1345 (Inoki et al., 2003). Active TSC2 can then inhibit Rheb, which is a GTPase of the RAS superfamily. Rheb has been proposed to control mTOR catalytic activity through multiple mechanisms: 1) Interaction with the mTOR kinase domain resulting in an increase in mTOR kinase activity (Long et al., 2005); 2) Rheb-GTP binds to the mTOR inhibitor FKBP (FK506-binding protein) 38, displacing it from mTOR (Bai et al., 2007); 3) Rheb-GTP interacts with phospholipase D₁ (PLD1), causing the generation of phosphatidic acid, which positively regulates mTOR (Sun et al., 2008).

Additionally, AMPK has been involved in the regulation of mTORC1 through Raptor. Raptor, as previously mentioned, is part of mTORC1 complex and it was shown to be necessary for mTOR signalling *in vivo* as well as *in vitro* (Hara et al., 2002; Kim et al., 2002). Specifically, Shaw and colleagues identified Raptor as a direct target of AMPK and revealed that phosphorylation of Raptor at Ser722 and Ser792 caused its binding to the 14-3-3 protein and reduction of mTOR activity. Moreover, in cells stimulated with the AMPK activators phenformin and AICAR, inhibition of mTORC1 was not efficient when a mutant form of Raptor, in which Ser722 and Ser792 were replaced with Alanine, was expressed, suggesting that AMPK phosphorylation of Raptor is required for inhibition of mTORC1 (Gwinn et al., 2008).

Further checkpoints activated by AMPK for the regulation of translation have been described over time. For example, AMPK can directly activate eEF2K

(Eukaryotic elongation factor-2 kinase) to block translation elongation (Leprivier et al., 2013). Overall, the modulation of multiple components of the TOR pathway makes AMPK a key regulator of translation during energetic stress.

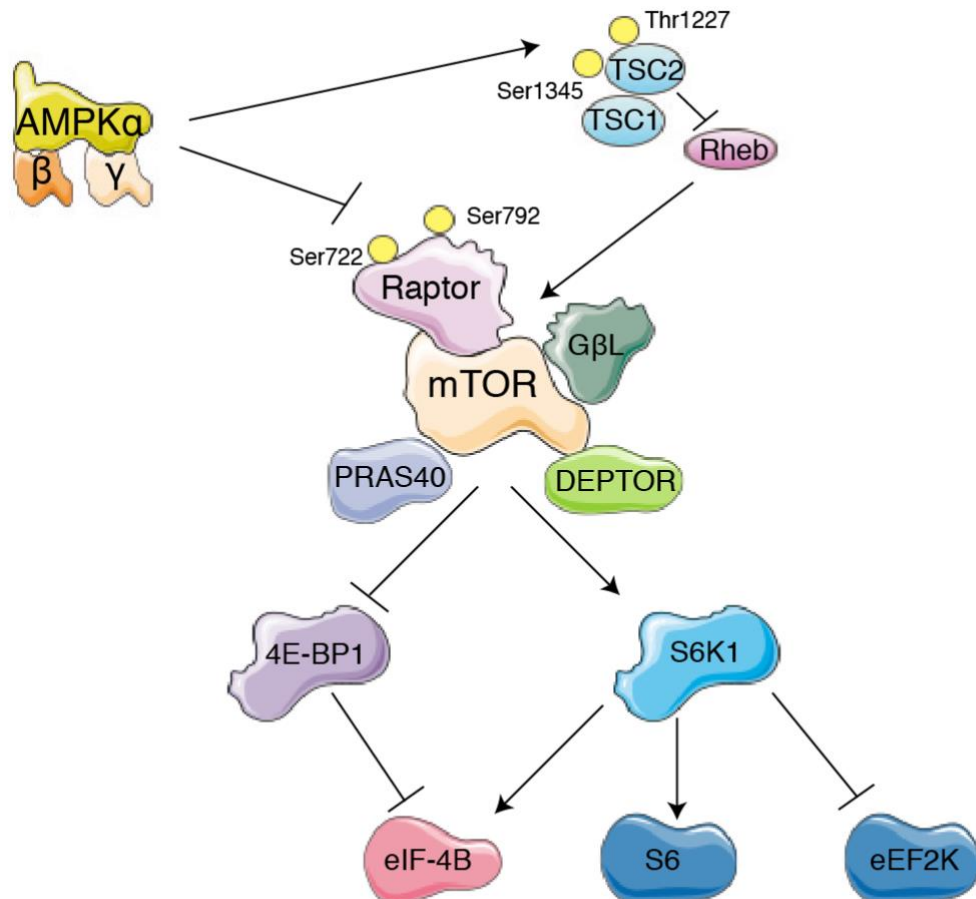


Figure 1. 3 – The mTORC1 signalling pathway.

The mTORC1 complex is formed by a catalytic subunit (mTOR) and regulatory components (Raptor, PRAS40, DEPTOR, GβL). Active mTOR transmits the signal to the downstream effectors 4E-BP1 and S6K1 to modulate mRNA translation. AMPK can inhibit protein synthesis by phosphorylation and inhibition of Raptor; alternatively, phosphorylation and induction of TSC2 results in inhibition of Rheb, which is a positive regulator of mTORC1 activity. Image made using items from Servier Medical Art.

1.1.5.2 Regulation of glucose and lipid metabolism

Glucose and lipids are an important source of energy for cells and AMPK can modulate pathways involved in their metabolism to maintain energetic homeostasis. AMPK can stimulate glucose uptake in the skeletal muscle by transcriptional regulation of the glucose transporter GLUT4 through phosphorylation and inactivation of the transcriptional repressor Histone Deacetylase 5 (HDAC5) (McGee et al., 2008) and by promoting GLUT4 translocation to the plasma membrane through phosphorylation and inhibition of TBC1D1 (Chavez et al., 2008; Chen et al., 2008). Furthermore, AMPK-mediated phosphorylation and inhibition of Thioredoxin-interacting protein (TXNIP), a negative regulator of GLUT1, was shown to contribute to enhanced glucose uptake (Wu et al., 2013).

To increase energy production, AMPK has been described to promote the oxidation of glucose via stimulation of the glycolytic enzyme 6-phosphofructo-2-kinase (PFK-2) in cardiac cells and activated monocytes (Marsin et al., 2000; Marsin et al., 2002). In addition, glucose storage has been reported to be modulated by AMPK in the liver and muscle through the inactivation of glycogen synthase (GS) (Bultot et al., 2012; Jorgensen et al., 2004).

Lipids are an alternative source of energy when glucose levels are low. Among the various substrates of the lipid metabolism modulated by AMPK, inhibition of Acetyl-CoA Carboxylase (ACC) represents a key event in the regulation of lipid biosynthesis and oxidation (Ha et al., 1994; Munday et al., 1988). ACC is expressed in two isoforms, ACC1 and ACC2, which differ in their cellular localization and tissue distribution. In eukaryotes, ACC1 is expressed in all tissues but it is particularly enriched in lipogenic tissues such as liver, mammary glands and adipose tissue; ACC2 is the predominant isoform in oxidative tissues such as skeletal and cardiac muscle. ACC1 regulates lipid biosynthesis by generation of malonyl-CoA in the cytoplasm. Conversely, the malonyl-CoA generated by ACC2 acts as inhibitor of the carnitine/palmitoyl-transferase 1 (CPT1), a mitochondrial enzyme involved in the movement of Acyl-CoA from the cytoplasm to the mitochondria for β -oxidation. Therefore, by inhibiting the two isoforms of ACC, AMPK can on one hand downregulate lipid biosynthesis and on the other hand it can stimulate lipid oxidation for energy production.

1.1.5.3 Regulation of mitochondria biogenesis and autophagy

Mitochondria are organelles with the important role of producing energy to support life. Indeed, as the key regulator of energy homeostasis, it is not surprising for AMPK to have been involved in the regulation of mitochondria biogenesis in response to energetic stress.

AMPK β 1/ β 2 deleted mice showed reduced activity and expression of mitochondrial enzymes such as citrate synthase and cytochrome c oxidase, as well as reduction in mitochondrial DNA copy number and alteration of mitochondria morphology (O'Neill et al., 2011). Moreover, AMPK was described to phosphorylate the proliferator-activated receptor γ coactivator 1 α (PGC-1 α), which is considered the master regulator of mitochondria biogenesis, causing the binding of PGC-1 α to its own promoter to increase its expression levels (Jager et al., 2007). More recently, Shaw's group revealed that following mitochondrial stress AMPK is activated to promote mitochondrial fission by phosphorylation of the mitochondrial fission factor (MFF), which is the receptor for the fission promoter dynamin-related protein 1 (DRP1) (Toyama et al., 2016). Mitochondrial fission is important for the generation of new mitochondria but also for their clearance when damaged and induction of this process by AMPK was suggested to prime cells for subsequent mitophagy. The term mitophagy refers to the mechanism of autophagy related to mitochondria, and represents an additional mechanism through which damaged mitochondria are removed.

In addition to a role in the degradation of dysfunctional proteins and organelles, mitophagy and more broadly autophagy are important cellular processes that allow the recycle of macromolecules in response to energetic needs. In agreement with its role as energy sensor, it was noted that AMPK activation under nutrient starvation could induce autophagy by phosphorylation of the autophagy-initiating kinase ULK1 (Egan et al., 2011; Kim et al., 2011).

Overall, by regulating both mitochondria biogenesis and clearance, as well as modulating autophagy in response to nutrient limitation, AMPK has established itself as a crucial coordinator of the cellular energetic engine.

1.1.6 Role of AMPK in the regulation of proliferation

Cell proliferation is a high energy-demanding process that not only requires new nucleotides for DNA and RNA synthesis, but also building blocks necessary to produce two daughter cells. Indeed, back in 1974 it was noticed that cells cultured in a shortage of amino acids, glucose and phosphate ions were entering in a quiescent status that was reverted by the addition of the limiting nutrient (Holley and Kiernan, 1974). In agreement with its role in maintaining the energetic balance, activation of AMPK was described to inhibit proliferation under glucose deprivation. In particular, AMPK was found to activate p53 through phosphorylation at Ser15, which induced cell cycle arrest at the G1 phase (Jones et al., 2005). Although the finding of AMPK-mediated induction of p53 was confirmed by other studies (Imamura et al., 2001), Ser15 does not appear to conform to the consensus motif of AMPK and evidence of a direct interaction between p53 and AMPK has not been provided, suggesting the possibility of an indirect effect. However, other investigations have revealed a potential role of AMPK in mitosis. In particular, during a study aimed to identify novel substrates of AMPK α 2, Banko and colleagues revealed 28 new targets, many of them involved in mitosis and cytokinesis. AMPK was found to contribute to proper completion of mitosis and cytokinesis through phosphorylation of protein phosphatase 1 regulatory subunit 12C (PPP1R12C) (Banko et al., 2011). The function of AMPK in promoting mitosis might not be in line with its role of cell cycle inhibitor. However, the authors claimed that the regulation of mitosis could not be related to the energy regulating role of AMPK, as the mechanism was not affected by glucose deprivation.

1.1.7 Role of AMPK in cancer

The established function of AMPK in the regulation of metabolism has led to an increased interest in its role in metabolic diseases and to exploit AMPK as a potential therapeutic target. For example, the increase in glucose uptake and utilization as a result of AMPK activation is beneficial in metabolic conditions such as type II diabetes that is characterized by elevated blood sugar levels, insulin resistance and reduced insulin production. Indeed, the well-known AMPK

activator Metformin has been successfully employed in clinic for the treatment of type II diabetes. Interestingly, a pilot case-study conducted on patients affected by type II diabetes that received treatment with Metformin revealed a decrease in the incidence of cancer (Evans et al., 2005). Similarly, aspirin, which is metabolized to Salicylate, a direct activator of AMPK, was shown to improve insulin sensitivity in diabetic patients and reduce the risk of cancer (Cuzick et al., 2009; Hundal et al., 2002). The metabolic and cancer preventive effects observed might be the overall result of additional effects on other tissues and beyond AMPK activation. Indeed, metformin has been reported to reduce insulin levels in non-diabetic patients affected by breast cancer (Goodwin et al., 2008), and patients affected by type II diabetes and hyperinsulinaemic have a higher risk of cancer development, thus suggesting that the reduction of insulin levels might contribute to the cancer preventive effect. Nevertheless, the role of AMPK in cancer remains of great interest. The features of uncontrolled proliferation and high metabolic demands of cancerous cells, often in a scenario of low availability of nutrients and oxygen, imply the intervention of AMPK to support energy homeostasis. However, there is still controversy on the role of AMPK as a friend or foe in cancer. Some studies have pointed towards a tumour suppressor role of AMPK. For example, it was reported that loss of AMPK α 1 cooperated with E μ -Myc in the acceleration of lymphomagenesis and caused a significant reduction in overall survival (Faubert et al., 2013). To note that the study made use of a full body knockout of AMPK α 1, giving rise to the possibility that deletion of AMPK in other compartments, such as stromal cells, could contribute to the observed phenotype.

Several suggestions of a tumour suppressor role for AMPK come from studies related to LKB1 loss. In fact, given that the tumour suppressor LKB1 is the master upstream kinase for AMPK, it has been assumed that the effect observed upon LKB1 loss are mediated by the consequent loss of AMPK function. For example, BRAF mutation in melanoma cells was described to cause LKB1 inactivation and consequent loss of function of AMPK, claiming a role of the LKB1/AMPK axis in mediating the oncogenic role of BRAF (Zheng et al., 2009). However, AMPK is not the only kinase downstream of LKB1 since, as elucidated in the next paragraph, several other AMPK-related kinases have been identified and they can mediate some of the functions of LKB1. In addition, genetic alterations of the AMPK subunits are not common events in cancer. Contrariwise,

we have highlighted a selective amplification of specific AMPK subunits in human cancer, which would suggest a tumour promoter role (Monteverde et al., 2015). Indeed, on one hand AMPK activity can counteract the growth of cancer cells by inhibiting proliferation and mTORC1 activity, but on the other hand the same functions can also help cancer cells to survive in stressful conditions and environments. In support of a tumour promoting role, increased AMPK activity was observed in the early phases of glioma development and was maintained throughout later stages (Jang et al., 2011). Moreover, an additional study revealed how the ability of AMPK to maintain NADPH levels by inhibition of ACC1 and ACC2 contributed to the survival of tumour cells (Jeon et al., 2012).

An intriguing aspect that has emerged in the recent years is to exploit the sensitivity to metabolic stress in case of impairments in the LKB1/AMPK axis. In particular, Shaw's group revealed an increased sensitivity to the metabolic drug phenformin of LKB1-deficient non-small cell lung cancer (Shackelford et al., 2013). In addition, a recent study demonstrated how the maintenance of Leukaemia-Initiating cells requires the activity of AMPK, as deletion of AMPK α 1/ α 2 from the hematopoietic cells enhanced the survival of mice affected by Acute Myeloid Leukaemia and sensitized tumour cells to metabolic stress induced by dietary restriction (Saito et al., 2015).

Further investigations are required to elucidate not only the context-dependent role of AMPK but also how different complexes might act as tumour promoters and suppressors before we can confidently manipulate AMPK for therapeutic purposes.

1.2 AMPK related kinases

AMPK was first named in 1988 by Hardie's group (Munday et al., 1988), although previous reports had described an ATP-dependent kinase that could regulate Acetyl coenzyme A carboxylase by phosphorylation (Carlson and Kim, 1974). The function of AMPK has been extensively studied over time and, based on sequence similarity, several other kinases related to AMPK, called AMPK related kinases (ARKs), have emerged (Manning et al., 2002) (Fig. 1.4). Twelve other members have been included in the AMPK family: BRSK1 (SAD-B), BRSK2 (SAD-A), NUA1

(ARK5), NUAK2 (SNARK), SIK1 (SIK), SIK2 (QIK), SIK3 (QSK), MARK1, MARK2, MARK3 (PAR1A or C-TAK1), MARK4 and MELK.

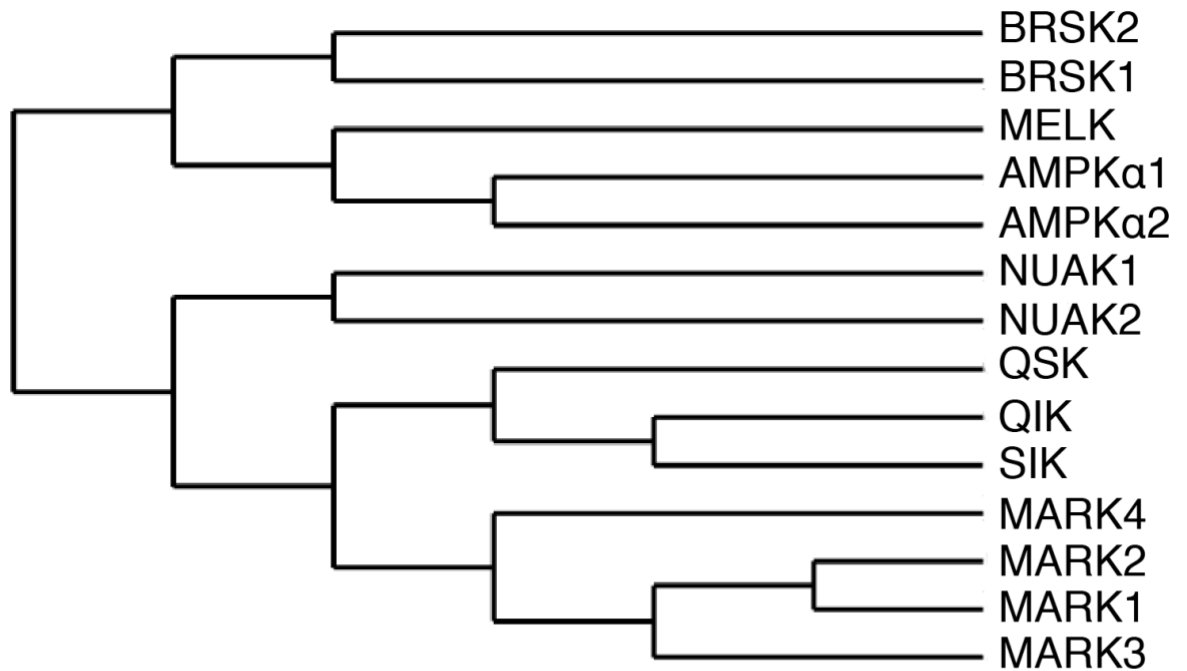


Figure 1. 4 – Dendrogram of the AMPK related kinases.

Dendrogram obtained by the analysis of the full-length amino acid sequence of the 12 AMPK related kinases (ARKs) and AMPK using a freely available online tool from www.phylogeny.fr.

These ARKs exert multiple biological functions, some of them shared with AMPK. In particular, the Microtubule affinity-regulating kinases (MARKs) and the Brain-specific kinases (BRSK) are important regulator of cell polarity. The three isoforms of the salt-inducible kinases (SIK) exerts a variety of functions. Specifically, SIK1, first identified from the adrenal glands of rats that were fed on a high-salt diet (Wang et al., 1999), has been involved in cell cycle regulation, gluconeogenesis and lipogenesis regulation, muscle growth and differentiation; SIK2 is highly expressed in the adipose tissue but it has also been implicated in neuronal survival (Sasaki et al., 2011); SIK3 is thought to be important for cell proliferation as its downregulation resulted in chromosome abnormalities. The Maternal embryonic leucine zipper kinase (MELK) has been involved in the regulation of cell cycle and pre-mRNA splicing. NUAK2 activation

was described to play a role in the induction of cell-cell detachment (Suzuki et al., 2003b) and in the protection of tumour cells from CD95-mediated apoptosis (Legembre et al., 2004). In addition, NUA2 was also described to promote cell migration (Namiki et al., 2011) and to share some functions and substrates with NUA1, its closest AMPK related kinase, as further elucidated in the following paragraphs.

1.2.1 Activation modalities of ARKs

ARKs are characterized by a similar structure of the catalytic domain. However, the regulation of ARKs appears to be different from AMPK. Indeed, they do not contain regulatory subunits (Al-Hakim et al., 2005) and do not seem to be modulated by adenine nucleotides binding, although NUA1 was reported to be activated by AMP and, similarly to NUA2, by AICAR (an analogue of AMP) (Fisher et al., 2005; Lefebvre et al., 2001; Suzuki et al., 2003a). However, the evidence provided by the studies is not biochemically compelling as the response of the kinases to stimulation with AICAR or AMP was evaluated either exclusively by a cross-reacting antibody or employing a kinase assay that cannot completely preclude that the observed effect is mediated by other ARKs. In addition, an alternative study provided opposite evidence, as stimulation of MEFs with AICAR did not affect NUA2 kinase activity (Lizcano et al., 2004a), questioning that other ARKs might be activated by AMP.

Additionally, initial evidence suggested that AMPK was the only member to be responsive to increased intracellular Ca^{2+} levels. By using the AMARA peptide (a minimal phosphorylation substrate for the members of the AMPK family) multiple ARKs were tested for their ability to be activated in response to treatment with the calcium ionophore A23187. The assay revealed that none of the ARKs tested (SIK1/2/3, NUA2, MARK1/2/3/4) was responsive to A23187, claiming that AMPK was the only member modulated by Ca^{2+} levels (Fogarty et al., 2010). However, the AMARA peptide may not be the optimal substrate for all the ARKs as it has been shown that they can phosphorylate peptide substrates at dissimilar rates, suggesting a different substrate specificity (Lizcano et al., 2004a). Additionally, and a more recent study has disputed the theory of AMPK being the only member to be responsive to Ca^{2+} , as SIK2 was shown to be activated by an increase in

intracellular Ca^{2+} levels (Miranda et al., 2016). Therefore, further investigations and the development of more specific assays to test ARKs activity might reveal additional and surprising mechanisms of regulation.

1.2.2 Regulation of ARKs by upstream kinases

The finding that the Threonine 172 in the activation loop of $\text{AMPK}\alpha 1/\alpha 2$ was conserved across the other ARKs (Fig. 1.5) led to the hypothesis that the family members could share the upstream kinases. In this regard, Lizcano and colleagues identified the LKB1/MO25/STRAD complex to be a common upstream kinase of the AMPK family members, responsible for phosphorylation of the conserved threonine residue in the T-loop leading to over 50-fold increase in activity of the ARKs. The only exception was MELK, which was shown to autophosphorylate the T-loop without the requirement of LKB1 (Lizcano et al., 2004a).

```

159- DFGLSNMMSDGE---FLRT*SCGSPNYAAPE AMPKα1
157- DFGLSNMMSDGE---FLRTSCGSPNYAAPE AMPKα2
196- DFGLSNLYQKDK---FLQTFCGSPLYASPE NUAK1
193- DFGLSNLYHQGK---FLQTFCGSPLYASPE NUAK2
174- DFGMASLQVGDS---LLETSCGSPHYACPE BRSK1
159- DFGMASLQVGDS---LLETSCGSPHYACPE BRSK2
167- DFGFGNFYKSGE---PLSTWCGSPPYAAPE SIK1
160- DFGFGNFFKSGE---LLATWCGSPPYAAPE SIK2
206- DFGFSNLFTPGQ---LLKTWCGSPPYAAPE SIK3
200- DFGFSNEFTVGN---KLDTFCGSPPYAAPE MARK1
160- DFGFSNEFTFGN---KLDTFCGSPPYAAPE MARK2
196- DFGFSNEFTVGG---KLDTFCGSPPYAAPE MARK3
198- DFGFSNEFTLGS---KLDTFCGSPPYAAPE MARK4
150- DFGLCAPKGNKDYHLQTCCGSLAYAAPE MELK

```

Figure 1. 5 – ARKs sequence homology of the kinase domain.

Alignment of the T-loop amino acid sequence of the AMPK related kinases. Highlighted in red are the conserved amino acids across the kinases; the star denotes the conserved threonine in the activation loop.

CaMKK β has been recognised as an alternative upstream kinase for AMPK and modulates its response to increased intracellular Ca²⁺ levels (Hurley et al., 2005; Woods et al., 2005). However, CaMKK β has been disclaimed from being an upstream kinase for other ARKs. In particular, whereas expression of CaMKK β was shown to enhance AMPK activation, the other ARKs tested did not respond similarly (Fogarty et al., 2010). In addition, in the same study BRSK1 activity appeared to be modulated by increased expression of CaMKK α , which was also reported to interact with BRSK1 (Fujimoto et al., 2008), although Fogarty and colleagues suggested it to be a poor substrate for CaMKK α .

TAK1, the third suggested alternative kinase for AMPK, is not known to modulate any other ARKs. However, alternative upstream kinases have been shown to modulate some ARKs. For example, using a proteomic approach, the atypical protein kinase PKC λ was found to interact with MARK4 (Brajnovic et al., 2004). A later study identified an additional atypical PKC, PKC ζ , to phosphorylate MARK2 at Thr595 and negatively affect its association to the plasma membrane as well as activity (Hurov et al., 2004). In addition, GSK3 β was documented to inhibit MARK2 activity through phosphorylation at Ser212 (Timm et al., 2008).

The three isoforms of SIK have been shown to be modulated by cAMP/Protein kinase A (PKA). In particular, phosphorylation at Ser577 by PKA was described to be required for nuclear translocation of SIK1 (Takemori et al., 2002), whereas phosphorylation of SIK2 on multiple serine and threonine residues by PKA was reported to affect cellular localization (Henriksson et al., 2012; Henriksson et al., 2015) and inhibit SIK3 activity in adipocytes (Berggreen et al., 2012). Additionally, AKT2 was shown to induce SIK2 activity by phosphorylation at Ser358 (Dentin et al., 2007). Finally, as already mentioned, SIK2 was found to be activated in response to increased Ca²⁺ signalling, although the responsible kinase was not identified in the study (Miranda et al., 2016).

1.3 NUAK1

1.3.1 Structure and expression profile of NUAK1

NUAK1 was identified during the analysis of its close member SNARK (NUAK2) performed by Suzuki and colleagues. By using an antibody developed against the SNARK peptide, they observed a cross-reacting protein by Western blot, which further analysis based on sequence homology revealed to be an additional member of the AMPK family (Suzuki et al., 2003a).

The human NUAK1 gene is located on chromosome 12 and encodes a protein of 661 amino acids, with a molecular weight of 78 kDa, whereas the mouse orthologous gene, *Omphk1*, is located on chromosome 10 and encodes for a 658 amino acids protein. Expression of NUAK1 is conserved across species: from mammals to Zebrafish and *Drosophila*, with two homologous (NUAK1 and NUAK2) in vertebrates and only one in *Drosophila melanogaster* and *Caenorhabditis elegans*. Currently, there is no crystal structure available for NUAK1, but protein sequence analysis indicates a 55, 47 and 45.8% identity to NUAK2, AMPK α 1 and AMPK α 2, respectively, with a conserved threonine residue at position 211 in the activation loop (Fig. 1.5).

The tissue distribution of mouse NUAK1 was analysed at mRNA levels and revealed high expression in oxidative tissues such as the cerebellum, heart and soleus muscle. In addition, analysis of protein levels confirmed high expression in the skeletal muscles (Inazuka et al., 2012).

1.3.2 Upstream kinases regulating NUAK1

LKB1 has been described as the master kinase for the members of the AMPK family. However, alternative upstream regulators have been identified for AMPK and other ARKs, as elucidated in the previous paragraphs. Regarding NUAK1, its activation was reported to be predominantly regulated by LKB1, as its deletion in mouse embryonic fibroblasts abolished NUAK1 basal activity (Zagorska et al., 2010). However, a residual basal activity of NUAK1 was detected in HeLa cells, which are functionally null for LKB1. Furthermore, NUAK1 levels and activity

could still be increased by treatment with EDTA, described in the same study to induce NUA1 activation, although to a lesser extent in comparisons to HeLa cells stably expressing LKB1 (Zagorska et al., 2010). Therefore, there are experimental suggestions for the presence of alternative kinases upstream of NUA1. Indeed, the analysis of NUA1 sequence revealed the presence of a putative site for AKT phosphorylation and *in vitro* analysis indicated that AKT could phosphorylate NUA1 at Ser600. Activation of NUA1 by AKT was described to promote ATM induction, which resulted in the phosphorylation of its target p53 to support cell survival under glucose starvation (Suzuki et al., 2003a). However, additional analysis reported that the S600A mutation of NUA1 did not affect the kinase activity (Humbert et al., 2010), suggesting that the AKT signalling may not play a direct role in NUA1 activity or that this mechanism of regulation might not be conserved in various contexts.

The nuclear dbf2-related kinase 2 (NDR2) has been suggested in an isolated study as an additional alternative kinase for NUA1. NDR1 and NDR2 were identified with a BLAST search for proteins with homology to the catalytic domain of LKB1 and CAMKK β . Moreover, NDR2 was found to phosphorylate NUA1 at Thr211 in response to IGF-1 stimulation. Interestingly, in the study the deletion of LKB1 did not affect IGF-1-mediated phosphorylation of NUA1 at Thr211, implicating that LKB1 does not mediate NUA1 activation under these specific conditions (Suzuki et al., 2006). Although additional kinases other than LKB1 have been suggested to modulate NUA1 activity, more work will be required to confirm those findings and clarify their functional relevance.

1.3.3 Lesson on NUA1's physiological role from *in vivo* studies

The physiological role of NUA1 has been highlighted by some *in vivo* studies carried out in mouse models. In particular, during the search of genes involved in brain development, the mouse homologous of NUA1, Omphalocle kinase (Omphk1), was found to be enriched in the brain and a mutant form of the gene was shown to induce defects in the abdominal wall closure during embryogenesis, even though it did not cause brain morphological abnormalities (Hirano et al., 2006). A following study reported that a mouse double knockout mutant for NUA1 and NUA2 displayed facial clefting, spina bifida and

exencephaly, which is a malformation of the cranium that results in the external protrusion of brain tissue (Ohmura et al., 2012). Additionally, together with LKB1, NUAK1 was found to be involved in neuronal axon branching and growth by regulating the mitochondrial immobilization at the presynaptic site (Courchet et al., 2013).

To obtain more insights on the function of NUAK1 in adult tissues, Esumi's group developed the first conditional knockout mouse model for Nuak1. Furthermore, in light of the tissue expression analysis of NUAK1, they specifically focused on its role in the skeletal muscle by controlling the deletion of the gene using a muscle Creatin kinase (Mck)-Cre (MNUAK1KO) (Inazuka et al., 2012). Whereas constitutive deletion of Nuak1 is embryonically lethal, the conditional knockout mice did not display any abnormality. In addition, the analysis of the muscle fibres composition and size revealed no significant difference between MNUAK1KO and wild type animals. However, when the authors investigated the effect of Nuak1 deletion on glucose metabolism it was revealed that MNUAK1KO mice were characterized by lower body weight, fasting blood glucose and free fatty acids levels in comparison to wild type animals when fed on a high-fat diet. A further analysis of the mechanism of the observed regulation of glucose metabolism revealed that, in response to acute administration of glucose, Nuak1 deletion resulted in enhanced membrane translocation of the glucose transporter GLUT4, through the increased phosphorylation of TBC1D4 at Thr649, which is known to regulate insulin-dependent trafficking of GLUT4. Phosphoproteomic analysis of isolated soleus muscle from MNUAK1KO and wild type mice exposed a decrease of the inhibitory phosphorylation of multiple proteins involved in glucose metabolism, such as the Insulin receptor substrate 1 (IRS1), Glycogen synthase and Protein kinase θ , indicative of a higher insulin sensitivity and glycogen synthesis. Overall, data obtained from the muscle-specific knockout of Nuak1 revealed a role of this AMPK-related kinase in the negative regulation of insulin signalling in soleus muscle (Inazuka et al., 2012).

1.3.4 Additional biological roles of NUAK1

Investigations carried out in cancer cell lines contributed to the improvement of our knowledge of NUAK1 function and provided key indications on its potential use as target for cancer therapy. As a matter of fact, NUAK1 has been involved in a plethora of biological processes that can be exploited by cancer cells to support their survival and help them to disseminate to distant sites.

1.3.4.1 Migration and Invasion

Multiple independent studies have established over time a crucial role of NUAK1 in cell migration and invasion to such an extent that initial reports were using those processes as a readout for NUAK1 activity.

An initial study that highlighted NUAK1's involvement in cell migration was carried out in a human pancreatic cancer cell line (PANC-1). Overexpression of NUAK1 in PANC-1 cells significantly increased their invasive capacity, which was further enhanced by IGF-1 stimulation and attenuated by AKT inhibition, suggesting an IGF/AKT regulatory mode. The mechanism through which NUAK1 contributed to cell invasion was suggested to involve increased activity of metalloproteinase 2 and 9 (MMP-2 and MMP-9), as a higher activity of those two enzymes was detected in NUAK1 overexpressing PANC-1 cells. In addition, the increased invasion upon NUAK1 overexpression was also confirmed *in vivo*. Subcutaneous tumours derived from transplantation of PANC-1 cells stably overexpressing NUAK1 displayed an extensive degree of invasion of the muscle layer and metastasis at multiple organs were also detected at earlier stages in comparison to PANC-1 cells expressing endogenous levels of NUAK1 (Suzuki et al., 2004). Additional investigations have further establishing the pivotal role of NUAK1 in cell migration and invasion in multiple cancer settings (Chang et al., 2012; Lu et al., 2013; Shi et al., 2014).

1.3.4.2 Cell adhesion

A proteomic study carried out on immunoprecipitated NUAK1 identified interactors belonging to the myosin phosphatase complex, which is responsible for dephosphorylation of proteins such as Myosin light chain 2 (MLC2) and Polo-like kinase-1 (PLK1) (Zagorska et al., 2010). The myosin phosphatase complex is formed by a catalytic subunit represented by the Protein Phosphatase 1 (PP1), and two regulatory subunits termed Myosin phosphatase target subunit (MYPT), which is expressed in three isoforms, and M20, of unknown function. NUAK1 was reported to interact with the complex formed by PP1 β and MYPT1 and phosphorylate the latter at three different sites, Ser445, Ser472, Ser910 to promote binding of 14-3-3 protein to MYPT1, resulting in the inhibition of the myosin phosphatase complex (Zagorska et al., 2010). The described function of NUAK1 was shown to depend on the upstream kinase LKB1, since phosphorylation of MYPT1 was reduced in cells with LKB1 deletion. Moreover, inhibition of the myosin phosphatase complex following activation of the LKB1/NUAK1 axis was shown to result in higher phosphorylation levels of MLC2, which promotes cell detachment (Fig. 1.6). In addition, the study also identified the presence of a Gly-Ile-Leu-Lys (GILK) motif in NUAK1 sequence that mediates the interaction with the MYPT1-PP1 β complex. Interestingly, NUAK2 was also shown to contain the GILK motif and to interact with the MYPT1-PP1 β complex, sharing with NUAK1 the same phosphorylation sites on MYPT1, confirming previous reports that indicated MYPT1 phosphorylation by NUAK2 (Yamamoto et al., 2008; Zagorska et al., 2010). NUAK1 and NUAK2 are the only AMPK related kinases containing a GILK motif and evidence provided by Zagorska's study also indicated that they are the only kinases of the family able to interact with MYPT1-PP1 β .

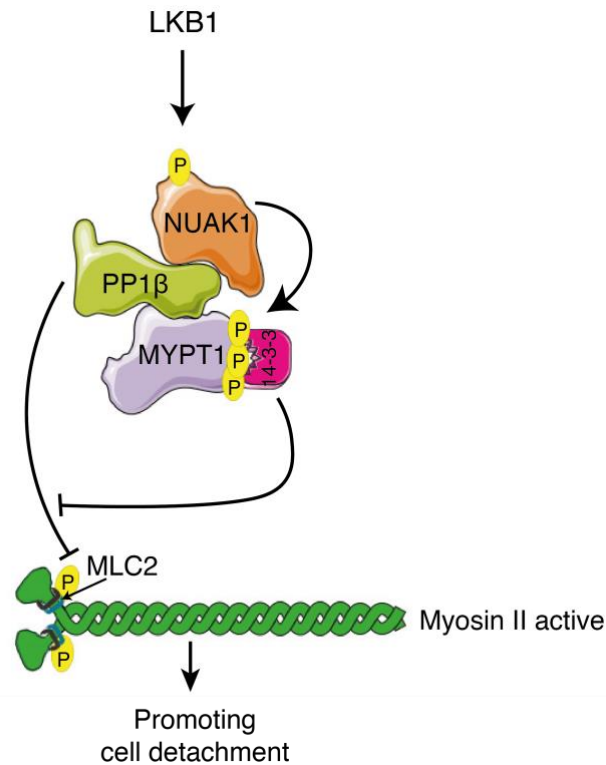


Figure 1. 6 – Mechanism of regulation of cell adhesion by NUAK1.

Following phosphorylation and activation by LKB1, NUAK1 forms a complex with the Protein Phosphatase 1 β (PP1 β) and with its regulatory subunit Myosin phosphatase target subunit (MYPT1). NUAK1 then phosphorylates MYPT1 at Ser445, Ser472, Ser910 to promote binding of 14-3-3 protein to MYPT1 and inhibition of the phosphatase activity of PP1 β . The overall outcome represented in the diagram is the increased phosphorylation of the myosin light chain 2 (MLC2) which promotes Myosin II activation and cell detachment. Image adapted from (Zagorska et al., 2010) using items from Servier Medical Art.

1.3.4.3 Cell proliferation and senescence

Experimental evidence has suggested that NUAK1 takes part in the regulation of cell proliferation, although with contradictory findings on its role as promoter or inhibitor of cell cycle progression. Specifically, NUAK1 was found to interact and phosphorylate p53 at Ser15 and Ser392, causing induction of p21 and cell cycle arrest at the G1/S checkpoint (Hou et al., 2011). In contrast, a function as positive regulator of cell cycle was suggested by Alessi's group. In their study inhibition of NUAK1 activity using the selective inhibitor HTH-01-015 reduced the percentage of cells in the S-phase of the cell cycle and restricted the progression to the mitotic phase. A more detailed analysis of the mechanism

revealed an interplay between NUA1 and Polo like kinase 1 (PLK1). The inhibition of the phosphatase activity of the PP1 β ^{MYPT1} complex upon NUA1 induction was suggested to increase PLK1 phosphorylation and activity to promote G2/M transition. In addition, active PLK1 was shown to phosphorylate NUA1 at Ser476 and Ser480, inducing the interaction of SCF β ^{TrCP} E3 ubiquitin ligase complex with NUA1 for its ubiquitylation and degradation. Thus, reciprocal modulation of PLK1 and NUA1 levels during the different phases of cell cycle was suggested to orchestrate cell cycle progression (Banerjee et al., 2014b). Further studies have supported a positive role of NUA1 in cell cycle regulation as its downregulation resulted in cell cycle arrest (Perumal et al., 2016) and its overexpression was described to enhance proliferation (Huang et al., 2014).

NUA1 has also been involved regulation of ploidy and senescence (Humbert et al., 2010). During a screening to identify genes involved in senescence, downregulation of NUA1 was found to increase the replicative potential of senescent cells. Additional analysis revealed that NUA1-induced senescence was related to its role in the regulation of cell ploidy. In particular, NUA1 was reported to induce aneuploidy via the negative regulation of the protein levels of the Large Tumour Suppressor kinase 1 (LATS1) (Humbert et al., 2010), known to promote cytokinesis (Yang et al., 2004).

1.3.4.4 Metabolic homeostasis

In addition to a biological role in adhesion, invasion and cell proliferation, NUA1 was reported to regulate metabolic homeostasis and promote the survival of MYC-overexpressing cells. In particular, NUA1 was identified in a synthetic lethality screening carried out to search for genes for which the loss of function was lethal only in the presence of MYC overexpression (Liu et al., 2012). In addition to the intriguing discovery that NUA1 depletion led to cell death of MYC-overexpressing cells, the study confirmed some of the previous findings, such as a cell cycle arrest in the S-phase upon NUA1 depletion, but most importantly it revealed new functions in the regulation of metabolic homeostasis. Indeed, NUA1 was found to contribute to the maintenance of ATP levels by two major mechanisms: inhibition of the mTOR pathway and promotion

of the expression of components of the mitochondrial respiratory chain. Activation of MYC resulted in an increased induction of AMPK and in a decrease of mTORC1 activity. However, NUA1 depletion ablated the increase in AMPK activity, resulting in an overall enhancement of protein synthesis, probably due to the inability of AMPK to restrain mTORC1. Treatment with Rapamycin, an mTORC1 inhibitor, could protect cells from death by relieving the metabolic stress induced by NUA1 depletion, supporting NUA1 contribution to cell survival through restraining mTORC1 activity. Furthermore, NUA1 was shown to sustain metabolic homeostasis through the maintenance of the mitochondrial respiratory chain, as NUA1 depletion caused a significant decrease in the expression of multiple subunits of the electron transport chain. Finally, analysis of a tumour model obtained by the transplantation of hepatoma cells expressing MYC revealed that downregulation of NUA1 reduced the incidence of tumour formation but also increased survival of mice in comparison to the NUA1 wild type counterpart (Liu et al., 2012). Therefore, overall the study suggested important implications of NUA1 in metabolism and proposed targeting of NUA1 as therapeutic approach in cancer.

1.3.5 Clinical relevance for NUA1

Some of the investigations on NUA1 function have been carried out in tumour cell lines, elucidating not only its roles but also a relevance for tumour biology and cancer therapy. Although NUA1 gene alterations do not frequently occur in the four most common human cancers, with the exception of neuroendocrine prostate cancer (Fig. 1.7), studies done in human samples have strengthened the idea of a tumour promoter role.

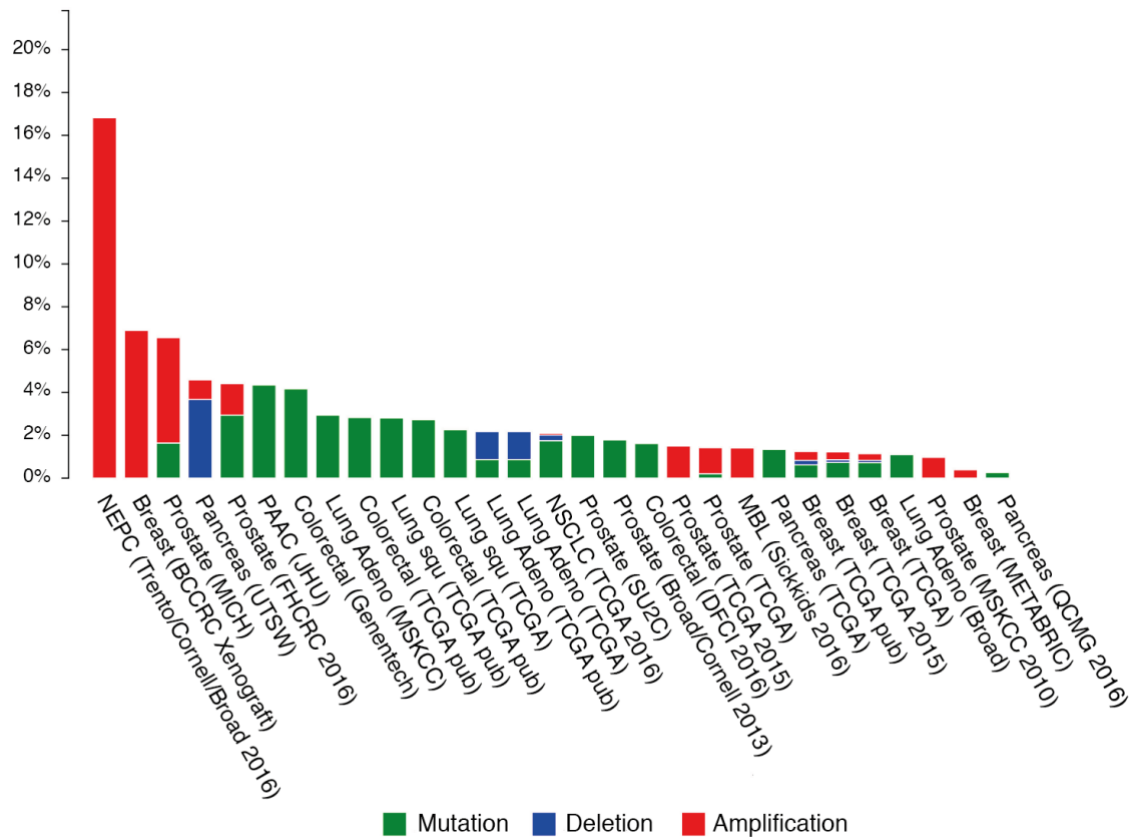


Figure 1. 7 – NUAK1 gene alteration frequency in human cancer.

The histogram represents the alteration frequency in NUAK1 gene across the four most lethal human cancers: pancreatic, breast, lung and colorectal cancer. NEPC, neuroendocrine prostate cancer; PAAC, Acinar Cell carcinoma of the pancreas; MBL, Mutational profiles of metastatic breast cancer. Graphic obtained from cBioportal and truncated from the right to omit non-relevant data.

Multiple investigations have underlined a negative correlation between NUAK1 expression levels and survival of patients affected by a number of cancer types. For example, analysis of samples derived from patients affected by colorectal cancer revealed higher levels of NUAK1 expression in the tumours compared to the normal adjacent tissue. Additionally, in agreement with a described role in invasion, NUAK1 was highly expressed in liver metastasis (Kusakai et al., 2004). Similarly, investigation of NUAK1 expression in tumour samples from patients affected by hepatocellular carcinoma and glioma indicated higher levels in the tumour tissue compared to normal adjacent tissue. Moreover, high expression levels of NUAK1 correlated with a poor prognosis for both glioma and hepatocellular carcinoma (Cui et al., 2013; Lu et al., 2013). The analysis of NUAK1 expression in human gastric and non-small cell lung cancer samples

similarly revealed high levels in the tumour samples, a negative correlation with prognosis and a positive correlation with the depth of invasion and lymph node metastasis (Chen et al., 2013; Ye et al., 2014).

Most studies have highlighted a role of NUA1 in invasion and metastasis. However, to date no genetically engineered mouse (GEM) models have been employed to characterize NUA1 role in the early and late phases of tumour progression. In fact, given the variety of biological functions described, its role in cancer might not be limited to the metastatic process. In addition, the master upstream kinase LKB1 has been established as an important tumour suppressor in lung tumorigenesis, therefore we cannot exclude that NUA1 might mediate some of tumour suppressive function in specific cancer types, such as lung cancer. Therefore, the use of GEM models could improve our understanding of NUA1 role in cancer and suggest new therapeutic approaches.

1.3.6 Exploiting the synthetic lethal interaction between NUA1 and MYC in cancer therapy

The important finding of a synthetic lethal interaction between NUA1 and MYC opened the door to a new therapeutic strategy for cancer.

The proto-oncogene c-MYC, together with the family members N-MYC and L-MYC, is a basic helix-loop-helix-leucine zipper (bHLH-LZ) transcription factor that controls the expression of a large number of genes. Upon dimerization with the protein partner MAX, MYC binds to the E-box element CACGTG to induce gene expression, whereas upon interaction with the transcriptional activator Miz-1, MYC causes repression of Miz-1 target genes. Extensive studies carried out in the last decades have revealed that 15% of all genes belong to the network of targets regulated by MYC. These genes are involved in several biological processes, such as cell cycle regulation, anabolic metabolism (biosynthesis of amino acids, nucleotides and lipids), ribosome biogenesis, mitochondrial biogenesis and metabolic pathways (glycolysis, glutaminolysis) (Dang, 2012). Therefore, given its crucial role in cell metabolism and proliferation, it is not surprising that MYC is frequently dysregulated in human cancer. For example, MYC translocation to one of the immunoglobulin loci gives rise to Burkitt lymphoma (Dalla-Favera et al., 1982). In other cases, dysregulation of MYC

occurs via overexpression, while somatic mutations are not frequent events in cancer. In particular, MYC gene amplification has been frequently detected in many cancer types such as breast cancer, in which a correlation with disease progression has been suggested (Deming et al., 2000). Furthermore, upregulation of MYC can also be due to oncogenic activation of upstream signalling pathways that can promote MYC stability, i.e. RAS activation. Therefore, given its incontrovertible role in cancer, MYC targeting has been the focus of many therapeutic strategies. However, its inhibition has proved difficult to achieve because the lack of enzymatic activity limits the use pharmacological inhibitors and its localization in the nucleus prevents access to antibody-based therapies. Thus, the identification of synthetic lethal interactors, such as NUA1, might represent a more successful strategy to challenge cancer addiction to MYC.

1.4 Lung cancer

1.4.1 Heterogeneity of lung cancer

Lung cancer is the second most common cancer in both males and females, secondary for incidence to prostate and breast cancer, respectively. Although the incidence and mortality has experienced a reduction over the last 30 years, it still represents the leading cause of cancer-related death worldwide.

Lung cancer can be classified in two major groups: Non-small cell lung cancer (NSCLC) and Small cell lung cancer (SCLC). The former accounts for the majority of cases (80%), and can be further classified in three groups based on histological characteristics: squamous cell carcinoma (SCC), adenocarcinoma (ADC) and large-cell carcinoma. Half of all cases of NSCLC are categorized as adenocarcinomas, which are malignant tumours with glandular histology and derive from the distal airways, particularly from bronchiolar and alveolar epithelial cells. Squamous cell carcinomas, which occurs in 40% of cases, typically derive from bronchial epithelial cells and are characterized by squamous differentiation, whereas large-cell carcinomas have a lower incidence and are diagnosed based on the lack of squamous or glandular differentiation.

The specific cell or cells of origin is a contributor to the histological diversity of NSCLC. Although over the recent years the cell of origin for ADC has been

debated, the use of genetically engineered mouse models has facilitated the investigation of the topic. To date, three types of cells have been considered for their potential to give rise to ADC: Clara cells (or Club cells), alveolar epithelial type 2 (AT2) cells and bronchioalveolar stem cells (BASCs). Conversely, the limited availability of GEM models for the study of SCC has restricted the investigation of the histogenesis of this specific subtype, however basal cells are thought to be the at the origin of SCC (Chen et al., 2014) (Fig. 1.8).

The classification of the multiple subtypes of NSCLC has been recently revisited by the World Health Organization, with the inclusion of several histological subtypes (Tab 1.1), and the recommendation for the use of immunohistochemistry along with morphological criteria for classification (Travis et al., 2015). In particular, in agreement with the protein expressed by the cell of origin, ADC displays positivity for markers like surfactant protein C (SPC), Keratin 7 (KRT7) and thyroid transcription factor 1 (TTF1), whereas SCC is characterized by expression of basal cells markers such as p63 and Keratin 5 (KRT5) (Fig. 1.8).

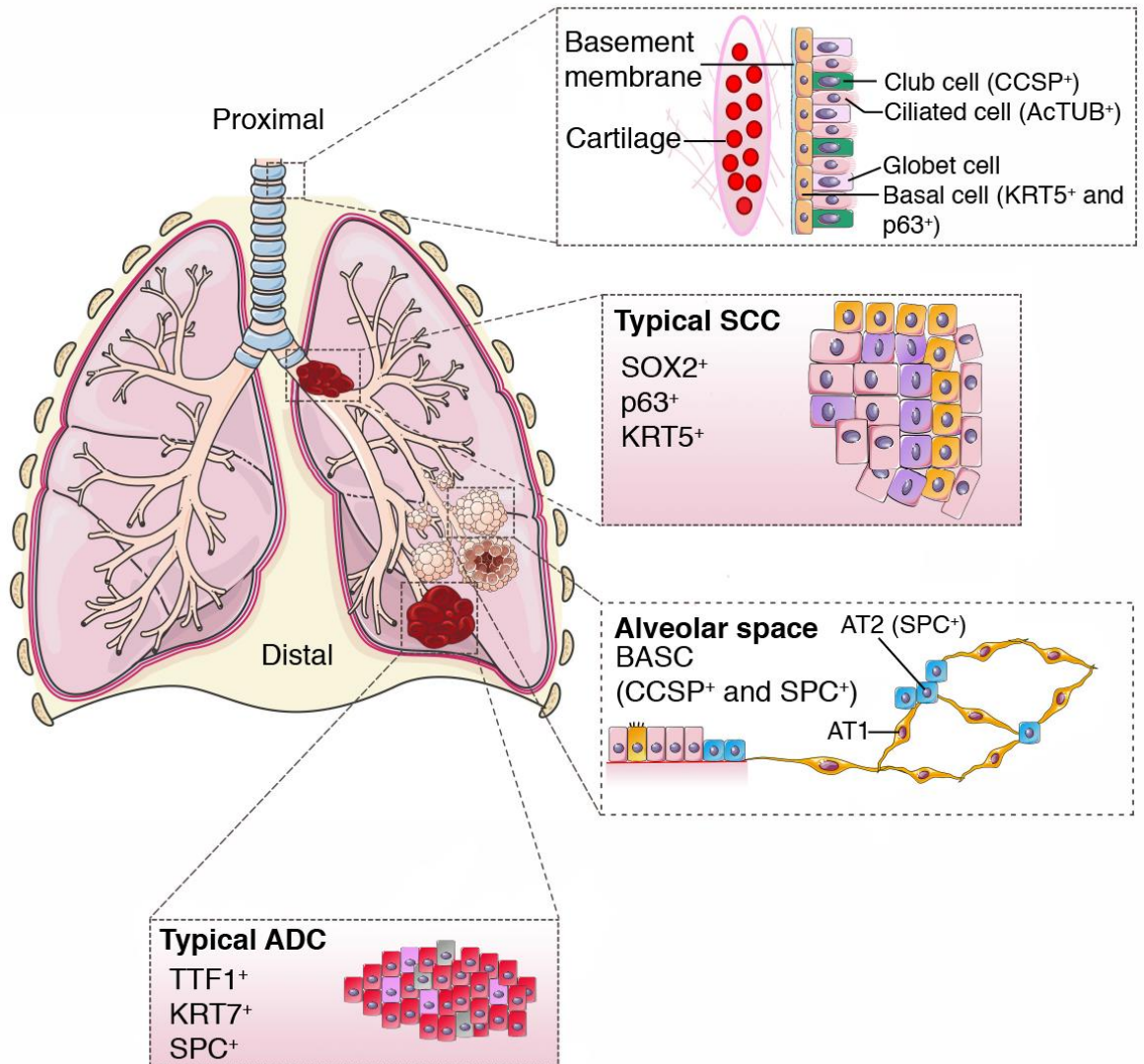


Figure 1. 8 – Histogenesis and molecular markers of Adenocarcinoma and Squamous cell carcinoma.

The distinct cell populations that give rise to Squamous cell carcinoma and Adenocarcinoma are depicted in the diagram. Squamous cell carcinoma typically origin from basal cells in the proximal lung whereas Adenocarcinoma is thought to arise from distal airways. TTF1, Thyroid transcription factor 1; KRT7, Keratin 7; SPC, surfactant protein C; KRT5, Keratin 5. Image adapted from (Chen et al., 2014) and generated using items from Servier Medical Art.

2015 WHO CLASSIFICATION OF LUNG TUMOURS
Histological types and subtypes

Adenocarcinoma	Squamous cell carcinoma
Lepidic adenocarcinoma	Keratinizing squamous cell carcinoma
Acinar adenocarcinoma	Nonkeratinizing squamous cell carcinoma
Papillary adenocarcinoma	Basaloid squamous cell carcinoma
Micropapillary adenocarcinoma	Preinvasive lesion
Solid adenocarcinoma	Squamous cell carcinoma in situ
Invasive mucinous adenocarcinoma	Large cell carcinoma
Mixed invasive mucinous and nonmucinous adenocarcinoma	
Colloid adenocarcinoma	
Fetal adenocarcinoma	
Enteric adenocarcinoma	
Minimally invasive adenocarcinoma	
Nonmucinous	
Mucinous	
Preinvasive lesions	
Atypical adenomatous hyperplasia	
Adenocarcinoma in situ	
Nonmucinous	
Mucinous	

Table 1. 1 - Histological types and subtypes of NSCLC.

A summary of the histological types and subtypes of Non-small cell lung cancer (NSCLC) as for classification by the World Health Organization (Travis et al., 2015).

1.4.2 Molecular profiling of NSCLC

The accumulation of genetic alterations leads ultimately to the dysregulation of the normal physiology of the cells and their transformation into cancerous cells. The development of new technologies such as Next Generation Sequencing has allowed the dissection of the genetic abnormalities in human cancer, providing us with a greater knowledge of the disease but simultaneously revealing its impressive complexity. The genetic investigation of SCC and ADC has added another level of separation between the two subtypes. Somatic mutations in PIK3CA, PTEN, are frequently detected in SCC, whereas mutations in EGFR, KRAS and ROS1 are more common in ADC. In addition, recent molecular profiling carried out on hundreds of tumour samples derived from patients with lung adenocarcinoma has uncovered several genetic aberrations and chromosomal rearrangements, placing lung ADC as one of the cancers with the highest mutation rate (The Cancer Genome Atlas Research, 2014). Interestingly, the mutation rates of some genes differ according to ethnicity and they also strongly correlate with tobacco smoke. For example, mutation in EGFR and ERBB2 are more frequent in never-smokers and Asian patients (Shigematsu et al., 2005), and tobacco smokers showed a higher number of mutations in comparison to never-smokers (Govindan et al., 2012).

The study of genetically engineered mouse models for NSCLC has enormously contributed to our current knowledge of the molecular mechanisms that drive the disease. However, pre-clinical studies of lung adenocarcinoma have been primarily conducted at the expense of squamous cell carcinoma, due to the limited availability of mouse models for the latter. Although numerous genes are being investigated for their potential tumorigenic role in lung adenocarcinoma, activating mutations of EGFR and KRAS have been established as important drivers of the disease and targeting of their aberrant activity has been a major clinical goal in the recent years.

1.4.2.1 EGFR and the ERBB signalling network

The dysregulation of the epidermal growth factor receptor (EGFR) in lung cancer was described already three decades ago (Veale et al., 1987), when immunostaining of tumour sections indicated higher levels of EGFR relative to normal lung tissue. Since then remarkable progresses have been made in the understanding of its role in lung cancer and overexpression of EGFR, detected in 62% of cases, is now considered a common event in NSCLC, with activating mutations present in approximately 15% of lung adenocarcinoma.

EGFR (also known as ERBB1 or HER1) belongs to the ERBB family of receptor tyrosine kinases together with ERBB2 (HER2), ERBB3 (HER3) and ERBB4 (HER4). These receptors are ubiquitously expressed as transmembrane proteins, characterized by an extracellular ligand-binding domain and an intracellular tyrosine kinase domain (Fig. 1.9). Although ERBB3 lacks a kinase domain and no ligand has been shown to bind to ERBB2, these two members can still function upon dimerization with EGFR and ERBB4. In addition, ERBB2-containing heterodimers have been shown to occur preferentially due to its peculiar conformation that resemble an active state that facilitates interaction with other ERBB receptors (Garrett et al., 2003).

ERBB receptors are activated by several ligands that belong to the family of EGF-related peptide growth factors (Fig. 1.9). These ligands are usually produced as transmembrane precursors that can be cleaved and released in the extracellular space by the enzymatic activity of the sheddases ADAMs (ADAM9, ADAM10, ADAM15 and ADAM17). Upon ligand binding, ERBB monomers form homo- and heterodimers, which triggers trans-phosphorylation of tyrosine residues of the intracellular kinase domain and stimulate the recruitment of effector proteins.

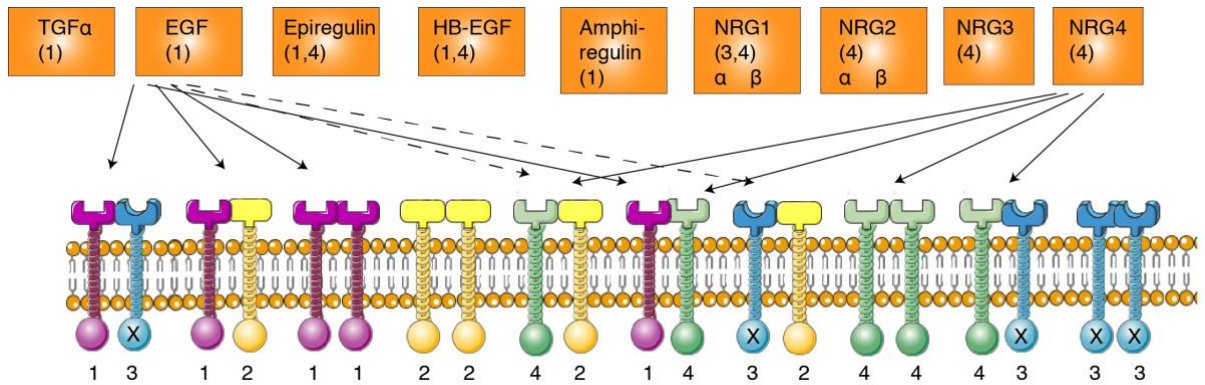


Figure 1. 9 – The ERBB signalling network.

Representation of the homo- and heterodimers formed by the ERBB family of receptor tyrosine kinases (EGFR (1), ERBB2 (2), ERBB3 (3), ERBB4 (4)) and their ligands. Numbers below each ligand indicate the high-affinity for the respective ERBB receptors, but arrows are only shown for EGF and NRG4 for simplicity of the graph. The cross on the intracellular domain of ERBB3 indicates the lack of kinase activity, whereas the filled extracellular domain of ERBB2 indicates the absence of a ligand interacting with the receptor. Image adapted from (Yarden and Sliwkowski, 2001) and generated using items from Servier Medical Art.

Multiple downstream signalling pathways are modulated by activation of the ERBB receptors and experimental evidence suggests that the type of ligand and heterodimer formed controls the selection of the effector proteins (Dankort et al., 2001; Sordella et al., 2004). Overall, the ERBB network modulates a number of biological processes: from cell proliferation and survival to cell migration and differentiation, with PI3K/AKT, RAS, PKC, JAK/STAT representing some of the several downstream effectors of the ERBB receptors.

1.4.2.2 RAS signalling

The story of the oncogene RAS goes back to 1960s, when Jennifer Harvey and Werner Kirsten discovered that a virus preparation from leukemic rat could induce sarcomas when injected in new-born rats (Ras= rat sarcoma). The homologous of the viral Ras sequence was identified in rat, mouse and humans in the following decades, and despite the extensive time and efforts spent in studying its function and, most importantly, its targeting, we are still in search of its Achilles' heel.

The RAS family is frequently mutated in human cancer and consists of three genes: H-RAS, K-RAS and N-RAS. KRAS is the isoform more frequently mutated in lung cancer (30% of lung adenocarcinoma), with activating mutation first described in 1984 by Mariano Barbacid (Santos et al., 1984).

RAS is a small GTPase that cycle between an off-state when bound to GDP to an on-state when bound to GTP. However, because of its poor intrinsic GTPase activity, it relies on two classes of proteins to switch between the on and off states: GTPase activating proteins (RASGAPs) and guanine nucleotide exchange factors (RASGEFs). In particular, RASGAPs stimulate the hydrolysis of GTP to GDP, promoting inactivation of RAS, whereas the RASGEFs induce the exchange of GDP for GTP, leading to RAS activation. Binding of GTP to RAS induces a conformational change in two regions, named Switch I and Switch II, resulting in an increased affinity and interaction of RAS with effector proteins (Vetter and Wittinghofer, 2001). Activating mutations impair RAS sensitivity to the activity of RASGAPs, which leads to a persistently active GTP-bound RAS (Malumbres and Barbacid, 2003).

Mutations in KRAS frequently occur at codon 12, but the frequency of the type of substitution changes according to the type of cancer. In lung cancer, the mutation G12C is the most recurrent, followed by G12V and G12D (Cox et al., 2014). Interestingly, the different substitutions have been shown to have a different correlation with cigarette smoke, with G12C and G12V being associated more with tobacco exposure than G12D (Riely et al., 2008), but also to engage different downstream effectors of RAS (Ihle et al., 2012).

Regarding the downstream effectors, over 11 families have been identified as mediators of RAS function, but the Raf/MEK/ERK cascade and AKT pathway are among the major downstream effectors (Fig. 1.10).

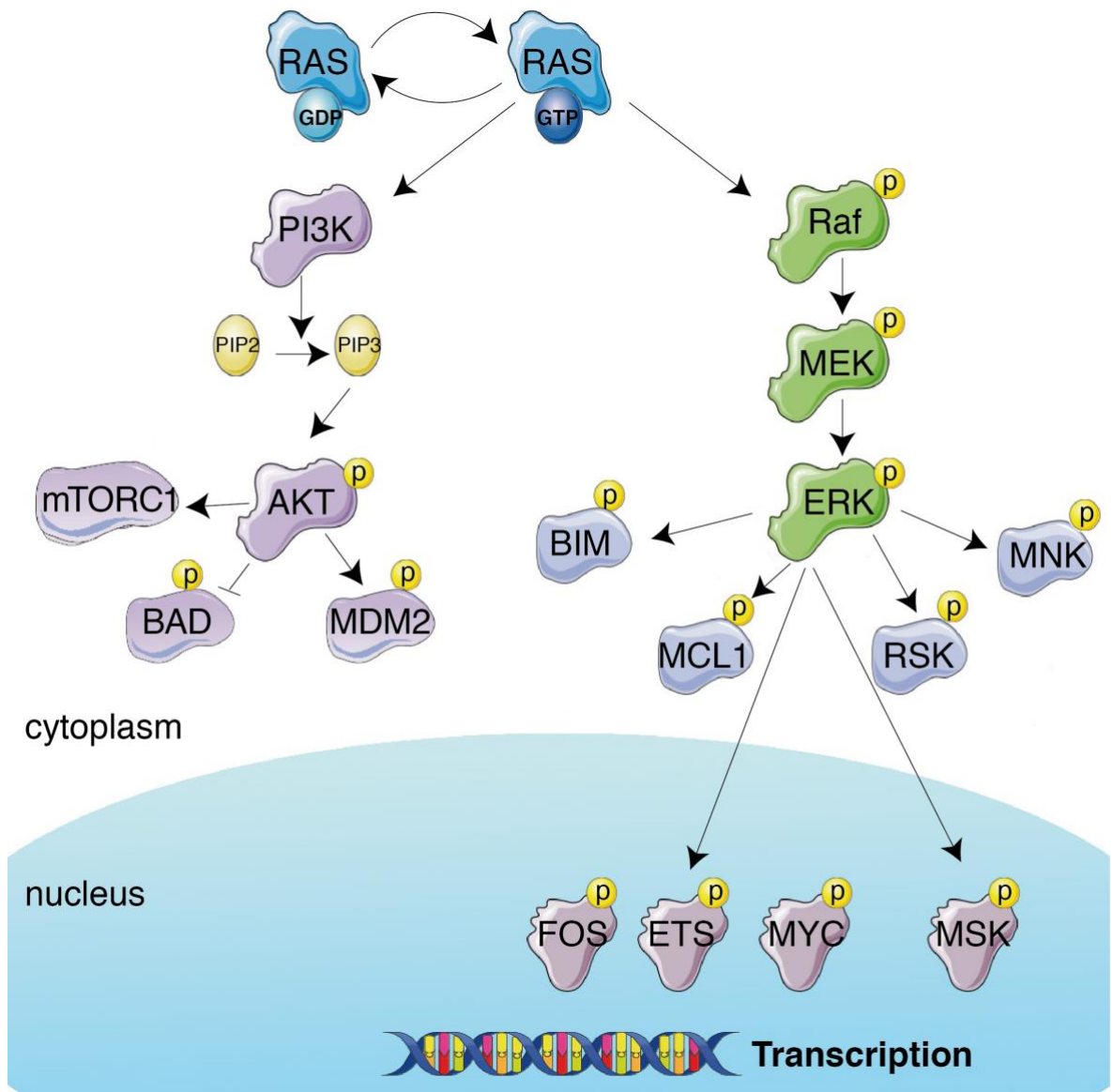


Figure 1. 10 - Downstream targets of RAS.

Active RAS in the GTP-bound state can stimulate multiple downstream pathways, among which the PI3K/AKT and the Raf/MEK/ERK cascade are the most important effectors. The PI3K/AKT axis support cell survival and proliferation through induction of mTORC1, the downregulation of the pro-apoptotic protein BAD and activation of MDM2, negative regulator of p53. On the other hand, RAS mediates activation of Raf, which culminates with the phosphorylation and activation of ERK, responsible for the regulation of several substrates located in the cytoplasm and in the nucleus, such as transcription factors, to support cell survival and proliferation. Only some of the targets are represented in the image. PIP2, phosphatidylinositol-4,5-bisphosphate; PIP3, phosphatidylinositol-3,4,5-trisphosphate. Image generated using items from Servier Medical Art.

The Raf/MEK/ERK signalling is one of the Mitogen-activated protein kinase (MAPK) cascade and transduces signals to regulate cell growth, differentiation and migration. The first step that triggers the pathway is the interaction and

phosphorylation of the Raf (MAPKKK) kinase by RAS. There are three isoforms of Raf (Raf-1, A-Raf, B-Raf), which differ not only in tissue distribution but also in their capability to activate the downstream effector MEK (Mitogen-activated protein kinase kinase or MAPKK). B-Raf is the isoform that most effectively activates the two isoforms of MEK (MEK1/2), followed by Raf-1, as opposed to the weak activation by A-Raf (Pritchard et al., 1995). This cascade of phosphorylation and activation events culminates with MEK catalysing a dual phosphorylation of a regulatory threonine and tyrosine on ERK. The serine/threonine kinase ERK (extracellular signal-regulated kinases or MAPK) is the only physiological substrate known of MEK and is encoded in two isoforms, ERK1 and ERK2, although several splicing forms are also produced. Once activated, ERK can regulate multiple targets located in the cytoplasm but also modulate nuclear transcription factors (Fig. 1.10).

An additional and crucial downstream effector of RAS is the PI3K/AKT axis (Fig. 1.10). This pathway is an important regulator of cell proliferation and survival and thus often dysregulated in cancer. Mechanisms of dysregulation include aberrant upstream signalling, i.e. EGFR or RAS mutation, as well as somatic mutations of its components (Vivanco and Sawyers, 2002). The first element of the signalling pathway is the Phosphoinositide 3-kinase (PI3K), a family of lipid kinases that consists of three classes: class I (further divided into subclasses IA and IB), class II and class III. Class IA of the PI3K family is the best characterized and plays a prominent role in cancer (Thorpe et al., 2015). It is formed by a p85 regulatory subunit and a p110 catalytic subunit, both of them being expressed as multiple isoforms. Active PI3K can phosphorylate phosphatidylinositol-4,5-bisphosphate (PIP₂) to form phosphatidylinositol-3,4,5-trisphosphate (PIP₃), which functions as second messenger and activator of AKT and additional numerous effector proteins. There are three genes encoding as many forms of AKT: AKT1, AKT2 and AKT3. Upon activation of PI3K, AKT is recruited to the plasma membrane where the binding of PIP₃ to the PH domain of AKT causes a change to an active conformation that facilitates the access of upstream kinases for phosphorylation. Phosphorylation of AKT1 at Thr308 and Ser473 by PDK1 and mTORC2, respectively, is required for the full activation of the kinase. Phosphorylation also occurs on the corresponding sites in AKT2 (Thr309 and Ser474) and AKT3 (Thr305 and Ser472). As phosphorylation and PIP₃ are

important factors in triggering AKT activity, its inactivation is mediated by phosphatases and by the tumour suppressor PTEN, which is responsible for dephosphorylation of PIP₃ (Manning and Toker, 2017). Although over 100 substrates for AKT have been suggested, not all of them have been validated. Nonetheless, multiple effector proteins belonging to a variety of signalling pathways have been established as key mediators of AKT function. For example, in its role to promote cell survival, AKT can phosphorylate and inhibit the pro-apoptotic protein BAD and regulate the tumour suppressor p53 (Datta et al., 1997; Ogawara et al., 2002); furthermore, AKT can stimulate cell growth by promoting mTORC1 activity through inhibition of the repressors TSC2 and PRAS40 (Inoki et al., 2002; Sancak et al., 2007).

1.4.3 Targeted therapies for NSCLC

Despite the tremendous efforts made in the last decades to improve current treatments and introduce new therapies, patients affected by advanced lung cancer still have a 5-year survival rate of only 15%. However, the identification of genetic drivers of the disease has allowed the clinical use of targeted therapies that, in some instances, offer a better therapeutic outcome in comparisons to standard chemotherapy. For example, patients with activating mutations in EGFR can benefit from EGFR tyrosine kinase (TK) inhibitors. Responsiveness of patients with EGFR mutation to treatment with Gefitinib, an EGFR inhibitor, was firstly described in 2004 (Santos et al., 1984), almost twenty years after the discovery of EGFR dysregulation in lung cancer. Subsequent clinical studies have described the benefit of EGFR TK inhibitors, accountable for a longer median progression-free survival and also a higher response rate over standard chemotherapy in lung cancer patients selected based on EGFR mutations (Maemondo et al., 2010). However, the emergence of resistance to long-term treatments represents a major clinical problem, to which the response has involved the use of second and third generation TK inhibitors, mutant-specific inhibitors or targeting additional upregulated kinases. A wide range of resistance mechanisms to EGFR inhibition has been identified over time, such as activation of collateral pathways (MET amplification or activation of ERBB2

signalling), but also secondary mutations in EGFR, such as the T790M substitution, which affects the binding of the small molecule inhibitors (Kobayashi et al., 2005; Turke et al., 2010; Yonesaka et al., 2011). Overall, introduction of TK inhibitors in combination with patients' stratification based on mutation status has revolutionized the therapeutic strategy for non-small cell lung cancer and many other cancer types. Nevertheless, limited targeted therapies are available for patients bearing mutations in the alternative oncogenic driver KRAS, as its inhibition has been extremely challenging to achieve. In particular, the development of GTP-competitive inhibitors that could impair RAS activity has proved to be unsuccessful due to the picomolar affinity of GTP for RAS (Spiegel et al., 2014). In addition, a broad inhibition of RAS, without distinction between the mutant and wild type form, might exhibit significant toxicity given its fundamental role in the biology of normal tissues. Therefore, in the recent years researchers have been trying to develop inhibitors that specifically target the mutant forms of RAS, with some promising results that need to be evaluated in clinical trials (Ostrem et al., 2013).

Alternatively, researchers have tried to impair RAS function by targeting those mechanisms that are required for its activity and its ability to engage with effector proteins. For example, localization of RAS to the plasma membrane is a key prerequisite for its function and requires the attachment of a farnesyl group to the CAXX motif that is present in all RAS isoforms. However, upon inhibition of the farnesyltransferase (FT) enzyme, which catalyses the farnesylation, RAS can be post-translationally modified by geranylgeranyltransferase (GGT). Simultaneous inhibition of both FT and GGT has proved to be highly toxic in preclinical models, limiting its clinical application (Lobell et al., 2001). Additionally, inhibition of the downstream effectors of RAS represents an alternative therapeutic strategy. A major effector of RAS is the MAPK pathway, which is hyper activated in 30% of cancers. Several pharmacological inhibitors of the components of the MAPK cascade have been developed and reached clinical evaluation over time. For example, MEK inhibitors have been approved for clinical use in B-RAF mutant metastatic melanoma and combination of Selumetinib (MEK inhibitor) with standard chemotherapy (docetaxel) resulted in an increase of the median progression-free survival in comparison to chemotherapy alone in a phase II trial in advanced KRAS-mutant NSCLC (Janne et al., 2013). However, a phase II trial suggested that inhibition of MEK using

Trametinib was not beneficial over chemotherapy with docetaxel in lung cancer patients selected for KRas mutation (Blumenschein et al., 2015). Further studies suggested the potential mechanism responsible for the lack of therapeutic efficacy of MEK inhibition alone. Specifically, Bernards group revealed that MEK inhibition resulted in upregulation of ERBB2 and ERBB3, which can sustain tumour cell growth through upregulation of the PI3K/AKT pathway. Therefore, a combinatorial therapy with ERBB receptors and MEK inhibitors was shown to be more effective and overcome resistance to MEK inhibition (Sun et al., 2014). Overall, preclinical and clinical data suggest that the success of a single-agent therapy is highly unlikely given the ability of tumour cells to rewire their signalling to support viability in the presence of inhibitory drugs.

1.5 PhD objectives

The great magnitude of studies in the cancer research field has contributed to make an impressive progress in the understanding and treatment of cancer. However, they have also highlighted the high complexity of cancer and how it cannot be defined as a single disease but as an extremely heterogeneous set of diseases. Although key oncogenes have been identified decades ago for their crucial role in the onset and maintenance of tumour cells viability, many of them still remain 'undruggable' and their targeting represents a major clinical goal.

The recent finding of the requirement of NUA1 in cells overexpressing the oncogene MYC gave rise to a new therapeutic potential of this AMPK related kinase. Although other studies have revealed a clinical relevance for NUA1 targeting in cancer, our knowledge about its regulation and biological function remains limited. In addition, experimental evidence has suggested a tumour promoter role for NUA1, albeit its location downstream of the tumour suppressor LKB1. Therefore, the objective of this work are:

- Improve our knowledge of the mechanisms of NUA1 regulation;
- Understand NUA1's role in metabolic homeostasis and specifically explore its involvement in lung tumorigenesis;

- Enhance our understanding of the molecular mechanisms of Non-small cell lung cancer to develop new therapeutic approaches.

Chapter 2 - Materials and Methods

2.1 Materials

2.1.1 Chemicals

Reagent	Supply
2-mercaptoethanol	Sigma-Aldrich
2-propanol	Fisher Scientific
30% Acrylamide	VWR
96-Well PCR plates	Biorad
Ammonium persulfate (APS)	Sigma-Aldrich
Anti-FLAG M2 affinity gel	Sigma-Aldrich
APC Annexin V	Biologend
BSA	Sigma-Aldrich
CaCl ₂ solution	Sigma-Aldrich
Captisol	Selleckchem
Chloroform	Fisher Scientific
DMSO	Sigma-Aldrich
DNase/RNase free water	Qiagen
Dulbecco's Modified Eagle Medium (DMEM)	Life Technologies
ECL Western blotting substrate	Pierce
Fetal Bovine Serum (FBS)	Thermo Fisher
L-Glutamine	Life Technologies
Lipofectamine 3000	Thermo Fisher
Lipofectamine RNAiMAX	Thermo Fisher
Milk powder	Marvel
Minimum Essential Media (MEM), powder	Thermo Fisher
N,N,N',N'-Tetramethylethylenediamine (TEMED)	Sigma-Aldrich
Nitrocellulose membrane (0.2 µm pore size)	GE Healthcare Life Sciences
Normal Goat Serum (NGS)	Vector labs
NP-40	Sigma-Aldrich

Opti-MEM	Thermo Fisher
PageRuler Prestained Protein Ladder	Thermo Fisher
Peanut oil	Sigma-Aldrich
PEG 400	Sigma-Aldrich
Penicillin/Streptomycin	Life Technologies
Phosphatase inhibitor cocktail 2	Sigma-Aldrich
Phosphatase inhibitor cocktail 3	Sigma-Aldrich
Polybrene	Sigma-Aldrich
Ponceau S	Sigma-Aldrich
Propidium Iodide	Sigma-Aldrich
Protease inhibitor cocktail	Sigma-Aldrich
Puromycin	
Spectra multicolour high range protein ladder	Thermo Fisher
SuperSignal West Dura	Pierce
Tris HCl	Sigma-Aldrich
Trizol	Thermo Fisher
Trypsin	Life Technologies
Tween-20	Sigma-Aldrich
Glycerol	Sigma-Aldrich

Table 2. 1 – Chemicals and Suppliers

2.1.2 Kits

Kit	Supplier
ApopTag Peroxidase <i>in situ</i> Apoptosis Detection kit	Millipore
Pierce BCA Protein Assay kit	Thermo Fisher
Quantitect-Rev. transcription kit	Qiagen
Vectastain ABC HRP Kit	Vector Laboratories
SYBR green Fast Mix	VWR

Table 2. 2 – Kits

2.1.3 Solutions

Solution	Recipe
Whole cell extract lysis buffer	150 mM NaCl, 50 mM Tris (pH 7.5), 1% NP-40 (v/v), 0.5% Sodium deoxycholic acid (w/v), 1% SDS (v/v), protease and phosphatase inhibitor cocktails
IP lysis buffer	50 mM Tris HCl (pH 7.5), 1% NP-40 (v/v), 0.27M sucrose, phosphatase and protease inhibitors
IP washing buffer	50 mM Tris HCl (pH 7.5), phosphatase inhibitors
Annexin V Binding Buffer	10 mM HEPES (pH 7.4), 140 mM NaCl, 2.5 mM CaCl ₂
5X Sample Buffer	0.3 M Tris (pH 6.8), 50% Glycerol (v/v), 10% SDS (w/v), 0.5% Bromophenol Blue (w/v), 4% 2-mercaptoethanol
Ponceau S	0.1% Ponceau S (w/v), 5% acetic acid
PBS	137 mM NaCl, 2.7 mM KCl, 10 mM Na ₂ HPO ₄ , KH ₂ PO ₄ ,
PBS/T	PBS, 0.1% Tween-20 (v/v)
TBS	10 mM Tris HCl pH7.4, 150 mM NaCl
TBS/T	TBS, 0.1% Tween-20 (v/v)
Sodium Citrate Buffer	10 mM Sodium citrate (pH 6.0)
Running Buffer	10% SDS, 250 mM Tris, 1.92 M Glycine
Transfer Buffer	0.1% SDS, 25 mM Tris, 0.192 M Glycine, 20% Methanol

Table 2. 3 – Recipes of solutions

2.1.4 Primary Antibodies

Protein	Species	Antibody	Supplier
Phospho-ACC (Ser79)	Rabbit	3661	Cell Signaling
ACC	Rabbit	3676	Cell Signaling
Phospho-RAPTOR (Ser792)	Rabbit	2083	Cell Signaling

RAPTOR	Rabbit	2280	Cell Signaling
Phospho-4E-BP1 (Thr37/46)	Rabbit	2855	Cell Signaling
4E-BP1	Rabbit	9644	Cell Signaling
Phospho-p70 S6 Kinase (Thr389)	Rabbit	9234	Cell Signaling
p70 S6 Kinase	Rabbit	2708	Cell Signaling
Phospho-AMPK (Thr172)	Rabbit	2535	Cell Signaling
AMPK α 1/ α 2	Rabbit	2532	Cell Signaling
AMPK β 1/ β 2	Rabbit	4150	Cell Signaling
AMPK γ 1	Rabbit	32508	Abcam
NUAK1	Rabbit	4458	Cell Signaling
Phospho-NUAK1 (Thr211)	Rabbit	NA	Eurogentec
NUAK2	Sheep	S225B	MRC PPU
Phospho-(Ser) PKC substrate	Rabbit	2261	Cell Signaling
Phospho-PKC α / β II (Thr638/641)	Rabbit	9375	Cell Signaling
PKC α	Rabbit	2056	Cell Signaling
phospho-MARCKS (Ser159/163)	Rabbit	11992	Cell Signaling
anti-MARCKS	Rabbit	72459	Abcam
Phospho-MYPT1 (Ser445)	Sheep	S508C	MRC PPU
MYPT1	Rabbit	8574	Cell Signaling
MYC	Rabbit	32073	Abcam
Phospho-EGFR (Tyr1068)	Rabbit	3777	Cell Signaling
EGFR	Rabbit	06-847	Millipore
Phospho-ERBB2 (tyr1248)	Rabbit	06-229	Millipore
ERBB2	Mouse	OP15L	Merk-Millipore
Phospho-ERBB3 (Tyr1197)	Rabbit	4561	Cell Signaling
ERBB3	Mouse	05-390	Millipore
Phospho-ERK (Tyr204)	Mouse	7383	Santa Cruz
ERK	Rabbit	4695	Cell Signaling
Phospho-AKT (Ser473)	Rabbit	4060	Cell Signaling
AKT	Mouse	2920	Cell Signaling
FLAG	Mouse	F1804	Sigma-Aldrich
Vinculin	Rabbit	129002	Abcam
β -Actin	Mouse	A5441	Sigma-Aldrich
γ -Tubulin	Mouse	173831	Abcam

H2B	Rabbit	1790	Abcam
-----	--------	------	-------

Table 2. 4 – Primary antibodies

2.1.5 Secondary Antibodies

Protein	Species	Antibody	Supplier
HRP anti-rabbit	Sheep	NA934	Ge Healthcare
HRP anti-mouse	Sheep	NA931	Ge Healthcare
HRP anti-sheep	Rabbit	31480	Pierce

Table 2. 5 – Secondary antibodies

2.1.6 siRNA

Target	SiRNA	Supplier
Non-targeting control	FlexiTube 1022076	Qiagen
NUAK1 #1	FlexiTube SI00108388	Qiagen
NUAK1 #2	FlexiTube SI00108388	Qiagen
NUAK2	FlexiTube SI02660224	Qiagen
PKC α #1	FlexiTube SI00605934	Qiagen
PKC α #2	FlexiTube SI00605927	Qiagen
MYC #1	FlexiTube SI00300902	Qiagen
MYC #2	FlexiTube SI02662611	Qiagen
MYC #3	FlexiTube SI03101847	Qiagen

Table 2. 6 – siRNA used for RNA interference experiments

2.1.7 shRNA

Target	Sequence	Supplier
Non-targeting control	Renilla	Mirimus Inc
MYC #1	CTGAGTCTTGAGACTGAAAGAT	Mirimus Inc
MYC #2	CGCCTCCCTCCACTCGGAAGGA	Mirimus Inc

Table 2. 7 – shRNA used for RNA interference experiments

2.1.8 Primers

Primer	Sequence
ITPR1 forward	5'-GAAGGCATCTTTGGAGGAAGT-3'
ITPR1 reverse	5'-ACCCTGAGGAAGGTTCTG-3'
PKC α forward	5'-CAAGGGATGAAATGTGACACC-3'
PKC α reverse	5'-CCTCTTCTCTGTGTGATCCATTC-3'
NUAK1 forward	5'-CCGCTCACTGATGTAATC-3'
NUAK1 reverse	5'-GTCATCTCTCAACCATCCTCAT-3'
CaMKK β forward	5'-GGAGGTCGAGAACTCAGTCAA-3'
CaMKK β reverse	5'-CATGGTCTTCACCAGGATCA-3'
β -Actin forward	5'-CCAACCGCGAGAAGATGA-3'
β -Actin reverse	5'-CCAGAGGCGTACAGGGATAG-3'
β 2m forward	5'-ACCTCCATGATGCTGCTTAC-3'
β 2m reverse	5'-GGACTGGTCTTTCTATCTCTTGAC-3'

Table 2. 8 – qPCR primer sequences

2.1.9 Acrylamide gels

	Separating Gel			Stacking Gel
	7.5%	10%	13%	
30% Acrylamide	3.75 ml	5.1 ml	6.8 ml	650 μ l
1M Tris pH8.9	5.6 ml	5.6 ml	5.6 ml	-
1M Tris pH6.8	-	-	-	600 μ l
H ₂ O	5.5 ml	4.2 ml	2.5 ml	3.6 ml
10% SDS	150 μ l	150 μ l	150 μ l	50 μ l
20% APS	75 μ l	75 μ l	75 μ l	25 μ l
TEMED	15 μ l	15 μ l	15 μ l	5 μ l

Table 2. 9 – Acrylamide gels composition

2.1.10 Drugs

Reagent	Supplier
A23187	Abcam
A769662	Abcam
BAPTA-AM	Tocris
Erlotinib	LC Labs
Gö6976	Tocris
HTH-01-015	Cambridge Bioscience
Ionomycin	Abcam
MG132	Sigma-Aldrich
Neratinib	Carbosynth
phenformin	Sigma-Aldrich
Rapamycin	Sigma-Aldrich
Sto-609	Sigma-Aldrich
Trametinib	Insight Biotechnology
WZ 4003	Tocris

Table 2. 10 – Drugs and Suppliers

2.2 Methods

2.2.1 Cell Culture

2.2.1.1 Tumour Cells

U2OS and HeLa cells were maintained in Dulbecco's modified Eagle's medium (DMEM) containing 4.5 g/L glucose, 2 mM L-Glutamine, 100 U/ml of penicillin, 100 µg/ml of streptomycin, 10% foetal bovine serum (FBS) and incubated at 37 °C in 5% CO₂. Cells were passaged when they reached 70% confluency and kept in culture until a maximum of 20 passages.

To split cells, the medium was removed and cells were washed once with PBS. Cells were then incubated with Trypsin-EDTA at 37 °C until complete detachment of the adherent cells was observed. Trypsin was then quenched by the addition of complete culture medium and cells were counted using a hemocytometer or an automated cell counter (Innovate) and re-seeded at the desired density for further experiments or for maintaining cells in culture.

All cell lines were routinely tested for mycoplasma contamination and were validated by STR profiling using an in-house validation service (CRUK-BICR).

2.2.1.2 Primary mouse embryonic fibroblasts

Pregnant females were euthanized by CO₂ at 13.5 days after plugging was observed. The uterus was dissected using dissecting forceps and each embryo was released from the yolk sac and placed in individual petri dishes containing PBS; embryos were then decapitated and a piece of tissue was used for genotyping purposes. After the removal of the embryonic internal organs, the embryo body was transferred into a fresh petri dish containing 2 ml of PBS and finely minced using a scalpel. Minced tissue was transferred to a falcon tube containing 1 ml of Trypsin-EDTA and incubated at room temperature for 15 minutes with occasional shaking. The tissue suspension was then placed in a 10 cm diameter petri dishes containing complete Dulbecco's modified Eagle's medium (DMEM) and incubated at 37 °C and 3% of Oxygen. The entire procedure was carried out in sterile conditions in a laminar flow hood. Cells were passaged

every 3 days using the same protocol as described in section 2.2.1.1, and re-seeded at a density of 1.3×10^6 into a 10 cm petri dish.

To induce recombination of the loxP-flanked regions, wild type and Rosa26-lsl-MYC MEFs were infected with 300 multiplicity of infection (MOI) of Adenovirus (University of Iowa) expressing Cre recombinase. Briefly, Adenovirus Cre, stored at $-80\text{ }^\circ\text{C}$, was thawed on ice and mixed with the minimum sufficient volume of DMEM complete medium to cover the plate. Polybrene ($4\text{ }\mu\text{g/ml}$) was also added to the vector-medium solution to increase the transduction efficiency and the final mixture was added to the cells. Culture medium was removed after 6-8 hours post-transduction and replaced with fresh complete medium. Nuak1^{FL/FL} MEFs were infected with retrovirus expressing tamoxifen-inducible CreER and selected on $1\text{ }\mu\text{g/ml}$ puromycin.

SV40 T antigen-immortalised Prkaa1^{FL/FL}; Prkaa2^{FL/FL} MEFs were generously provided by Russell Jones, McGill University, and infected with 300 MOI of Adenovirus-Cre or Adenovirus-LacZ.

2.2.1.3 Cryopreservation and resuscitation of cells

For long-term storage, cells were cryopreserved when in log-phase growth, i.e. when cells were below the confluent density. Culture medium was removed and cells were washed once with PBS. Trypsin-EDTA was then added to detach the cells, which were re-suspended in freezing medium (10% DMSO, 90% FBS). The cell suspension was aliquoted into cryovials, which were transferred into Mr Frosty freezing containers filled with 2-propanol and stored at $-80\text{ }^\circ\text{C}$ before long-term storage in liquid nitrogen.

For resuscitation of frozen cells, cryovials containing cells were quickly thawed by incubation in a $37\text{ }^\circ\text{C}$ water bath for 3-5 minutes. The cell suspension was then transferred to a 15 ml falcon tube containing complete culture medium and centrifuged at 1200 rpm for 5 minutes. After centrifugation, the supernatant was removed and the cell pellet was re-suspended in complete culture medium, transferred to appropriate culture plates and incubated at $37\text{ }^\circ\text{C}$.

For resuscitation of Mouse Embryonic Fibroblasts, cryovials were quickly thawed as described above and the cell suspension was added drop-wise to culture

plates containing complete medium, avoiding the centrifugation step, and incubated at 3% Oxygen.

2.2.2 Plasmid transfection

Cells were seeded at 1.5×10^6 cells per 10 cm and incubated overnight at 37 °C. The next day, 3 µg of DNA was re-suspended in 500 µl OPTI-MEM, with the subsequent addition of 6 µl of p3000 reagent. At the same time, 5 µl of Lipofectamine 3000 was added to 500 µl of Opti-MEM. Then, the two solutions were mixed together and incubated at room temperature for 15 min, as for manufacturer's instructions. The DNA-lipid complex was added drop-wise to the cells in Pen/Strep free DMEM medium, following incubation at 37 °C. After 12 hours, medium was replaced with complete DMEM and cells re-seeded for further experiments and analysed as per figure legends.

shRNA-encoding plasmids, containing a puromycin resistance gene, were transfected as described above. In addition, cells were selected using 1 µg/mL of puromycin before subsequent experiments. Non-transfected cells treated with the same antibiotic were used as control to assess the antibiotic response.

FLAG- tagged NUA1 T211A mutant plasmid was generously provided by David Bernard, Cancer Research Center of Lyon, and was reverted to the wild type form using a mutagenesis kit (QuikChange XL Site-Directed Mutagenesis Kit, Agilent Technologies).

2.2.3 siRNA transfection

Cells were seeded at 1×10^6 cells per 10 cm and the incubated overnight at 37 °C. Next day, the desired volume of siRNA, as per figure legends, was re-suspended in 500 µl OPTI-MEM and 10 µl of Lipofectamine RNAiMAX was also diluted in a second vial containing 500 µl Opti-MEM. The diluted siRNA was then added to the diluted Lipofectamine RNAiMAX and the solution obtained was incubated at room temperature for 5 minutes before adding it drop-wise to the cells in Pen/Strep free DMEM medium. Cells were incubated at 37 °C and re-seeded for further experiments as per figure legends.

2.2.4 RNA extraction and Quantitative Real-Time PCR

2.2.4.1 RNA extraction

Cells were seeded at 1×10^5 cells per well in a 6 well plate in triplicates. To isolate RNA, they were first rinsed in PBS and then harvested by adding 1 mL of Trizol. 200 μ l of Chloroform was then added and the cell suspension was centrifuged at 14,000 rpm for 15 minutes at 4 °C. The upper aqueous phase was transferred to a fresh tube and mixed with an equal volume of isopropanol. The mix was incubated on ice for 20 minutes before centrifugation at 15,000 rpm for 10 minutes at 4 °C. The supernatant was removed and the RNA pellet was washed by the addition of 500 μ l of 70% ethanol followed by centrifugation at 8,000 rpm for 5 min at 4 °C. The washing step was repeated a second time before air-drying the RNA pellet to completely remove the residual ethanol. Finally, RNA was re-suspended in 30 μ l of RNase and DNase free water and incubated at 56 °C for 10 min. RNA concentration was measured using NanoDrop 2000c (ThermoFisher).

2.2.4.2 cDNA synthesis

Reverse transcription of 1 μ g RNA into cDNA was carried out using QuantiTect Reverse Transcription Kit, according to manufacturer's instructions. Briefly, 1 μ g of RNA was added to 2 μ l of gDNA Wipeout buffer and a final volume of 14 μ l was reached with the addition of RNase free water. The mixture was incubated at 42 °C for 2 minutes to remove contamination with genomic DNA and then samples were transferred on ice. For the reverse transcription of RNA into cDNA, 1 μ l of Quantiscript Reverse Transcriptase, 4 μ l of Quantiscript RT buffer and 1 μ l of RT Primer mix were added to each RNA sample and incubated first at 42 °C for 15 minutes and then at 95 °C for 3 minutes to inactivate the reverse transcriptase enzyme.

2.2.4.3 qPCR primers design and analysis

Primers for amplification of the gene of interest were designed using the Assay Design Centre freely available from Roche website, using an intron spanning assay. They were then analysed for the formation of hairpins, self- and heterodimers with the OligoAnalyzer 3.1 freely available from IDT (Integrated DNA Technology).

2.2.4.4 Quantitative Real-Time PCR

Real time quantification was performed using SYBR Green Fast Mix. Specifically, 1 μ l of cDNA was added to a mix containing 5 μ l of SYBR Green Fast MIX, 0.1 μ l of each Reverse and Forward primers (10 μ M stock), and 3.8 μ l of DNAase/RNase free water to reach a final volume of 10 μ l. Samples not containing the cDNA template were included to test the primer formation of homo- or heterodimers. Samples were plated in triplicates in a 96-well PCR plate and the qPCR reaction was carried out using a C1000 thermal cycler (Bio-Rad). A three-step protocol was used for the qPCR reaction:

Temperature ($^{\circ}$ C)	Time	Cycle number
95	5 minutes	1
95	30 seconds	} 35
60	20 seconds	
72	10 minutes	1
65	10 seconds	1
95	30 seconds	1

Table 2. 11 – Cycling conditions for qPCR reaction

The relative quantification of gene expression was performed using the comparative $\Delta\Delta$ Ct method, with normalization of the target gene to the control genes β 2-macroglobulin or Actin.

2.2.5 Immunoprecipitation and immunoblotting

2.2.5.1 Immunoprecipitation

FLAG-NUAK1 wild type, mutant (T211A) or empty vector transiently overexpressed HeLa cells were rinsed with ice-cold PBS and then lysed in IP Lysis Buffer (Tab. 2.3). Protein content of the cell lysates was quantified using the BCA quantification kit according to manufacturer's instructions and 1 mg of proteins were incubated overnight at 4 °C with anti-FLAG M2 Affinity gel. Immunoprecipitated were centrifuged at 2,000 rpm at 4 °C for 1 minute, the supernatant was discarded and pellet washed twice with IP Washing Buffer (Tab. 2.3). After the final washing step, the immunoprecipitated were re-suspended in 30 µl of 2X SDS Sample Buffer.

2.2.5.2 Preparation of whole cell proteins extracts

For whole cell extracts, cells were rinsed twice with ice-cold PBS and then lysed *in situ* with ice-cold lysis buffer (Tab. 2.3). Lysates were then sonicated to reduce viscosity and diluted in 5X SDS Sample Buffer.

2.2.5.3 SDS-PAGE

Immunoprecipitated and whole cell extract proteins were resolved by SDS-PAGE. Samples were boiled at 95 °C for 10 minutes and centrifuged at 5,000 rpm for 2 minutes before loading onto hand-cast acrylamide gels of 1.5 mm thickness and of various percentage (Tab. 2.9) according to the molecular weights intended to separate. Electrophoresis was performed using a Bio-Rad Electrophoresis chamber containing Running Buffer (Tab. 2.3) and gels were run at 90 V until samples reached the separating gel and then the run was continued at 120 V until the visualization of the protein ladder indicated the preferred separation.

2.2.5.4 Western Blotting

Proteins were transferred to nitrocellulose membrane using a Bio-Rad tank transfer system, in which gels and membranes are submerged under transfer buffer (Tab. 2.3). Transfer was performed at 250 mA for a maximum of 2.5 hours.

The membrane was quickly stained using a Ponceau S solution to observe the quality of the transfer process and then rinsed with TBS/T before adding a blocking solution of 5% milk in TBS/T for 1 hour at room temperature with gentle shaking. The membrane was then rinsed in TBS/T before the overnight incubation with primary antibodies diluted in either 5% BSA or 1% milk in TBS/T at 4 °C.

Membranes were then washed three times, for 10 minutes each, in TBS/T and incubated with gentle shaking for 1 hour at room temperature with a 1:5000 dilution of the appropriate HRP-conjugated secondary antibody in 5% milk in TBS/T. Membranes were thoroughly washed three times in TBS/T to remove the secondary antibody and then incubated with the ECL Western blotting substrate for 1 minute. For detection of low intensity signal, membranes were incubated with SuperSignal West Dura Extended Duration Substrate in place of ECL Western blotting substrate. Membranes were then placed in a plastic sheet protector and transferred in a film cassette for detection of the chemiluminescent signal by autoradiography using X-ray film and a Kodak X-Omat 488 X-ray film processor.

2.2.6 Cell death analysis

Cells were seeded in triplicates at 10×10^4 cells per well in a 6-well plate and on the day of the analysis the supernatant was collected in round-bottom polystyrene tubes kept on ice. Cells were rinsed in PBS, following by the addition of 500 μ l of 1X trypsin. Trypsin was quenched with 100 μ l of FBS and cells were collected and transferred in to the polystyrene tubes for centrifugation at 300 g for 5 min at 4 °C. The supernatant was discarded and the cell pellet was incubated in 200 μ l Annexin V Binding Buffer (Tab. 2.3) containing 2 μ l of APC Annexin_V (5 μ g/ml stock) for 10 min at room temperature in the dark. 100 μ l of

a 1 mg/ml propidium iodide solution was added prior to the analysis with FACSCalibur (BD Biosciences).

2.2.7 Determination of protein synthesis rates

Cells were seeded in triplicates at 9×10^4 cells per well in a 12-well plate after siRNA transfection and incubated with 30 $\mu\text{Ci/ml}$ ^{35}S -methionine label (EasyTag from Perkin Elmer) for 30 minutes. Medium was then removed and cells washed with ice cold PBS before lysis. Protein precipitation was performed using a final concentration of 12.5% trichloroacetic acid and precipitated collected by vacuum filtration onto glass filter paper (Whatmann). Filters were then washed with 70% ethanol and acetone before counting scintillation (Ecoscint) for 2 minutes. An aliquot of the lysates was used for a BCA assay (Pierce) to normalise scintillation counts per minute to total protein.

2.2.8 Animals

2.2.8.1 Mouse Models

Multiple Genetically Engineered Mouse (GEM) models were used for research purposes and provided by different research groups. Specifically, *R26-lsl-MYC* mice were generated by Daniel Murphy (Neidler and Murphy, unpublished), *lsl-Kras^{G12D}* mice (Jackson et al., 2001) were obtained from Jackson lab and *Nuak1^{F/F}* mice were generously provided by Hiroyasu Esumi (Inazuka et al., 2012). *Lkb1^{F/F}* mice (Sakamoto et al., 2005) were provided by Owen Sansom and *Hprt-lsl-Irfp* mice were generated by Hock Andreas in collaboration with the Transgenic Production facility at the Beatson Institute (Hock et al., 2017).

2.2.8.2 Breeding and Maintenance

All animal work was carried out in accordance with UK Home Office guidelines in line with Animals (Scientific Procedures) Act 1986 and the European Directive

2010/63/EU. Experimental cohorts and breeding stocks were kept in a light/dark 12 hours cycle, bred and maintained at the Beatson Institute Animal Facility. All breeding stocks and experimental cohorts were regularly checked for health concerns. Ear notching and general maintenance (food, water and housing) was carried out by the Biological Services Unit at the Beatson Institute. Animals were euthanized according to Schedule 1 techniques. Genotyping was carried out using ear notch tissue by Transnetyx (Cordova, TN, US). All experimental procedures were carried out under the Project Licence No. 70-7950 and my personal licence No. ICB9550E7.

2.2.8.3 Intranasal instillation of Adenovirus

Administration of Adenovirus Cre was carried out according to the following protocol in animals aged between 8 and 10 weeks.

Minimum Essential Medium (MEM) was prepared by dissolving MEM powder in distillate water and pH was adjusted at 7.86 using NaOH. Medium was then filter-sterilised using a 0.22 μm filter.

Adenovirus expressing Cre recombinase, stored at $-80\text{ }^{\circ}\text{C}$, was thawed on ice and diluted to obtain the desired concentration in the prepared MEM medium. To create virus particle precipitates, CaCl_2 was added to a final concentration of 4 mM to the diluted virus and incubated at room temperature for approximately 30 minutes.

Mice were anesthetized using a combination of Medetomidine (0.25 mg/Kg) and Ketamine (50 mg/Kg) diluted in 0.9% NaCl and administered by intraperitoneal injection. The depth of the anesthesia was checked by pinching animal's feet before proceeding with the administration of 45 μl of Adenovirus Cre precipitates through the nostrils. Animals were then kept in recovery cages placed on heated plates to help maintain their body temperature. Once mice were fully recovered from the anaesthesia, they were housed in filter-top cages and maintained in a contained room for two weeks.

2.2.8.4 Administration of drugs

Rapamycin was administered by intraperitoneal injection (i.p.) for 3 days at a dose of 10 mg/kg. A stock solution of 50 mg/ml was prepared in 100% Ethanol and 500 μ l was further diluted in 9.5 ml of vehicle (5% PEG400, 5% Tween 20, PBS).

Neratinib and Trametinib were dissolved in peanut oil and sonicated in an ultrasonic bath. Both drugs were administered daily by i.p. injection, for the duration indicated as per figure legends, at a dose of 80 mg/Kg and 1 mg/Kg, respectively.

Erlotinib was dissolved in 6% captisol (w/v) in water and administered at a dose of 100 mg/Kg for 4 weeks by daily gavage.

Animals under treatment were frequently monitored for sides effects and sacrificed in case of excessive adverse response.

2.2.8.5 *In vivo* imaging

In vivo iRFP imaging was carried out using the Pearl Trilogy Small Animal Imaging System (LI-COR). To minimize the signal background originating from the stomach and intestine due to standard diet, mice were fed with alfalfa-free chow (AIN-93M, DBM Scotland) for at least 7 days prior to imaging. Briefly, animals were anesthetized under 2% isoflurane-mixed oxygen and the hair of the thorax and abdominal regions was removed using Nair depilatory cream. Animals were then imaged for the acquisition of the iRFP fluorescence in the 700 channel using the Pearl imaging system. Quantification of the iRFP signal intensity was performed with Image Studio v5 (LI-COR).

2.2.8.6 Tissue collection

To isolate the lungs for histological and pathological analysis, animals were euthanized according to Schedule 1 protocol by asphyxiation with carbon dioxide (CO₂) followed by cervical dislocation. To clear the internal organs of red blood cells, a whole-body perfusion was carried out through the heart by injecting PBS solution in the left ventricle and making an incision in the right ventricle to

allow for the discharge of the blood flow. To ensure a proper fixation of the lungs, 10% neutral buffered formalin was injected through the trachea using a 18g needle until the lungs were completely inflated. Lungs were then removed and placed in a conical tube containing 10% neutral buffered formalin. Tissue was fixed for approximately 16-20 hours before further histological processing was carried out by the Histology Service at the Beatson Institute.

2.2.8.7 Protein isolations from lung tumours

To isolate proteins from lung tumours, animals were sacrificed according to Schedule 1 protocol. Whole-body perfusion with PBS was carried out as described in paragraph 2.2.8.6 and lungs were quickly removed and placed in a petri dish containing PBS. Lung tumours were then dissected and placed in pre-chilled tubes containing 10 volumes of ice-cold lysis buffer (Tab. 2.3) for 1 volume of tissue sample. The tumour samples were homogenised using polypropylene pestles attached to a motor-driven grinder and then centrifuged at 12,000 rpm for 10 minutes at 4 °C. Supernatant was transferred to a fresh tube and stored at -20 °C for further analysis. Protein concentration was determined by BCA protein assay prior to Western blot analysis.

2.2.9 Histology

2.2.9.1 Immunohistochemistry

Paraffin-embedded tissue sections of 4 µm thickness were routinely cut and stained with Hematoxylin & Eosin by the Histology Service at the Beatson Institute.

Immunohistochemical staining for specific antigens was performed by initial de-paraffinization of the tissue sections through the incubation in three washes of xylene for 5 minutes each. Sections were then rehydrated by washing in a decreasing concentration of ethanol series (100%, 70%, 50%, 30%) for 2 minutes each, followed by incubation in dH₂O for 5 minutes.

Heat-induced antigen retrieval was carried out to unmask the antigen and allow for its recognition by the primary antibody by placing the tissue sections in pre-warmed sodium citrate buffer (pH 6.0) and heated for 6 minutes at 120 °C in a pressure cooker using a microwave. Sections were left to cool down for at least 30 minutes before washing in dH₂O for 5 minutes.

To prevent non-specific signal or high background staining due to endogenous peroxidase activity, sections were incubated in 3% hydrogen peroxide (H₂O₂) for 10 minutes to block the endogenous peroxidase. Sections were then washed for 5 minutes in TBS/T before incubation in the appropriate blocking solution for 30 minutes at room temperature.

Primary antibodies were diluted as indicated in Table 2.12 and sections incubated overnight at 4 °C in a humidified chamber. To remove the excess of primary antibody, sections were washed twice in TBS/T for 5 minutes per wash. Detection of the primary antibody bound to the antigen was carried out using the Vectastain ABC HRP Kit, which allows the amplification of the signal by exploiting the Avidin/Biotin complex formation. In particular, the use of a protein with high affinity-binding to biotin (avidin), allows the formation of a molecular bridge between the biotinylated secondary antibody and the biotinylated peroxidase enzyme, resulting in an enhanced signal detection upon addition of the enzyme substrate.

Tissue sections were incubated for 30 minutes with the appropriate biotinylated secondary antibody (Vectastain ABC HRP Kit) diluted in 5% Normal goat serum (NGS) diluted in TBS/T. At the same time, the ABC (Avidin/Biotinylated enzyme Complex) reagent was prepared as for manufacturer's instructions (Vectastain ABC HRP Kit) and incubated at room temperature for 30 minutes.

Sections were washed twice in TBS/T for 5 minutes each and incubated with the ABC reagent for 30 minutes in a humidified chamber. They were rinsed twice in TBS/T for 5 minutes and then DAB (3,3'-diaminobenzidine) was applied to each section and the staining monitored closely using a bright field microscope to establish the optimal incubation time. The peroxidase enzyme, in complex with Avidin and the biotinylated secondary antibody, determines the oxidation of DAB resulting in the deposition of a brown, alcohol-insoluble precipitate at the site of enzymatic activity. As soon as the signal of the desired intensity was developed, sections were rinsed in dH₂O and then counterstained for 1-2 minutes with a solution of Hematoxylin to stain cell's nucleus. They were then rinsed in gently

running tap water before and after dipping into a differentiation solution (Acid Alcohol) to remove excess staining and define nuclei, following by 30 seconds incubation in a blueing reagent (Scott's tap water) to transform the initial soluble colour of the Hematoxylin within the nucleus to an insoluble blue colour. Finally, tissue sections were dehydrated by washing in an increasing concentration of ethanol series (70%, 95%, 100%) for 2 minutes each and then incubated in two washes of xylene for 5 minutes per wash. Coverslips were mounted using a drop of DPX mounting media.

Antigen	Antibody (Supplier)	Blocking Buffer	Dilution
Ki67	RM-9106-SO (Fisher Scientific)	1% BSA in TBS/T	1:200
BrdU		1% NGS in TBS/T	1:200
p-ERK	4370 (Cell Signaling)	5% NGS in PBS	1:500
p-AKT (Ser473)	4060 (Cell Signaling)	5% NGS in TBS/T	1:25
p-4E-BP1 (Thr37/46)	2855 (Cell Signaling)	5% NGS in TBS/T	1:500
p-S6 (Ser235/236)	4858 (Cell Signaling)	5% NGS in TBS/T	1:800
p63	Sc-8431 (Santa Cruz)	No blocking	1:1000
SPC	AB3786 (Millipore)	3% NGS in PBS	1:1000
CD31	28364 (Abcam)	No blocking	1:75

Table 2. 12 – Primary antibodies used for Immunohistochemistry

2.2.9.2 TUNEL staining

Detection of apoptosis was performed using the ApopTag Peroxidase *In Situ* Apoptosis detection kit which consists of digoxigenin-conjugated nucleotide and the terminal deoxynucleotidyl transferase (TdT) enzyme. Apoptotic cells are characterized by fragmented DNA with free 3'-OH ends. The TdT enzyme can incorporate digoxigenin-conjugated nucleotide to the free 3'-OH ends, labelling the DNA fragments localized in apoptotic bodies. The digoxigenin-nucleotide can

then be detected by an HRP conjugated anti-digoxigenin antibody. Therefore, upon the addition of DAB, the HRP enzyme will catalyse the conversion of the chromogenic substrate into a visible brown coloured product, identifying the fragmented DNA.

Briefly, tissue sections were de-paraffinised and re-hydrated as already described in section 2.2.9.1, and antigen retrieval was carried out by incubation in a Coplin jar containing a solution of proteinase K (20 $\mu\text{g}/\text{ml}$ in PBS) for 15 minutes at room temperature with gentle shaking. Sections were washed twice with dH_2O for 2 minutes per wash and endogenous peroxidase activity was blocked by incubation in 3% H_2O_2 in PBS for 5 minutes at room temperature. After rinsing twice in PBS for 5 minutes each, 75 μl of Equilibration buffer was added to each section and incubated for 10 seconds. The TdT Enzyme was diluted 1:10 in Reaction Buffer and, after aspiration of the Equilibration buffer, 60 μl of the solution was added to each section for incubation at 37 $^\circ\text{C}$ for 30 minutes in a humidified chamber. Sections were incubated in a Coplin jar containing the STOP Buffer (1 ml STOP buffer+ 34 ml dH_2O) for 10 minutes at room temperature and then washed three times in PBS for 1 minute per wash. The HRP- conjugate anti-digoxigenin antibody was applied to each section and incubated at room temperature for 30 minutes in a humidified chamber. Sections were rinsed three times in PBS for two minutes per wash before addition of the DAB substrate for 2-3 minutes. Optimal staining time was established by monitoring the brown colour development under the microscope. Counterstaining with hematoxylin and coverslip mounting were performed as described in section 2.2.9.1.

2.2.10 Tumour burden quantification and Immunohistochemistry scoring

Lung tissue sections were scanned using the Aperio Digital Pathology Slides Scanner (Leica) and tumour burden ($n \geq 3$ per genotype) was quantified with SlidePath Digital Image Hub.

For quantification of Ki67 and TUNEL staining, images of lung tissue sections at 20X magnification were taken of at least 5 fields of view ($n=3$ per genotype) and

scoring was performed by counting the percentage of positively stained nuclei within tumours using ImageJ software.

Quantification of BrdU and CD31 staining was performed using SlidePath Digital Image Hub.

2.2.11 Laser-Capture Microdissection and RNA-SEQ analysis

Formalin-fixed paraffin-embedded (FFPE) sections of 10 μm thickness were mounted on framed membrane slides (Leica). To identify phospho-ERK positive regions, adjacent sections were mounted on standard glass slides and stained for phospho-ERK. Tissue mounted on membrane slides was stained with ice-cold 1% cresyl violet after de-paraffinization and rehydration. Selected phospho-Erk^{Low} and phospho-Erk^{High} tumour regions were micro-dissected using a Leica DM 6000B microscope and harvested into separate tubes before combining tissue obtained from multiple sections for each of 4 mice. RNA was then isolated using the RNEasy FFPE kit (Qiagen) according to manufacturer's instructions and depletion of ribosomal RNA was achieved using Ribo-Zero (Epicentre). Synthesis of cDNA was performed using the SMARTER Stranded random primed RNA-SEQ kit (Takara/Clontech), resulting in cDNA libraries flanked by Illumina indexing primers. Libraries were standardized to 10 nM after quantification (Quant-IT Pico green kit, Invitrogen), denatured and diluted to 10 pM for subsequent analysis by paired-end sequencing using an Illumina GA11X deep sequencer. Statistical analysis was performed by a combination of HTSeq and the R 3.0.2 environment, utilizing packages from the Bioconductor data analysis suite and differential gene expression analysis based on the negative binomial distribution using the EdgeR package (Robinson et al., 2010). Pathway modulation analysis was performed using Metacore GeneGO (Thompson Reuters). For analysis of individual gene expression, data were normalized internally to B2M for each mouse, and fold change and false discovery rates were recalculated.

2.2.12 Statistical analysis

Statistical analysis was carried out by GraphPad 6.0 software. Comparison of two data sets was performed with unpaired or paired t-tests, as indicated per figure legend. To compare more than two data sets, ANOVA with a post-hoc Tukey's multiple comparison test was used.

Log-rank Mantel-Cox test was used for statistical analysis of survival data. Statistical significance is indicated in each figure legend, with $p < 0.05$ considered as significant.

Chapter 3 - Investigating the role of NUA1 in cell survival under metabolic stress

In this chapter, we elucidate the contribution of NUA1 to AMPK activation. In addition, we examine the activity of NUA1 in the absence of the upstream kinase LKB1 and investigate an alternative pathway in NUA1 activation that involves PKC α . Finally, we give more insights on the mechanism contributing to the synthetic lethal interaction between NUA1 and MYC and further explore how NUA1 sustains cell viability in MYC-overexpressing cells.

Some of the results of the presented work have been published in (Monteverde et al., 2017).

3.1 Introduction

NUA1, also known as ARK5, is a serine/threonine kinase belonging to the AMPK family (Suzuki et al., 2003a). LKB1, in complex with STRAD-MO25, is the major upstream kinase of the family, responsible for the activation of NUA1 through phosphorylation of the Thr211 in the active T loop (Lizcano et al., 2004b). NUA1 has been involved in a variety of biological processes: from cell adhesion (Zagorska et al., 2010) to proliferation (Hou et al., 2011) and axon branching (Courchet et al., 2013). Interestingly, Liu et al. identified NUA1 as being required for survival of tumour cells that overexpress MYC. Particularly, the study revealed that depletion of NUA1 led to an increase in mTORC1 activity and a collapse in ATP levels, resulting in apoptotic cell death (Liu et al., 2012).

Rapidly growing cells, like cancer cells, require an enhanced production of building blocks, such as amino acids and nucleotides, to sustain cell growth and proliferation. As these processes are energy-demanding, the maintenance of the energetic balance is essential for the survival of cells under metabolic stress. AMP-activated protein kinase is a key regulator of energy homeostasis and its activation to re-establish the energetic balance is crucial for cell survival (Hardie et al., 2012; Shaw et al., 2004b). In fact, it has been shown that cells that overexpress the oncogene c-MYC undergo metabolic stress that triggers the

activation of AMPK. Importantly, NUA1 was shown to be required for activation of AMPK as downregulation of NUA1 resulted in an impaired AMPK response to MYC-induced metabolic stress (Liu et al., 2012).

MYC is found to be amplified or, less frequently, mutated in multiple cancers and its role in tumour initiation as well as in tumour maintenance has been well documented (Beroukhi et al., 2010; Nesbit et al., 1999) but the lack of enzymatic activity has limited the application of pharmacological inhibitors as a therapeutic approach. Therefore, the synthetic lethal interaction between NUA1 and MYC is an attractive strategy for cancer therapy. However, a better understanding of the biological roles of NUA1 might shed more lights on its potential to be used as therapeutic target.

LKB1, the master upstream regulator of NUA1, is recognised as a critical tumour-suppressor gene responsible for the Peutz-Jeghers syndrome, a hereditary disorder characterized by gastrointestinal hamartomatous polyps and a higher risk of cancer. In addition, LKB1 is frequently mutated in lung cancer and occasionally mutated in other sporadic cancers (Monteverde et al., 2015). Loss of *Lkb1* has been shown to accelerate KRas-driven lung cancer as well as enhance the metastatic process (Ji et al., 2007). Although other kinases have been suggested to contribute to NUA1 activation, such as AKT (Suzuki et al., 2003a), an alternative kinase that could regulate NUA1 in the absence of LKB1 has not been identified.

Protein Kinase C (PKC) is a family of serine/threonine kinase that consists of numerous isozymes divided in three major groups: conventional PKC (cPKC: PKC α , PKC β _I, PKC β _{II} and PKC γ), novel PKC (nPKC: PKC ϵ , PKC δ , PKC η PKC θ) and atypical PKC (aPKC: PKC ζ and PKC τ). cPKC isozymes are activated by Ca²⁺ and phorbol esters or diacylglycerol (DAG), whereas nPKCs require DAG but not Ca²⁺ for activation and aPKC do not respond to either Ca²⁺ nor DAG. Remarkably, the PKC family regulates a diverse set of cellular processes including cell proliferation, survival and migration. However, although multiple isozymes share some common functions and substrates, the physiological role of each of them can completely differ depending on the specific cell type. Thus, two isoforms can exert opposite roles in the same setting and the same isoform can behave differently in two distinct cell types (Garg et al., 2014b). For example,

proliferative and anti-proliferative roles have been attributed to PKC α . In particular, PKC α was described to promote cell cycle arrest at the G1 phase in intestinal epithelial cells by induction of the cyclin-dependent kinase inhibitors p21^{Cip1} and p27^{Kip} (Frey et al., 1997) and to mediate downregulation of cyclin D1 (Guan et al., 2007). Similarly, activation of PKC α was shown to induce cell cycle arrest through p21^{Cip1} in pancreatic cancer cells (Detjen et al., 2000). Conversely, PKC α downregulation was reported to reduce proliferation of human hepatocellular carcinoma cells (Wu et al., 2008) and its overexpression resulted in increased proliferation of glioma and breast cancer cells (Mandil et al., 2001; Ways et al., 1995).

Multiple studies have established a positive role of PKC α in the regulation of cell invasion and metastasis. Specifically, PKC α downregulation was described to impair the migration of several cancer cell lines (Byers et al., 2010; Haughian and Bradford, 2009; Wu et al., 2008) and its activation was shown to promote motility and invasion of breast cancer cells through downregulation of E-cadherin and upregulation of matrix metalloproteinase protein 1 and 9 (MMP-1/9) (Kim et al., 2012a). In addition, through the phosphorylation of the myristoylated alanine-rich C-kinase substrate (MARCKS), which is an actin- and membrane-binding protein, PKC α can further exert a control role on cell motility and morphogenesis (Disatnik et al., 2002; Ott et al., 2013).

A link between PKC and cancer was already identified three decades ago, when cells transformed with KRas or HRas were shown to have higher levels of DAG as well as increased activity of PKC (Wolfman and Macara, 1987). Moreover, cells with increased levels of PKC were found to be more inclined to transformation with KRas (Hsiao et al., 1989). However, the specific contribution to the tumorigenic aspect of each PKC isozymes has been difficult to delineate due to the context-dependent and diversity of their functions. Indeed, until now researchers have been debating on their actual value as therapeutic targets in cancer. In addition, the lack of a clear description of PKCs substrates and the difficulties encountered in the identification of isoform-specific targets has challenged a comprehensive understanding of the biology of PKCs and, consequently, of their role in cancer.

3.2 Results

3.2.1 NUAK1 does not regulate AMPK subunits nor basal activity

To elucidate the molecular mechanism of the role played by NUAK1 in the activation of AMPK (Liu et al., 2012), we first analysed the effect of NUAK1 inhibition and downregulation on the catalytic ($\alpha1/\alpha2$) and the regulatory subunits ($\beta1/\beta2$, $\gamma1$, $\gamma2$, $\gamma3$) of the AMPK complex. As shown in figure 3.1A, acute treatment up to 4 hours with the selective inhibitor of NUAK1, HTH-01-015, identified by Gray and colleagues (Banerjee et al., 2014a), did not affect the protein levels of the regulatory and catalytic subunits of AMPK. Note that no signal was detected for the $\gamma2$, $\gamma3$ subunits as probably they are not expressed in U2OS cells (data not shown). NUAK1 downregulation by two independent siRNAs resulted in a modest increase of AMPK $\beta2$ protein levels but only one siRNA caused a slight increase of AMPK $\alpha1/\alpha2$ and AMPK $\gamma1$ protein levels (Fig. 3.1B). Therefore, the overall analysis suggested that NUAK1 does not influence the protein levels of the AMPK subunits.

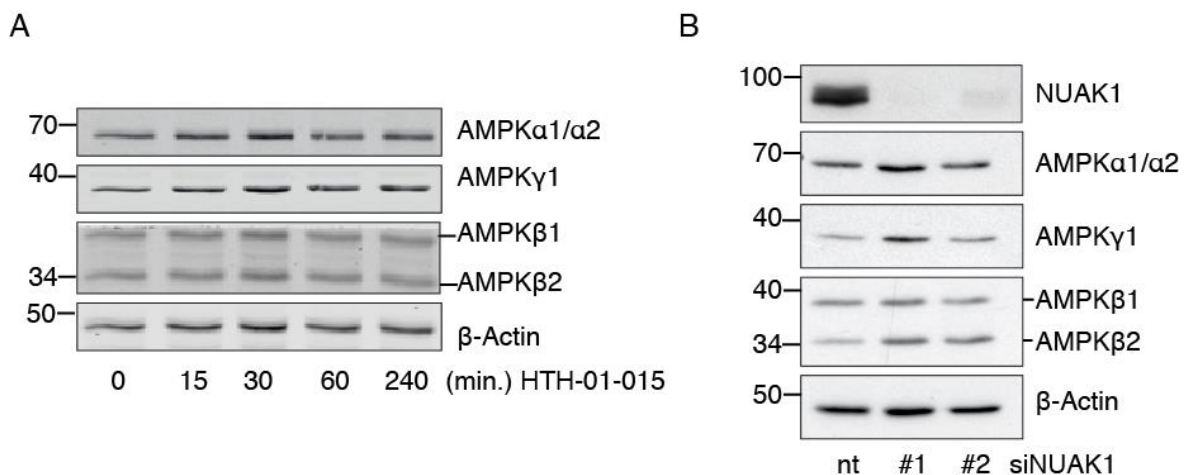


Figure 3. 1 - NUAK1 is not required for the maintenance of AMPK subunits.

A, U2OS cells were treated for the indicated time points with HTH-01-015 (10 μ M) and lysates immunoblotted with the indicated antibodies. **B**, U2OS cells were transfected with 10 nM of two siRNAs targeting NUAK1 or control siRNA (nt). After 48 hours, cells were harvested in lysis buffer and lysates immunoblotted with the indicated antibodies. All images are representative of at least 3 independent experiments.

Alternatively, we asked if acute NUA1 inhibition could have a more prominent effect on the activation of AMPK rather than the subunit protein levels. As shown in figure 3.2, treatment of U2OS cells with HTH-01-015 for 1 hour was sufficient to efficiently reduce levels of MYPT1 phosphorylation at Ser445, a known and validated NUA1 substrate (Zagorska et al., 2010), in a dose-dependent manner. In contrast, the basal levels of AMPK activation were not affected upon inhibition of NUA1, as revealed by the unchanged phosphorylation of Acetyl-CoA Carboxylase (ACC), a well characterized substrate of AMPK (Ha et al., 1994).

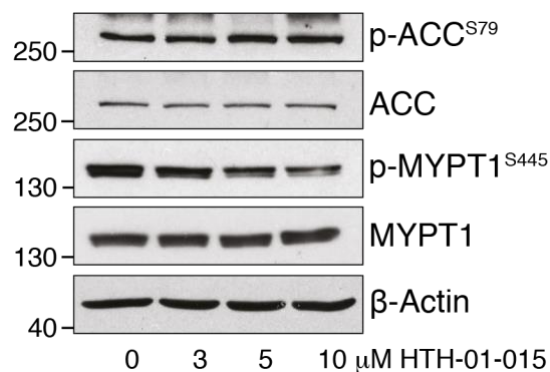


Figure 3. 2 - NUA1 is not required for the maintenance of AMPK basal activity.

U2OS cells were treated with the indicated concentrations of HTH-01-015 for 1 hour and whole cell extracts were immunoblotted with the indicated antibodies. The antibody against ACC may cross react with ACC2. Images are representative of at least 3 independent experiments.

3.2.2 NUA1 is specifically required for Ca²⁺-mediated activation of AMPK

After excluding a role of NUA1 on influencing the basal activity of AMPK, we were interested to investigate if NUA1 regulation of AMPK activation was context-specific rather than a general phenomenon. Therefore, we analysed the AMPK response to multiple activators that mimic the different activation pathways in the presence of NUA1 inhibition. Particularly, we employed phenformin, an inhibitor of the mitochondrial complex I that activates AMPK through the generation of an energetic imbalance; A769662, a synthetic compound that can directly interact with the AMPK complex causing its allosteric activation; finally, we used the calcium ionophore A23187 to increase the

intracellular levels of Ca^{2+} and study the aspect of Ca^{2+} -mediated activation of AMPK. As expected, the different activators could induce the activation of AMPK, as shown by the increased phosphorylation of ACC. Interestingly, NUA1 inhibition did not affect the response to A769662 whereas the efficiency of ACC phosphorylation in response to A23187 and phenformin was impaired (Fig. 3.3).

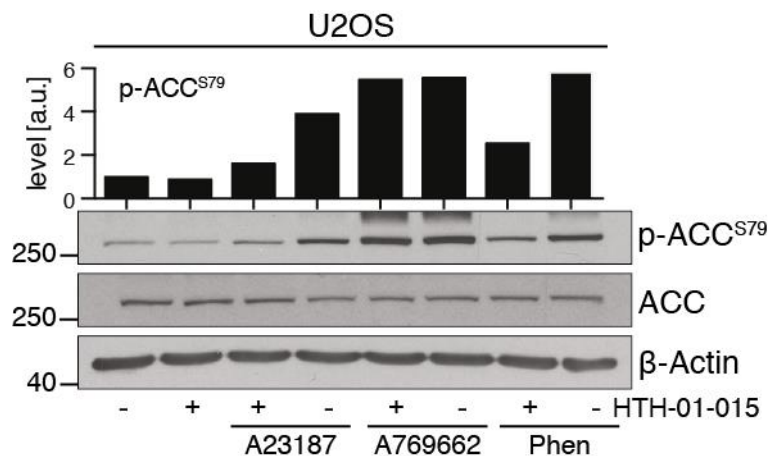


Figure 3. 3 - AMPK response to increase in intracellular Ca^{2+} is impaired by NUA1 inhibition.

U2OS cells were pre-treated with HTH-01-015 (10 μM) for 1 hour and then stimulated with phenformin (10 mM), A769662 (100 μM) for 1 hour and with A23187 (3 μM) for 10 min. Whole cell protein extracts were immunoblotted for the detection of phospho-ACC^{S79} and total ACC. Densitometric analysis shown in the bar graph. All images are representative of at least 3 independent experiments.

LKB1 is known to be the major upstream kinase for NUA1 (Lizcano et al., 2004b). However, the contribution of NUA1 to Ca^{2+} -dependent activation of AMPK suggested an LKB1-independent regulation of the kinase. Therefore, we repeated the analysis of NUA1 contribution to AMPK activation in HeLa cells, which do not express LKB1 (Fig. 3.4A). As already documented by others (Fogarty et al., 2010), stimulation of HeLa cells with phenformin did not induce a significant phosphorylation of ACC, and only a moderate increase was observed following A769662 treatment. Nevertheless, in both instances the levels of ACC phosphorylation were not affected by NUA1 inhibition. In contrast, A23187 was more effective in inducing ACC phosphorylation, which was reduced by NUA1 inhibition (Fig. 3.4B). Overall, the analysis carried out in U2OS and HeLa cells,

strongly pointed towards a role of NUA1 in Ca^{2+} signalling and independent of LKB1.

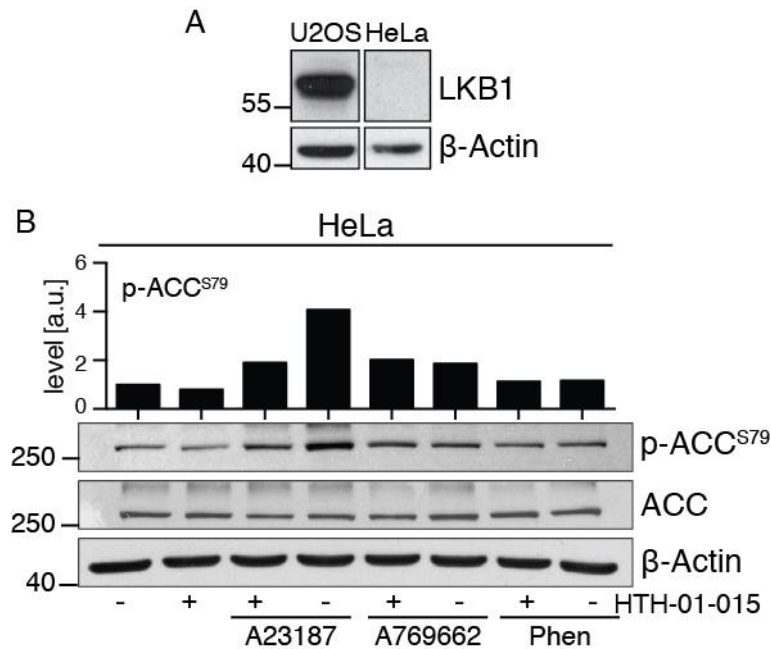


Figure 3. 4 - NUA1 is still required for AMPK response to increase in intracellular Ca^{2+} in the absence of LKB1.

A, Western blot showing LKB1 protein expression in U2OS and HeLa cells. Images are from the same gel & immunoblot, but rearranged to omit extraneous data. **B**, HeLa cells were pre-treated with HTH-01-015 (10 μM) for 1 hour and then stimulated with phenformin (10 mM), A769662 (100 μM) for 1 hour and with A23187 (3 μM) for 10 min. Whole cell protein extracts were immunoblotted for the detection of phospho-ACC^{S79} and total ACC. Densitometric analysis shown in the bar graph. All images are representative of at least 3 independent experiments.

3.2.3 NUA1 is activated by Ca^{2+} signalling by an LKB1-independent pathway

To further elucidate the activity of NUA1 in the absence of LKB1, we assessed the phosphorylation levels of its substrate, MYPT1, following NUA1 inhibition. As shown in figure 3.5A, treatment of HeLa cells with HTH-01-015 resulted in a dose-dependent decrease of MYPT1 phosphorylation at Ser445. In addition, MYPT1 phosphorylation was also affected by NUA1 downregulation in the same cells by two independent siRNAs, confirming that NUA1 is indeed active in LKB1-null cells (Fig.3.5B).

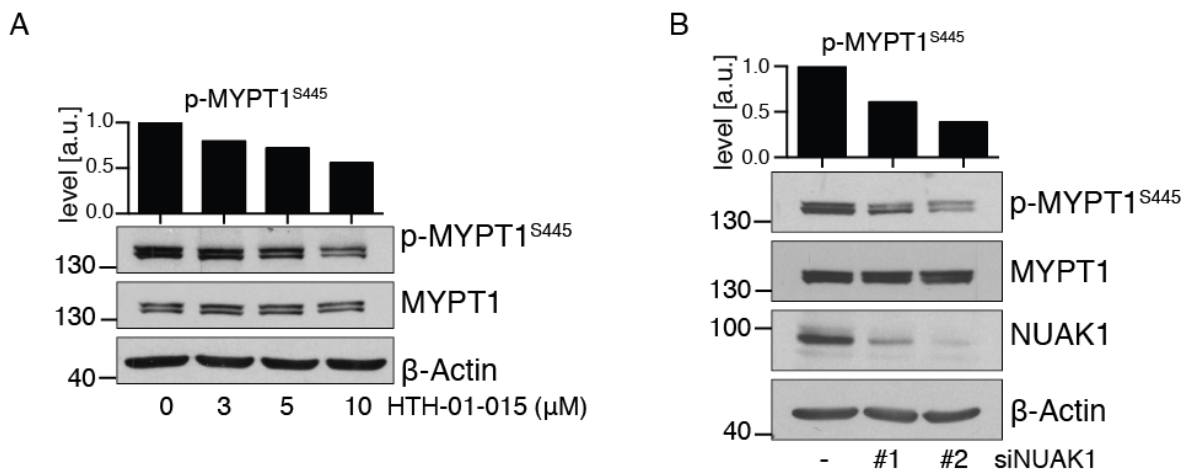


Figure 3.5 - NUAK1 is active and can be modulated in LKB1-null cells.

A, HeLa cells were treated with the indicated concentrations of HTH-01-015 for 1 hour and whole cell protein extracts were immunoblotted for phospho-MYPT1^{S445} and total MYPT1. Densitometric analysis shown in the bar graph. **B**, HeLa cells were transfected with 10 nM of two siRNAs targeting NUAK1 or control siRNA (nt). After 48 hours, cells were harvested in lysis buffer and lysates immunoblotted with the indicated antibodies. Densitometric analysis shown in the bar graph. All images are representative of at least 3 independent experiments.

3.2.4 *CaMKKβ* does not mediate Ca^{2+} -induced activation of NUAK1

Having established the activity of NUAK1 in the absence of the upstream kinase LKB1, we asked which alternative pathway could be engaged to regulate the kinase activity.

It is known that AMPK can be activated by CaMKKβ in response to increase in intracellular Ca^{2+} levels (Woods et al., 2005). Given the observed role of NUAK1-mediated activation of AMPK during Ca^{2+} signalling, we asked if CaMKKβ could be an alternative upstream kinase for NUAK1 as it is for AMPK. To test the hypothesis, we treated HeLa cells with the CaMKKβ inhibitor Sto-609. Inhibition of CaMKKβ efficiently reduced the phosphorylation of AMPK and its target ACC, but no effect was observed on the basal levels of MYPT1^{S445} phosphorylation (Fig 3.6). Moreover, stimulation of cells with the Ca^{2+} ionophore A23187 induced a striking increase in phospho-MYPT1^{S445} that was not affected by Sto-609 treatment.

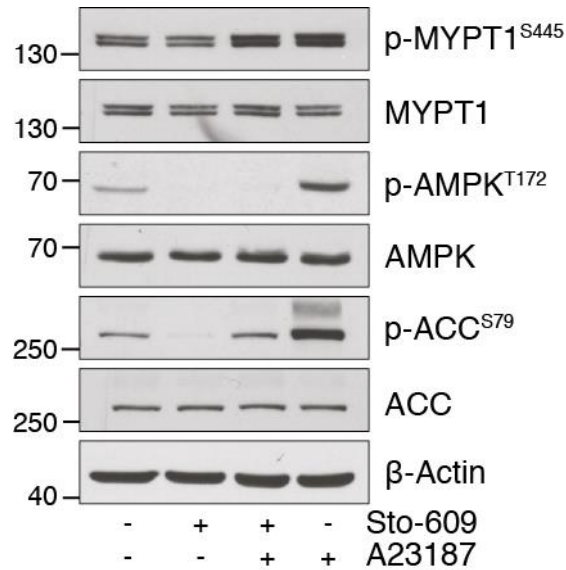


Figure 3. 6 - CaMKK β is not an upstream kinase for NUAK1.

HeLa cells were pre-treated with Sto-609 (5 μ g/mL) for 1 hour and then stimulated with A23187 (3 μ M) for 10 min. Whole cell protein extracts were immunoblotted with the indicated antibodies. Image representative of at least 3 independent experiments.

In agreement with the observed Ca²⁺-mediated activation of NUAK1, treatment of HeLa cells with two different Ca²⁺ ionophores, Ionomycin and A23187, induced an increase in MYPT1^{S445} phosphorylation that was attenuated by NUAK1 inhibition with HTH-01-015 (Fig. 3.7A). Conversely, chelation of the intracellular Ca²⁺ by treatment with BAPTA-AM resulted in the decrease of phospho-MYPT1^{S445} (Fig. 3.7B). Taken together, these results revealed that Ca²⁺ signalling could modulate NUAK1 activation, but not through CaMKK β .

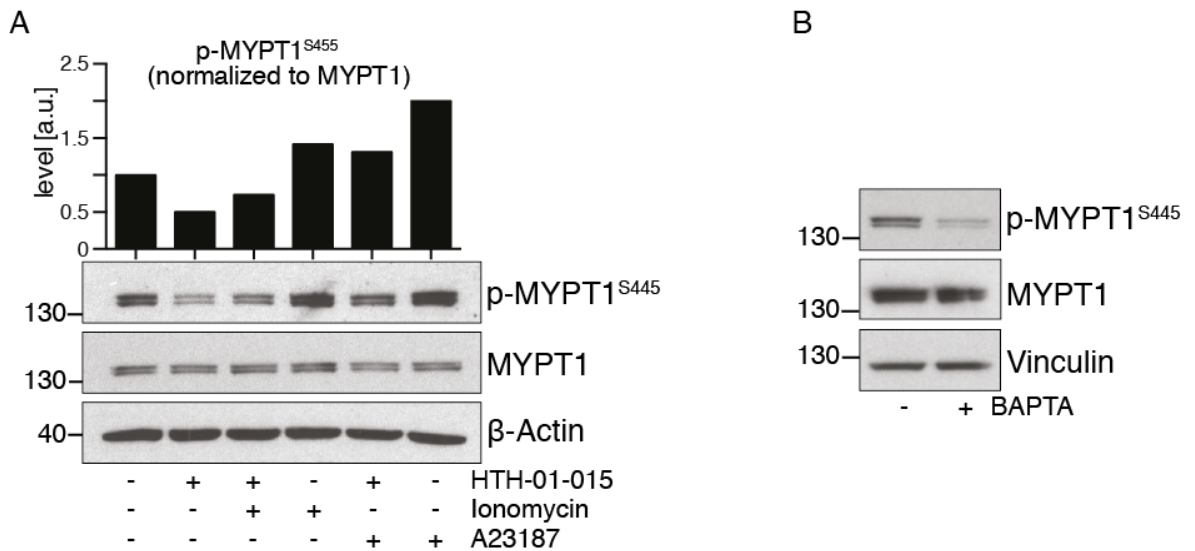


Figure 3. 7 - Modulation of intracellular Ca²⁺ levels impacts on NUAK1 activation.

A, HeLa cells were pre-treated with HTH-01-015 (10 μM) for 1 hour and then stimulated with A23187 (3 μM) or Ionomycin (3 μM) for 10 min. Whole cell protein extracts were immunoblotted for phospho-MYPT1^{S445} and total MYPT1. N=3. Densitometric analysis shown in the bar graph. **B**, HeLa cells were treated with BAPTA-AM (20 μM) for 30 min. Whole cell extracts were prepared and immunoblotted with the indicated antibodies. N=2.

3.2.5 Both NUAK1 and NUAK2 phosphorylate MYPT1^{S445} in response to increased intracellular Ca²⁺

The observation that NUAK1 inhibition could not completely abrogate MYPT1^{S445} phosphorylation in response to increase in intracellular Ca²⁺ levels suggested that other kinases might be involved in the same pathway. Particularly, NUAK2 has been previously shown to phosphorylate MYPT1 at Ser445 (Zagorska et al., 2010). Therefore, we asked if the remaining phosphorylation of MYPT1 after NUAK1 inhibition could be attributed to NUAK2 activation. As shown in figure 3.8A, downregulation of NUAK2 by siRNA resulted in a partial decrease of phospho-MYPT1^{S445}. However, the combination of NUAK2 downregulation with inhibition of NUAK1 by HTH-01-015 resulted in a striking decrease of phospho-MYPT1^{S445}, confirming that the two kinases share the same target. In addition, the phosphorylation of MYPT1^{S445} in response to A23187 could be more efficiently prevented when both NUAK1 and NUAK2 were inhibited and downregulated, respectively (Fig. 3.8A). Similarly, the simultaneous inhibition of NUAK1 and

NUAK2 using WZ4003, an inhibitor previously shown to have high selectivity for both kinases (Banerjee et al., 2014a), led to the abrogation of phosphorylation of MYPT1^{S445} in response to increased Ca²⁺ signalling compared to the partial effect obtained with NUAK1 inhibition alone using HTH-01-015 (Fig. 3.8B). Therefore, NUAK1 and NUAK2 are both induced by Ca²⁺ and mediate the increase in phospho-MYPT1^{S445} in response to stimulation with A23187.

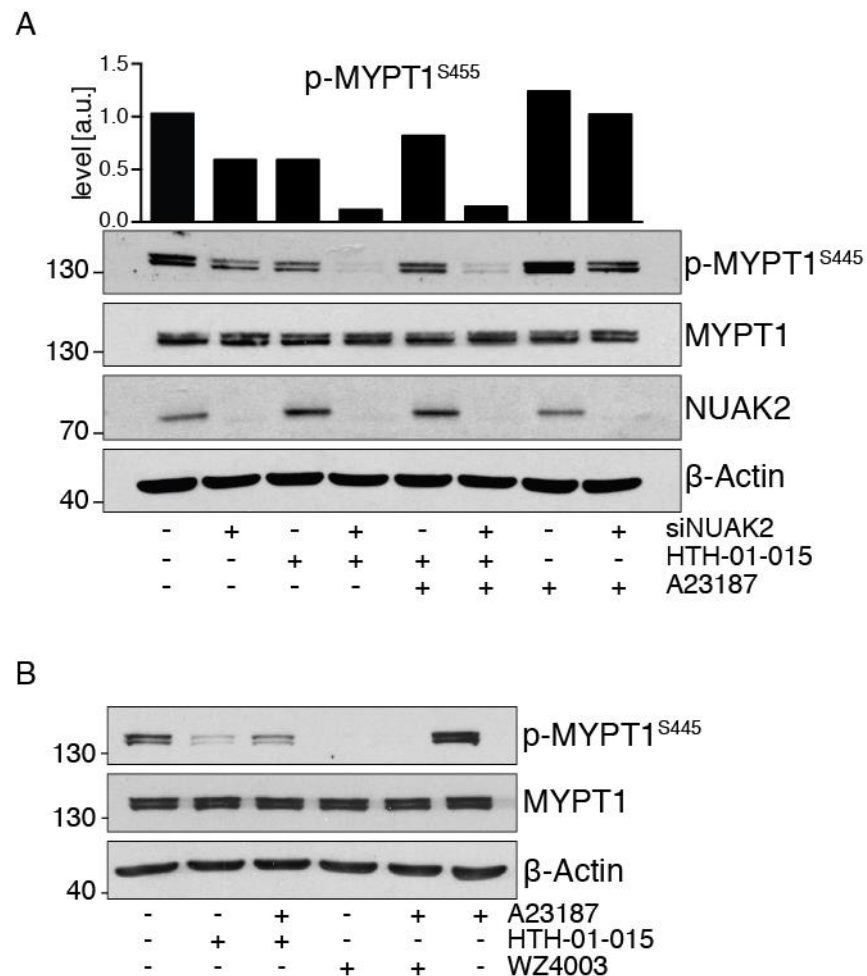


Figure 3. 8 - Simultaneous depletion of NUAK1 and NUAK2 abrogates modulation of phospho-MYPT1^{S445} in response to calcium.

A, HeLa cells were transfected with siRNA targeting NUAK2 (20 nM) and pre-treated with HTH-01-015 (10 μM) for 1 hour and then stimulated with A23187 (3 μM) for 10 min. N=3. Densitometric analysis shown in the bar graph. **B**, HeLa cells were pre-treated with HTH-01-015 (10 μM) or WZ4003 for 1 hour and then stimulated with A23187 (3 μM) for 10 min. Whole cell protein extracts were immunoblotted for phospho-MYPT1^{S445} and total MYPT1. N=2.

3.2.6 MYC modulates activation of PKC

Calcium ions are extremely important second messengers in eukaryotic cells and they can activate a number of kinases that mediate the signal transduction to modulate various cellular processes that range from gene transcription to muscle contraction (Clapham, 2007). Multiple studies have suggested an interconnection between MYC and Calcium signalling. It has been reported that MYC expression can induce an increase in intracellular Ca^{2+} in B cells (Habib et al., 2007) but also that Ca^{2+} can drive MYC gene expression in various settings (Quesada et al., 2002) (Todorova et al., 2009). Considering the link between Ca^{2+} and MYC and also the previously described synthetic lethal interaction between NUA1 and MYC, we wondered if MYC could regulate the expression of a kinase, which is part of the Ca^{2+} signalling pathways, that could also be involved in NUA1 activation. To test that, we compared the transcriptome of wild type and MYC-overexpressing Mouse Embryonic Fibroblasts (MEFs). Interestingly, the transcriptome analysis (data not shown) revealed that components of the Ca^{2+} signalling pathway, such as $\text{Pkc}\alpha$, Itpr1 and $\text{CaMKK}\beta$, were upregulated and the same results were confirmed by qPCR analysis (Fig. 3.9A). Enhancement of Ca^{2+} signalling in MYC-overexpressing cells was further reflected by the increased phosphorylation levels of ACC, downstream of AMPK, upon A23187 stimulation (Fig. 3.9B). In addition, MYC overexpression resulted in a Ca^{2+} -dependent increase in PKC activity, as shown by the higher phosphorylation levels of its downstream target MARCKS (Aderem, 1992), which were sensitive to Ca^{2+} chelation and PKC inhibition with BAPTA and Gö6976, respectively (Fig. 3.9C). Moreover, MARCKS phosphorylation levels were diminished upon downregulation of MYC by three independent siRNAs in HeLa cells, indicating that MYC-dependent activation of PKC is conserved across species (Fig. 3.9D).

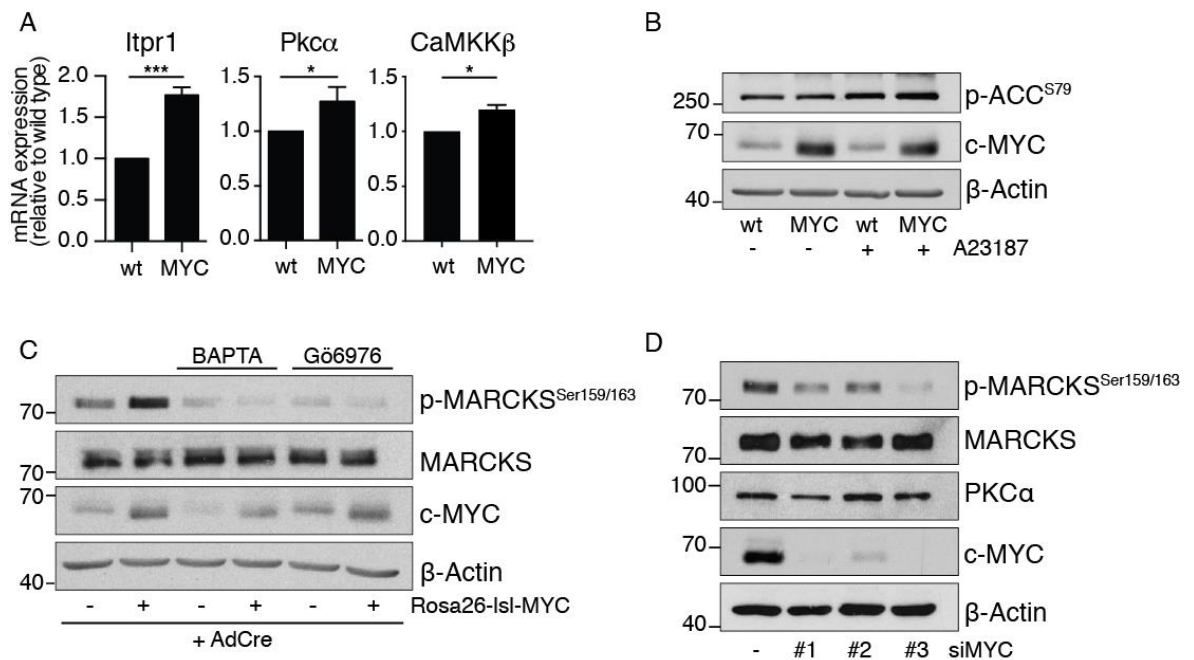


Figure 3. 9 - Overexpression of MYC induces upregulation of components of the Ca²⁺ signalling pathway.

A, R26-lsl-MYC or wild type MEFs were infected with 300 MOI of Adenovirus-Cre and 24 hours later analysed for mRNA expression levels of Pkcα, Itpr1 and CaMKKβ. Bar graph representing the Mean and SD from biological triplicates. * p<0.05 and *** p<0.001 determined by two-tailed unpaired T-tests. **B**, Adenovirus-Cre infected R26^{lsl-MYC} or wild type MEFs were stimulated with A23187 (6 μM) for 10 min and whole cell protein extracts were immunoblotted with the indicated antibodies. **C**, Adenovirus-Cre infected R26^{lsl-MYC} or wild type MEFs were treated with BAPTA (10 μM) or Gö6976 (1 μM) for 3 hours prior to lysis. Whole cell protein extracts were immunoblotted with the indicated antibodies. **D**, HeLa cells were transfected with three independent siRNAs (20 nM) targeting MYC and whole cell protein extracts immunoblotted with the indicated antibodies. All images are representative of at least 3 independent experiments, except (D) where n=2.

3.2.7 PKCα mediates NUAK1 activation by Ca²⁺ signalling

The conventional class of PKC (cPKC) is a subgroup of the PKC family known for being activated by Ca²⁺ and includes four isozymes: PKCα, PKCβ_I, PKCβ_{II} and PKCγ. Therefore, cPKC represented a good candidate for the upstream calcium-mediated regulation of NUAK1. To test if that was the case, HeLa cells were treated acutely with Gö6976, a potent PKCα and PKCβ_I inhibitor, which induced a dose-dependent decrease of phospho-MYPT1^{S445} (Fig. 3.10A). Phospho-(Ser) PKC substrate antibody was used as readout of PKC activity in response of Gö6976

treatment. Notably, whereas HTH-01-015 could sustain MYPT1^{S445} inhibition over a treatment period of 16 hours, phosphorylation levels of MYPT1^{S445} and Phospho-(Ser) PKC substrates recovered after treatment with Gö6976 for the same time frame, suggesting a transient effect of the PKC inhibitor (Fig. 3.10B). Additionally, acute inhibition of PKC resulted in an attenuation of Ca²⁺-induced MYPT1^{S445} phosphorylation (Fig.3.10C), indicating its contribution to the pathway that leads to MYPT1 phosphorylation.

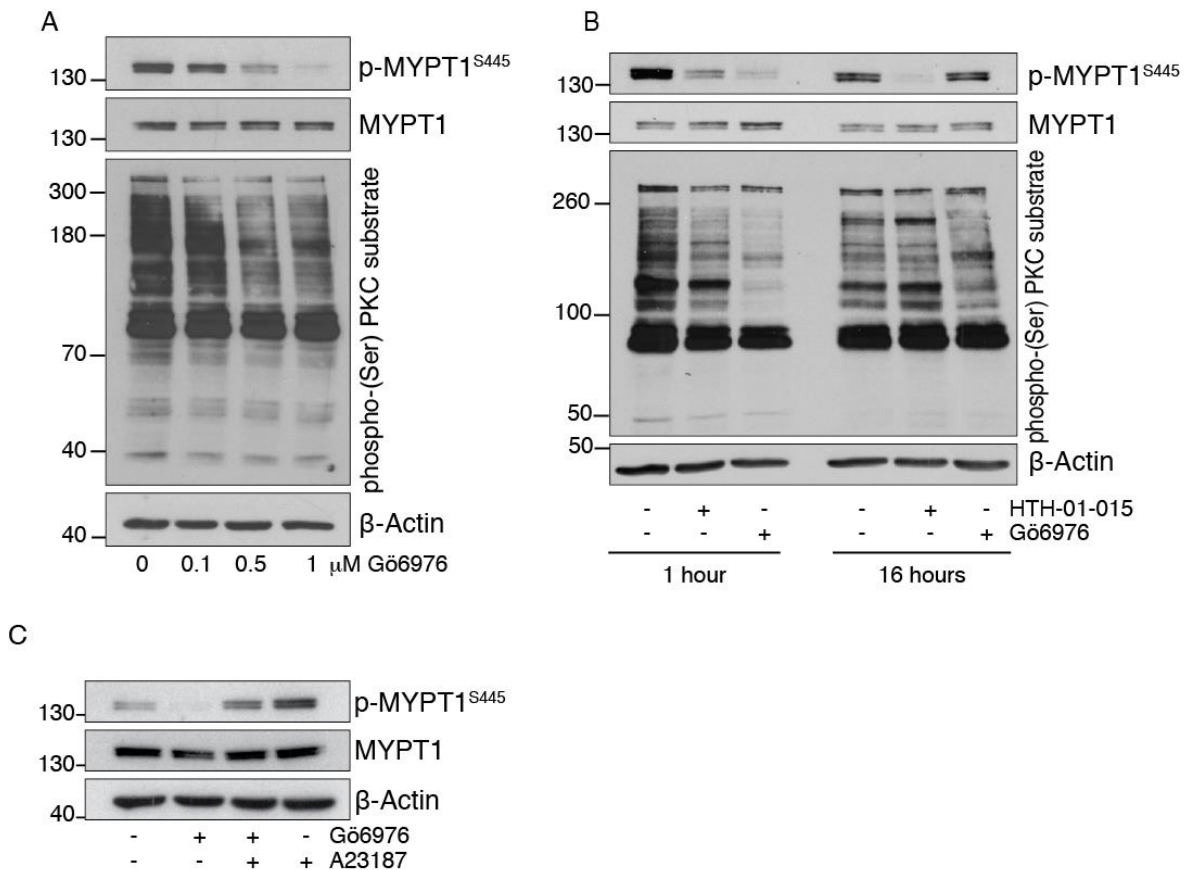


Figure 3. 10 - Inhibition of PKC impairs MYPT1^{S445} phosphorylation.

A, HeLa cells were treated with the indicated concentrations of Gö6976 for 1 hour and whole cell protein extracts were immunoblotted with the indicated antibodies. **B**, HeLa cells were treated with HTH-01-015 (10 μM) or Gö6976 (0.5 μM) for 1 hour and 16 hours and whole cell protein extracts were immunoblotted with the indicated antibodies. **C**, HeLa cells were pre-treated with Gö6976 (0.5 μM) for 1 hour and then stimulated with A23187 (3 μM) for 10 min. Lysates were immunoblotted for phospho-MYPT1^{S445} and total MYPT1. All images are representative of at least 3 independent experiments.

Given that Gö6976 can inhibit two of the four conventional PKC isoforms, PKCα and PKCβ₁, we sought to determine whether one or both isoforms were mediating the observed effect of Ca²⁺-induced phosphorylation of MYPT1^{S445}.

Downregulation of PKC α by two different siRNAs (Fig. 3.11A) resulted in a decrease of MYPT1^{S445} phosphorylation, which was not further reduced by simultaneous depletion of PKC β_1 (Fig. 3.11B). Note that downregulation of PKC β_1 could not be confirmed, as no protein or mRNA expression could be detected in HeLa cells, probably indicating that this isoform is not expressed in this cell line (data not shown).

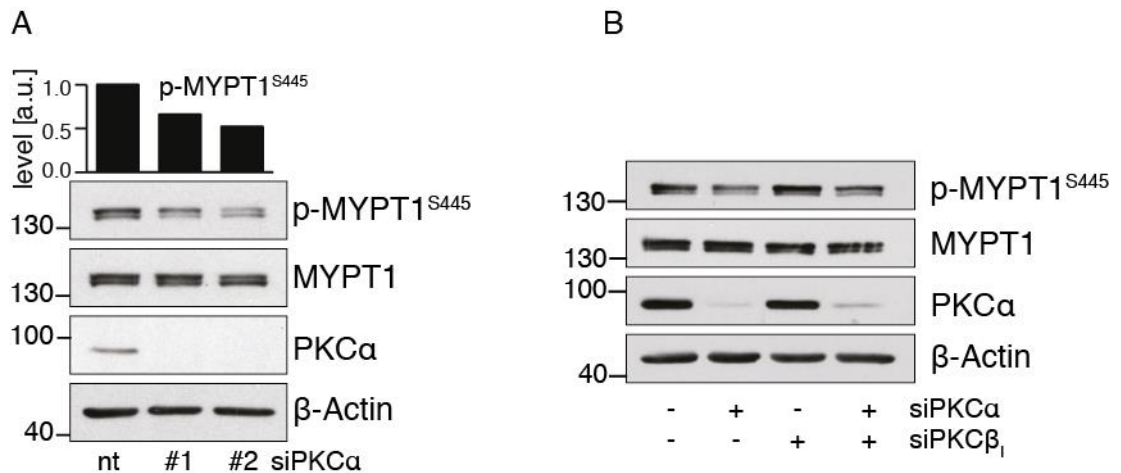


Figure 3. 11 - PKC α and not PKC β_1 regulates downstream phosphorylation of MYPT1^{S445}.

HeLa cells were transfected with 20 nM of two siRNAs targeting PKC α and control siRNA (nt) (A) or with a combination of siRNAs targeting PKC α (20 nM) and PKC β (20nM) (B). After 48 hours, cells were harvested in lysis buffer and lysates immunoblotted for phospho-MYPT1^{S445}, total MYPT1 and PKC α . Densitometric analysis shown in the bar graph (A). All images are representative of at least 3 independent experiments.

Phosphorylation of MYTP1^{S455} has proved to be mediated by both NUAK1 and NUAK2, therefore, we sought to obtain a more direct indication of the effect of PKC inhibition on NUAK1 phosphorylation at Thr211 in the activation loop. Thus, to study phospho-NUAK1^{T211} we made use of an antibody against phospho-AMPK^{T172} that was previously shown to detect phosphorylation at Thr211 of overexpressed NUAK1 (Fisher et al., 2005). A23187 treatment induced an increase in the phosphorylation of the immunoprecipitated FLAG-tagged NUAK1 that was prevented by treatment with Gö6976, whereas no signal was detected for the T211A mutant, confirming the specificity of the antibody (Fig. 3.12A). The same results could be reproduced with a newly developed polyclonal

antibody raised against Thr211 of human NUA1 (Fig. 3.12B). Overall, we obtained strong evidence for PKC α regulation of NUA1 activity and its ability to phosphorylate the downstream target MYPT1 in response to Ca²⁺ signalling.

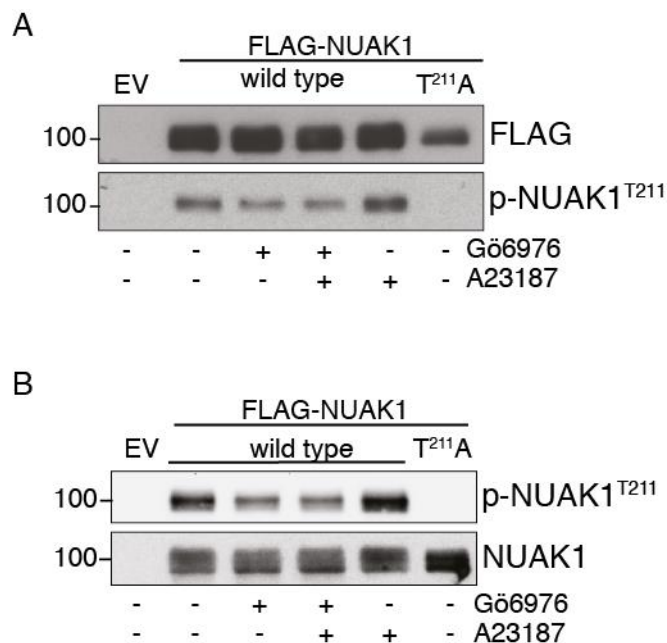


Figure 3. 12 - Phosphorylation of NUA1 is decreased by PKC inhibition.

A-B, HeLa cells were transfected with expression plasmids encoding either wild type or mutant (T211A) FLAG-NUA1. Forty-eight hours post-transfection, FLAG-NUA1 wild type cells were pre-treated with Gö6976 (0.5 μ M) for 1 hour and then stimulated with A23187 (3 μ M) for 10 min. Cells were then lysed and FLAG-tagged proteins were immunoprecipitated and immunoblotted with the indicated antibodies. Detection of phospho-NUA1^{T211} was performed by cross-reaction of the phospho-AMPK^{T172} antibody (n=3) (**A**) or by a newly developed antibody raised against phospho-NUA1^{T211} (n=2) (**B**). Cells transfected with Empty Vector were used as negative control.

3.2.8 PKC α regulates NUA1 protein levels

Upon depletion of PKC α by two independent siRNAs we observed a marked reduction of NUA1 protein levels, suggesting that PKC α regulates NUA1 protein stability. Indeed, as shown in Figure 3.13A-B, the decrease in NUA1 protein levels upon PKC α downregulation was rescued by proteasome inhibition using MG132. In addition, NUA1 mRNA expression levels were not significantly

affected by PKC α depletion, confirming a regulation at protein levels as opposed to a transcriptional modulation (Fig. 3.13C).

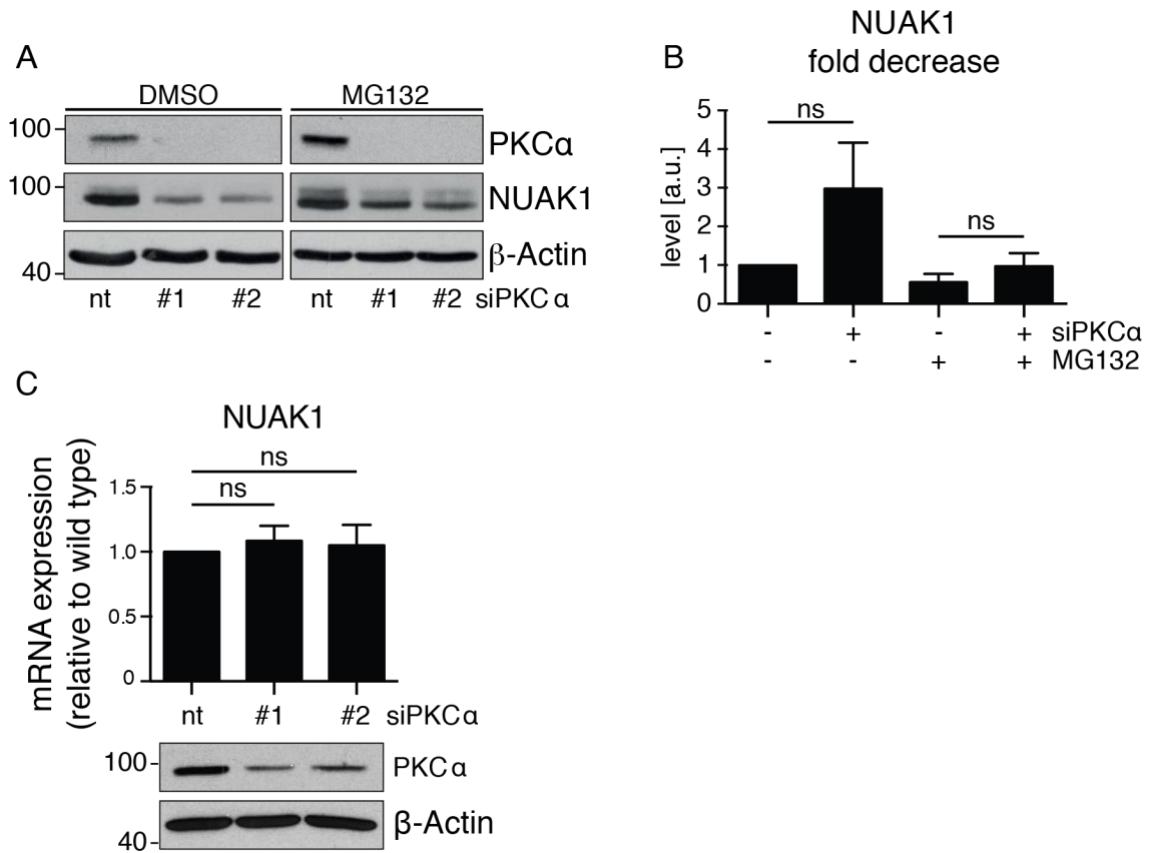


Figure 3. 13 - PKC α depletion induces NUA1 degradation.

A, HeLa cells were transfected with 20 nM of two siRNAs targeting PKC α or control siRNA (nt) and treated with MG132 (20 μ M) for 5 hours prior to lysis. Whole cell protein extracts were then immunoblotted with the indicated antibodies. N=2. **B**, Bar graph indicating the Mean and SD fold decrease in NUA1 protein expression in HeLa cells depleted for PKC α and treated with MG132 (20 μ M) or DMSO control. N=3. ns= not significant. P value calculated with one-way ANOVA, Tukey's multiple comparison. **C**, HeLa cells were transfected with two independent siRNAs targeting PKC α (20 nM) or control siRNA (nt) and NUA1 mRNA levels analysed by qPCR. Bar graph indicating the Mean and SD fold change of NUA1 mRNA expression relative to control (nt). ns= not significant. P value calculated with one-way ANOVA, Tukey's multiple comparison.

3.2.9 NUAK1 and NUAK2 reside in two distinct pathways for the regulation of MYPT1^{S445} phosphorylation in response to Ca²⁺ signalling

Notably, PKC α downregulation only induced a partial reduction of MYPT1^{S445} phosphorylation (Fig. 3.11A) and treatment with the PKC inhibitor Gö6976 did not completely abrogate phospho-MYPT1^{S445} levels in response to A23187 stimulation (Fig. 3.10C). In light of our data showing a contribution of NUAK2 to Ca²⁺-induced phosphorylation of MYPT1^{S445} (Fig. 3.8A-B), we asked if the incomplete inhibition of phospho-MYPT1^{S445} upon PKC α depletion and inhibition could be attributed to NUAK2. Co-depletion of NUAK1 and PKC α in HeLa cells minimally affected phospho-MYPT1^{S445} levels in comparison to NUAK1 depletion alone, consistent with the two kinases residing in the same pathway. Conversely, phospho-MYPT1^{S445} levels were further reduced upon co-depletion of NUAK2 and PKC α in comparison to their individual downregulation, indicating that NUAK2 and PKC α mediate Ca²⁺-dependent phosphorylation of MYPT1 from two different signal axes (Fig. 3.14).

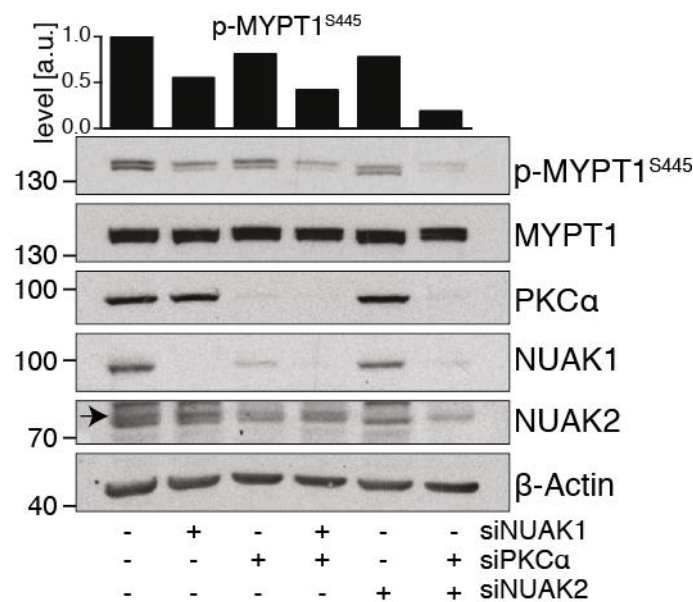


Figure 3. 14 – PKC α and NUAK2 co-depletion further decreases phospho-MYPT1^{S445} levels.

HeLa cells were transfected with siRNA targeting PKC α (20 nM) and/or NUAK1 (10 nM) or NUAK2 (20 nM). Whole cell protein extracts were then immunoblotted with the indicated antibodies. N=2. The arrow indicates the correct band for NUAK2. Densitometric analysis shown in the bar graph.

3.2.10 The PKC α -NUAK1 pathway supports viability of MYC overexpressing cells

A previous synthetic lethality screening carried out by Liu et al., identified NUAK1 as being required to support survival of MYC-overexpressing cells (Liu et al., 2012). In agreement with that, inhibition of NUAK1 by HTH-01-015 treatment in HeLa cells, which express high levels of MYC (Shen et al., 2017), induced a significant increase in apoptotic cell death compared to control cells. Interestingly, cell death was observed only at 10 μ M of HTH-01-015, whereas partial inhibition of NUAK1 with a lower concentration of the inhibitor did not affect cell survival (Fig. 3.15A). Similarly, in the same cells, downregulation of NUAK1 with two different siRNAs resulted in a significant increase in cell death only when NUAK1 expression was more strongly suppressed (Fig. 3.15B).

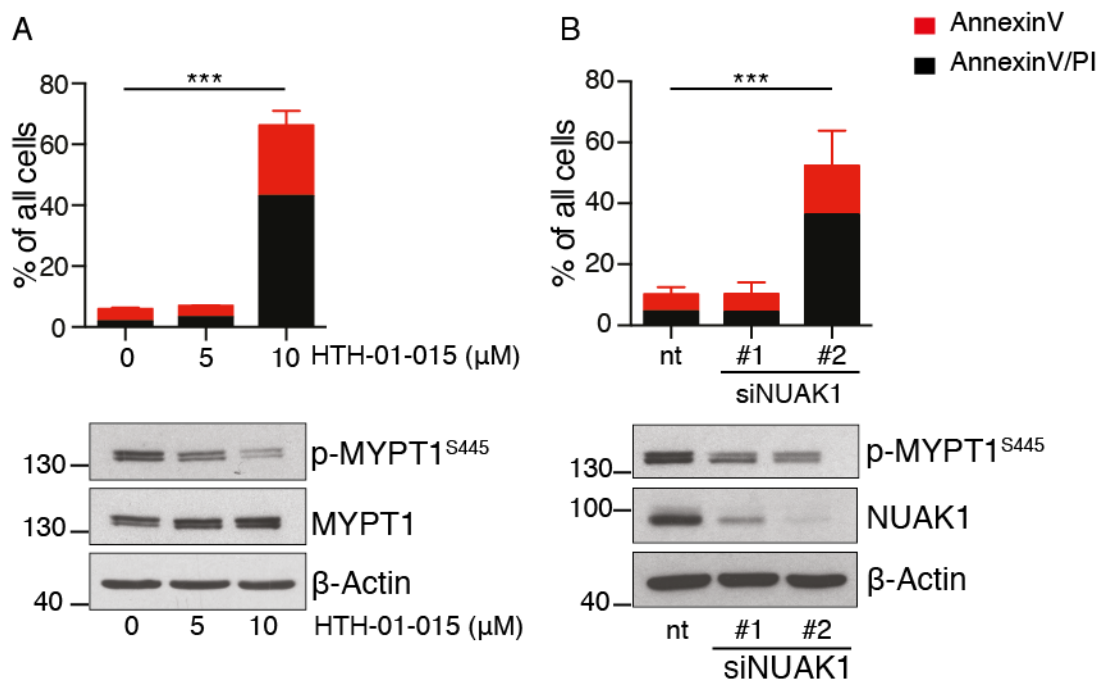


Figure 3. 15 - NUAK1 inhibition and depletion is lethal in HeLa cells.

A, HeLa cells were treated with the indicated concentrations of HTH-01-015. Forty-eight hours later, induction of apoptosis was analysed by Annexin V/Propidium iodide FACS (top) and whole cell protein extracts were immunoblotted with the indicated antibodies (bottom). Error bars represent the SD of the mean of three independent experiments. *** $p < 0.001$ calculated with one-way ANOVA, Tukey's multiple comparison.

B, HeLa cells were transfected with 10 nM of two siRNAs targeting NUAK1 or control siRNA. At day 3 post-transfection, induction of apoptosis was analysed by Annexin V/PI staining (top) and whole cell protein extracts were immunoblotted with the indicated antibodies (bottom). Error bars represent the SD of the mean of three independent experiments. *** $p < 0.001$ calculated with one-way ANOVA, Tukey's multiple comparison.

Thus, our results suggested that NUA1 expression at low levels was still able to support cell survival, establishing a threshold of NUA1 expression below which cells are no longer able to sustain viability. Next, we asked if the synthetic lethal interaction of NUA1 and MYC was indeed responsible for the observed cell death upon NUA1 inhibition in HeLa cells. MYC reduction by two independent shRNAs (Fig. 3.16B) significantly decreased the levels of cell death caused by NUA1 inhibition, consistent with a synthetic lethal interaction (Fig. 3.16A).

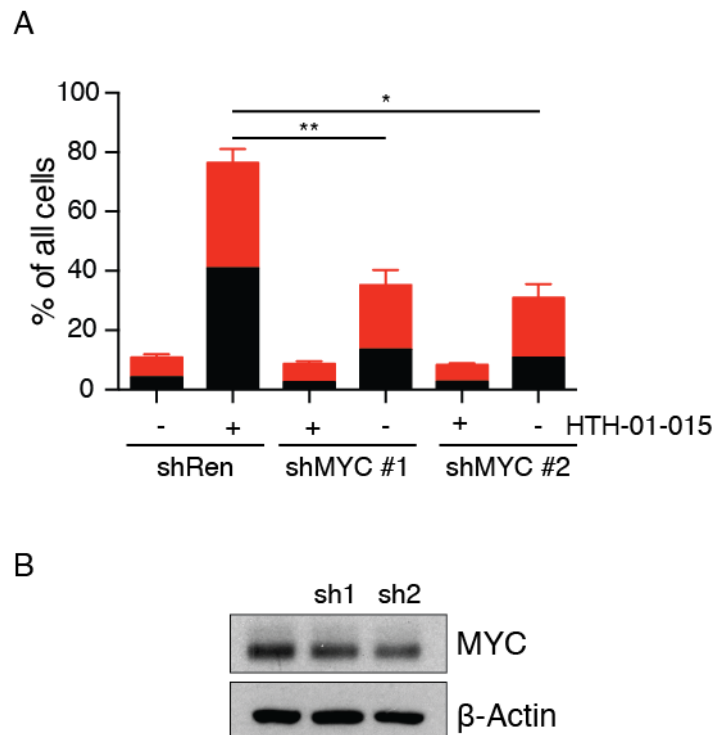


Figure 3. 16 - Cell death induced by NUA1 inhibition is rescued by MYC downregulation.

HeLa cells were transfected with two shRNA-encoding plasmids targeting MYC or a non-targeting control (shRen). After puromycin selection, cells were treated with HTH-01-015 (10 μ M) and 48 hours after treatment analysed by Annexin V/PI staining for apoptosis induction (A). Error bars reflect the standard deviation of biological triplicate samples from one experiment and statistical analysis was performed on a total of five independent experiments. ** $p < 0.01$, * $p < 0.05$ calculated with one-way ANOVA, Tukey's multiple comparison. Whole cell protein extracts were immunoblotted with the indicated antibodies (B).

Furthermore, PKC α downregulation by two independent siRNAs also induced a significant increase in cell death in HeLa cells (Fig. 3.17A), and PKC inhibition with Gö6976 more efficiently induced death in cell treated with a low dose of HTH-01-015 (Fig. 3.17B-C), corroborating a role of PKC α upstream of NUA1.

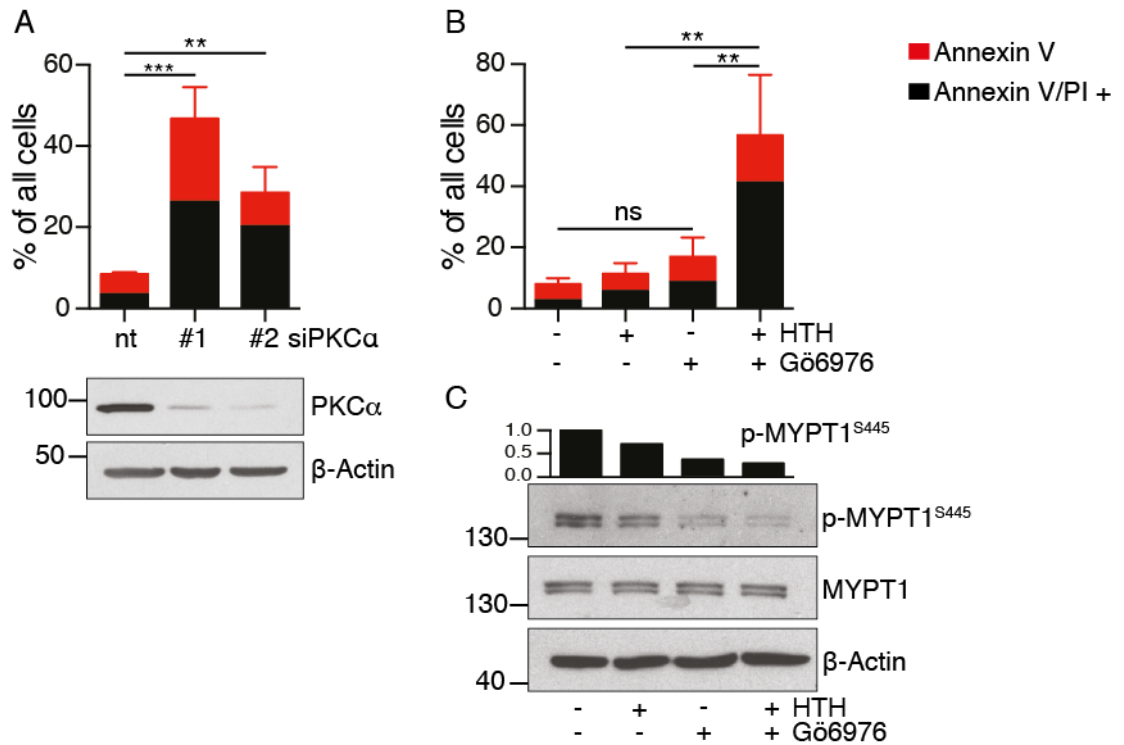


Figure 3. 17 - PKC α depletion and inhibition is lethal in HeLa cells.

A, HeLa cells were transfected with 20 nM of two siRNAs targeting PKC α or control siRNA (nt). At day 3 post-transfection, induction of apoptosis was analysed by Annexin V/PI staining (top) and whole cell protein extracts were immunoblotted with the indicated antibodies (bottom). Error bars represent the SD of the mean of three independent experiments. *** p <0.001, ** p <0.01 calculated with one-way ANOVA, Tukey's multiple comparison. **B**, HeLa cells were treated with Gö6976 (1 μ M) and HTH-01-015 (5 μ M) and, 48 hours post treatment, induction of apoptosis was analysed by Annexin V/PI staining. Error bars represent the SD of the mean of three independent experiments. Ns= not significant, ** p <0.01 calculated with one-way ANOVA, Tukey's multiple comparison. **C**, Whole cell protein extracts from HeLa cells stimulated as per **B**, were isolated after 1 hour of treatment and immunoblotted with the indicated antibodies. Densitometric analysis shown in the bar graph.

3.2.11 The *PKC α -NUAK1* pathway regulates activation of *mTORC1* via *Raptor*

Cells that express higher levels of MYC are characterized by increased protein synthesis, which is required to sustain the increase in proliferation (van Riggelen et al., 2010). Therefore, cells in those conditions are highly metabolically demanding and the activation of metabolic checkpoints becomes crucial to cope with energetic stress. Restraining mTOR activity is a mechanism that protects cells from metabolic stress and AMPK is well known to control mTORC1 activation for the maintenance of energetic balance. Particularly, it has been shown that AMPK can inhibit Raptor through phosphorylation of Ser792 (Gwinn et al., 2008). Indeed, as shown in figure 3.18, stimulation of HeLa cells with A23187 induced activation of AMPK and phosphorylation of Raptor^{S792}, which resulted in a dynamic response of mTORC1. In particular, whereas phospho-Raptor^{S792} levels increased steadily over time, phosphorylation levels of S6K and 4EBP1, mTORC1 substrates, decreased after an initial increase, in agreement with a dual effect of Ca²⁺ in activating mTORC1 (Li et al., 2016; Zhou et al., 2015) as well as inhibiting Raptor through activation of AMPK.

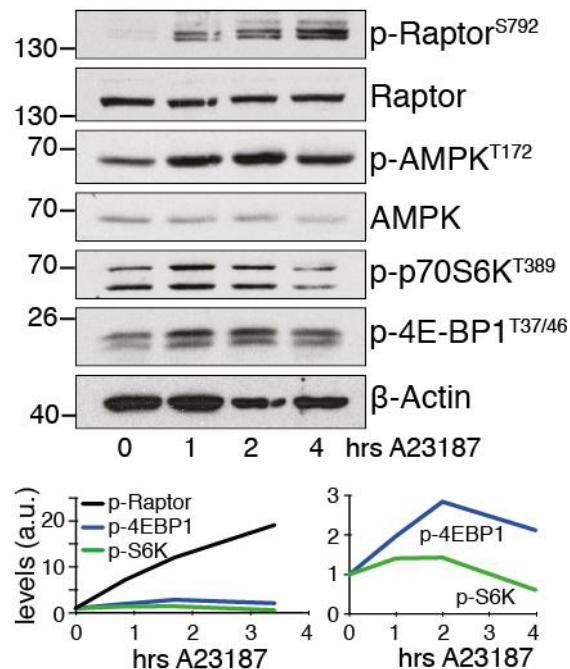


Figure 3. 18 – Dynamic Ca²⁺-dependent modulation of mTORC1.

HeLa cells were treated for the indicated time points with A23187 (3 μ M) and whole cell protein extracts immunoblotted with the indicated antibodies.

Surprisingly, downregulation of PKC α and NUA1 in HeLa cells resulted in an impaired inhibition of Raptor at basal levels as well as in response to A23187 treatment, as observed by the decreased phosphorylation at Ser792 (Fig. 3.19A). Furthermore, NUA1-mediated regulation of Raptor^{S792} phosphorylation was similarly observed in U2OS cells, which retain LKB1 function. Particularly, as shown in Figure 3.19B-C, acute inhibition of NUA1 with HTH-01-015 or downregulation by two independent siRNAs significantly impaired the inhibitory phosphorylation of Raptor in response to multiple AMPK activators, such as phenformin, Salicylate and A23187, suggesting a higher mTORC1 basal activity but also the inability of AMPK to efficiently control Raptor in the absence of NUA1.

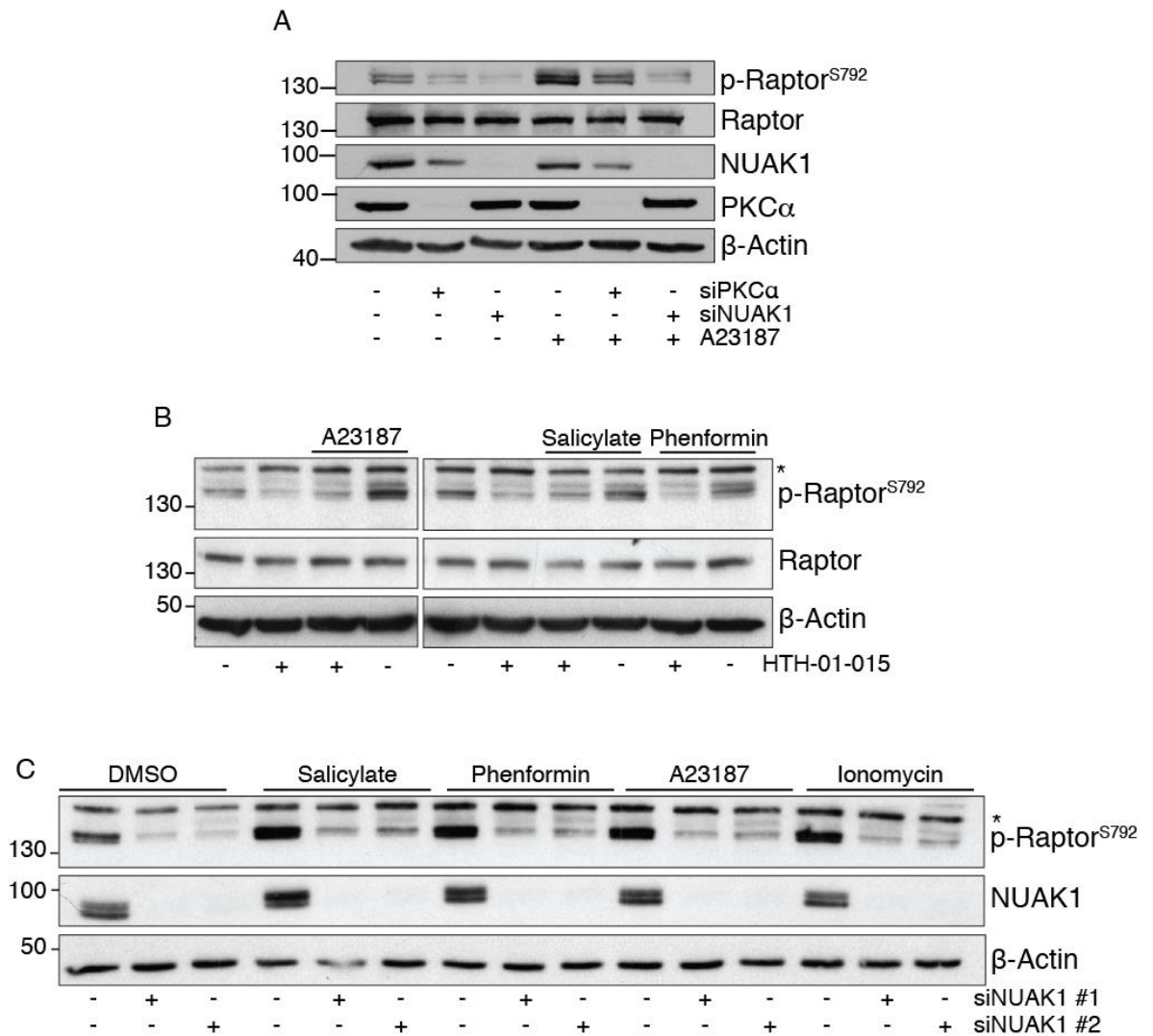


Figure 3. 19 - PKC α and NUAK1 depletion impairs Raptor inhibition at basal levels and in response to AMPK stimulation.

A, HeLa cells were transfected with siRNA targeting PKC α (20 nM), NUAK1 (10 nM) or control siRNA. At day 1 post-transfection, cells were stimulated with A23187 6 μ M for 10 minutes and whole cell protein extracts were immunoblotted with the indicated antibodies. **B**, U2OS cells were pre-treated with HTH-01-015 (10 μ M) for 1 hour and then stimulated with phenformin (10 mM), Salicylate (10 mM) for 1 hour and with A23187 (3 μ M) for 10 min. Whole cell protein extracts were immunoblotted with the indicated antibodies. Images are from the same gel & immunoblot, but rearranged to omit extraneous data. **C**, U2OS cells were transfected with 10 nM of two independent siRNAs targeting NUAK1 (10 nM) or control siRNA. At day 2 post-transfection, cells were stimulated with phenformin (10 mM), Salicylate (10 mM) for 1 hour and with A23187 and Ionomycin (3 μ M) for 10 min. Whole cell protein extracts were immunoblotted with the indicated antibodies. The star in B and C indicates a cross-reacting band.

Consistent with a role of NUAK1 in regulating mTORC1 activity, its downregulation in HeLa and U2OS cells resulted in a significant increase in protein synthesis, as underlined by an increase in ^{35}S -Methionine incorporation in comparisons to control cells (Fig. 3.20). In addition, depletion of PKC α in HeLa cells also caused a significant increase in protein synthesis, corroborating its involvement in NUAK1 signalling pathway.

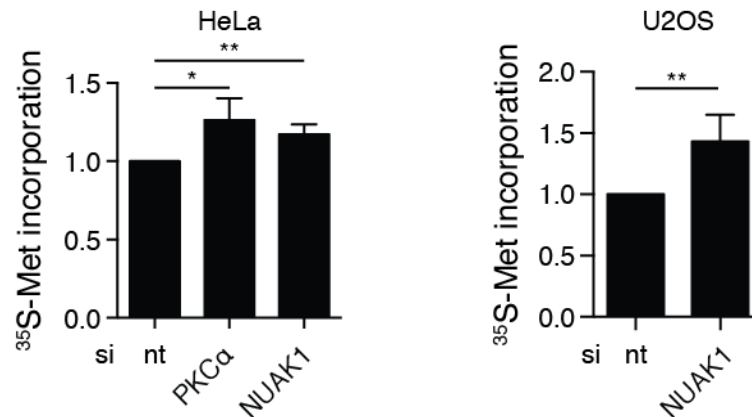


Figure 3. 20 - NUAK1 downregulation increases protein translation.

HeLa were transfected with siRNA targeting PKC α (20 nM), NUAK1 (10 nM) or a non-targeting control (nt); U2OS cells were transfected with siRNA targeting NUAK1 (10 nM) or control siRNA (nt). At day 2 post-transfection, both cell lines were analysed for ^{35}S -Methionine incorporation. Bar graph represents Mean and SD from 3 independent experiments. *p<0.05 and **p<0.01 calculated with one-tailed unpaired T-test. Data generated in collaboration with Dr John Knight from the Beatson Institute.

In agreement with a role of the PKC α /NUAK1 axis to support cell viability by restraining mTORC1 activity through inhibition of Raptor, treatment of HeLa cells with the mTORC1 inhibitor Rapamycin could significantly rescue the cell death induced by either NUAK1 or PKC α downregulation (Fig. 3.21).

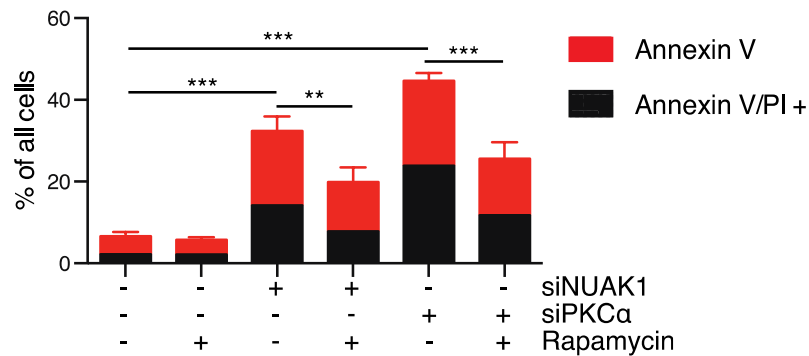


Figure 3. 21 - mTORC1 inhibition rescues cell death induced by PKC α or NUAK1 depletion.

HeLa cells were transfected with siRNA targeting PKC α (20 nM) and NUAK1 (10 nM) and treated with Rapamycin (100 nM) at day 1 post-transfection. 48 hours after treatment cells were analysed by Annexin V/PI staining for apoptosis induction. Error bars represent the SD of the mean of three independent experiments. *** p <0.001, ** p <0.01 calculated with 2-way ANOVA, Sidak's multiple comparison test.

Among the family members only AMPK has previously been described to inhibit Raptor by phosphorylation at Ser792 (Gwinn et al., 2008). Therefore, we asked if NUAK1 was mediating AMPK phosphorylation of Raptor or if it could regulate Raptor independently of AMPK. Thus, we studied the effect of NUAK1 inhibition on RAPTORS⁷⁹² phosphorylation in Mouse Embryonic Fibroblast depleted of both α 1 and α 2 catalytic subunits of AMPK. As shown in figure 3.22, AMPK depletion moderately reduced phosphorylation of RAPTORS⁷⁹². However, inhibition of NUAK1 by HTH-01-015 decreased phospho-RAPTORS⁷⁹² levels both in wild type and AMPK depleted cells, suggesting an AMPK-independent regulation of Raptor by NUAK1.

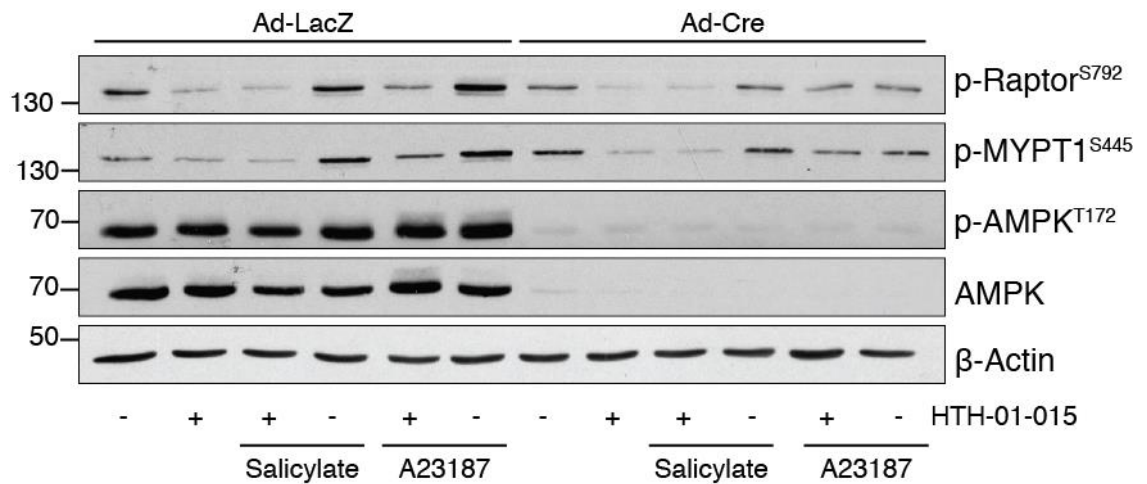


Figure 3. 22 - NUA1 regulates Raptor^{S792} phosphorylation in the absence of AMPK. AMPK α 1/ α 2 floxed MEFs were infected with 300 MOI of Adenovirus expressing Cre (Ad-Cre) or LacZ (Ad-LacZ). Cells were pre-treated with HTH-01-015 (10 μ M) for 1 hour and then stimulated with Salicylate (10 mM) for 1 hour and with A23187 (3 μ M) for 10 min. Whole cell extracts were immunoblotted with the indicated antibodies.

3.3 Discussion

NUAK1 was identified as a member of the AMPK family based on its 47% and 45% sequence homology to AMPK α 1 and α 2, respectively. Since its discovery, few research groups have worked on understanding its biological functions, and NUAK1 role in migration and invasion together with cell proliferation and metabolic homeostasis has suggested an application of its targeting in cancer therapy. However, not many of the suggested targets or upstream kinases of NUAK1 have been further validated and a more comprehensive understanding of its function and regulation is needed to effectively and fully exploit its therapeutic potential.

The discovery of a synthetic lethal interaction between NUAK1 and MYC opened the door to a novel approach of targeting NUAK1 in MYC-driven cancers. Results reported in this chapter have further investigated the mechanism through which NUAK1 contributes to survival of MYC-overexpressing cells, uncovering a novel Calcium-mediated activation of NUAK1 through PKC α .

Cells overexpressing the oncogene MYC were shown to upregulate AMPK activity, possibly as a mechanism of protection from the energetic stress resulting from

MYC induction (Liu et al., 2012). In addition, the same study suggested that AMPK increased activity was dependent on NUA1, as its depletion was reported to prevent AMPK phosphorylation at Thr172 and also to decrease the protein levels of the regulatory subunit AMPK β 1. However, we have shown that inhibition or downregulation of NUA1 in U2OS cells did not affect the protein levels of either the regulatory or catalytic subunits of AMPK (Fig. 3.1A-B). Therefore, data obtained in our study exclude the modulation of the AMPK subunits as part of the mechanism of NUA1-mediated regulation of AMPK. However, the analysis performed by Liu and colleagues employed a type of U2OS cells in which a modified form of MYC (MYC-ER) is constitutively overexpressed but can only translocate to the nucleus, thus being activated, upon treatment with 4-Hydroxytamoxifen (4-OHT). Therefore, the discrepancy between our results and data from Liu and colleagues might reside in a basal induction of MYC activity in the absence of 4-OHT treatment, due to a leakiness of the system, that could change the dynamic of the effect of NUA1 depletion on the AMPK complex, a hypothesis that will require further analysis.

Our data revealed that the requirement for NUA1 with regards to AMPK activation is context dependent, as NUA1 inhibition could consistently impair activation of AMPK specifically in response to modulation of intracellular Ca²⁺ levels in the two cell lines tested, U2OS and HeLa (Fig. 3.3 & Fig. 3.4B). We have not currently characterized the mechanism of the observed phenomenon and additional investigations will be required to understand if NUA1 can mediate AMPK activation by promoting its phosphorylation by upstream kinases, or perhaps through its own kinase activity, or protect AMPK from dephosphorylation.

Notably, the requirement of NUA1 for a complete response of AMPK to increased intracellular Ca²⁺ levels was preserved in LKB1-null cells (HeLa, Fig. 3.4A-B). Moreover, the observations that NUA1 activity could be efficiently modulated in HeLa cells (Fig. 3.5A-B) and that it was responsive to Ca²⁺ modulation (Fig. 3.7A-B) strengthen the theory of a novel Ca²⁺-dependent and LKB1-independent regulation of NUA1. In particular, upon treatment with two Ca²⁺ ionophores, A23187 and Ionomycin, we observed an increase in phospho-MYPT1^{S445} (Fig. 3.7A), which is a downstream target shared by both NUA1 and NUA2 (Zagorska et al., 2010). Indeed, our data indicate that both kinases can

be activated by Ca^{2+} and mediate the increase in phospho-MYPT1^{S445} (Fig. 3.8A-B).

In our search for an upstream kinase mediating NUAK1 activation by Ca^{2+} signalling we could firstly exclude the involvement of CaMKK β (Fig. 3.6), which is known to mediate the Ca^{2+} -dependent phosphorylation of AMPK (Woods et al., 2005). A role of Ca^{2+} and CaMKK β in the activation of other AMPK-related kinases (ARKs) has been previously investigated and excluded based on the inability of the ARKs to phosphorylate the AMARA peptide in response to A23187 treatment or expression of CaMKK β (Fogarty et al., 2010). Our data partially agree with the experimental evidence provided by Fogarty and colleagues, as we have excluded a role for CaMKK β in mediating the Ca^{2+} -dependent activation of NUAK1 and NUAK2, assessed by the unchanged phosphorylation of their downstream target MYPT1 upon CaMKK β inhibition (Fig.3.6). However, our observations support an effect of Ca^{2+} in NUAK1 and NUAK2 activation as an optimal phosphorylation of MYPT1 in response to A23187 was impaired when both kinases were inhibited (Fig. 3.8A-B), which was rejected by Fogarty et al. with regards to NUAK2, whereas NUAK1 was not included in their biochemical analysis. This inconsistency might be attributed to the use of the AMARA peptide, which was initially considered as a common substrate for all the ARKs but that has been since revisited as a preferential substrate for SIK and AMPK.

Interestingly, multiple experimental evidence suggested a reciprocal regulation between Ca^{2+} and MYC. The calcium ionophore A23187 was shown to induce MYC expression in Human promyelocytic leukemia cells (HL-60) (Salehi and Niedel, 1990). More recently, calcium was shown to affect MYC activity in addition to its expression, as Ca^{2+} -loaded Calmodulin was described to interact with MYC and enhance its transcription activity (Raffener et al., 2017). On the other hand, MYC was shown to amplify calcium signalling through the downregulation of the Ca^{2+} efflux pump PMCA4b (Habib et al., 2007) and to bind the promoter of components of the Ca^{2+} -signalling pathway, such as CaMKK β , ITPR1 and PKC α (Walz et al., 2014). In agreement with Walz et al., upon MYC overexpression we observed an increase in mRNA levels of CaMKK β , *Itpr1* and *Pkc α* (Fig. 3.9A), a higher sensitivity of AMPK to calcium modulation, as shown by the increased levels of ACC phosphorylation upon A23187 treatment (Fig. 3.9B) and, most importantly, an increased Ca^{2+} -dependent activity of PKC, as revealed by the

increased phosphorylation levels of the downstream target MARCKS (Fig. 3.9C). Taken together these results agree with the previously reported role of MYC in the amplification of Ca^{2+} signalling and established a new important link between MYC and NUA1 through $\text{PKC}\alpha$ (Fig. 3.23).

We identified $\text{PKC}\alpha$ as a novel regulator of NUA1 activity and protein levels. Specifically, downregulation or inhibition of PKC resulted in decreased phosphorylation levels of MYPT1^{S445} (Fig. 3.10A & 3.11A). In addition, PKC inhibition could prevent phosphorylation of NUA1 at Thr211 in response to A23187 (Fig. 3.12 A-B) and $\text{PKC}\alpha$ downregulation induced proteasome-dependent degradation of NUA1 (Fig. 3.13 A-B). Overall, our data strongly indicate that $\text{PKC}\alpha$ is the upstream kinase regulating NUA1 basal activity and in response to Calcium, while we additionally report that NUA2, although it is responsive to Ca^{2+} , is not similarly regulated by $\text{PKC}\alpha$ (Fig. 3.14).

Notably, phospho-NUA1^{T211} levels were not completely abolished by inhibition of PKC using Gö6976, but nevertheless they did not increase upon combination of Gö6976 and A23187 (Fig. 3.12 A-B). Taken together, this evidence suggests that PKC is the only kinase mediating NUA1 phosphorylation in response to A23187 but also that NUA1 maintains a basal level of phosphorylation at the Thr211 site. This residual phosphorylation might be explained by the presence of an additional upstream kinase or by an auto-phosphorylation activity of NUA1, thus further biochemical investigations are needed to confirm any of the hypothesis. Interestingly, AMPK has been shown to undergo auto-phosphorylation in response to oxidation induced by peroxide (Zmijewski et al., 2010) and unpublished data from our laboratory suggest a similar mechanism of activation of NUA1 by oxidative stress, opening to the possibility of an auto-phosphorylation reaction for NUA1.

The Thr211 in the activation loop of NUA1 (QKDKFLQ^tFCGSPLY) does not conform to the canonical phospho-PKC Substrate Motif (K/RXpSXK/R). However, other sites appear to be a more suitable match for PKC, such as Ser367 (VMLERQRsLKKSKKE) on human NUA1, which opens to the possibility of $\text{PKC}\alpha$ phosphorylating an alternative site that could influence phosphorylation of Thr211 and support protein stability due to regulatory mechanisms that are not yet understood.

The regulation of NUA1 activity by an alternative phosphorylation would not be surprising, as AKT has been previously suggested to modulate NUA1 activity by phosphorylation at Ser600 (Suzuki et al., 2003a). Furthermore, phosphorylation of additional sites to the threonine residue in the T loop for the modulation of the activity of other ARKs has been reported by multiple experimental evidence (Henriksson et al., 2012; Timm et al., 2008). In any case, further investigations will be required to identify phosphorylation sites on NUA1 upon Ca^{2+} stimulation and understand which of them might be regulated by $\text{PKC}\alpha$, contemplating also the possibility of a second kinase, downstream of $\text{PKC}\alpha$, mediating the observed effects.

Inhibition or downregulation of NUA1 resulted in a significant increase in death of HeLa cells (Fig. 3.15A-B), which express high levels of MYC due to the upstream genomic integration of the Human papilloma virus 18 (HPV-18) (Adey et al., 2013; Shen et al., 2017). Similarly, downregulation of $\text{PKC}\alpha$ caused a significant increase in cell death (Fig. 3.17A), consistent with a role of $\text{PKC}\alpha$ upstream of NUA1. In agreement with the synthetic lethality interaction between NUA1 and MYC, downregulation of MYC in HeLa cells decreased the cell death induced by NUA1 inhibition (Fig. 3.16A-B). The synthetic lethal interaction between MYC and NUA1 appears to be independent of LKB1 status, as it was firstly identified in U2OS cells that are proficient for LKB1 (Liu et al., 2012) and confirmed in this thesis in HeLa cells, which are LKB1-deficient. Therefore, given the observed requirement of $\text{PKC}\alpha$ for survival of HeLa cells, additional investigations could be carried out to elucidate if $\text{PKC}\alpha$ depletion might be synthetic lethal with MYC overexpression in the presence of LKB1.

Depletion of NUA1 was described to be lethal in combination with MYC overexpression and the mechanism for the synthetic lethality interaction involved an unrestrained mTORC1 activity, attributed to the impaired activation of AMPK in the absence of NUA1 (Liu et al., 2012). However, our data indicated that NUA1 itself can regulate mTORC1 activity, as downregulation of the $\text{PKC}\alpha$ /NUA1 axis resulted in increased protein synthesis (Fig. 3.20). In addition, our data suggested that NUA1 regulation of mTORC1 involved the inhibition of Raptor, a positive regulator of the mTORC1 complex, although this mechanism has been previously attributed to AMPK (Gwinn et al., 2008). Specifically,

inhibition or downregulation of NUA1 resulted in a decreased phosphorylation of Raptor at Ser792, a function that was conserved among cell lines and not dependent on LKB1 status (Fig. 3.19). Importantly, Raptor^{S792} phosphorylation in AMPK α 1/ α 2-depleted MEFs was still sensitive to NUA1 inhibition (Fig. 3.22), indicating that NUA1 exerts a direct and prominent role in the mechanism rather than simply assisting AMPK-mediated regulation of mTORC1.

Activation of metabolic checkpoints that restrain mTORC1, particularly under energy stress conditions, has been shown to be required for cell survival, as failure in mTORC1 inhibition ultimately leads to apoptotic cell death (Gwinn et al., 2008). Thus, taken together, our data indicate an active role of NUA1 in the inhibition of Raptor to modulate a metabolic checkpoint that favours survival of MYC-overexpressing cells. As the regulation of Raptor by NUA1 is independent of LKB1 status, it would be interesting to explore the contribution of PKC α to the regulation of NUA1 in the presence of LKB1. Previously published data have highlighted how deletion of Lkb1 strikingly reduced the levels of MYPT1^{S445} phosphorylation, indicating a major control exerted by LKB1 (Zagorska et al., 2010). However, the analysis of a single substrate might not be representative of the kinase activity as the specificity towards substrates might differ according to the type of stimulus or conditions. In addition, the physiological relevance of Ca²⁺-mediated activation of NUA1 should be explored in other conditions, as activation of receptors such as the Epidermal growth factor receptor (EGFR) by the binding of growth factors is known to generate an acute increase in intracellular Ca²⁺ levels that contributes to the downstream signal propagation. Therefore, further biochemical investigations are needed to explore additional physiological roles of the PKC α /NUA1 axis and understand its contribution to various cellular process also in the presence of LKB1.

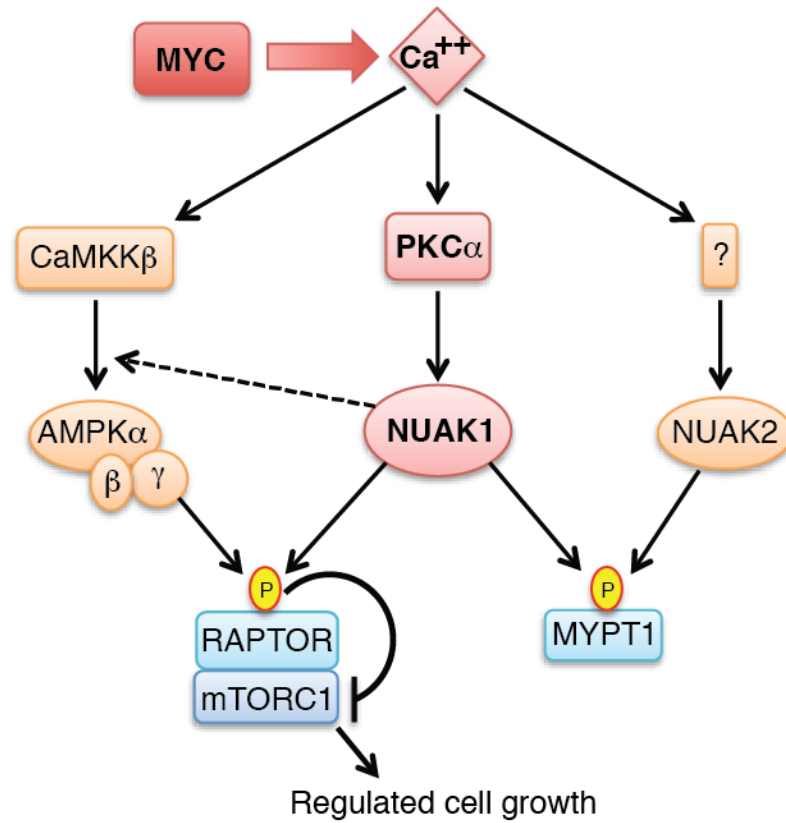


Figure 3. 23 – Proposed model for the MYC-PKC α -NUAK1 signalling pathway.

MYC amplification of Ca²⁺ signalling results in activation of downstream pathways that include the Ca²⁺-sensitive kinases CaMKK β and PKC α . The former leads to activation of AMPK, whereas the latter modulates NUAK1 activity. Activation of NUAK1 and AMPK, in part mediated by NUAK1, contributes to restrain mTORC1 activity through the inhibition of Raptor. In addition, Ca²⁺ signalling mediates the phosphorylation of MYPT1 through the induction of the PKC α /NUAK1 axis and NUAK2, for which the upstream kinase has not been identified.

Chapter 4 - Investigation of NUAK1 role in lung tumorigenesis

4.1 Introduction

Lung cancer is currently the leading cause of cancer-related deaths worldwide, with about 46,000 new cases being diagnosed in the United Kingdom every year. It can be classified in two major groups: small cell lung cancer (SCLC) and non-small cell lung cancer (NSCLC), the latter representing the 80% of all lung cancer cases. Adenocarcinoma is the predominant histological subtype of non-small cell lung cancer and it shows a high rate of somatic mutations and genomic rearrangements, making it a very complex disease. Particularly, mutations in KRAS, found in approximately 30% of patients with lung adenocarcinoma, can drive the tumorigenic process and are associated with poor prognosis and a high risk of cancer recurrence (Meng et al., 2013). Among frequently mutated genes in lung adenocarcinoma, LKB1, also known as STK11, has the third highest mutation rate after TP53 and KRAS (Ding et al., 2008). Specifically, it is altered in about 20-30% of cases of NSCLC, with a tendency towards co-occurrence with KRAS mutations (The Cancer Genome Atlas Research, 2014). In addition, pre-clinical models have established the important function of LKB1 as tumour suppressor in lung cancer (Ji et al., 2007; Sanchez-Cespedes et al., 2002).

The AMPK family is a key downstream effector of LKB1, which can positively modulate the AMPK-related kinases (ARKs) (Lizcano et al., 2004b). Through the activation of multiple ARKs, LKB1 can regulate a wide range of biological processes: from cell polarity and metabolism to angiogenesis and chromosome segregation (Bonaccorsi et al., 2007; Kottakis et al., 2016; Londesborough et al., 2008). Despite the tumour suppressor role of LKB1, multiples members of the AMPK family have been associated with a tumour-promoting role. For example, expression of NUAK1 has been linked to poor prognosis in various cancer types, such as ovarian and colorectal cancer and hepatocellular carcinoma (Cui et al., 2013; Kusakai et al., 2004; Phippen et al., 2016). In addition, the role of NUAK1 in cell adhesion and migration has been shown to contribute to tumour invasion and metastasis (Chen et al., 2017). Shi and colleagues have shown a tumour-promoting role of NUAK1 in lung cancer, as it was found to promote migration

and invasion of NSCLC cells (Shi et al., 2014). Therefore, NUA1 represents a promising target for cancer therapy.

Although a tumour-promoting role of NUA1 has been suggested in various cancer settings, with particular emphasis to its contribution to migration and invasion, the role of NUA1 in the early phases of the lung tumorigenic process has not been elucidated yet. Therefore, in this chapter we investigate the role of NUA1 in KRas-driven non-small cell lung cancer and try to understand if NUA1 exerts some of the tumour suppressor function attributed to its upstream kinase LKB1. In addition, given that MYC is dysregulated in lung cancer as result of KRAS hyperactivation (Sears et al., 2000), and also found to be amplified in a fraction of lung adenocarcinomas (Iwakawa et al., 2011), we sought to determine if the synthetic lethal interaction of NUA1 and MYC could be beneficial from a therapeutic perspective in a mouse model of NSCLC characterized by MYC overexpression.

4.1.1 Mouse models

To study the mechanism of progression of lung adenocarcinoma and investigate the contribution of NUA1 to the tumorigenic process, we made use of a mouse model in which lung tumorigenesis is driven by KRas mutation. In particular, we used a conditional strain characterized by a G12D point mutation in the exon 1 of the endogenous KRas gene. Expression of mutant KRas is prevented by a lox-stop-lox (lsl) cassette inserted in the first intron of the gene, which generates a loss of function of endogenous KRas (Jackson et al., 2001). Since homozygosity for loss of KRas is embryonically lethal, only heterozygous animals with KRas G12D mutation were obtained for the experiments. *KRas^{G12D}* was then bred to a conditional knockout of Nuak1 (*Nuak1^{F/F}*), in which the exon 3 of endogenous Nuak1 is flanked by loxP sites (Inazuka et al., 2012), to generate *lsl-KRas^{G12D}/Nuak1^{F/F}* mice (Fig. 4.1). *KRas^{G12D}/Lkb1^{F/F}* mice, in which the exon 4 of endogenous Lkb1 and a cDNA construct encoding the remainder of the LKB1 sequence, inserted in replacement of exons 5-7, are flanked by loxP sites (Sakamoto et al., 2005), were additionally used for phenotypic comparison of Lkb1 loss with Nuak1 loss.

Adenovirus-Cre, delivered intranasally, mediates the recombination of the loxP sites causing the excision of either the stop cassette preceding mutant *KRas* or the floxed exon of *Nuak1* or *Lkb1*, resulting in the induction of *KRas*^{G12D} and deletion of *Nuak1* or *Lkb1* specifically in the lungs and in a time-controlled manner.

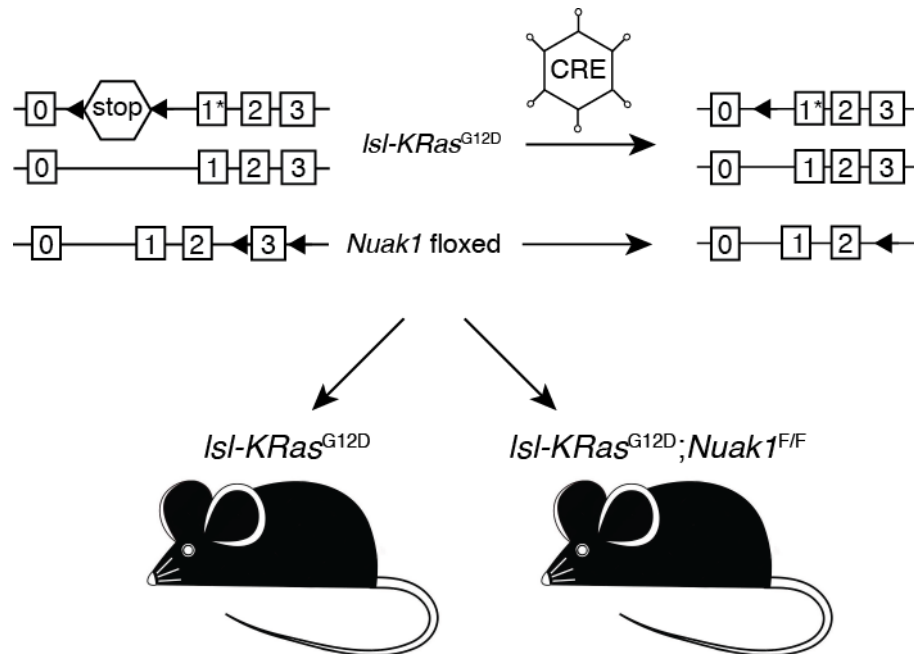


Figure 4. 1 – Schematic representation of conditional *Isl-KRas*^{G12D} and *Isl-KRas*^{G12D};*Nuak1*^{F/F} mouse model.

4.2 Results

4.2.1 *KRas*-mutant lung tumours develop as adenocarcinoma even in the absence of *Nuak1*

Squamous cell carcinoma (SCC) and Adenocarcinoma (ADC) are the two major histological types of non-small cell lung cancer. Previous studies have indicated that *KRas*^{G12D} and *KRas*^{G12D}/*p53*^{F/F} mice develop only adenocarcinoma (Jackson et al., 2005; Jackson et al., 2001; Rekhtman et al., 2012) whereas loss of function of the tumour suppressor LKB1, the major upstream kinase of NUAK1, has been observed in both lung adenocarcinoma and squamous cell carcinoma (Ji et al., 2007; Sanchez-Cespedes et al., 2002). In addition, it has been shown that *Lkb1* deletion resulted in trans-differentiation of adenocarcinoma into squamous cell

carcinoma in a mouse model of non-small cell lung cancer driven by *KRas*^{G12D} mutation, giving rise to a more complex phenotype (Li et al., 2015a). Therefore, we asked if *Nuak1* deletion could phenotypically resemble *Lkb1* deletion and contribute to tumour heterogeneity.

KRas^{G12D} only, *KRas*^{G12D}/*Lkb1*^{F/F} and *KRas*^{G12D}/*Nuak1*^{F/F} mice were induced with the same dose of Adenovirus-Cre and lungs were harvested at 16 weeks post Adeno-Cre infection. As expected, histological examination of lung lesions from *KRas*^{G12D}/*Lkb1*^{F/F} revealed a heterogeneity of tumours, some characterized by solid or papillary growth, typical of the adenocarcinoma subtype (Fig. 4.2, panel A), and others characterized by keratin pearls and cell nests forming round nodules, typical of squamous cell carcinoma (Fig. 4.2, panel B). Contrariwise, *KRas*^{G12D} only and *KRas*^{G12D}/*Nuak1*^{F/F} tumours displayed characteristics of the ADC subtype (Fig. 4.2, panel C and D, respectively). The histological subtypes were then confirmed by immunohistochemical staining for SCC and ADC markers: p63 and the surfactant apoprotein-C (SP-C), respectively. Indeed, *KRas*^{G12D}/*Lkb1*^{F/F} tumours with SCC features were positive for p63 staining while ADC stained positively for SP-C; all *KRas*^{G12D} only and *KRas*^{G12D}/*Nuak1*^{F/F} tumours were negative for p63 but positive for SP-C (Fig. 4.2). Therefore, *Nuak1* deletion did not contribute to the trans-differentiation from ADC to SCC driven by *Lkb1* loss, as ADC was the only histological subtype observed in *KRas*^{G12D}/*Nuak1*^{F/F} lung tumours.

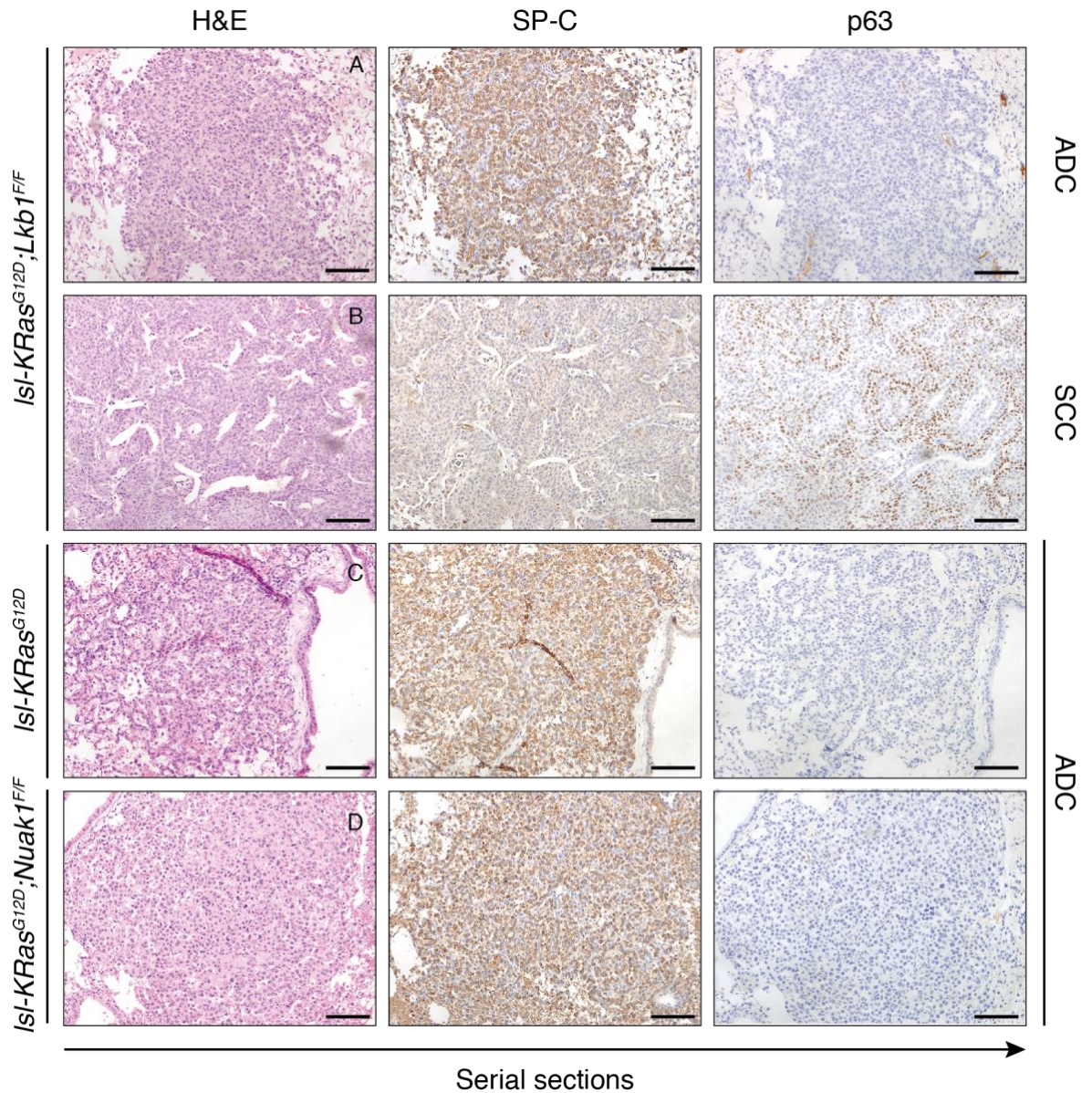


Figure 4. 2 – KRas^{G12D}/Nuak1^{F/F} mice develop only lung adenocarcinoma.

Representative images of lsl-KRas^{G12D};Lkb1^{F/F}, lsl-KRas^{G12D};Nuak1^{F/F} and lsl-KRas^{G12D} lung tumour sections stained with Hematoxylin & Eosin, SP-C and p63. Scale bars = 200 μm.

4.2.2 Deletion of *Nuak1* does not affect the cell of origin of *KRas*-mutant lung adenocarcinoma

Although multiple studies have tried to identify the cell of origin of lung adenocarcinoma, there is still some controversy on its histogenesis. Alveolar type 2 cells (AT2) and Clara cells are the two cell types that have been debated for being the initiating cells in *KRas*-mutant lung adenocarcinoma, as tumours stain positively for AT2 and Clara cells markers such as SP-C and CC10, respectively (Jackson et al., 2001; Sutherland et al., 2014). To investigate if *Nuak1* deletion could influence the cell of origin of *KRas*-driven lung adenocarcinoma, tissue sections of *KRas*^{G12D}/*Nuak1*^{F/F} and *KRas*^{G12D} tumours were stained for SP-C and CC10 markers. As already shown in figure 4.2, *KRas*^{G12D} and *KRas*^{G12D}/*Nuak1*^{F/F} adenomas stained positive for SP-C, whereas epithelial hyperplasia of the bronchioles (EH) showed positivity for the CC10 marker (Fig. 4.3A). In addition, as previously revealed by Jackson and colleagues (Jackson et al., 2001), regions of epithelial hyperplasia that were continuous with atypical adenomatous hyperplasia (AAH) in *KRas*^{G12D}/*Nuak1*^{F/F} and *KRas*^{G12D} mice stained positive for both SP-C and CC10 (Fig.4.3B). Overall, *Nuak1* deletion does not appear to influence the histogenesis of *KRas*^{G12D} tumours.

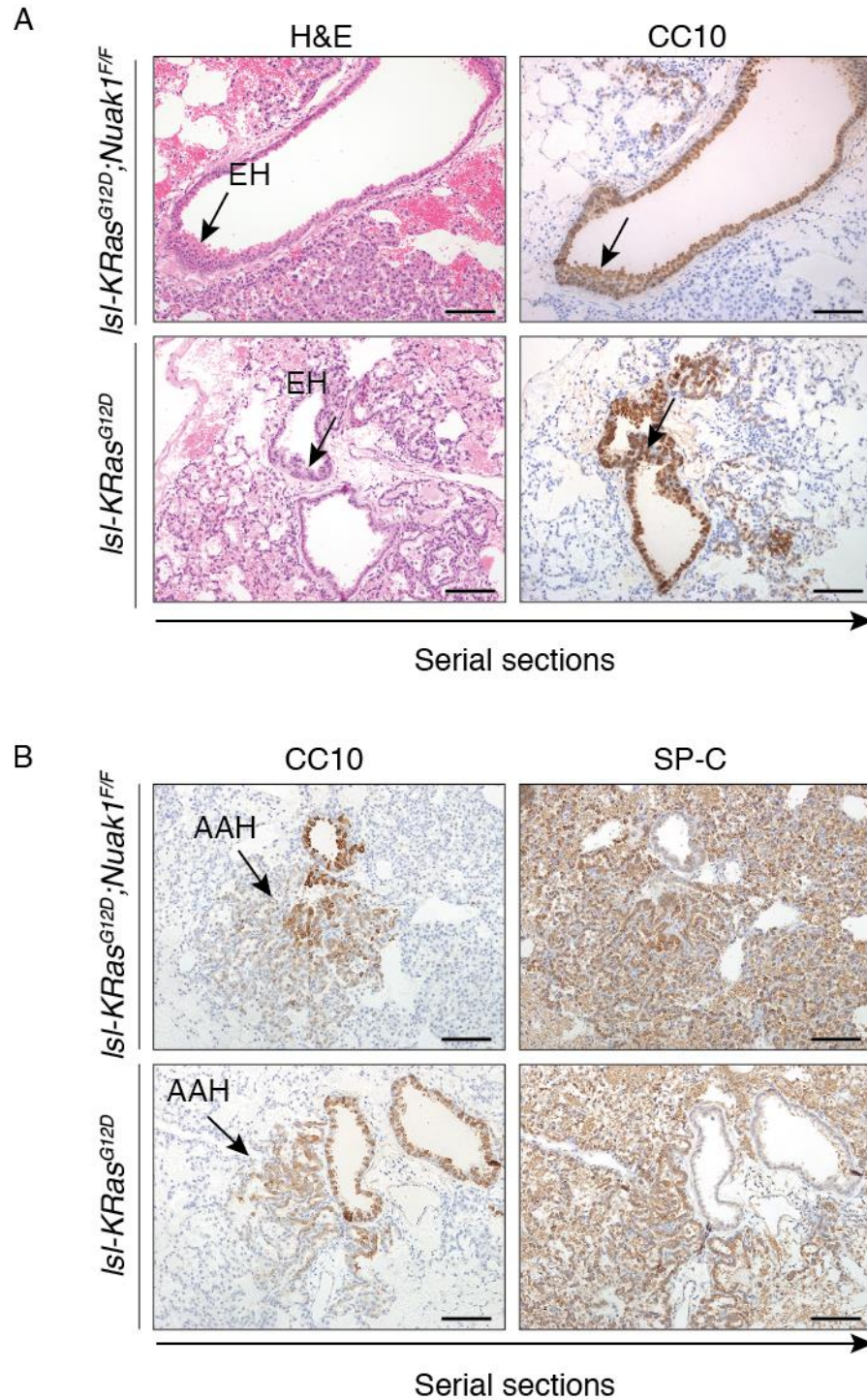


Figure 4. 3 – Nuak1 deletion does not affect the histogenesis of KRas^{G12D} lung adenocarcinoma.

A, Representative pictures of epithelial hyperplasia of the bronchioles (EH) in *Isl-KRas^{G12D};Nuak1^{F/F}* and *Isl-KRas^{G12D}* lung tumour sections at 16 weeks post Adeno-Cre infection stained for H&E and CC10. Scale bars = 200 μ m. **B**, Representative pictures of EH lesions continuous with atypical adenomatous hyperplasia (AAH) in *Isl-KRas^{G12D};Nuak1^{F/F}* and *Isl-KRas^{G12D}* lung tumour sections stained with SP-C and CC10.

4.2.3 *Nuak1* deletion does not affect *KRas*-driven tumorigenic process

The tumour suppressor LKB1, which is the master upstream kinase of NUA1, has been previously shown to exert an important tumour suppressor role in lung tumorigenesis, as loss of *Lkb1* gave rise to a more aggressive disease in a mouse model of non-small cell lung cancer driven by *KRas*^{G12D} mutation (Ji et al., 2007). Therefore, we sought to investigate if *Nuak1* could also function as tumour suppressor in the same setting. The tumour burden of *KRas*^{G12D}/*Nuak1*^{F/F} and *KRas*^{G12D} only mice, infected with the same dose of Adenovirus-Cre, was analysed at 16 weeks post infection. The analysis revealed that *Nuak1* deletion did not affect the tumorigenic process driven by *KRas*^{G12D}, as no significant difference in tumour burden was observed in *KRas*^{G12D}/*Nuak1*^{F/F} mice compared to *KRas*^{G12D} only (Fig. 4.4).

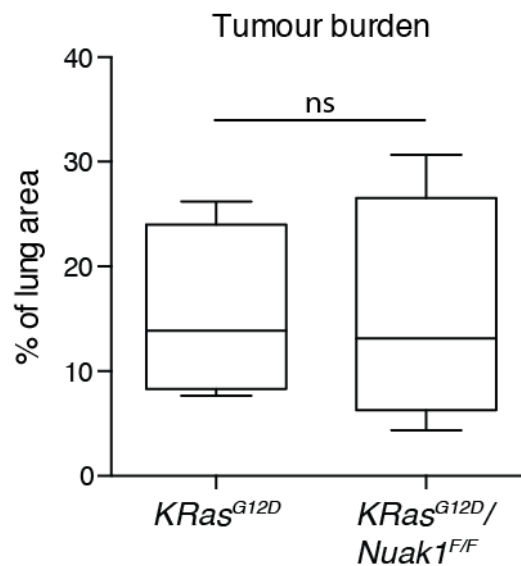


Figure 4. 4 – *Nuak1* deletion does not affect *KRas*^{G12D}-driven lung tumorigenesis. Box plots representing the tumour burden (Mean \pm SEM) of *KRas*^{G12D} (n=4) and *lsl-KRas*^{G12D};*Nuak1*^{F/F} (n=4) mice at 16 weeks post Adeno-Cre infection. ns = not significant. P value calculated with two-tailed unpaired T test.

4.2.4 Characterization of *Nuak1* deletion in *KRas*^{G12D}/*MYC* lung adenocarcinoma

Given the previously described synthetic lethal interaction between *MYC* and *NUAK1* in *MYC*-overexpressing cells (Liu et al., 2012), we were interested in exploring the effect of *Nuak1* deletion in a mouse model driven by *KRas* G12D mutation with the addition of *MYC* overexpression. Therefore, *KRas*^{G12D} mice were bred with a conditional model of *MYC* overexpression, in which *lsl*-human *MYC* is expressed under the control of the *Rosa26* (*R26*) locus. Homozygous animals for the *R26-lsl-MYC* allele were used in all the experiments.

The *lsl-KRas*^{G12D}/*R26-lsl-MYC* NSCLC mouse model (referred to as KM) has been previously characterized by a former colleague, Dr Sarah Neidler, who showed how a moderate overexpression of *MYC* can drastically accelerate the lung tumorigenic process driven by *KRas* G12D mutation, as indicated by the significant increase in tumour burden in KM mice compared to *KRas*^{G12D} only (Fig. 4.5A-B).

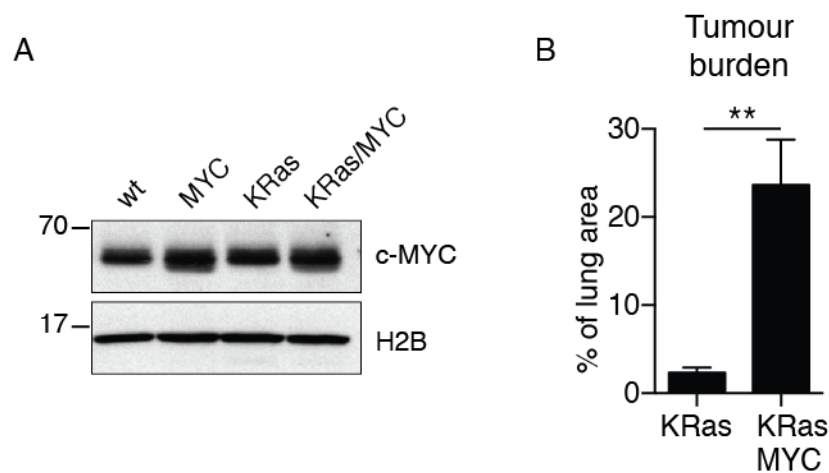


Figure 4. 5 - Moderate overexpression of *MYC* accelerates *KRas*^{G12D}-driven lung cancer.

A, Mouse Embryonic Fibroblasts of the indicated genotypes were infected with Adenovirus-Cre and whole cell protein extracts immunoblotted for c-MYC and H2B. B, Box plots representing the tumour burden (Mean \pm SEM) of *lsl-KRas*^{G12D} (n=4) and *lsl-KRas*^{G12D};*R26-lsl-MYC* (n=4) mice at 6 weeks post Adeno-Cre infection (data generated by Sarah Neidler). ** $p < 0.01$ value calculated with two-tailed unpaired T test.

To investigate the role of Nuak1 in lung tumorigenesis in a setting of MYC overexpression, *KRas*^{G12D}/MYC and *KRas*^{G12D}/MYC/*Nuak1*^{F/F} mice (referred to as KMN) were infected with the same dose of Adenovirus-Cre and lungs harvested at 6 weeks post infection.

Histological examination of *KRas*^{G12D}/MYC lungs revealed the presence of multiple lesions: from epithelial hyperplasia of the bronchioles (EH) to atypical adenomatous hyperplasia and adenomas (Fig. 4.6, panel A, B, C, respectively). Furthermore, the observed adenomas were characterized by a predominant papillary structure, displaying a fibrovascular core lined by tumour cells with slightly enlarged nuclei and prominent nucleoli. Similarly, lesions observed in *KRas*^{G12D}/MYC/*Nuak1*^{F/F} mice were also represented by EH, atypical adenomatous hyperplasia and adenomas (Fig. 4.6, panel D, E, F). However, upon Nuak1 deletion adenomas presented an acinar-predominant pattern, in which tumours formed glandular structures and presented cord-like arranged tumour cells (Fig. 4.6, panel F).

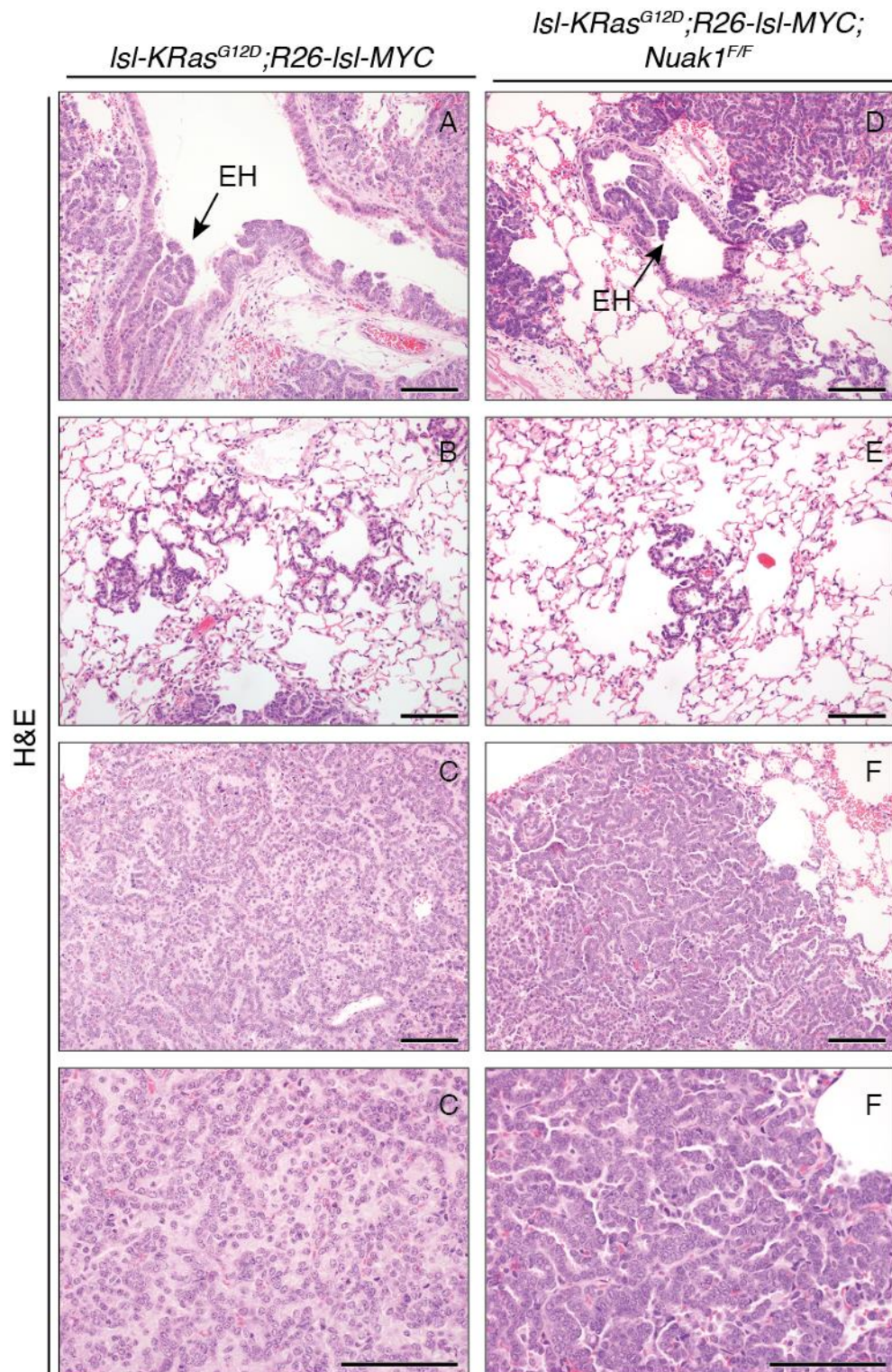


Figure 4. 6 – Histological examintaion of KM and KMN tumours.

Representative H&E pictures of epithelial hyperplasia of the bronchioles (EH, A-D), adenomatous hyperplasia (B-E) and adenoma (C-F) of *lsl-KRas^{G12D};R26-lsl-MYC;Nuak1^{F/F}* and *lsl-KRas^{G12D};R26-lsl-MYC* lung sections at 6 weeks post Adeno-Cre infection. Scale bars = 200 μ m.

4.2.5 MYC overexpression is not synthetically lethal with Nuak1 deletion in KRas-driven NSCLC

To further characterize the effect of Nuak1 deletion in *KRas*^{G12D}/*MYC* lung tumours, the analysis of the proliferation rate was carried out by examination of the incorporation of Bromodeoxyuridine (BrdU), the synthetic analogue of thymidine, into newly synthesized DNA of cancer cells. KMN tumours did not differ in the levels of BrdU incorporation in comparison to KM tumours, as indicated by the quantification of the immunohistochemistry staining (Fig. 4.7A). In agreement with the comparable levels of proliferation, the tumour burden at 6 weeks post infection was not significantly different in KMN mice compared to KM (Fig. 4.7B).

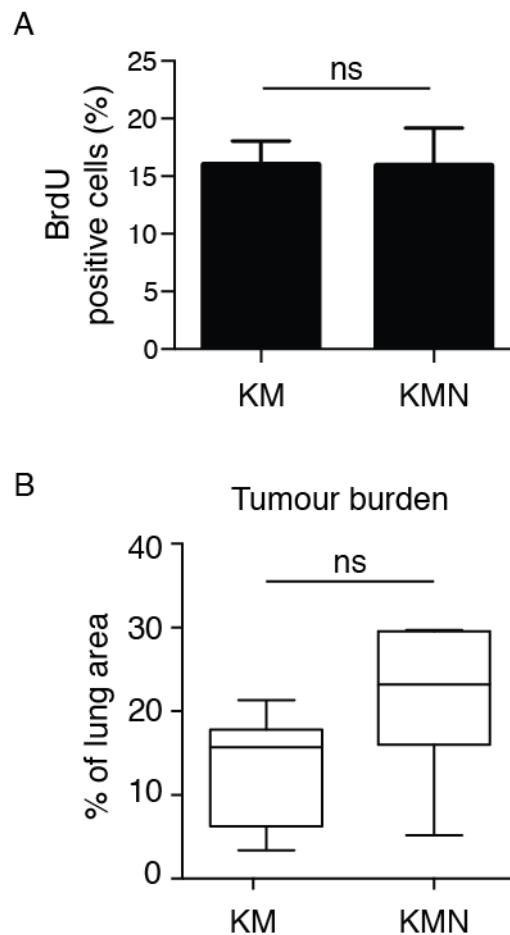


Figure 4. 7 – Deletion of Nuak1 does not affect growth of KRas/MYC lung tumours. A, Bar graphs representing the Mean \pm SEM of BrdU positively stained cells from KM (n=3) and KMN (n=3) lung tumours at 6 weeks post Adeno-Cre infection. B, Box plots representing the tumour burden (Mean \pm SEM) of KM (n=7) and KMN (n=7) mice at 6 weeks post Adeno-Cre infection. ns = not significant. P value calculated with two-tailed unpaired T test.

4.2.6 Upregulation of the PI3K/AKT pathway in *Nuak1* deleted lung tumours

The Raf/MEK/ERK cascade is a major effector downstream of RAS and is a very important contributor to cell survival and proliferation, often dysregulated in cancer. In addition, increased activation of ERK1/2, as indicated by increased phosphorylation levels, has been correlated with more advanced and aggressive tumours in patients with NSCLC (Vicent et al., 2004). Therefore, we sought to assess ERK1/2 activation status in *KRas*^{G12D}/*MYC* lung tumours and we observed a minority of adenomas characterized by areas that were positive for immunohistochemical staining with phospho-ERK (Fig. 4.8A, panel ii). Interestingly, those specific regions also featured a distinctive morphology, indicative of a more aggressive phenotype: a much lower degree of organization and a loss of cell polarity (Fig. 4.8A, panel i). Furthermore, histological examinations of lungs after 4-5 months from Adeno-Cre infection revealed a higher and wider occurrence of phospho-ERK positive regions, suggesting that the distinctive tumour regions identified at 6 weeks are aggressive sub-clones that predominate as tumours progress to a more advanced disease (Fig. 4.8B). In contrast, analysis of phospho-ERK in *KRas*^{G12D}/*MYC*/*Nuak1*^{F/F} adenomas at 6 weeks post infection showed a significant reduction of the number of phospho-ERK positive tumours (Fig. 4.8C).

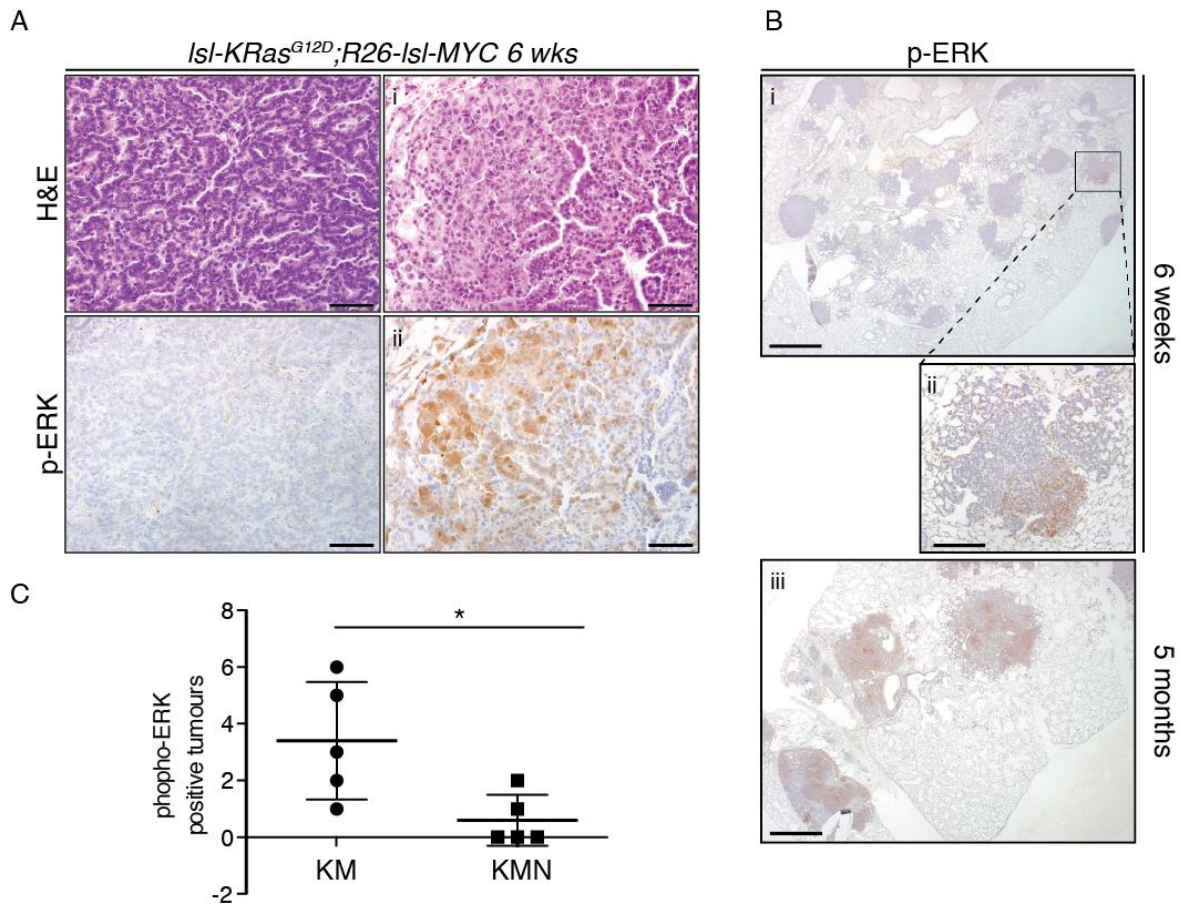


Figure 4. 8 – Nuak1 deletion decreases signalling through ERK.

A, Representative pictures of KM lung tumours stained for H&E and phospho-ERK at 6 weeks post Adeno-Cre infection, depicting the morphological changes associated with progression (panel i and ii). Scale bars = 50 μ m. **B**, Representative pictures of KM lung tumours stained for phospho-ERK at 6 weeks (panel i and ii) in comparison to 5 months post Adeno-Cre infection (panel iii). Scale bars = 1 mm (i and iii), 200 μ m (ii). **C**, Scatter dot plot representing the number \pm SEM of phospho-ERK positive lung tumours per mouse from KM (n=5) and KMN (n=5) mice at 6 weeks post Adeno-Cre infection. * $p < 0.05$ calculated with two-tailed unpaired T test.

A similar phenotype has been previously observed in *KRas^{G12D}/Lkb1^{F/F}* lung tumours, which showed decreased phospho-ERK levels in comparison to *KRas^{G12D}* tumours (Chen et al., 2012). In addition, the same study revealed an increased activity of the AKT and SRC pathways, suggesting that *Lkb1* deleted tumours rewire their dependency from MEK/ERK to AKT and SRC pathways to sustain their growth. Therefore, given the observed decrease in phospho-ERK levels upon *Nuak1* deletion, we were interested in exploring if upregulation of the PI3K/AKT pathway represented an alternative mechanism to sustain tumour growth in *KRas^{G12D}/MYC/Nuak1^{F/F}* as in *KRas^{G12D}/Lkb1^{F/F}* mice.

Staining for phospho-AKT^{S473} revealed an increased positivity of lung tumours when Nuak1 was deleted compared to wild type controls (Fig. 4.9).

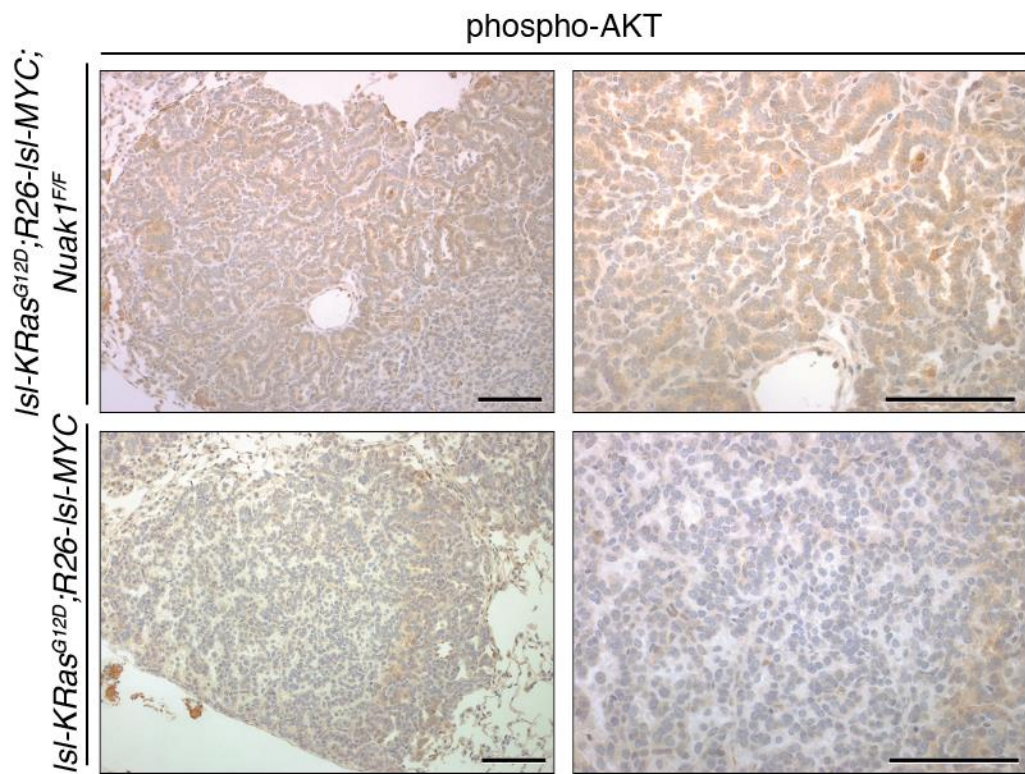


Figure 4. 9 – Nuak1 deletion results in increased AKT phosphorylation in lung tumours.

Representative pictures of phospho-AKT (Ser473) staining of KM and KMN lung tumours at 6 weeks post Adeno-Cre infection. Scale bars = 200 μ m.

4.2.7 Deletion of Nuak1 does not sensitize lung tumours to mTORC1 inhibition

One of the major effectors of the PI3K/AKT signalling cascade is mTORC1, which positively regulates protein synthesis to sustain cell growth. Given the higher AKT phosphorylation observed in Nuak1 deleted lung tumours and considering the regulation of the mTORC1 subunit Raptor by NUA1, highlighted in our studies (Chapter 3), we decided to investigate the activation of mTORC1 in our tumour model. Thus, we performed immunohistochemical staining for downstream effectors of mTORC1: phospho-4E-BP1 and phospho-S6. As shown in figure 4.10, deletion of Nuak1 resulted in an increase in phospho-4E-BP1 staining compared

to wild type tumours, whereas no significant difference was observed regarding phospho-S6.

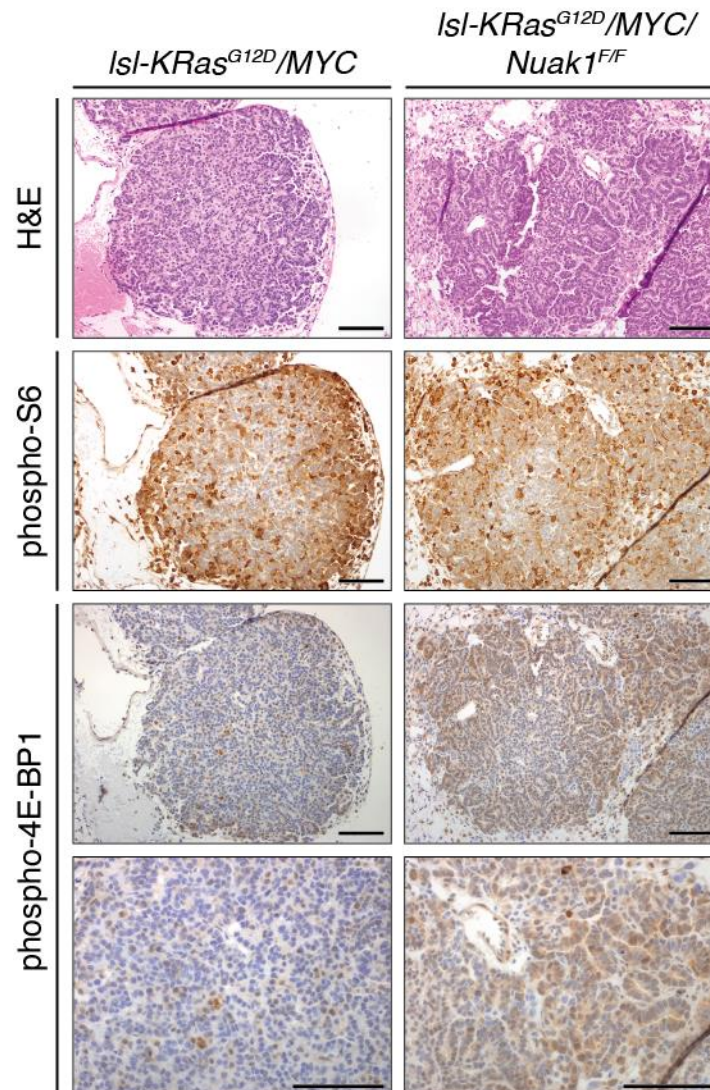


Figure 4. 10 – Nuak1 deletion results in increased phosphorylation of 4E-BP1.

Representative pictures of KM and KMN lung tumour sections at 6 weeks post Adeno-Cre infection stained with H&E, phospho-S6 (Ser235/236) and phospho-4E-BP1 (Thr37/46). Scale bars = 200 μ m.

LKB1 has been shown to negatively regulate mTORC1 (Shaw et al., 2004a) and LKB1-deficient NSCLC cells displayed a higher sensitivity to inhibition of the PI3K-mTORC1 signalling pathways (Whang et al., 2016). Thus, in light of the higher mTORC1 activity observed in Nuak1 deleted tumours, we sought to test the effect of mTORC1 inhibition.

KMN and KM mice at 6 weeks post Adeno-Cre infection were treated acutely with the mTORC1 inhibitor Rapamycin. As shown in figure 4.11A, Rapamycin could efficiently inhibit tumour cell proliferation in both KM and KMN lung tumours, as assessed by BrdU incorporation, but no increased sensitivity was observed in correlation to Nuak1 deletion. In addition, apoptotic levels in response to rapamycin treatment were not significantly different between KM and KMN tumours (Fig. 4.11B), suggesting overall that Nuak1 deletion did not confer higher sensitivity to inhibition of mTORC1 activity.

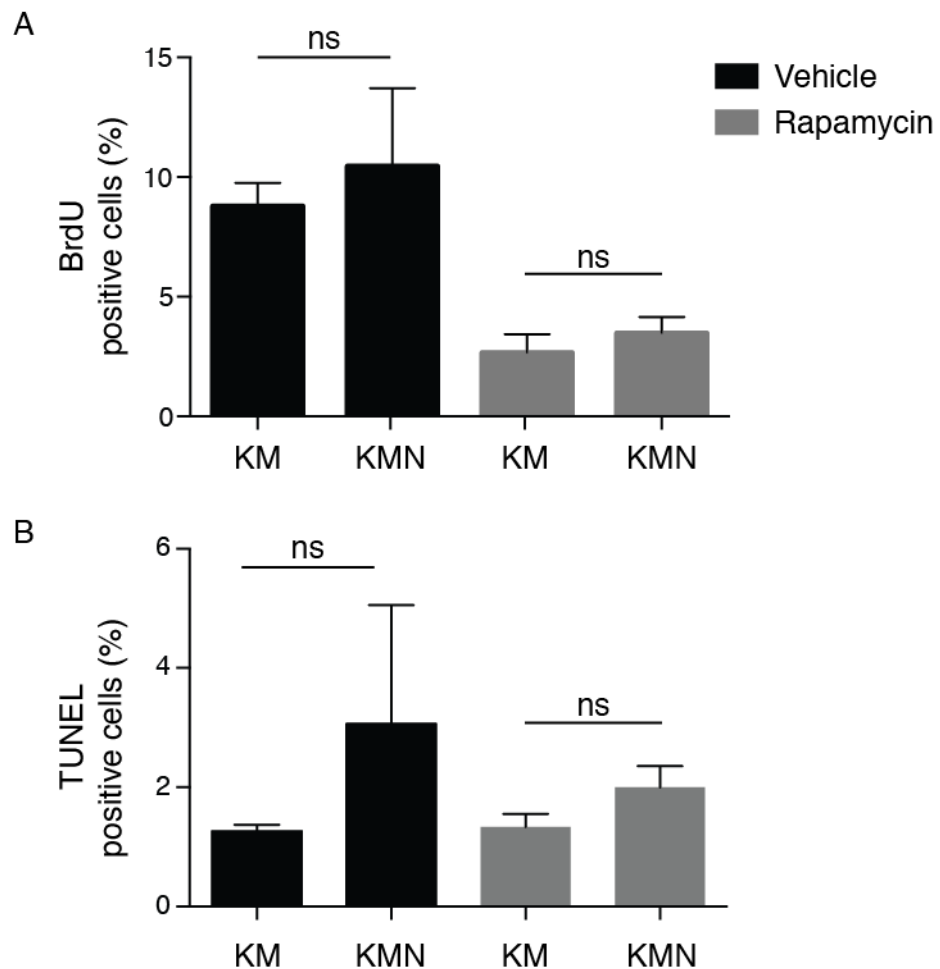


Figure 4. 11 – Nuak1 deletion does not sensitize tumours to mTORC1 inhibition.

Bar graphs representing the Mean \pm SEM of BrdU (A) and TUNEL (B) positively stained lung tumour cells from KM (n=3) and KMN (n=3) mice treated with vehicle or Rapamycin for 3 days at 6 weeks post Adeno-Cre infection. ns= not significant. P value calculated with one-way ANOVA, Tukey's multiple comparison.

4.2.8 Deletion of Nuak1 confers a survival advantage to *KRas*^{G12D}/*MYC* mice

Although the tumour burden analysed at 6 weeks post infection did not significantly differ between KM and KMN mice, the observation of phospho-ERK positive regions in KM adenomas, which were absent in KMN tumours, suggested that Nuak1 deletion affected the onset of aggressive tumour sub-clones. Interestingly, a negative correlation between high cytoplasmic phospho-ERK levels and survival of patients with NSCLC has been previously described (Vicent et al., 2004). In addition, preliminary data on the immunohistochemical analysis of CD31 staining, marker of endothelial cells, at 6 weeks post infection revealed a significant reduction in the number of blood vessels in KMN tumours in comparison to KM (Fig. 4.12).

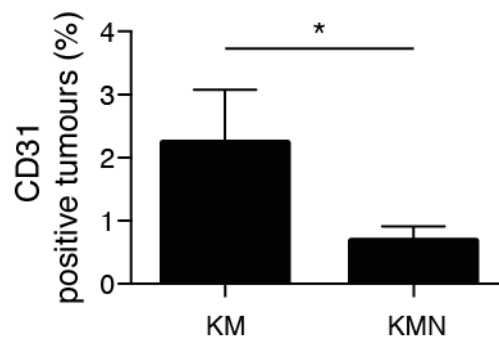


Figure 4. 12 – Nuak1 deletion affects tumour blood vessels.

Bar graphs representing the Mean \pm SEM of CD31 positively stained lung tumour blood vessels from KM (n=2) and KMN (n=3) mice at 6 weeks post Adeno-Cre infection. * p<0.05 calculated with two-tailed unpaired T test. Data generated in collaboration with Lisa Neilson and Dr Sara Zanivan from the Beatson Institute.

Thus, we sought to determine if Nuak1 deletion could have an impact on overall survival in our tumour model. Given the asphyxia caused by the large tumour load obtained with the high dose of Adenovirus-Cre used in the previous experiments, which limits an adequate study of long term survival benefits, KM and KMN mice were infected with a lower dose of Adenovirus-Cre and sacrificed at clinical end-point, i.e. when animals showed signs of respiratory distress, deterioration of body conditions and behavioural changes. As shown in figure

4.13, Nuak1 deletion resulted in a significant increase in survival of KM mice, suggesting a long-term benefit of Nuak1 deletion in NSCLC.

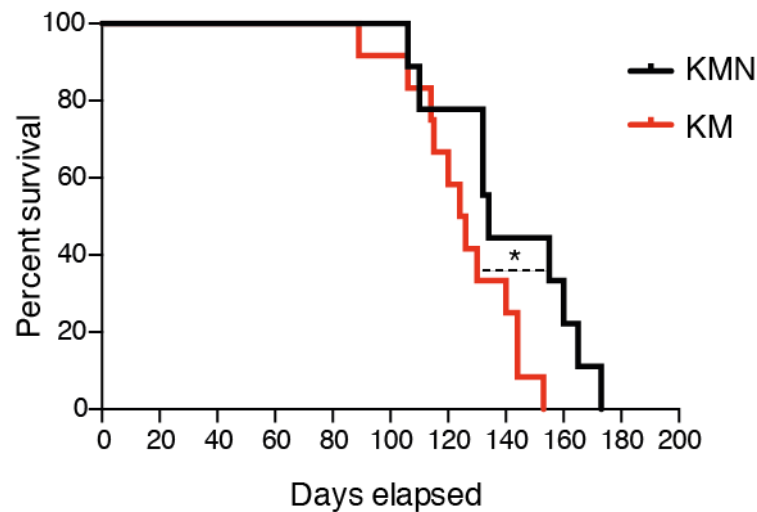


Figure 4. 13 – Nuak1 deletion enhances survival of KRas^{G12D}/MYC lung tumours-bearing mice.

Kaplan-Meier survival analysis of KM (n=12) and KMN (n=9) mice induced with a low titer of Adenovirus-Cre (3×10^5 pfu). * $p < 0.05$ determined by log-rank (Mantel-Cox) test.

4.3 Discussion

The Liver Kinase B1 (LKB1), also known as *STK11*, has been identified as the third most frequently mutated gene in lung adenocarcinoma. In addition, the tumour suppressor role of LKB1 in lung cancer has been compellingly determined in pre-clinical models of lung cancer. Specifically, deletion of *Lkb1* in a mouse model of NSCLC driven by KRas^{G12D} showed an acceleration of the disease with enhanced metastatic potential (Ji et al., 2007). However, the data described in this chapter suggest that NUAK1, as downstream effector of LKB1, does not reflect the potent tumour suppressor role of its upstream kinase. Our results indicate that Nuak1 deletion in the lungs does not accelerate the tumorigenic process driven by mutant KRas, as simultaneous deletion of Nuak1 and expression of KRas^{G12D} did not affect the tumour burden in comparison to KRas^{G12D} only (Fig. 4.4). Also, whereas *Lkb1* deletion has been shown to mediate trans-differentiation of lung adenocarcinoma into squamous cell carcinoma (Li et al., 2015a), here we provide evidence that Nuak1 deletion does not recapitulate

a similar phenotype as only the adenocarcinoma subtype was detected in *KRas*^{G12D}/*Nuak1*^{F/F} lungs at 16 weeks post Adeno-Cre infection (Fig. 4.2).

Although deletion of *Nuak1* did not have an impact on the tumorigenic process driven by mutant *KRas* in the lungs, other studies have suggested a beneficial effect of NUA1 inhibition in multiple cancer settings. Particularly, a previous synthetic lethality screening done by Liu and colleagues identified NUA1 as being required for survival of *MYC*-overexpressing cells (Liu et al., 2012). Interestingly, the study showed that depletion of NUA1 impaired the graft of hepatoma cells expressing *MYC* and resulted in a significant extension in survival of tumour-bearing mice. We characterized the effect of *Nuak1* deletion in a genetically engineered mouse model for NSCLC driven by *KRas*^{G12D} mutation and accelerated by *MYC* overexpression (KM model). Remarkably, upon *Nuak1* deletion (KMN model) we observed a change of the histological features of lung adenomas, which were characterized by predominant acinar structures in contrast to *Nuak1* wild type tumours that presented a papillary predominant growth. Despite these morphological differences, at 6 weeks post infection the levels of tumour cells proliferation did not significantly differ between KM and KMN lung tumours (Fig. 4.7A), in agreement with the observation of the unchanged tumour burden (Fig. 4.7B). Clinical data have suggested that there is not a significant difference in terms of survival between the papillary and acinar types of tumours, whereas the micropapillary subtype has been reported to have the worst survival outcome (Russell et al., 2011). Therefore, currently the biological meaning and clinical implications of the transition from a papillary to an acinar subtype are not yet understood.

The MEK/ERK cascade downstream of Ras is frequently dysregulated in cancer and we identified enhanced ERK activation, suggested by increased phosphorylation levels, as KM tumours progress to more advanced stages. Furthermore, increased phospho-ERK levels were associated with tumour regions featuring morphological hallmarks of progression, such as loss of cell polarity and enlarged nuclei (Fig. 4.8A-B). Although *Nuak1* deletion did not affect the tumour burden of KM mice at 6 weeks post Adeno-Cre infection, it resulted in a reduced level of ERK activation while increasing AKT phosphorylation (Fig. 4.8C and 4.9). AKT has been suggested as an alternative kinase for NUA1 but a reciprocal role of NUA1 regulating AKT has not been described yet. Further

analyses are needed to uncover the mechanism of the observed upregulation of AKT in the absence of NUAK1. Moreover, analysis of phospho-4E-BP1 and phospho-S6, which are targets of mTORC1, a downstream effector of AKT, revealed higher phosphorylation levels of 4E-BP1 in KMN tumours in comparison to KM tumours (Fig. 4.10).

Raptor has been shown to recruit 4E-BP1 to the mTORC1 complex, facilitating its phosphorylation (Hara et al., 2002). Therefore, as we uncovered that NUAK1 contributes to Raptor inhibition (Fig. 3.15), it is possible that the preferential phosphorylation of 4E-BP1 over S6 is a result of Raptor activation in Nuak1 deleted lung tumours.

The LKB1/AMPK axis is well known for regulating protein synthesis (Shaw et al., 2004a). In particular, AMPK can modulate mTORC1 activity through the negative regulation of Raptor and the positive regulation of TSC2, an inhibitor of mTORC1. In addition, Lkb1 deletion has been shown to increase mTORC1 activation both *in vitro* and *in vivo* and our data suggested a similar role for Nuak1 (Fig. 3.10 and Fig. 4.10). Therefore, targeting the increased protein synthesis that is required for highly proliferative cells, such as tumour cells, to sustain their growth appeared as a potential therapeutic strategy. Although Nuak1 deletion resulted in an increase of mTORC1 activity it did not sensitise tumour cells to Rapamycin. However, there is discordant evidence on the efficacy of mTORC1 inhibition in inducing cell death of LKB1-null cancer cells. Particularly, an *in vitro* study carried out by Whang and colleagues using wild type and LKB1-null human lung cancer cell lines highlighted the higher sensitivity of the latter to mTORC1 inhibition using Rapamycin, as demonstrated by the decreased viability and colony formation of LKB1-null cells as compared to LKB1 wild type cells upon treatment (Whang et al., 2016). Conversely, other studies have disproved the increased sensitivity of LKB1-null cells to mTOR inhibitors, suggesting a feedback activation of the AKT pathway that overcomes mTOR inhibition (Xiao et al., 2015). Similarly, Momcilovic and colleagues have shown the lack of relation between LKB1 status and sensitivity to the mTOR inhibitor MLN0128 (Momcilovic et al., 2015). Moreover, multiple studies have suggested that Rapamycin has a differential effect on 4E-BP1 and S6K, which is the upstream kinase of S6. Treatment with Rapamycin was shown to repress S6K activity in a sustained manner, whereas phosphorylation levels of 4E-BP1 were re-established after an initial inhibition (Choo et al., 2008). Given the increase

of phospho-4E-BP1 but not of phospho-S6 observed in Nuak1 deleted tumour, one possibility is that the inefficiency of Rapamycin to inhibit 4E-BP1 is the cause of the lack of enhanced sensitivity of KMN tumours. We have not established whether phosphorylation of 4E-BP1 occurs independently of mTORC1 activation in our model, as it has been suggested an AKT-dependent modulation of the substrate, in which case inhibition of AKT might represent a better therapeutic approach. However, testing of ATP-competitors for mTORC1 that more efficiently inhibit 4E-BP1 phosphorylation might give more information on the contribution of mTORC1 to proliferation and survival of Nuak1 deleted tumour cells.

An important finding of this study that will be confirmed and further explored is the potential role of NUAK1 in tumour angiogenesis, as the percentage of tumour blood vessels was decreased in Nuak1 deleted lung tumours in comparison to wild type (Fig. 4.12). Interestingly, a role of LKB1 in angiogenesis has been previously highlighted by multiple research groups, although with conflicting findings. In particular, deletion of *Lkb1* was reported to cause vascular abnormalities, among others, in the developing embryos, with alterations in sprouting and maturation of blood vessels (Ylikorkala et al., 2001). An additional study carried out in adult mice described a similar role of LKB1 in supporting angiogenesis, since it was observed that formation of new blood vessels following an ischemic insult was impaired in mice bearing *Lkb1* deletion in endothelial cells (Ohashi et al., 2010). However, other studies have provided evidence towards an antiangiogenic role of LKB1. For example, it was recently described that tumour implanted in mice with endothelial deletion of *Lkb1* displayed increased angiogenesis in comparison to *Lkb1* wild type endothelial cells (Zhang et al., 2017). Additional investigations have corroborated an antiangiogenic function of LKB1, proposing multiple mechanisms: from regulation of VEGF to degradation of the angiogenic receptor neuropilin-1 (NRP-1) (Liang et al., 2014; Okon et al., 2014). Overall, LKB1 might play a dual role in angiogenesis, which could differ according to tissues or development stage.

We have not established if the angiogenic role of NUAK1 in our tumour model is dependent on the upstream kinase LKB1, which will require additional analysis. However, we also need to consider that the observed involvement of NUAK1 in tumour angiogenesis might not be related to LKB1 because, as highlighted by

data obtained in this chapter, LKB1 does not seem to mediate its tumour suppression functions in lung tumorigenesis through NUA1. Moreover, some functions exerted by NUA1 are not shared by LKB1 but actually contradicting with it. For example, whereas LKB1 has been shown to suppress cell invasion and its deletion to increase the metastatic potential, NUA1 role in promoting invasion and metastasis has been compellingly established in multiple settings. Therefore, it appears that the two kinases may not lie within the same path for all their functions.

Further investigations in our KMN model might clarify NUA1's involvement in angiogenesis and elucidate the mechanisms through which its deletion contributed to the observed extension of survival (Fig. 4.13). Deletion of *Nuak1* did not affect tumour cells proliferation in the presence of *MYC* overexpression at 6 weeks post infection. However, previous studies and also unpublished data from our laboratory indicate that NUA1 expression increases with tumour progression. Therefore, the progression to more advanced stages and the related increase in metabolic stress might impose a more prominent and long-term dependence on NUA1 for survival of *MYC* overexpressing cells. Furthermore, *Nuak1* deletion might contribute to the inhibition of the metastatic process and together with an impairment in tumour vasculature, which is essential in providing oxygen and nutrients to tumour cells as well as a route for metastatic dissemination, oppose cancer progression, establishing itself as tumour promoter in NSCLC as opposed to LKB1.

Chapter 5 - The role of the ERBB network in supporting KRas mutant lung adenocarcinoma

5.1 Introduction

KRAS is a member of the RAS family of small GTPase together with the H- and N-RAS isoforms. The RAS family of genes is often mutated in cancer, with activating mutations in KRAS frequently found in three of the four most lethal cancers: pancreatic adenocarcinoma, colorectal adenocarcinoma and lung adenocarcinoma (Oikonomou et al., 2014). Most mutations are found at the residue G12 of KRAS and they cause the formation of a persistent GTP-bound form, which represents a constitutively active state. Interestingly, alterations of RAS genes are events that occur in the early phases of tumour initiation but multiple experimental evidence point towards a role of continued expression of mutant RAS in tumour maintenance as well, corroborating its important role in the different stages of cancer progression (Brummelkamp et al., 2002; Singh et al., 2009).

Despite the significant progress made in the understanding of RAS biology since the first detection of its activating mutations in human cancer in 1982 (Parada et al., 1982; Santos et al., 1982), targeted therapies for KRAS mutant cancers are lacking and they still represent a challenge for clinical oncology. Many attempts have been made to inhibit RAS and over time the efforts have been broadened from targeting RAS activity to affecting RAS function by interfering with its localization or by inhibiting RAS effectors. However, whereas patients with EGFR-mutant lung cancer can benefit from therapy with EGFR tyrosine kinase inhibitors (TKI), KRAS mutations have been suggested as negative predictors of response to therapies with EGFR TKI (Linardou et al., 2008; Massarelli et al., 2007).

The study of the role of Nuak1 in the tumorigenic process driven by KRas shed some light on the potential benefit of NUA1 inhibition. However, it is unlikely that targeting of NUA1 alone would be therapeutically sufficient in lung cancer. Therefore, we focused on the investigation of the mechanisms associated with

tumour progression of a $KRas^{G12D}/MYC$ NSCLC mouse model in order to identify new therapeutic targets.

In this chapter, we elucidate the role of the ERBB network in the lung tumorigenic process driven by KRas, challenging the dogma that inhibition of ERBB receptors is not beneficial in patients affected by KRAS mutant NSCLC. Data provided in this chapter are part of a broader study carried out in collaboration with Björn Kruspig and Sarah Neidler.

5.1.1 Mouse models

Most of the experiments were performed using a $lsl-KRas^{G12D}/R26-lsl-MYC^{Hom}$ NSCLC mouse model (referred to as $KRas^{G12D}/MYC$ or KM), in which the KRas G12D point mutation is preceded by a lox-stop-lox (*lsl*) sequence, and *lsl*-human MYC is expressed under the control of the Rosa26 (*R26*) locus. In addition, to monitor tumour growth in live animals we employed the near-infrared fluorescent protein encoded by the *lrfp* gene, which was inserted in the endogenous *Hprt* locus and preceded by a lox-stop-lox cassette to control its expression (Hock et al., 2017). Upon administration of Adenovirus-Cre, the simultaneous induction of mutant KRas, exogenous MYC and iRFP, when present, was achieved (Fig.5.1).

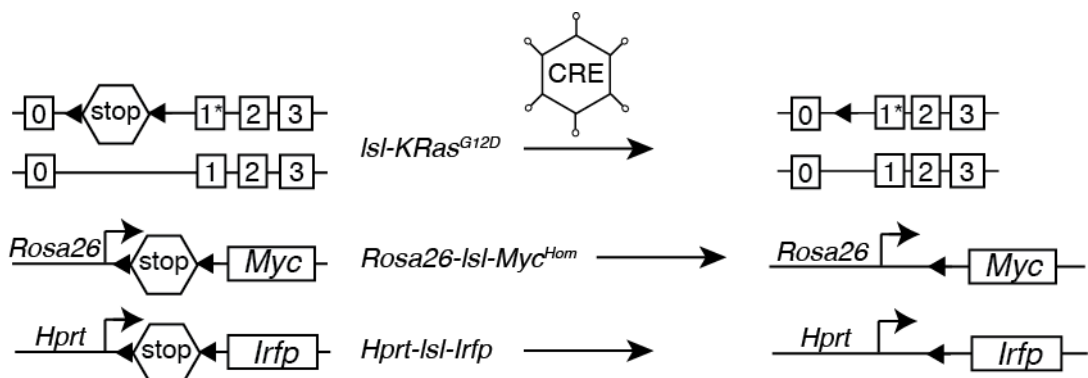


Figure 5. 1 – Schematic representation of the $lsl-KRas^{G12D}/R26-lsl-MYC/Hprt-lsl-Irfp$ mouse model.

5.2 Results

5.2.1 Upregulation of the ERBB network during progression of KRas mutant lung adenocarcinoma

As mentioned in Chapter 4, histological examination of lungs of *KRas*^{G12D}/*MYC* (KM) mice after six weeks from Adeno-Cre infection revealed the presence of more aggressive sub-populations within the tumour, characterized by different morphological features (Fig. 4.8A). In addition, exclusively these tumour areas were positive for immunohistochemical staining with phospho-ERK, a downstream effector of KRAS and a marker associated with tumour progression (Vicent et al., 2004). To identify the underlying molecular events involved in the observed morphological transition to a more advanced phenotype, we compared the transcriptome of isolated phospho-ERK^{high} regions to phospho-ERK^{low} regions of lung adenomas after 6 weeks from Adeno-Cre infection. GeneGO analysis of the data set obtained from the RNA sequencing analysis revealed that multiple pathways associated with regulation of cell adhesion, cell motility and cytoskeletal remodelling were upregulated in phospho-ERK^{high} regions (data not shown). Surprisingly, multiple components of the ERBB signalling network were found to be enriched in the phospho-ERK^{high} regions (Table 5.1). In particular, expression of ERBB receptors such as ERBB2 and ERBB3 was increased, together with multiple ERBB ligands such as Epiregulin, Amphiregulin and Tgf α . Upregulation of LamC2, Fabp5 and Keratine 19, all shown to enhance signalling through EGFR/ERBB family RTKs (Garg et al., 2014a; Powell et al., 2015), was also identified. Furthermore, increased expression of the sheddase ADAM9 and ADAM10, proteolytic enzymes responsible for the release of soluble form of receptor ligands, was observed. Overall, the analysis strikingly indicated a potential role of the ERBB network in the progression of *KRas*^{G12D}/*MYC* lung adenomas.

High phospho-ERK associated gene expression	Δ (fold)	FDR
ERBB family ligands		
Epiregulin	24.82	2.78e-13
Amphiregulin	4.25	4.98e-11
Transforming Growth Factor alpha	2.69	0.0048
Heparin-bound EGF	2.31	0.020
ERBB ligand sheddases		
Adam9	2.00	0.0001
Adam10	1.89	0.0016
ERBB Receptors/Receptor Tyrosine Kinases		
ErbB2	1.55	0.060
ErbB3	1.53	0.054
ERBB Accessory proteins		
IQGAP2	5.30	0.0004
LamC2	3.48	2.56e-9
Keratin 19	2.96	2.06e-6
FABP5	2.79	6.15e-3
RAS pathway		
Raf1	1.86	0.0178
BRaf	1.52	0.063
CRaf	1.80	0.0037

Table 5. 1- Overexpression of genes belonging to the ERBB network in phospho-ERK^{high} tumour regions.

Phospho-Erk^{high} and phospho-ERK^{low} tumour regions from KM mice (n = 4) were isolated by laser-capture microdissection and gene expression measured by RNA-SEQ. The table represents normalized Ras and ERBB network gene expression in phospho-Erk^{high} relative to phospho-Erk^{low} tumour regions. FDR = false discovery rate. Data generated by Sarah Neidler.

Interestingly, Western blot analysis of protein lysates isolated from multiple lung tumours at 6 weeks post infection showed detectable levels of phospho-EGFR, phospho-ERBB2 and phospho-ERBB3, indicating activity of the ERBB receptors in the developing adenomas (Fig. 5.2).

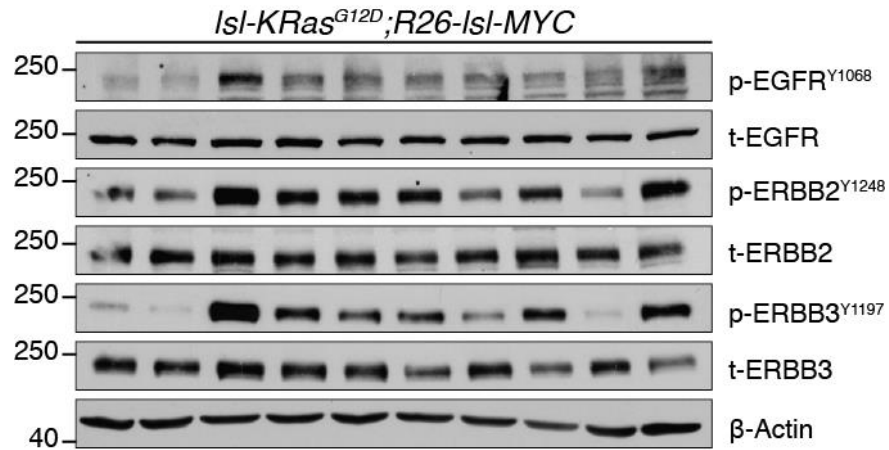


Figure 5. 2 – ERBB receptors are active in KRas^{G12D}/MYC lung adenomas.

Protein extracts were isolated from KM lung tumours at 6 weeks post Adeno-Cre infection and were immunoblotted with the indicated antibodies. Each lane represents an individual lung tumour; all the ten tumours were harvested from a single mouse.

5.2.2 KRas^{G12D}/MYC lung tumours are sensitive to ERBB inhibition

The observed upregulation of the ERBB network in developing *KRas*/*MYC* lung tumours indicated a potential contribution of the ERBB signalling in sustaining tumour progression. To test the sensitivity of ERBB receptors inhibition in our *KRas^{G12D}/MYC* NSCLC mouse model, we made use of the clinically approved drug Neratinib, which is an irreversible inhibitor of EGFR and ERBB2 (Subramaniam et al., 2015). As shown in figure 5.3A, acute Neratinib treatment resulted in an efficient inhibition of EGFR and ERBB2, as suggested by their decreased phosphorylation levels in comparisons to vehicle treated controls. Most importantly, Neratinib treatment caused a significant decrease of tumour cell proliferation, as suggested by the reduction of the proliferation marker Ki67, and in a significant increase of apoptosis, as indicated by TUNEL staining, compared to vehicle treated controls (Fig. 5.3B-C).

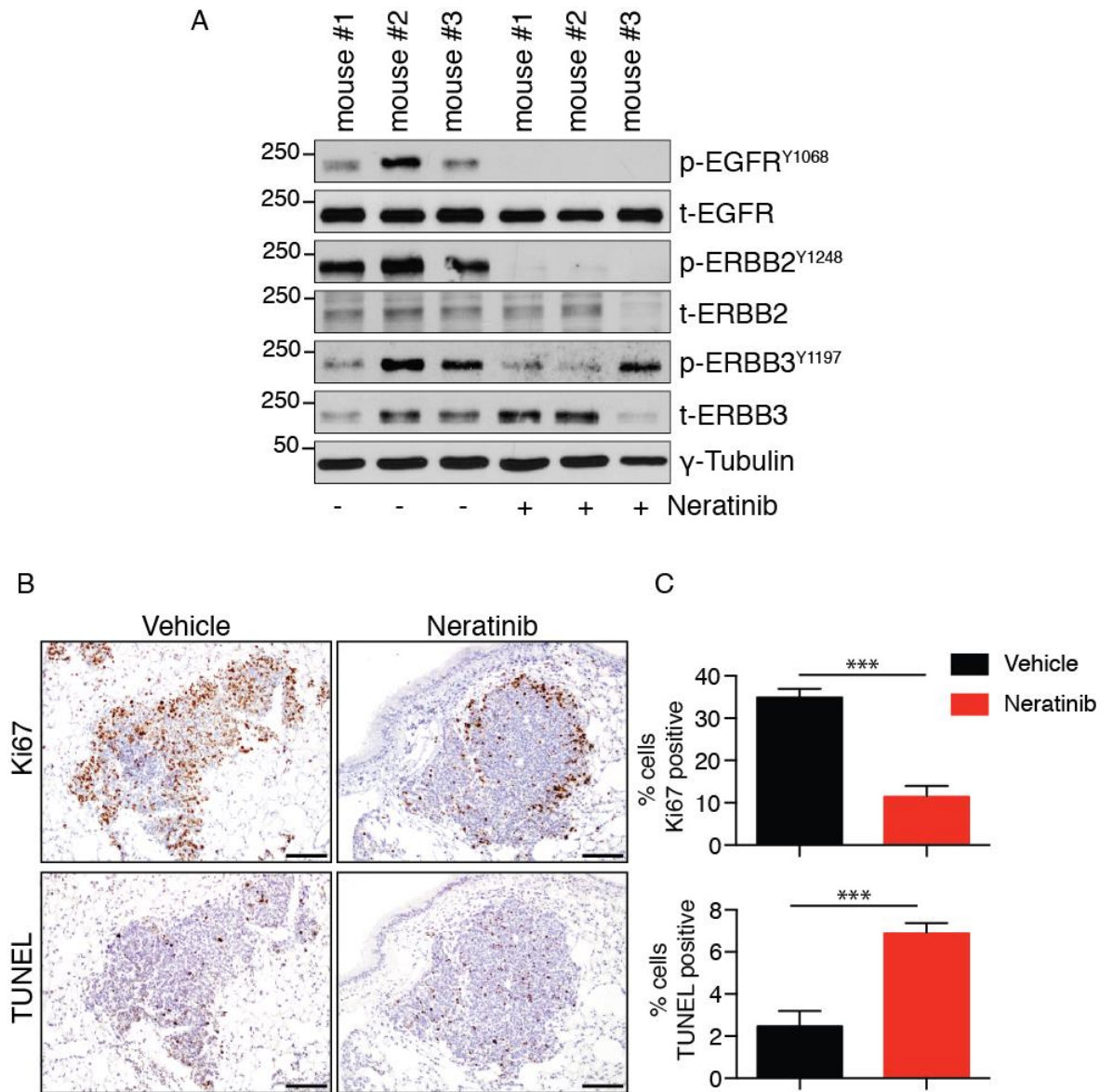


Figure 5. 3 – ERBB inhibition induces growth arrest and cell death in KM lung tumours.

A, KM mice at 6 weeks post Adeno-Cre infection were treated with Neratinib (n=3) or vehicle control (n=3) for three days before harvesting tumour tissue for protein isolation. Whole cell protein extracts were immunoblotted with the indicated antibodies. B, Representative images of lung tissue sections of KM mice at 6 weeks post Adeno-Cre infection treated for three days with Neratinib or vehicle control immunostained for Ki67 and TUNEL. Scale bars = 100 μ m. C, Bar graphs representing the Mean \pm SEM of Ki67 and TUNEL positively stained lung tumour cells from KM mice treated with vehicle (n=3) or Neratinib (n=3) for three days. ***p<0.01 calculated with two-tailed unpaired T test.

5.2.3 Inhibition of the ERBB receptors impairs KRas-driven tumorigenesis

Having established the sensitivity of KM tumours to inhibition of ERBB receptors by Neratinib treatment, we sought to investigate the extent of the contribution of the ERBB signalling to the tumorigenic process driven by mutant KRas. To achieve that, *KRas*^{G12D}/*MYC* mice were treated daily with Neratinib for 4 weeks, starting at 2 weeks post infection, a time point when only early lesions such as atypical adenomatous hyperplasia and epithelial hyperplasia of the bronchioles could be detected. Strikingly, continuous Neratinib treatment impaired the tumorigenic process driven by mutant KRas as shown by the significant decrease in tumour burden in KM treated mice compared to control mice. Conversely, prolonged inhibition of EGFR only, by treatment with a daily dose of Erlotinib, did not have a significant impact on tumour burden in comparison to vehicle treatment (Fig. 5.4A-B). Overall, these results suggested that multiple ERBB receptors are required since the early stages of the tumorigenic process of *KRas*^{G12D}/*MYC* lung cancer.

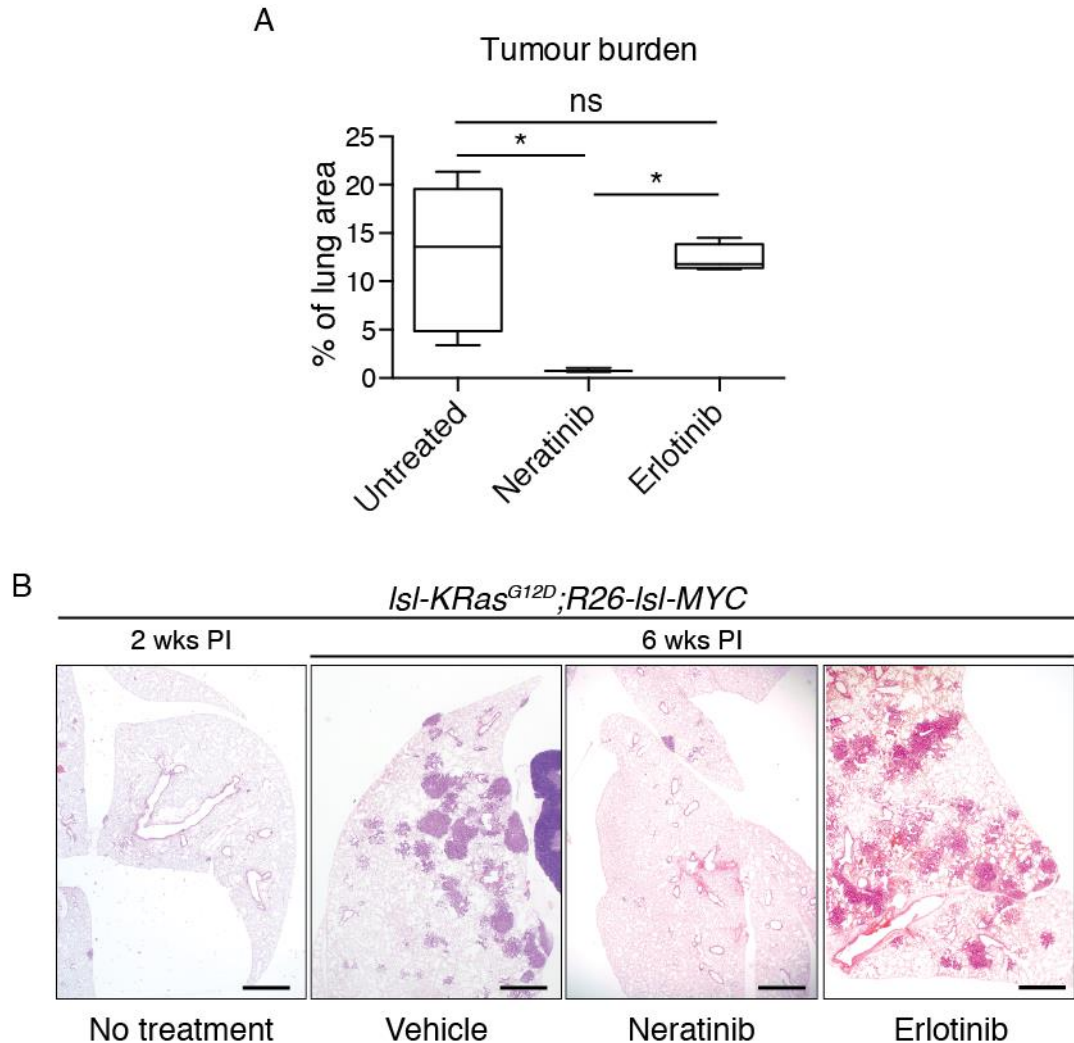


Figure 5. 4 – Neratinib but not Erlotinib treatment reduces lung tumour burden of KM mice.

A, Box plots indicating the tumour burden (Mean \pm SEM) and **B**, representative H&E images of KM mice treated with either Neratinib (n=3), Erlotinib (n=4) or vehicle control (n=6) for 4 weeks, starting at 2 weeks post Adeno-Cre infection (PI). ns= not significant, * $p < 0.05$ calculated with one-way ANOVA, Tukey's multiple comparison. Scale bars = 1 mm.

5.2.4 ERBB blockade enhances therapeutic impact of MEK inhibition in KRas mutant lung adenocarcinoma

The observed tumour preventive effect of the ERBB receptors inhibition in *KRas^{G12D}/MYC* lung tumorigenesis prompted us to investigate the therapeutic outcome of Neratinib treatment. However, daily treatment of established *KRas^{G12D}/MYC* lung tumours for 7 days with Neratinib did not have a significant effect on overall survival in comparison to vehicle treatment (Fig. 5.5).

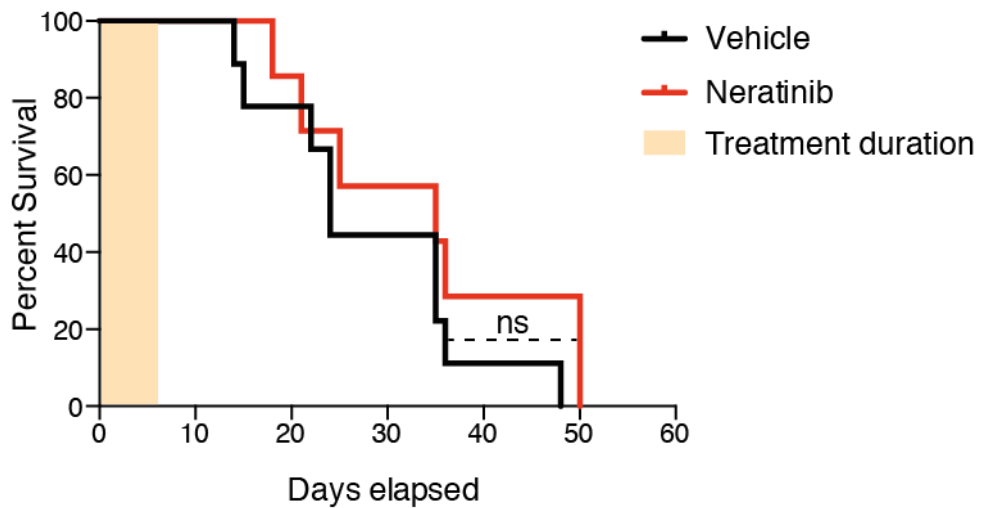


Figure 5. 5 – Neratinib treatment does not increase the overall survival of KM mice. Kaplan-Meier survival analysis of KM mice treated with Neratinib (n=7) or vehicle control (n=9) for 7 days starting at 6 weeks post Adeno-Cre infection, which is indicated as time 0 in the graph. ns= not significant. P value determined by log-rank (Mantel-Cox) test.

Further *in vitro* studies on KRAS mutant human lung cancer cell lines (H2009, H358, A549) revealed that Neratinib treatment did not induce a significant increase in cell death in two of three cell lines. However, the achievement of a more pronounced inhibition of the MEK/ERK cascade by combination of ERBB and MEK inhibition using Neratinib and Trametinib, respectively, could efficiently and significantly enhance cell death in all the lines tested, as compared to single drugs and vehicle control treatment (Fig. 5.6).

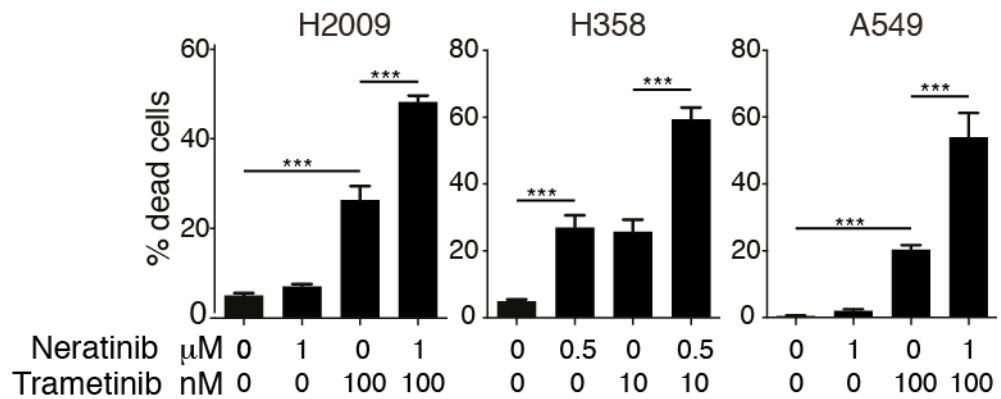


Figure 5. 6 – Combination of ERBB and MEK inhibition more efficiently induces cell death in KRas mutant human lung cancer cell lines.

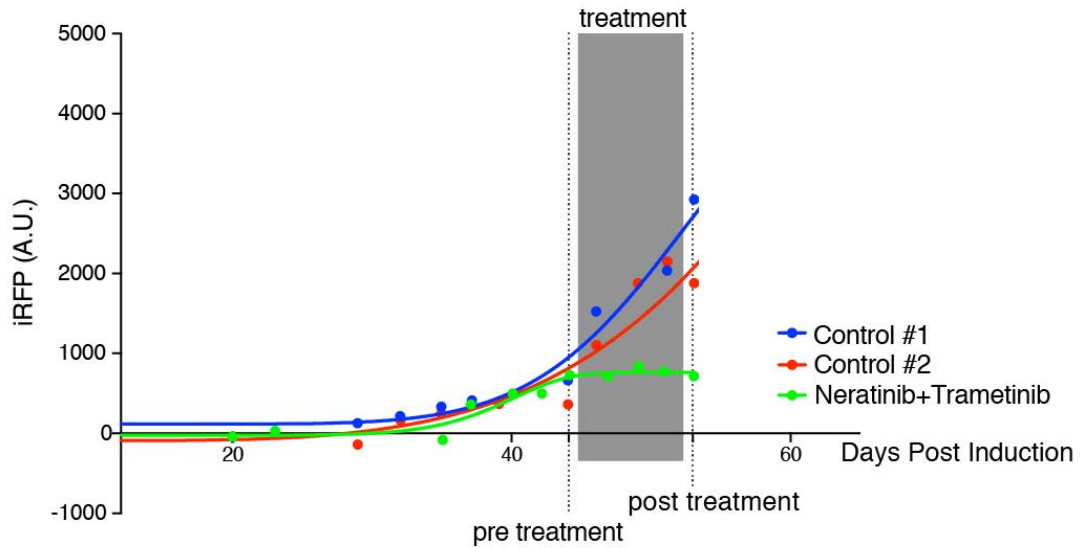
Bar graph representing the Mean \pm SEM of cell death induced by the indicated doses of Neratinib and/or Trametinib in human NSCLC cells, measured 48hrs after treatment. Cell death was analysed by Incucyte live-cell imaging system in the presence of Sytox green and corrected for confluence. N=3. Data generated by Björn Kruspig.

Given the efficacy of the combination of Neratinib with Trametinib in inducing cell death in the human lung cancer cell lines tested *in vitro*, we sought to determine the therapeutic effect of the combinatorial treatment in our *KRas*^{G12D}/*MYC* NSCLC *in vivo* model.

Following Adenovirus-Cre administration, *KRas*^{G12D}/*MYC*/*Irfp* animals were monitored weekly for detection of iRFP signal using the PEARL system for near-infrared fluorescent imaging (LI-COR), starting at 2 weeks post infection. When the intensity of the iRFP signal, which correlates with tumour burden, reached a threshold of approximately 800 units, daily treatment with Neratinib in combination with Trametinib was carried out for 5 consecutive days.

As shown by quantification in figure 5.7A, we could attest that the tumour growth followed an exponential trend in untreated mice, as suggested by the exponential increase of the iRFP signal intensity over time. On the contrary, treatment with the combination of Neratinib and Trametinib caused a plateau of the iRFP signal, indicating an arrest in the tumour growth during the treatment period. Similarly, representative pictures in figure 5.7B indicated an increase of the iRFP signal intensity over the treatment period in mice that received the vehicle control whereas the iRFP signal was reduced in the presence of the combinatorial therapy.

A



B

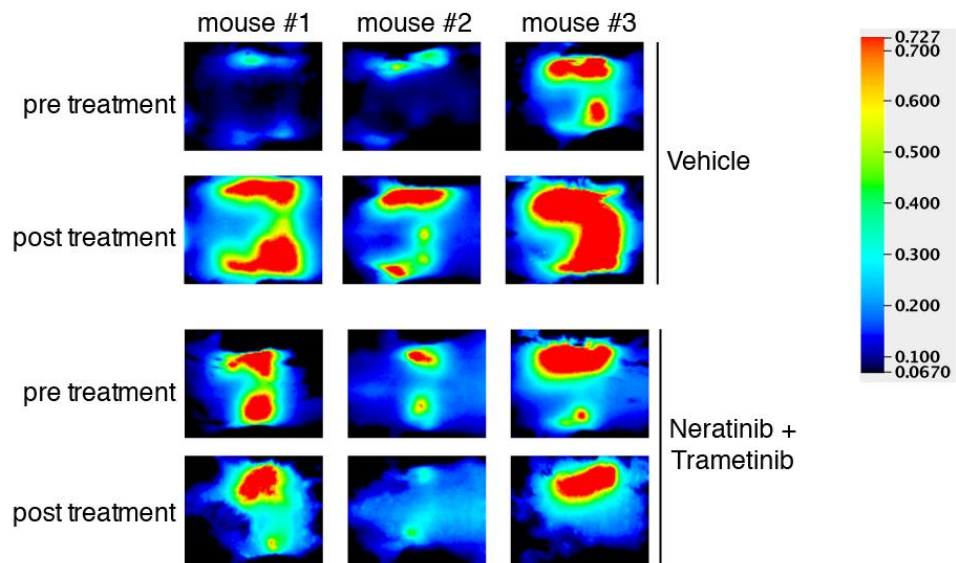


Figure 5. 7 – iRFP signal detection identified impaired growth of lung tumours treated with Neratinib in combination with Trametinib.

A, iRFP signal in KM mice was monitored using a PEARL imaging system (LI-COR) and intensity curves calculated using the Weibull growth equation. iRFP signal is represented as baseline corrected values. Treatment with Neratinib & Trametinib was started when the signal threshold (800 arbitrary units) was reached and continued for five days. Each dot represents a day of imaging. B, Representative LI-COR PEARL images of lung tumours from KM mice treated with Neratinib & Trametinib or vehicle control.

Furthermore, in agreement with the observed arrest in tumour growth, the combination of Trametinib and Neratinib could significantly further extended overall survival, in comparisons to single treatments and vehicle control (Fig. 5.8).

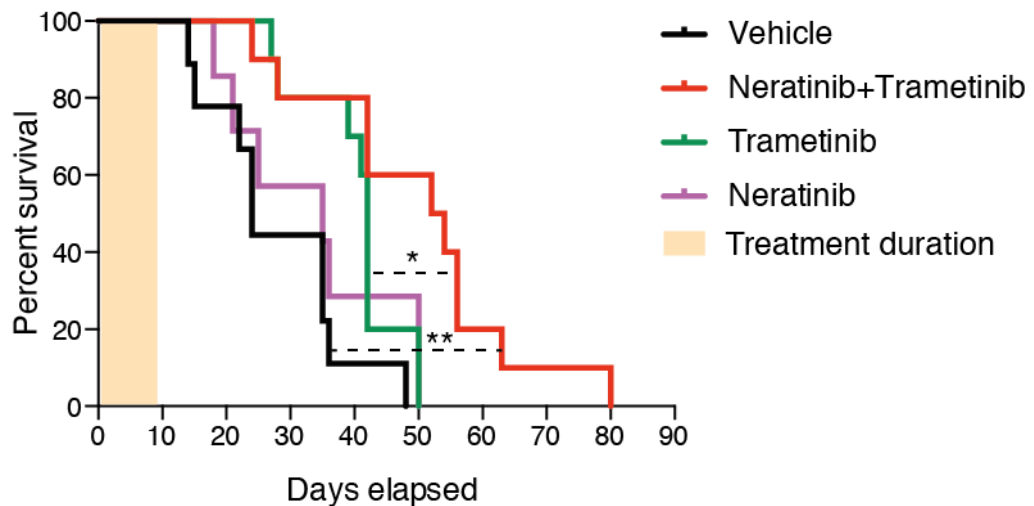


Figure 5. 8 – Combination of Neratinib with Trametinib enhances survival of KM mice.

Kaplan-Meier survival analysis of KM mice treated with vehicle control (n=9), Neratinib (n=7), Trametinib (n=10) or a combination of the two drugs (n=10) for 7 days starting at 6 weeks post Adeno-Cre infection, which is indicated as time 0 in the graph. * $p < 0.05$, ** $p < 0.001$ determined by log-rank (Mantel-Cox) test.

Western blot analysis of tumour samples isolated from KM mice treated acutely with Neratinib and/or Trametinib revealed an increase in AKT phosphorylation upon Trametinib treatment, which has been previously documented by Sun and colleagues (Sun et al., 2014). Moreover, Neratinib treatment could reduce the Trametinib-mediated increase in AKT phosphorylation to basal levels and, whereas the levels of phospho-ERK were only modestly reduced by Neratinib, combination with Trametinib efficiently abrogated phosphorylation of ERK (Fig. 5.9). Overall, combination of Neratinib with Trametinib appeared to be more effective than the single treatments in inhibiting two key pathways that sustain tumour cell survival and proliferation downstream of ERBB receptors and KRAS, the mitogen-activated protein kinase (MAPK)- and the PI3K/AKT pathways.

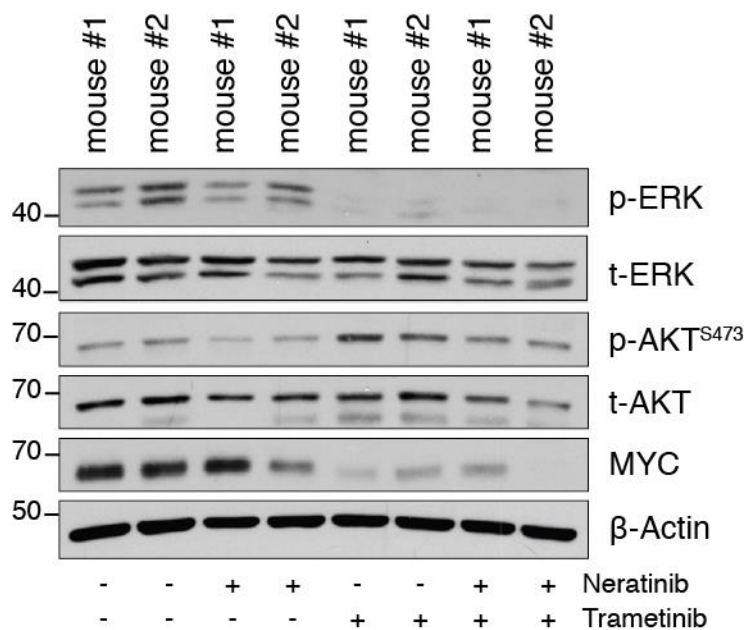


Figure 5. 9 – Simultaneous inhibition of the ERBB receptors and MEK impacts on AKT activation.

Protein extracts were isolated from lung tumours of KM mice treated for three days with Neratinib (n=2), Trametinib (n=2), a combination of both drugs (n=2) or vehicle control (n=2) at 6 weeks post Adeno-Cre infection, and immunoblotted with the indicated antibodies.

5.3 Discussion

Activating mutations of the oncogene Ras are among the main drivers of the tumorigenic process in several tissues. In particular, somatic mutations in RAS are detected in 20% of human tumours, of which more than 80% are related to KRAS isoform. Although RAS was the first mutated gene to be identified in human cancer and its biological functions extensively studied over the years, we are still battling with the search of a successful therapeutic strategy that tackles its oncogenic activity. Therefore, the investigations reported in this chapter intended to provide with a better understanding of the molecular mechanisms at the base of KRas-driven tumour progression in the lung to develop novel therapeutic approaches.

Experimental evidence obtained in this study have surprisingly uncovered a functional role of the ERBB signalling in supporting KRas driven tumorigenesis. Specifically, tumour regions with morphological and molecular features of progression were found to be characterized by the upregulation of multiple

components of the ERBB network, such as the ERBB receptors and their ligands (Tab. 5.1). In addition, inhibition of the ERBB receptors with Neratinib significantly reduced tumour cell proliferation and increased apoptotic levels in established tumours (Fig. 5.3), and most strikingly, it impaired tumour initiation when treatment was started at an early stage of tumorigenesis (2 weeks post-Adeno-Cre infection) (Fig. 5.4). Overall, these findings not only support a functional requirement of the ERBB signalling in developing KRas mutant lung tumours but also in the tumour initiation process.

These surprising but important observations challenge the current field on several aspects and are supported by recently published data that change our understanding of Ras biology. Firstly, as the three common KRAS mutations in lung cancer (G12C, G12D, G12V) confer a persistent activation status, it has been inferred that upstream signals, such as modulation by the ERBB receptors, can no longer influence RAS activity. However, a recent study has questioned that concept by providing evidence of a maintained basal GTPase activity of mutant KRas^{G12C} that could be targeted with high affinity by a novel small molecule inhibitor (ARS853), which was able to reduce the levels of GTP-bound RAS and impair the signalling to the downstream effectors Raf and ERK (Lito et al., 2016). Thus, the new finding of mutant KRas still cycling between an on and off state has indicated that its activity can be modulated by upstream signalling. In addition, the mutual exclusive occurrence of KRAS and EGFR activating mutations has been attributed to their redundant function due to localization in the same or overlapping signalling pathways. Therefore, the mutual exclusivity would further support that hyperactivation of the ERBB receptors would not be required due to their redundancy in a setting of KRAS mutation. However, two recent studies have revealed an alternative and intriguing explanation for the absence of concomitant mutations in KRAS and EGFR. In particular, co-expression of mutant KRAS and EGFR in human lung cancer cell lines induced hyperactivation of the MAPK pathway (ERK, p38 and JNK) and cell death, suggesting a synthetic lethal interaction between the two mutant oncogenes (Unni et al., 2015). Additionally, by using an elegant double-inducible *in vivo* system of KRas^{G12V} and EGFR^{L858R}, Santamaria's group has described how induction of mutant EGFR in established KRas-driven lung adenocarcinoma caused an initial increase in tumour cells death that was followed by restoration of tumour progression together with a decreased activity of the MAPK and PI3K

pathways (Ambrogio et al., 2017). Therefore, it is possible that a distinct threshold of the ERBB signalling influences tumour survival and progression outcome. Thus, despite constitutive activation of EGFR, i.e. in case of mutations, might be detrimental to KRas driven tumours due to unsustainable levels of oncogenic signalling, our data suggested that a modest increase of ERBB signalling could support KRas driven tumorigenesis.

Secondly, the sensitivity of KRas mutant lung tumours to ERBB inhibition therapy addresses the reported clinical failure of EGFR inhibition in patients with KRAS mutant NSCLC. In particular, EGFR tyrosine kinases inhibitors (TKI) and anti-EGFR monoclonal antibodies have been successfully used in cancer patients with EGFR mutations, whereas KRAS mutations have been suggested as a negative predictor for the response to both therapies. Data from our KM mouse model reported in this chapter agree with the clinical observation that EGFR-inhibition alone, using Erlotinib, does not affect the tumorigenic process driven by mutant KRas (Fig. 5.4). However, the observed reduction of tumour burden upon inhibition of multiple ERBB receptors using Neratinib, suggests that the clinical outcome could be improved by the inhibition of multiple ERBB receptors.

Continuous treatment of established tumours with Neratinib for seven days did not result in a survival advantage in comparison to vehicle control (Fig. 5.5). Although a more prolonged treatment could improve the therapeutic outcome, the inability of Neratinib to induce a significant increase in cell death in human lung cancer cell lines (Fig. 5.6) suggested that inhibition of ERBB signalling was not sufficient to impair tumour growth.

The increased ERK phosphorylation as tumours progressed to more advanced stages (Chapter 4, Fig. 4.8) indicated the importance of the MAPK cascade in support of this process. Indeed, components of the cascade, such as the three isoforms of Raf, were modestly upregulated in the phospho-ERK^{High} tumour regions together with the ERBB network (Tab. 5.1). Therefore, a more profound inhibition of the MAPK cascade by dual targeting of ERBB signalling and the downstream effector MEK could more efficiently induce cell death in the human cancer cell lines tested (Fig. 5.6) and, most importantly, cause an arrest in tumour growth *in vivo* (Fig. 5.7) that translated in an increased overall survival of KM mice in comparisons to single treatments (Fig. 5.8).

Although MEK inhibition alone induced a significant increase in cell death in all cell lines tested (Fig. 5.6) and significantly increased KM survival in comparison to vehicle treatment ($p < 0.05$) (Fig. 5.8), clinical studies have obtained discouraging results for lung cancer. For example, Trametinib was shown to induce a similar response rate and progression-free survival as standard chemotherapy with docetaxel in patients with previously treated KRAS mutant NSCLC (Blumenschein et al., 2015). Further studies have tried to address the lack of therapeutic effect of MEK inhibition and combine it with the targeting of additional pathways for an improved outcome. Recent experimental evidence has suggested that inhibition of MEK results in upregulation of the Fibroblast growth factor 1 (FGFR1) as a compensatory response mechanism. Thus, a combinatorial therapy with inhibition of MEK and FGFR1 was proposed to be more effective for treating KRAS-mutant lung cancer (Manchado et al., 2016). An alternative mechanism of resistance to MEK inhibition was suggested to be mediated by the transcriptional induction of ERBB2 and ERBB3. Indeed, ERBB inhibition was shown to have a synergistic effect with MEK inhibition with a more efficient induction of cell death in colon and lung cancer cells (Sun et al., 2014). Therefore, although originating from a different contextualization of the ERBB network function in KRas mutant lung cancer as in our model upregulation of the receptors represents an intrinsic property of KM tumours rather than an induced consequence of MEK inhibition, our data are in agreement with the findings of Sun and colleagues in supporting the use of a combinatorial ERBB and MEK inhibition therapy. In particular, the increase in AKT activity observed due to MEK inhibition using Trametinib was prevented by combination with Neratinib (Fig. 5.9), suggesting that inhibition of the AKT pathway could be part of the synergistic mechanism of Trametinib and Neratinib treatment. However, further studies will be required to delineate the molecular details of the combinatorial therapy, assess the potential emergence of resistance, as it represents a major mechanism of failure of long term treatments, and establish the possible molecular mechanisms of resistance.

MYC gene amplifications are detected in approximately 10% of lung adenocarcinoma (cBioPortal) and we have shown that a moderate overexpression of MYC could significantly contribute to accelerate KRas driven lung tumorigenesis (Chapter 4, Fig. 4.5). Therefore, combination of KRas^{G12D} with

MYC overexpression provided with a good model to study both the initial and later phases of the tumorigenic process. However, we can exclude that the molecular phenotype described in this chapter is an artificial result of the engagement of the ERBB receptors to sustain exogenous MYC overexpression as we have previously reported that expression from the Rosa26 locus is refractory to growth factor signalling (Murphy et al., 2008). In addition, we can also exclude that the tumour regions featuring signs of progression reflect a differential expression efficiency of the exogenous MYC, as RNA-SEQ analysis did not reveal any difference in MYC expression levels between phospho-ERK^{High} and phospho-ERK^{Low} regions (data not shown). Therefore, we can conclude that the phenotype observed is not simply driven by exogenous MYC and that our findings, in support to available data, strongly suggest a renewed potential of targeting the ERBB network in KRAS mutant NSCLC.

Chapter 6 – Final Discussion

Since the relatively recent identification of NUAK1 in 2003 (Suzuki et al., 2003a), multiple studies have revealed its role in a variety of cellular processes that established a connection with cancer. Enhancement of proliferative signalling, resistance to cell death and activation of invasion and metastasis are some of the so called “hallmarks of cancer” in which NUAK1 has been shown to play a role. In addition, NUAK1 expression has been reported to correlate with tumour stage and survival outcome in many cancer types (Cui et al., 2013; Kusakai et al., 2004; Lu et al., 2013), indicating that its targeting could be clinically relevant. However, our knowledge of NUAK1 regulation and function can be considered still limited particularly in comparison to AMPK, which has been the main focus of investigation among all the AMPK related kinases (ARKs). Indeed, currently only a restricted number of NUAK1 substrates and upstream regulators are well characterized, while a more in depth understanding of NUAK1 network is lacking.

Data presented in this thesis describe a novel modality of regulation of NUAK1 that involves modulation by Ca^{2+} levels. This activation modality was initially considered a peculiarity of AMPK, not shared by other AMPK related kinases (Fogarty et al., 2010). However, recent published data reported a Ca^{2+} -mediated activation of SIK2 (Miranda et al., 2016) and we propose a similar activation for NUAK1 and NUAK2. Therefore, increase in intracellular Ca^{2+} levels might represent an activation modality common for the AMPK family or at least shared by multiple ARKs.

The Ca^{2+} /calmodulin-dependent protein kinase kinase-beta ($\text{CaMKK}\beta$) has been established as the upstream kinase regulating AMPK activation in response to Ca^{2+} (Woods et al., 2005), whereas the kinase mediating the activation of SIK2 has not been identified yet. Our experimental evidence has indicated that Protein Kinase C α ($\text{PKC}\alpha$) is the Ca^{2+} -responsive kinase that regulates NUAK1 activation, whereas NUAK2 does not appear to be modulated by the same kinase.

The tumour suppressor LKB1 has been described as the master kinase for the AMPK family members and deletion of *Lkb1* was shown to abolish NUAK1 activity

in non-transformed MEFs (Zagorska et al., 2010). However, a dominant regulation of NUAK1 by LKB1 is puzzling to some extent. Some aspects of NUAK1 cellular functions are in agreement with the reported roles of LKB1 and experimental evidence has compellingly demonstrated that NUAK1 mediates some of LKB1 physiological functions. For example, LKB1 was described for its role in axon specification during neuronal polarization (Barnes et al., 2007; Shelly et al., 2007) and subsequent studies have underlined its role in axon branching of cortical neurons through activation of NUAK1 (Courchet et al., 2013). In addition, the LKB1/NUAK1 axis has been involved in the regulation of phosphorylation of Myosin Light chain 2 (MLC2) (Zagorska et al., 2010), which plays an important role in cell adhesion and polarity (Vicente-Manzanares et al., 2009). However, molecular connections between LKB1 and NUAK1 in the control of metastasis have not been recognised. Several studies have established the incontrovertible role of NUAK1 as a positive regulator of cell migration and invasion (Chang et al., 2012; Chen et al., 2017; Chen et al., 2013), whereas most data available indicate an opposite role for LKB1 (Chan et al., 2014; Deguchi et al., 2010; Goodwin et al., 2014). Therefore, it is possible that the function of NUAK1 in migration might be regulated by an alternative kinase.

In particular, our identification of PKC α as a kinase modulating NUAK1 activation in response to Ca²⁺ stimulation opens new frontiers to the understanding of the biology of NUAK1. Notably, PKC α , which has been established as a positive regulator of cell migration and invasion, might regulate NUAK1 in regard to the metastatic process and potentially many others. As new biological roles for NUAK1 continue to emerge, more aspects of its tumour promoter role are being described but also additional degrees of separation from LKB1 are revealed. For example, NUAK1 has been recently involved in the induction of epithelial-to-mesenchymal transition (EMT) (Obayashi et al., 2016; Xu et al., 2016), which has been debated for playing a role in the metastatic process but also implicated in the mechanisms of drug resistance (Fischer et al., 2015; Shibue and Weinberg, 2017). Similarly to NUAK1, PKC α has been shown to promote EMT and mediate drug resistance (Abera and Kazanietz, 2015), whereas LKB1 has been suggested to inhibit EMT (Carretero et al., 2010; Roy et al., 2010). Therefore, evaluation of the PKC α /NUAK1 axis in the induction of EMT might be an additional aspect to consider from a physiological point of view but also as therapeutic approach to chemoresistance.

Intriguingly, we have exposed a new role of PKC α in its function as a linker between NUAK1 and MYC. Particularly, MYC was found to amplify Ca²⁺ signalling through the transcriptional upregulation of multiple components such as ITPR1, CaMKK β and PKC α . Importantly, MYC overexpression induced a more prominent effect at the level of activity of PKC rather than at expression levels. In addition, depletion of either NUAK1 or PKC α was shown to be lethal in HeLa cells, which express high levels of the oncogene MYC, consistent with a role of the PKC α /NUAK1 axis in supporting the survival of MYC overexpressing cells.

NUAK1 has already been described to promote survival of MYC-overexpressing cells by restraining mTORC1 activity (Liu et al., 2012). In our studies, we were further able to delineate the mechanism underlying the involvement of NUAK1 in the regulation of mTORC1. Particularly, our data revealed a direct role of NUAK1 in the inhibition of Raptor, which might represent an important metabolic checkpoint that contributes to the pro-survival mechanism in the setting of MYC oncogene-induced stress.

MYC is an emblematic oncogene in its function as it is known to drive proliferation but also to induce apoptosis. In particular, a threshold level of MYC has been suggested to determine cell fate. Indeed, whereas low expression levels of MYC can sustain aberrant proliferation, elevated levels of MYC trigger a tumour suppressive function with the induction of ARF/p53 and apoptotic pathways (Murphy et al., 2008). PKC α has been suggested to exert a pro-survival function through phosphorylation of the anti-apoptotic protein BCL-2 (Ruvolo et al., 1998) and enhancement of AKT activity (Li et al., 1999). Therefore, a potential function of PKC α would be to protect cells from death induced by high levels of MYC, mitigating MYC tumour suppressive role in favour of its oncogenic activity.

Overall, our data strengthen the rationale for the therapeutic targeting of NUAK1 and provide insights for the inhibition of PKC α , which so far has produced mixed and largely negative outcomes in clinical oncology (Marshall et al., 2004; Paz-Ares et al., 2006; Villalona-Calero et al., 2004), as a potential therapeutic strategy in MYC-deregulated cancers.

NUAK1 has been indicated to act as a tumour promoter, since an increased expression has been reported in more advanced tumour stages and has been

associated with poor survival for different cancer types. Our studies conducted in a mouse model of Non-small cell lung cancer (NSCLC) driven by mutant $KRas^{G12D}$ have demonstrated that NUAK1 does not share the tumour suppressive role of LKB1, whose deletion has been reported to accelerate lung tumorigenesis (Ji et al., 2007). At 16 weeks post infection, deletion of Nuak1 did not affect the tumour burden in the lungs of Kas^{G12D} mice, although a survival analysis might offer a more exhaustive interpretation of its role. Indeed, Nuak1 deletion increased the survival of mice in which lung tumorigenesis was driven by $KRas^{G12D}$ and accelerated by MYC overexpression. The synthetic lethal interaction between MYC and Nuak1 might contribute to the observed survival benefit but it is also possible that deletion of Nuak1 results in the loss of its intrinsic tumour supportive mechanisms. For example, preliminary results have suggested a potential role of NUAK1 in tumour angiogenesis, as we observed a decrease in tumour blood vessels formation upon Nuak1 deletion, which might represent a novel biological function of NUAK1, not related to MYC. The pro-angiogenic role of NUAK1 could be partially responsible for the observed increase in survival of Nuak1 deleted mice, as blood vessels are essential in providing nutrients and oxygen to the highly metabolic tumour cells, other than representing the preferential way for tumour dissemination to distant sites. On the other hand, a reduction in tumour blood vessel might represent an obstacle for an efficient systemic delivery of chemotherapeutic agents. However, an analysis of the structure and permeability of the remaining blood vessels together with a pharmacokinetics and tumor uptake study might indicate if the observed reduction in tumour blood vessels could considerably affect drug delivery.

We observed a decrease of phospho-ERK levels in $KRas^{G12D}/MYC/Nuak1^{F/F}$ tumours, which might delay the development of aggressive sub-clones, responsible for a rapid progression of the disease, and reflect the observed survival benefit. Notably, Nuak1 deletion also resulted in an increase in AKT activation, which might be supported by an enhanced insulin sensitivity as previously described in a Nuak1 knockout mouse model (Inazuka et al., 2012). Therefore, it is possible that Nuak1 deletion triggers a cross-inhibition between AKT and Raf to downregulate ERK phosphorylation, a mechanism previously reported (Moelling et al., 2002). However, further investigations will be required for a more comprehensive understanding of the mechanisms behind the observed

effects of Nuak1 deletion. Firstly, additional studies will be needed to confirm the pro-angiogenic role of NUA1 and explore the mechanism. In addition, given the established role of NUA1 in promoting invasion and metastasis, it will be of great interest to investigate the effect of Nuak1 deletion from a metastatic perspective in the *KRas*^{G12D}/*MYC* NSCLC mouse model.

Although therapeutic targeting of NUA1 in NSCLC might not be itself sufficient for a substantial regression of the disease, as we improve our understanding of the signalling network that includes NUA1 we might discover new aspects of its therapeutic potential. On the other hand, a more in-depth knowledge of the mechanisms that drive the progression of lung cancer might as well have multiple implications from a therapeutic point of view and offer new opportunities for NUA1 targeting.

With the study of the molecular mechanisms of NSCLC progression, we revealed that the ERBB network is significantly upregulated in *KRas* mutant lung adenocarcinoma and demonstrated its involvement in the initial phases of the tumorigenic process as well as in the progression of the disease to more advanced stages. Indeed, we have compellingly shown that inhibition of the ERBB network leads to a better therapeutic outcome when combined with MEK inhibition, which as single therapy failed to provide encouraging results in clinical trials (Blumenschein et al., 2015). Therefore, the dependence of *KRas* mutant lung tumours on the ERBB network might prompt the revisiting of current therapeutic regimes and identify new successful combinatorial therapies.

Interestingly, *LKB1* deletion was shown to sensitize NSCLC cell lines to EGFR inhibition (Whang et al., 2016). Additionally, a link between *PKC α* and ERBB receptors has been suggested by several studies. For example, *PKC α* was reported to increase ERBB2 protein levels in breast cancer, establishing a feedback loop in which activation of ERBB2 led to increased *PKC α* , which in turns contributed to sustain ERBB2 levels (Magnifico et al., 2007). In addition, upregulation of *PKC α* was suggested to mediated the resistance to EGFR inhibition in NSCLC cells (Abera and Kazanietz, 2015). As NUA1 resides downstream of both *PKC α* and *LKB1*, targeting of NUA1 in combination with inhibition of ERBB receptors might represent a new and more efficient therapeutic strategy to explore in NSCLC.

Collectively, data presented in this thesis have revealed novel mechanisms of regulation of NUA1, strengthening the molecular basis for its targeting in tumours addicted to MYC oncogene, and uncovered new potential physiological roles of NUA1. Indeed, the identification of PKC α as an alternative upstream kinase might be the beginning of a more comprehensive understanding of the NUA1 signalling network. In addition, by improving our knowledge of the mechanisms involved in lung cancer progression, we have provided new targets that could be exploited for therapeutic purposes not only in lung cancer but also in other tumours driven by mutant KRas, such as pancreatic ductal adenocarcinoma, that still represents a major challenge in clinical oncology.

References

- Abera, M. B., and Kazanietz, M. G. (2015). Protein kinase Calpha mediates erlotinib resistance in lung cancer cells. *Molecular pharmacology* *87*, 832-841.
- Aderem, A. (1992). The MARCKS brothers: a family of protein kinase C substrates. *Cell* *71*, 713-716.
- Adey, A., Burton, J. N., Kitzman, J. O., Hiatt, J. B., Lewis, A. P., Martin, B. K., Qiu, R., Lee, C., and Shendure, J. (2013). The haplotype-resolved genome and epigenome of the aneuploid HeLa cancer cell line. *Nature* *500*, 207-211.
- Al-Hakim, A. K., Goransson, O., Deak, M., Toth, R., Campbell, D. G., Morrice, N. A., Prescott, A. R., and Alessi, D. R. (2005). 14-3-3 cooperates with LKB1 to regulate the activity and localization of QSK and SIK. *Journal of cell science* *118*, 5661-5673.
- Ambrogio, C., Barbacid, M., and Santamaria, D. (2017). In vivo oncogenic conflict triggered by co-existing KRAS and EGFR activating mutations in lung adenocarcinoma. *Oncogene* *36*, 2309-2318.
- Bai, X., Ma, D., Liu, A., Shen, X., Wang, Q. J., Liu, Y., and Jiang, Y. (2007). Rheb activates mTOR by antagonizing its endogenous inhibitor, FKBP38. *Science (New York, NY)* *318*, 977-980.
- Banerjee, S., Buhrlage, S. J., Huang, H. T., Deng, X., Zhou, W., Wang, J., Traynor, R., Prescott, A. R., Alessi, D. R., and Gray, N. S. (2014a). Characterization of WZ4003 and HTH-01-015 as selective inhibitors of the LKB1-tumour-suppressor-activated NUA1 kinases. *The Biochemical journal* *457*, 215-225.
- Banerjee, S., Zagorska, A., Deak, M., Campbell, D. G., Prescott, A. R., and Alessi, D. R. (2014b). Interplay between Polo kinase, LKB1-activated NUA1 kinase, PP1betaMYPT1 phosphatase complex and the SCFbetaTrCP E3 ubiquitin ligase. *The Biochemical journal* *461*, 233-245.
- Banko, M. R., Allen, J. J., Schaffer, B. E., Wilker, E. W., Tsou, P., White, J. L., Villen, J., Wang, B., Kim, S. R., Sakamoto, K., *et al.* (2011). Chemical genetic screen for AMPKalpha2 substrates uncovers a network of proteins involved in mitosis. *Molecular cell* *44*, 878-892.
- Barnes, A. P., Lilley, B. N., Pan, Y. A., Plummer, L. J., Powell, A. W., Raines, A. N., Sanes, J. R., and Polleux, F. (2007). LKB1 and SAD kinases define a pathway required for the polarization of cortical neurons. *Cell* *129*, 549-563.
- Berggreen, C., Henriksson, E., Jones, H. A., Morrice, N., and Goransson, O. (2012). cAMP-elevation mediated by beta-adrenergic stimulation inhibits salt-inducible kinase (SIK) 3 activity in adipocytes. *Cellular signalling* *24*, 1863-1871.
- Beroukhi, R., Mermel, C. H., Porter, D., Wei, G., Raychaudhuri, S., Donovan, J., Barretina, J., Boehm, J. S., Dobson, J., Urashima, M., *et al.* (2010). The landscape of somatic copy-number alteration across human cancers. *Nature* *463*, 899-905.

- Betz, C., and Hall, M. N. (2013). Where is mTOR and what is it doing there? *The Journal of cell biology* 203, 563-574.
- Blumenschein, G. R., Jr., Smit, E. F., Planchard, D., Kim, D. W., Cadranel, J., De Pas, T., Dunphy, F., Udud, K., Ahn, M. J., Hanna, N. H., *et al.* (2015). A randomized phase II study of the MEK1/MEK2 inhibitor trametinib (GSK1120212) compared with docetaxel in KRAS-mutant advanced non-small-cell lung cancer (NSCLC)dagger. *Annals of oncology : official journal of the European Society for Medical Oncology* 26, 894-901.
- Bonaccorsi, S., Mottier, V., Giansanti, M. G., Bolkan, B. J., Williams, B., Goldberg, M. L., and Gatti, M. (2007). The Drosophila Lkb1 kinase is required for spindle formation and asymmetric neuroblast division. *Development (Cambridge, England)* 134, 2183-2193.
- Boudeau, J., Baas, A. F., Deak, M., Morrice, N. A., Kieloch, A., Schutkowski, M., Prescott, A. R., Clevers, H. C., and Alessi, D. R. (2003). MO25alpha/beta interact with STRADalpha/beta enhancing their ability to bind, activate and localize LKB1 in the cytoplasm. *Embo j* 22, 5102-5114.
- Brajenovic, M., Joberty, G., Kuster, B., Bouwmeester, T., and Drewes, G. (2004). Comprehensive proteomic analysis of human Par protein complexes reveals an interconnected protein network. *The Journal of biological chemistry* 279, 12804-12811.
- Brummelkamp, T. R., Bernards, R., and Agami, R. (2002). Stable suppression of tumorigenicity by virus-mediated RNA interference. *Cancer cell* 2, 243-247.
- Bultot, L., Guigas, B., Von Wilamowitz-Moellendorff, A., Maisin, L., Vertommen, D., Hussain, N., Beullens, M., Guinovart, J. J., Foretz, M., Viollet, B., *et al.* (2012). AMP-activated protein kinase phosphorylates and inactivates liver glycogen synthase. *The Biochemical journal* 443, 193-203.
- Byers, H. R., Boissel, S. J., Tu, C., and Park, H. Y. (2010). RNAi-mediated knockdown of protein kinase C-alpha inhibits cell migration in MM-RU human metastatic melanoma cell line. *Melanoma research* 20, 171-178.
- Carlson, C. A., and Kim, K. H. (1974). Regulation of hepatic acetyl coenzyme A carboxylase by phosphorylation and dephosphorylation. *Archives of biochemistry and biophysics* 164, 478-489.
- Carretero, J., Shimamura, T., Rikova, K., Jackson, A. L., Wilkerson, M. D., Borgman, C. L., Buttarazzi, M. S., Sanofsky, B. A., McNamara, K. L., Brandstetter, K. A., *et al.* (2010). Integrative genomic and proteomic analyses identify targets for Lkb1-deficient metastatic lung tumors. *Cancer cell* 17, 547-559.
- Chan, K. T., Asokan, S. B., King, S. J., Bo, T., Dubose, E. S., Liu, W., Berginski, M. E., Simon, J. M., Davis, I. J., Gomez, S. M., *et al.* (2014). LKB1 loss in melanoma disrupts directional migration toward extracellular matrix cues. *The Journal of cell biology* 207, 299-315.

Chang, X. Z., Yu, J., Liu, H. Y., Dong, R. H., and Cao, X. C. (2012). ARK5 is associated with the invasive and metastatic potential of human breast cancer cells. *Journal of cancer research and clinical oncology* 138, 247-254.

Chavez, J. A., Roach, W. G., Keller, S. R., Lane, W. S., and Lienhard, G. E. (2008). Inhibition of GLUT4 translocation by Tbc1d1, a Rab GTPase-activating protein abundant in skeletal muscle, is partially relieved by AMP-activated protein kinase activation. *The Journal of biological chemistry* 283, 9187-9195.

Chen, D., Liu, G., Xu, N., You, X., Zhou, H., Zhao, X., and Liu, Q. (2017). Knockdown of ARK5 Expression Suppresses Invasion and Metastasis of Gastric Cancer. *Cellular physiology and biochemistry : international journal of experimental cellular physiology, biochemistry, and pharmacology* 42, 1025-1036.

Chen, L., Jiao, Z. H., Zheng, L. S., Zhang, Y. Y., Xie, S. T., Wang, Z. X., and Wu, J. W. (2009). Structural insight into the autoinhibition mechanism of AMP-activated protein kinase. *Nature* 459, 1146-1149.

Chen, P., Li, K., Liang, Y., Li, L., and Zhu, X. (2013). High NUA1 expression correlates with poor prognosis and involved in NSCLC cells migration and invasion. *Experimental lung research* 39, 9-17.

Chen, S., Murphy, J., Toth, R., Campbell, D. G., Morrice, N. A., and Mackintosh, C. (2008). Complementary regulation of TBC1D1 and AS160 by growth factors, insulin and AMPK activators. *The Biochemical journal* 409, 449-459.

Chen, Z., Cheng, K., Walton, Z., Wang, Y., Ebi, H., Shimamura, T., Liu, Y., Tupper, T., Ouyang, J., Li, J., *et al.* (2012). A murine lung cancer co-clinical trial identifies genetic modifiers of therapeutic response. *Nature* 483, 613-617.

Chen, Z., Fillmore, C. M., Hammerman, P. S., Kim, C. F., and Wong, K. K. (2014). Non-small-cell lung cancers: a heterogeneous set of diseases. *Nature reviews Cancer* 14, 535-546.

Cheung, P. C., Salt, I. P., Davies, S. P., Hardie, D. G., and Carling, D. (2000). Characterization of AMP-activated protein kinase gamma-subunit isoforms and their role in AMP binding. *The Biochemical journal* 346 Pt 3, 659-669.

Choo, A. Y., Yoon, S. O., Kim, S. G., Roux, P. P., and Blenis, J. (2008). Rapamycin differentially inhibits S6Ks and 4E-BP1 to mediate cell-type-specific repression of mRNA translation. *Proceedings of the National Academy of Sciences of the United States of America* 105, 17414-17419.

Clapham, D. E. (2007). Calcium signaling. *Cell* 131, 1047-1058.

Cool, B., Zinker, B., Chiou, W., Kifle, L., Cao, N., Perham, M., Dickinson, R., Adler, A., Gagne, G., Iyengar, R., *et al.* (2006). Identification and characterization of a small molecule AMPK activator that treats key components of type 2 diabetes and the metabolic syndrome. *Cell metabolism* 3, 403-416.

Courchet, J., Lewis, T. L., Jr., Lee, S., Courchet, V., Liou, D. Y., Aizawa, S., and Polleux, F. (2013). Terminal axon branching is regulated by the LKB1-NUAK1 kinase pathway via presynaptic mitochondrial capture. *Cell* 153, 1510-1525.

- Cox, A. D., Fesik, S. W., Kimmelman, A. C., Luo, J., and Der, C. J. (2014). Drugging the undruggable RAS: Mission possible? *Nature reviews Drug discovery* 13, 828-851.
- Cui, J., Yu, Y., Lu, G. F., Liu, C., Liu, X., Xu, Y. X., and Zheng, P. Y. (2013). Overexpression of ARK5 is associated with poor prognosis in hepatocellular carcinoma. *Tumour biology : the journal of the International Society for Oncodevelopmental Biology and Medicine* 34, 1913-1918.
- Cuzick, J., Otto, F., Baron, J. A., Brown, P. H., Burn, J., Greenwald, P., Jankowski, J., La Vecchia, C., Meyskens, F., Senn, H. J., and Thun, M. (2009). Aspirin and non-steroidal anti-inflammatory drugs for cancer prevention: an international consensus statement. *The Lancet Oncology* 10, 501-507.
- Dalla-Favera, R., Bregni, M., Erikson, J., Patterson, D., Gallo, R. C., and Croce, C. M. (1982). Human c-myc onc gene is located on the region of chromosome 8 that is translocated in Burkitt lymphoma cells. *Proceedings of the National Academy of Sciences of the United States of America* 79, 7824-7827.
- Dang, C. V. (2012). MYC on the path to cancer. *Cell* 149, 22-35.
- Dankort, D., Jeyabalan, N., Jones, N., Dumont, D. J., and Muller, W. J. (2001). Multiple ErbB-2/Neu Phosphorylation Sites Mediate Transformation through Distinct Effector Proteins. *The Journal of biological chemistry* 276, 38921-38928.
- Datta, S. R., Dudek, H., Tao, X., Masters, S., Fu, H., Gotoh, Y., and Greenberg, M. E. (1997). Akt phosphorylation of BAD couples survival signals to the cell-intrinsic death machinery. *Cell* 91, 231-241.
- Deguchi, A., Miyoshi, H., Kojima, Y., Okawa, K., Aoki, M., and Taketo, M. M. (2010). LKB1 suppresses p21-activated kinase-1 (PAK1) by phosphorylation of Thr109 in the p21-binding domain. *The Journal of biological chemistry* 285, 18283-18290.
- Deming, S. L., Nass, S. J., Dickson, R. B., and Trock, B. J. (2000). C-myc amplification in breast cancer: a meta-analysis of its occurrence and prognostic relevance. *British journal of cancer* 83, 1688-1695.
- Dentin, R., Liu, Y., Koo, S. H., Hedrick, S., Vargas, T., Heredia, J., Yates, J., 3rd, and Montminy, M. (2007). Insulin modulates gluconeogenesis by inhibition of the coactivator TORC2. *Nature* 449, 366-369.
- Detjen, K. M., Brembeck, F. H., Welzel, M., Kaiser, A., Haller, H., Wiedenmann, B., and Rosewicz, S. (2000). Activation of protein kinase Calpha inhibits growth of pancreatic cancer cells via p21(cip)-mediated G(1) arrest. *Journal of cell science* 113 (Pt 17), 3025-3035.
- Ding, L., Getz, G., Wheeler, D. A., Mardis, E. R., McLellan, M. D., Cibulskis, K., Sougnez, C., Greulich, H., Muzny, D. M., Morgan, M. B., *et al.* (2008). Somatic mutations affect key pathways in lung adenocarcinoma. *Nature* 455, 1069-1075.
- Disatnik, M. H., Boutet, S. C., Lee, C. H., Mochly-Rosen, D., and Rando, T. A. (2002). Sequential activation of individual PKC isozymes in integrin-mediated

muscle cell spreading: a role for MARCKS in an integrin signaling pathway. *Journal of cell science* 115, 2151-2163.

Egan, D. F., Shackelford, D. B., Mihaylova, M. M., Gelino, S., Kohnz, R. A., Mair, W., Vasquez, D. S., Joshi, A., Gwinn, D. M., Taylor, R., *et al.* (2011). Phosphorylation of ULK1 (hATG1) by AMP-activated protein kinase connects energy sensing to mitophagy. *Science (New York, NY)* 331, 456-461.

Evans, J. M., Donnelly, L. A., Emslie-Smith, A. M., Alessi, D. R., and Morris, A. D. (2005). Metformin and reduced risk of cancer in diabetic patients. *BMJ (Clinical research ed)* 330, 1304-1305.

Faubert, B., Boily, G., Izreig, S., Griss, T., Samborska, B., Dong, Z., Dupuy, F., Chambers, C., Fuerth, B. J., Viollet, B., *et al.* (2013). AMPK is a negative regulator of the Warburg effect and suppresses tumor growth in vivo. *Cell metabolism* 17, 113-124.

Fischer, K. R., Durrans, A., Lee, S., Sheng, J., Li, F., Wong, S. T., Choi, H., El Rayes, T., Ryu, S., Troeger, J., *et al.* (2015). Epithelial-to-mesenchymal transition is not required for lung metastasis but contributes to chemoresistance. *Nature* 527, 472-476.

Fisher, J. S., Ju, J. S., Oppelt, P. J., Smith, J. L., Suzuki, A., and Esumi, H. (2005). Muscle contractions, AICAR, and insulin cause phosphorylation of an AMPK-related kinase. *American journal of physiology Endocrinology and metabolism* 289, E986-992.

Fogarty, S., Hawley, Simon A., Green, Kevin A., Saner, N., Mustard, Kirsty J., and Hardie, D G. (2010). Calmodulin-dependent protein kinase kinase- β activates AMPK without forming a stable complex: synergistic effects of Ca²⁺ and AMP. *Biochemical Journal* 426, 109-118.

Frey, M. R., Saxon, M. L., Zhao, X., Rollins, A., Evans, S. S., and Black, J. D. (1997). Protein kinase C isozyme-mediated cell cycle arrest involves induction of p21(waf1/cip1) and p27(kip1) and hypophosphorylation of the retinoblastoma protein in intestinal epithelial cells. *The Journal of biological chemistry* 272, 9424-9435.

Fujimoto, T., Yurimoto, S., Hatano, N., Nozaki, N., Sueyoshi, N., Kameshita, I., Mizutani, A., Mikoshiba, K., Kobayashi, R., and Tokumitsu, H. (2008). Activation of SAD kinase by Ca²⁺/calmodulin-dependent protein kinase kinase. *Biochemistry* 47, 4151-4159.

Garg, M., Kanojia, D., Okamoto, R., Jain, S., Madan, V., Chien, W., Sampath, A., Ding, L. W., Xuan, M., Said, J. W., *et al.* (2014a). Laminin-5 γ -2 (LAMC2) is highly expressed in anaplastic thyroid carcinoma and is associated with tumor progression, migration, and invasion by modulating signaling of EGFR. *The Journal of clinical endocrinology and metabolism* 99, E62-72.

Garg, R., Benedetti, L. G., Abera, M. B., Wang, H., Abba, M., and Kazanietz, M. G. (2014b). Protein kinase C and cancer: what we know and what we do not. *Oncogene* 33, 5225-5237.

Garrett, T. P., McKern, N. M., Lou, M., Elleman, T. C., Adams, T. E., Lovrecz, G. O., Kofler, M., Jorissen, R. N., Nice, E. C., Burgess, A. W., and Ward, C. W. (2003). The crystal structure of a truncated ErbB2 ectodomain reveals an active conformation, poised to interact with other ErbB receptors. *Molecular cell* *11*, 495-505.

Goodwin, J. M., Svensson, R. U., Lou, H. J., Winslow, M. M., Turk, B. E., and Shaw, R. J. (2014). An AMPK-independent signaling pathway downstream of the LKB1 tumor suppressor controls Snail1 and metastatic potential. *Molecular cell* *55*, 436-450.

Goodwin, P. J., Pritchard, K. I., Ennis, M., Clemons, M., Graham, M., and Fantus, I. G. (2008). Insulin-lowering effects of metformin in women with early breast cancer. *Clinical breast cancer* *8*, 501-505.

Goransson, O., McBride, A., Hawley, S. A., Ross, F. A., Shpiro, N., Foretz, M., Viollet, B., Hardie, D. G., and Sakamoto, K. (2007). Mechanism of action of A-769662, a valuable tool for activation of AMP-activated protein kinase. *The Journal of biological chemistry* *282*, 32549-32560.

Govindan, R., Ding, L., Griffith, M., Subramanian, J., Dees, N. D., Kanchi, K. L., Maher, C. A., Fulton, R., Fulton, L., Wallis, J., *et al.* (2012). Genomic landscape of non-small cell lung cancer in smokers and never-smokers. *Cell* *150*, 1121-1134.

Gowans, G. J., Hawley, S. A., Ross, F. A., and Hardie, D. G. (2013). AMP is a true physiological regulator of AMP-activated protein kinase by both allosteric activation and enhancing net phosphorylation. *Cell metabolism* *18*, 556-566.

Guan, L., Song, K., Pysz, M. A., Curry, K. J., Hizli, A. A., Danielpour, D., Black, A. R., and Black, J. D. (2007). Protein kinase C-mediated down-regulation of cyclin D1 involves activation of the translational repressor 4E-BP1 via a phosphoinositide 3-kinase/Akt-independent, protein phosphatase 2A-dependent mechanism in intestinal epithelial cells. *The Journal of biological chemistry* *282*, 14213-14225.

Gwinn, D. M., Shackelford, D. B., Egan, D. F., Mihaylova, M. M., Mery, A., Vasquez, D. S., Turk, B. E., and Shaw, R. J. (2008). AMPK phosphorylation of raptor mediates a metabolic checkpoint. *Molecular cell* *30*, 214-226.

Ha, J., Daniel, S., Broyles, S. S., and Kim, K. H. (1994). Critical phosphorylation sites for acetyl-CoA carboxylase activity. *The Journal of biological chemistry* *269*, 22162-22168.

Habib, T., Park, H., Tsang, M., de Alboran, I. M., Nicks, A., Wilson, L., Knoepfler, P. S., Andrews, S., Rawlings, D. J., Eisenman, R. N., and Iritani, B. M. (2007). Myc stimulates B lymphocyte differentiation and amplifies calcium signaling. *The Journal of cell biology* *179*, 717-731.

Hara, K., Maruki, Y., Long, X., Yoshino, K., Oshiro, N., Hidayat, S., Tokunaga, C., Avruch, J., and Yonezawa, K. (2002). Raptor, a binding partner of target of rapamycin (TOR), mediates TOR action. *Cell* *110*, 177-189.

Hardie, D. G., Ross, F. A., and Hawley, S. A. (2012). AMPK: a nutrient and energy sensor that maintains energy homeostasis. *Nature reviews Molecular cell biology* 13, 251-262.

Haughian, J. M., and Bradford, A. P. (2009). Protein kinase C alpha (PKCalpha) regulates growth and invasion of endometrial cancer cells. *Journal of cellular physiology* 220, 112-118.

Hawley, S. A., Boudeau, J., Reid, J. L., Mustard, K. J., Udd, L., Makela, T. P., Alessi, D. R., and Hardie, D. G. (2003). Complexes between the LKB1 tumor suppressor, STRAD alpha/beta and MO25 alpha/beta are upstream kinases in the AMP-activated protein kinase cascade. *Journal of biology* 2, 28.

Hawley, S. A., Davison, M., Woods, A., Davies, S. P., Beri, R. K., Carling, D., and Hardie, D. G. (1996). Characterization of the AMP-activated protein kinase from rat liver and identification of threonine 172 as the major site at which it phosphorylates AMP-activated protein kinase. *The Journal of biological chemistry* 271, 27879-27887.

Hawley, S. A., Fullerton, M. D., Ross, F. A., Schertzer, J. D., Chevtzoff, C., Walker, K. J., Peggie, M. W., Zibrova, D., Green, K. A., Mustard, K. J., *et al.* (2012). The ancient drug salicylate directly activates AMP-activated protein kinase. *Science (New York, NY)* 336, 918-922.

Hawley, S. A., Pan, D. A., Mustard, K. J., Ross, L., Bain, J., Edelman, A. M., Frenguelli, B. G., and Hardie, D. G. (2005). Calmodulin-dependent protein kinase kinase-beta is an alternative upstream kinase for AMP-activated protein kinase. *Cell metabolism* 2, 9-19.

Henriksson, E., Jones, H. A., Patel, K., Peggie, M., Morrice, N., Sakamoto, K., and Goransson, O. (2012). The AMPK-related kinase SIK2 is regulated by cAMP via phosphorylation at Ser358 in adipocytes. *The Biochemical journal* 444, 503-514.

Henriksson, E., Sall, J., Gormand, A., Wasserstrom, S., Morrice, N. A., Fritzen, A. M., Foretz, M., Campbell, D. G., Sakamoto, K., Ekelund, M., *et al.* (2015). SIK2 regulates CRTCs, HDAC4 and glucose uptake in adipocytes. *Journal of cell science* 128, 472-486.

Hirano, M., Kiyonari, H., Inoue, A., Furushima, K., Murata, T., Suda, Y., and Aizawa, S. (2006). A new serine/threonine protein kinase, Omphk1, essential to ventral body wall formation. *Developmental dynamics : an official publication of the American Association of Anatomists* 235, 2229-2237.

Hock, A. K., Cheung, E. C., Humpton, T. J., Monteverde, T., Paulus-Hock, V., Lee, P., McGhee, E., Scopelliti, A., Murphy, D. J., Strathdee, D., *et al.* (2017). Development of an inducible mouse model of iRFP713 to track recombinase activity and tumour development in vivo. *Scientific reports* 7, 1837.

Holley, R. W., and Kiernan, J. A. (1974). Control of the initiation of DNA synthesis in 3T3 cells: low-molecular weight nutrients. *Proceedings of the National Academy of Sciences of the United States of America* 71, 2942-2945.

Hong, S. P., Leiper, F. C., Woods, A., Carling, D., and Carlson, M. (2003). Activation of yeast Snf1 and mammalian AMP-activated protein kinase by

- upstream kinases. *Proceedings of the National Academy of Sciences of the United States of America* *100*, 8839-8843.
- Hou, X., Liu, J. E., Liu, W., Liu, C. Y., Liu, Z. Y., and Sun, Z. Y. (2011). A new role of NUA1: directly phosphorylating p53 and regulating cell proliferation. *Oncogene* *30*, 2933-2942.
- Hsiao, W. L., Housey, G. M., Johnson, M. D., and Weinstein, I. B. (1989). Cells that overproduce protein kinase C are more susceptible to transformation by an activated H-ras oncogene. *Molecular and cellular biology* *9*, 2641-2647.
- Huang, X., Lv, W., Zhang, J. H., and Lu, D. L. (2014). miR96 functions as a tumor suppressor gene by targeting NUA1 in pancreatic cancer. *International journal of molecular medicine* *34*, 1599-1605.
- Humbert, N., Navaratnam, N., Augert, A., Da Costa, M., Martien, S., Wang, J., Martinez, D., Abbadie, C., Carling, D., de Launoit, Y., *et al.* (2010). Regulation of ploidy and senescence by the AMPK-related kinase NUA1. *Embo j* *29*, 376-386.
- Hundal, R. S., Petersen, K. F., Mayerson, A. B., Randhawa, P. S., Inzucchi, S., Shoelson, S. E., and Shulman, G. I. (2002). Mechanism by which high-dose aspirin improves glucose metabolism in type 2 diabetes. *The Journal of clinical investigation* *109*, 1321-1326.
- Hurley, R. L., Anderson, K. A., Franzone, J. M., Kemp, B. E., Means, A. R., and Witters, L. A. (2005). The Ca²⁺/calmodulin-dependent protein kinase kinases are AMP-activated protein kinase kinases. *The Journal of biological chemistry* *280*, 29060-29066.
- Hurov, J. B., Watkins, J. L., and Piwnica-Worms, H. (2004). Atypical PKC phosphorylates PAR-1 kinases to regulate localization and activity. *Current biology : CB* *14*, 736-741.
- Ihle, N. T., Byers, L. A., Kim, E. S., Saintigny, P., Lee, J. J., Blumenschein, G. R., Tsao, A., Liu, S., Larsen, J. E., Wang, J., *et al.* (2012). Effect of KRAS oncogene substitutions on protein behavior: implications for signaling and clinical outcome. *Journal of the National Cancer Institute* *104*, 228-239.
- Imamura, K., Ogura, T., Kishimoto, A., Kaminishi, M., and Esumi, H. (2001). Cell cycle regulation via p53 phosphorylation by a 5'-AMP activated protein kinase activator, 5-aminoimidazole- 4-carboxamide-1-beta-D-ribofuranoside, in a human hepatocellular carcinoma cell line. *Biochemical and biophysical research communications* *287*, 562-567.
- Inazuka, F., Sugiyama, N., Tomita, M., Abe, T., Shioi, G., and Esumi, H. (2012). Muscle-specific knock-out of NUA family SNF1-like kinase 1 (NUAK1) prevents high fat diet-induced glucose intolerance. *The Journal of biological chemistry* *287*, 16379-16389.
- Inoki, K., Li, Y., Zhu, T., Wu, J., and Guan, K. L. (2002). TSC2 is phosphorylated and inhibited by Akt and suppresses mTOR signalling. *Nature cell biology* *4*, 648-657.

- Inoki, K., Zhu, T., and Guan, K. L. (2003). TSC2 mediates cellular energy response to control cell growth and survival. *Cell* *115*, 577-590.
- Iwakawa, R., Kohno, T., Kato, M., Shiraishi, K., Tsuta, K., Noguchi, M., Ogawa, S., and Yokota, J. (2011). MYC amplification as a prognostic marker of early-stage lung adenocarcinoma identified by whole genome copy number analysis. *Clinical cancer research : an official journal of the American Association for Cancer Research* *17*, 1481-1489.
- Jackson, E. L., Olive, K. P., Tuveson, D. A., Bronson, R., Crowley, D., Brown, M., and Jacks, T. (2005). The differential effects of mutant p53 alleles on advanced murine lung cancer. *Cancer research* *65*, 10280-10288.
- Jackson, E. L., Willis, N., Mercer, K., Bronson, R. T., Crowley, D., Montoya, R., Jacks, T., and Tuveson, D. A. (2001). Analysis of lung tumor initiation and progression using conditional expression of oncogenic K-ras. *Genes & development* *15*, 3243-3248.
- Jager, S., Handschin, C., St-Pierre, J., and Spiegelman, B. M. (2007). AMP-activated protein kinase (AMPK) action in skeletal muscle via direct phosphorylation of PGC-1alpha. *Proceedings of the National Academy of Sciences of the United States of America* *104*, 12017-12022.
- Jang, T., Calaoagan, J. M., Kwon, E., Samuelsson, S., Recht, L., and Laderoute, K. R. (2011). 5'-AMP-activated protein kinase activity is elevated early during primary brain tumor development in the rat. *International journal of cancer* *128*, 2230-2239.
- Janne, P. A., Shaw, A. T., Pereira, J. R., Jeannin, G., Vansteenkiste, J., Barrios, C., Franke, F. A., Grinsted, L., Zazulina, V., Smith, P., *et al.* (2013). Selumetinib plus docetaxel for KRAS-mutant advanced non-small-cell lung cancer: a randomised, multicentre, placebo-controlled, phase 2 study. *The Lancet Oncology* *14*, 38-47.
- Jeon, S. M., Chandel, N. S., and Hay, N. (2012). AMPK regulates NADPH homeostasis to promote tumour cell survival during energy stress. *Nature* *485*, 661-665.
- Ji, H., Ramsey, M. R., Hayes, D. N., Fan, C., McNamara, K., Kozlowski, P., Torrice, C., Wu, M. C., Shimamura, T., Perera, S. A., *et al.* (2007). LKB1 modulates lung cancer differentiation and metastasis. *Nature* *448*, 807-810.
- Jones, R. G., Plas, D. R., Kubek, S., Buzzai, M., Mu, J., Xu, Y., Birnbaum, M. J., and Thompson, C. B. (2005). AMP-activated protein kinase induces a p53-dependent metabolic checkpoint. *Molecular cell* *18*, 283-293.
- Jorgensen, S. B., Nielsen, J. N., Birk, J. B., Olsen, G. S., Viollet, B., Andreelli, F., Schjerling, P., Vaulont, S., Hardie, D. G., Hansen, B. F., *et al.* (2004). The alpha2-5'AMP-activated protein kinase is a site 2 glycogen synthase kinase in skeletal muscle and is responsive to glucose loading. *Diabetes* *53*, 3074-3081.
- Kim, D. H., Sarbassov, D. D., Ali, S. M., King, J. E., Latek, R. R., Erdjument-Bromage, H., Tempst, P., and Sabatini, D. M. (2002). mTOR interacts with raptor

to form a nutrient-sensitive complex that signals to the cell growth machinery. *Cell* 110, 163-175.

Kim, J., Kundu, M., Viollet, B., and Guan, K. L. (2011). AMPK and mTOR regulate autophagy through direct phosphorylation of Ulk1. *Nature cell biology* 13, 132-141.

Kim, S., Han, J., Lee, S. K., Choi, M. Y., Kim, J., Lee, J., Jung, S. P., Kim, J. S., Kim, J. H., Choe, J. H., *et al.* (2012a). Berberine suppresses the TPA-induced MMP-1 and MMP-9 expressions through the inhibition of PKC-alpha in breast cancer cells. *The Journal of surgical research* 176, e21-29.

Kim, S. Y., Jeong, S., Jung, E., Baik, K. H., Chang, M. H., Kim, S. A., Shim, J. H., Chun, E., and Lee, K. Y. (2012b). AMP-activated protein kinase-alpha1 as an activating kinase of TGF-beta-activated kinase 1 has a key role in inflammatory signals. *Cell death & disease* 3, e357.

Kim, T., Davis, J., Zhang, A. J., He, X., and Mathews, S. T. (2009). Curcumin activates AMPK and suppresses gluconeogenic gene expression in hepatoma cells. *Biochemical and biophysical research communications* 388, 377-382.

Kobayashi, S., Boggon, T. J., Dayaram, T., Janne, P. A., Kocher, O., Meyerson, M., Johnson, B. E., Eck, M. J., Tenen, D. G., and Halmos, B. (2005). EGFR mutation and resistance of non-small-cell lung cancer to gefitinib. *The New England journal of medicine* 352, 786-792.

Kodiha, M., Rassi, J. G., Brown, C. M., and Stochaj, U. (2007). Localization of AMP kinase is regulated by stress, cell density, and signaling through the MEK-->ERK1/2 pathway. *American journal of physiology Cell physiology* 293, C1427-1436.

Kottakis, F., Nicolay, B. N., Roumane, A., Karnik, R., Gu, H., Nagle, J. M., Boukhali, M., Hayward, M. C., Li, Y. Y., Chen, T., *et al.* (2016). LKB1 loss links serine metabolism to DNA methylation and tumorigenesis. *Nature* 539, 390-395.

Kusakai, G., Suzuki, A., Ogura, T., Miyamoto, S., Ochiai, A., Kaminishi, M., and Esumi, H. (2004). ARK5 expression in colorectal cancer and its implications for tumor progression. *The American journal of pathology* 164, 987-995.

Lee, Y. S., Kim, W. S., Kim, K. H., Yoon, M. J., Cho, H. J., Shen, Y., Ye, J. M., Lee, C. H., Oh, W. K., Kim, C. T., *et al.* (2006). Berberine, a natural plant product, activates AMP-activated protein kinase with beneficial metabolic effects in diabetic and insulin-resistant states. *Diabetes* 55, 2256-2264.

Lefebvre, D. L., Bai, Y., Shahmolky, N., Sharma, M., Poon, R., Drucker, D. J., and Rosen, C. F. (2001). Identification and characterization of a novel sucrose-non-fermenting protein kinase/AMP-activated protein kinase-related protein kinase, SNARK. *The Biochemical journal* 355, 297-305.

Legembre, P., Schickel, R., Barnhart, B. C., and Peter, M. E. (2004). Identification of SNF1/AMP kinase-related kinase as an NF-kappaB-regulated anti-apoptotic kinase involved in CD95-induced motility and invasiveness. *The Journal of biological chemistry* 279, 46742-46747.

Leprivier, G., Remke, M., Rotblat, B., Dubuc, A., Mateo, A. R., Kool, M., Agnihotri, S., El-Naggar, A., Yu, B., Somasekharan, S. P., *et al.* (2013). The eEF2 kinase confers resistance to nutrient deprivation by blocking translation elongation. *Cell* 153, 1064-1079.

Li, F., Han, X., Li, F., Wang, R., Wang, H., Gao, Y., Wang, X., Fang, Z., Zhang, W., Yao, S., *et al.* (2015a). LKB1 Inactivation Elicits a Redox Imbalance to Modulate Non-small Cell Lung Cancer Plasticity and Therapeutic Response. *Cancer cell* 27, 698-711.

Li, R. J., Xu, J., Fu, C., Zhang, J., Zheng, Y. G., Jia, H., and Liu, J. O. (2016). Regulation of mTORC1 by lysosomal calcium and calmodulin. *eLife* 5.

Li, W., Zhang, J., Flechner, L., Hyun, T., Yam, A., Franke, T. F., and Pierce, J. H. (1999). Protein kinase C-alpha overexpression stimulates Akt activity and suppresses apoptosis induced by interleukin 3 withdrawal. *Oncogene* 18, 6564-6572.

Li, X., Wang, L., Zhou, X. E., Ke, J., de Waal, P. W., Gu, X., Tan, M. H., Wang, D., Wu, D., Xu, H. E., and Melcher, K. (2015b). Structural basis of AMPK regulation by adenine nucleotides and glycogen. *Cell research* 25, 50-66.

Liang, X., Li, Z. L., Jiang, L. L., Guo, Q. Q., Liu, M. J., and Nan, K. J. (2014). Suppression of lung cancer cell invasion by LKB1 is due to the downregulation of tissue factor and vascular endothelial growth factor, partly dependent on SP1. *International journal of oncology* 44, 1989-1997.

Linardou, H., Dahabreh, I. J., Kanaloupiti, D., Siannis, F., Bafaloukos, D., Kosmidis, P., Papadimitriou, C. A., and Murray, S. (2008). Assessment of somatic k-RAS mutations as a mechanism associated with resistance to EGFR-targeted agents: a systematic review and meta-analysis of studies in advanced non-small-cell lung cancer and metastatic colorectal cancer. *The Lancet Oncology* 9, 962-972.

Lito, P., Solomon, M., Li, L. S., Hansen, R., and Rosen, N. (2016). Allele-specific inhibitors inactivate mutant KRAS G12C by a trapping mechanism. *Science (New York, NY)* 351, 604-608.

Liu, L., Ulbrich, J., Muller, J., Wustefeld, T., Aeberhard, L., Kress, T. R., Muthalagu, N., Rycak, L., Rudalska, R., Moll, R., *et al.* (2012). Deregulated MYC expression induces dependence upon AMPK-related kinase 5. *Nature* 483, 608-612.

Lizcano, J. M., Goransson, O., Toth, R., Deak, M., Morrice, N. A., Boudeau, J., Hawley, S. A., Udd, L., Makela, T. P., Hardie, D. G., and Alessi, D. R. (2004a). LKB1 is a master kinase that activates 13 kinases of the AMPK subfamily, including MARK/PAR-1. *Embo j* 23, 833-843.

Lizcano, J. M., Göransson, O., Toth, R., Deak, M., Morrice, N. A., Boudeau, J., Hawley, S. A., Udd, L., Mäkelä, T. P., Hardie, D. G., and Alessi, D. R. (2004b). LKB1 is a master kinase that activates 13 kinases of the AMPK subfamily, including MARK/PAR-1. *The EMBO Journal* 23, 833-843.

Lobell, R. B., Omer, C. A., Abrams, M. T., Bhimnathwala, H. G., Brucker, M. J., Buser, C. A., Davide, J. P., deSolms, S. J., Dinsmore, C. J., Ellis-Hutchings, M. S., *et al.* (2001). Evaluation of farnesyl:protein transferase and geranylgeranyl:protein transferase inhibitor combinations in preclinical models. *Cancer research* 61, 8758-8768.

Londesborough, A., Vaahtomeri, K., Tiainen, M., Katajisto, P., Ekman, N., Vallenius, T., and Makela, T. P. (2008). LKB1 in endothelial cells is required for angiogenesis and TGFbeta-mediated vascular smooth muscle cell recruitment. *Development (Cambridge, England)* 135, 2331-2338.

Long, X., Lin, Y., Ortiz-Vega, S., Yonezawa, K., and Avruch, J. (2005). Rheb binds and regulates the mTOR kinase. *Current biology : CB* 15, 702-713.

Lu, S., Niu, N., Guo, H., Tang, J., Guo, W., Liu, Z., Shi, L., Sun, T., Zhou, F., Li, H., *et al.* (2013). ARK5 promotes glioma cell invasion, and its elevated expression is correlated with poor clinical outcome. *European journal of cancer (Oxford, England : 1990)* 49, 752-763.

Maemondo, M., Inoue, A., Kobayashi, K., Sugawara, S., Oizumi, S., Isobe, H., Gemma, A., Harada, M., Yoshizawa, H., Kinoshita, I., *et al.* (2010). Gefitinib or chemotherapy for non-small-cell lung cancer with mutated EGFR. *The New England journal of medicine* 362, 2380-2388.

Magnifico, A., Albano, L., Campaner, S., Campiglio, M., Pilotti, S., Menard, S., and Tagliabue, E. (2007). Protein kinase Calpha determines HER2 fate in breast carcinoma cells with HER2 protein overexpression without gene amplification. *Cancer research* 67, 5308-5317.

Malumbres, M., and Barbacid, M. (2003). RAS oncogenes: the first 30 years. *Nature reviews Cancer* 3, 459-465.

Manchado, E., Weissmueller, S., Morris, J. P. t., Chen, C. C., Wullenkord, R., Lujambio, A., de Stanchina, E., Poirier, J. T., Gainor, J. F., Corcoran, R. B., *et al.* (2016). A combinatorial strategy for treating KRAS-mutant lung cancer. *Nature* 534, 647-651.

Mandil, R., Ashkenazi, E., Blass, M., Kronfeld, I., Kazimirsky, G., Rosenthal, G., Umansky, F., Lorenzo, P. S., Blumberg, P. M., and Brodie, C. (2001). Protein kinase Calpha and protein kinase Cdelta play opposite roles in the proliferation and apoptosis of glioma cells. *Cancer research* 61, 4612-4619.

Manifava, M., Smith, M., Rotondo, S., Walker, S., Niewczas, I., Zoncu, R., Clark, J., and Ktistakis, N. T. (2016). Dynamics of mTORC1 activation in response to amino acids. *eLife* 5.

Manning, B. D., and Toker, A. (2017). AKT/PKB Signaling: Navigating the Network. *Cell* 169, 381-405.

Manning, G., Whyte, D. B., Martinez, R., Hunter, T., and Sudarsanam, S. (2002). The protein kinase complement of the human genome. *Science (New York, NY)* 298, 1912-1934.

Marshall, J. L., Eisenberg, S. G., Johnson, M. D., Hanfelt, J., Dorr, F. A., El-Ashry, D., Oberst, M., Fuxman, Y., Holmlund, J., and Malik, S. (2004). A phase II trial of ISIS 3521 in patients with metastatic colorectal cancer. *Clinical colorectal cancer* 4, 268-274.

Marsin, A. S., Bertrand, L., Rider, M. H., Deprez, J., Beauloye, C., Vincent, M. F., Van den Berghe, G., Carling, D., and Hue, L. (2000). Phosphorylation and activation of heart PFK-2 by AMPK has a role in the stimulation of glycolysis during ischaemia. *Current biology : CB* 10, 1247-1255.

Marsin, A. S., Bouzin, C., Bertrand, L., and Hue, L. (2002). The stimulation of glycolysis by hypoxia in activated monocytes is mediated by AMP-activated protein kinase and inducible 6-phosphofructo-2-kinase. *The Journal of biological chemistry* 277, 30778-30783.

Massarelli, E., Varella-Garcia, M., Tang, X., Xavier, A. C., Ozburn, N. C., Liu, D. D., Bekele, B. N., Herbst, R. S., and Wistuba, II (2007). KRAS mutation is an important predictor of resistance to therapy with epidermal growth factor receptor tyrosine kinase inhibitors in non-small-cell lung cancer. *Clinical cancer research : an official journal of the American Association for Cancer Research* 13, 2890-2896.

McGee, S. L., van Denderen, B. J., Howlett, K. F., Mollica, J., Schertzer, J. D., Kemp, B. E., and Hargreaves, M. (2008). AMP-activated protein kinase regulates GLUT4 transcription by phosphorylating histone deacetylase 5. *Diabetes* 57, 860-867.

Meng, D., Yuan, M., Li, X., Chen, L., Yang, J., Zhao, X., Ma, W., and Xin, J. (2013). Prognostic value of K-RAS mutations in patients with non-small cell lung cancer: a systematic review with meta-analysis. *Lung cancer (Amsterdam, Netherlands)* 81, 1-10.

Miranda, F., Mannion, D., Liu, S., Zheng, Y., Mangala, L. S., Redondo, C., Herrero-Gonzalez, S., Xu, R., Taylor, C., Chedom, D. F., *et al.* (2016). Salt-Inducible Kinase 2 Couples Ovarian Cancer Cell Metabolism with Survival at the Adipocyte-Rich Metastatic Niche. *Cancer cell* 30, 273-289.

Miyamoto, T., Rho, E., Sample, V., Akano, H., Magari, M., Ueno, T., Gorshkov, K., Chen, M., Tokumitsu, H., Zhang, J., and Inoue, T. (2015). Compartmentalized AMPK signaling illuminated by genetically encoded molecular sensors and actuators. *Cell reports* 11, 657-670.

Moelling, K., Schad, K., Bosse, M., Zimmermann, S., and Schweneker, M. (2002). Regulation of Raf-Akt Cross-talk. *The Journal of biological chemistry* 277, 31099-31106.

Momcilovic, M., Hong, S. P., and Carlson, M. (2006). Mammalian TAK1 activates Snf1 protein kinase in yeast and phosphorylates AMP-activated protein kinase in vitro. *The Journal of biological chemistry* 281, 25336-25343.

Momcilovic, M., McMickle, R., Abt, E., Seki, A., Simko, S. A., Magyar, C., Stout, D. B., Fishbein, M. C., Walser, T. C., Dubinett, S. M., and Shackelford, D. B. (2015). Heightening Energetic Stress Selectively Targets LKB1-Deficient Non-Small Cell Lung Cancers. *Cancer research* 75, 4910-4922.

Monteverde, T., Muthalagu, N., Port, J., and Murphy, D. J. (2015). Evidence of cancer-promoting roles for AMPK and related kinases. *The FEBS journal* 282, 4658-4671.

Monteverde, T., Tait-Mulder, J., Hedley, A., Knight, J. R., Sansom, O. J., and Murphy, D. J. (2017). Calcium signalling links MYC to NUA1. *Oncogene*.

Munday, M. R., Campbell, D. G., Carling, D., and Hardie, D. G. (1988). Identification by amino acid sequencing of three major regulatory phosphorylation sites on rat acetyl-CoA carboxylase. *European journal of biochemistry* 175, 331-338.

Murphy, D. J., Junttila, M. R., Pouyet, L., Karnezis, A., Shchors, K., Bui, D. A., Brown-Swigart, L., Johnson, L., and Evan, G. I. (2008). Distinct thresholds govern Myc's biological output in vivo. *Cancer cell* 14, 447-457.

Namiki, T., Tanemura, A., Valencia, J. C., Coelho, S. G., Passeron, T., Kawaguchi, M., Vieira, W. D., Ishikawa, M., Nishijima, W., Izumo, T., *et al.* (2011). AMP kinase-related kinase NUA2 affects tumor growth, migration, and clinical outcome of human melanoma. *Proceedings of the National Academy of Sciences of the United States of America* 108, 6597-6602.

Nesbit, C. E., Tersak, J. M., and Prochownik, E. V. (1999). MYC oncogenes and human neoplastic disease. *Oncogene* 18, 3004-3016.

O'Neill, H. M., Maarbjerg, S. J., Crane, J. D., Jeppesen, J., Jorgensen, S. B., Schertzer, J. D., Shyroka, O., Kiens, B., van Denderen, B. J., Tarnopolsky, M. A., *et al.* (2011). AMP-activated protein kinase (AMPK) beta1beta2 muscle null mice reveal an essential role for AMPK in maintaining mitochondrial content and glucose uptake during exercise. *Proceedings of the National Academy of Sciences of the United States of America* 108, 16092-16097.

Oakhill, J. S., Chen, Z. P., Scott, J. W., Steel, R., Castelli, L. A., Ling, N., Macaulay, S. L., and Kemp, B. E. (2010). beta-Subunit myristoylation is the gatekeeper for initiating metabolic stress sensing by AMP-activated protein kinase (AMPK). *Proceedings of the National Academy of Sciences of the United States of America* 107, 19237-19241.

Oakhill, J. S., Steel, R., Chen, Z. P., Scott, J. W., Ling, N., Tam, S., and Kemp, B. E. (2011). AMPK is a direct adenylate charge-regulated protein kinase. *Science (New York, NY)* 332, 1433-1435.

Obayashi, M., Yoshida, M., Tsunematsu, T., Ogawa, I., Sasahira, T., Kuniyasu, H., Imoto, I., Abiko, Y., Xu, D., Fukunaga, S., *et al.* (2016). microRNA-203 suppresses invasion and epithelial-mesenchymal transition induction via targeting NUA1 in head and neck cancer. *Oncotarget* 7, 8223-8239.

Ogawara, Y., Kishishita, S., Obata, T., Isazawa, Y., Suzuki, T., Tanaka, K., Masuyama, N., and Gotoh, Y. (2002). Akt enhances Mdm2-mediated ubiquitination and degradation of p53. *The Journal of biological chemistry* 277, 21843-21850.

Ohashi, K., Ouchi, N., Higuchi, A., Shaw, R. J., and Walsh, K. (2010). LKB1 deficiency in Tie2-Cre-expressing cells impairs ischemia-induced angiogenesis. *The Journal of biological chemistry* 285, 22291-22298.

Ohmura, T., Shioi, G., Hirano, M., and Aizawa, S. (2012). Neural tube defects by NUA1 and NUA2 double mutation. *Developmental dynamics : an official publication of the American Association of Anatomists* 241, 1350-1364.

Oikonomou, E., Koustas, E., Goulielmaki, M., and Pintzas, A. (2014). BRAF vs RAS oncogenes: are mutations of the same pathway equal? differential signalling and therapeutic implications. *Oncotarget* 5, 11752-11777.

Okon, I. S., Coughlan, K. A., Zhang, C., Moriasi, C., Ding, Y., Song, P., Zhang, W., Li, G., and Zou, M. H. (2014). Protein kinase LKB1 promotes RAB7-mediated neuropilin-1 degradation to inhibit angiogenesis. *The Journal of clinical investigation* 124, 4590-4602.

Ostrem, J. M., Peters, U., Sos, M. L., Wells, J. A., and Shokat, K. M. (2013). K-Ras(G12C) inhibitors allosterically control GTP affinity and effector interactions. *Nature* 503, 548-551.

Ott, L. E., Sung, E. J., Melvin, A. T., Sheats, M. K., Haugh, J. M., Adler, K. B., and Jones, S. L. (2013). Fibroblast Migration Is Regulated by Myristoylated Alanine-Rich C-Kinase Substrate (MARCKS) Protein. *PloS one* 8, e66512.

Owen, M. R., Doran, E., and Halestrap, A. P. (2000). Evidence that metformin exerts its anti-diabetic effects through inhibition of complex 1 of the mitochondrial respiratory chain. *The Biochemical journal* 348 Pt 3, 607-614.

Parada, L. F., Tabin, C. J., Shih, C., and Weinberg, R. A. (1982). Human EJ bladder carcinoma oncogene is homologue of Harvey sarcoma virus ras gene. *Nature* 297, 474-478.

Park, C. E., Kim, M. J., Lee, J. H., Min, B. I., Bae, H., Choe, W., Kim, S. S., and Ha, J. (2007). Resveratrol stimulates glucose transport in C2C12 myotubes by activating AMP-activated protein kinase. *Experimental & molecular medicine* 39, 222-229.

Paz-Ares, L., Douillard, J. Y., Koralewski, P., Manegold, C., Smit, E. F., Reyes, J. M., Chang, G. C., John, W. J., Peterson, P. M., Obasaju, C. K., *et al.* (2006). Phase III study of gemcitabine and cisplatin with or without aprinocarsen, a protein kinase C-alpha antisense oligonucleotide, in patients with advanced-stage non-small-cell lung cancer. *Journal of clinical oncology : official journal of the American Society of Clinical Oncology* 24, 1428-1434.

Perumal, D., Kuo, P. Y., Leshchenko, V. V., Jiang, Z., Divakar, S. K., Cho, H. J., Chari, A., Brody, J., Reddy, M. V., Zhang, W., *et al.* (2016). Dual Targeting of CDK4 and ARK5 Using a Novel Kinase Inhibitor ON123300 Exerts Potent Anticancer Activity against Multiple Myeloma. *Cancer research* 76, 1225-1236.

Phippen, N. T., Bateman, N. W., Wang, G., Conrads, K. A., Ao, W., Teng, P. N., Litzi, T. A., Oliver, J., Maxwell, G. L., Hamilton, C. A., *et al.* (2016). NUA1 (ARK5) Is Associated with Poor Prognosis in Ovarian Cancer. *Frontiers in oncology* 6, 213.

Polekhina, G., Gupta, A., van Denderen, B. J., Feil, S. C., Kemp, B. E., Stapleton, D., and Parker, M. W. (2005). Structural basis for glycogen recognition by AMP-activated protein kinase. *Structure (London, England : 1993)* 13, 1453-1462.

Powell, C. A., Nasser, M. W., Zhao, H., Wochna, J. C., Zhang, X., Shapiro, C., Shilo, K., and Ganju, R. K. (2015). Fatty acid binding protein 5 promotes metastatic potential of triple negative breast cancer cells through enhancing epidermal growth factor receptor stability. *Oncotarget* 6, 6373-6385.

Pritchard, C. A., Samuels, M. L., Bosch, E., and McMahon, M. (1995). Conditionally oncogenic forms of the A-Raf and B-Raf protein kinases display different biological and biochemical properties in NIH 3T3 cells. *Molecular and cellular biology* 15, 6430-6442.

Quesada, I., Rovira, J. M., Martin, F., Roche, E., Nadal, A., and Soria, B. (2002). Nuclear KATP channels trigger nuclear Ca(2+) transients that modulate nuclear function. *Proceedings of the National Academy of Sciences of the United States of America* 99, 9544-9549.

Raffeiner, P., Schraffl, A., Schwarz, T., Rock, R., Ledolter, K., Hartl, M., Konrat, R., Stefan, E., and Bister, K. (2017). Calcium-dependent binding of Myc to calmodulin. *Oncotarget* 8, 3327-3343.

Rekhtman, N., Paik, P. K., Arcila, M. E., Tafe, L. J., Oxnard, G. R., Moreira, A. L., Travis, W. D., Zakowski, M. F., Kris, M. G., and Ladanyi, M. (2012). Clarifying the spectrum of driver oncogene mutations in biomarker-verified squamous carcinoma of lung: lack of EGFR/KRAS and presence of PIK3CA/AKT1 mutations. *Clinical cancer research : an official journal of the American Association for Cancer Research* 18, 1167-1176.

Riely, G. J., Kris, M. G., Rosenbaum, D., Marks, J., Li, A., Chitale, D. A., Nafa, K., Riedel, E. R., Hsu, M., Pao, W., *et al.* (2008). Frequency and distinctive spectrum of KRAS mutations in never smokers with lung adenocarcinoma. *Clinical cancer research : an official journal of the American Association for Cancer Research* 14, 5731-5734.

Robinson, M. D., McCarthy, D. J., and Smyth, G. K. (2010). edgeR: a Bioconductor package for differential expression analysis of digital gene expression data. *Bioinformatics (Oxford, England)* 26, 139-140.

Ross, F. A., Jensen, T. E., and Hardie, D. G. (2016). Differential regulation by AMP and ADP of AMPK complexes containing different gamma subunit isoforms. *The Biochemical journal* 473, 189-199.

Roy, B. C., Kohno, T., Iwakawa, R., Moriguchi, T., Kiyono, T., Morishita, K., Sanchez-Cespedes, M., Akiyama, T., and Yokota, J. (2010). Involvement of LKB1 in epithelial-mesenchymal transition (EMT) of human lung cancer cells. *Lung cancer (Amsterdam, Netherlands)* 70, 136-145.

Russell, P. A., Wainer, Z., Wright, G. M., Daniels, M., Conron, M., and Williams, R. A. (2011). Does lung adenocarcinoma subtype predict patient survival?: A clinicopathologic study based on the new International Association for the Study of Lung Cancer/American Thoracic Society/European Respiratory Society

international multidisciplinary lung adenocarcinoma classification. *Journal of thoracic oncology : official publication of the International Association for the Study of Lung Cancer* 6, 1496-1504.

Ruvolo, P. P., Deng, X., Carr, B. K., and May, W. S. (1998). A functional role for mitochondrial protein kinase Calpha in Bcl2 phosphorylation and suppression of apoptosis. *The Journal of biological chemistry* 273, 25436-25442.

Saito, Y., Chapple, R. H., Lin, A., Kitano, A., and Nakada, D. (2015). AMPK Protects Leukemia-Initiating Cells in Myeloid Leukemias from Metabolic Stress in the Bone Marrow. *Cell stem cell* 17, 585-596.

Sakamoto, K., McCarthy, A., Smith, D., Green, K. A., Grahame Hardie, D., Ashworth, A., and Alessi, D. R. (2005). Deficiency of LKB1 in skeletal muscle prevents AMPK activation and glucose uptake during contraction. *Embo j* 24, 1810-1820.

Salehi, Z., and Niedel, J. E. (1990). Multiple calcium-mediated mechanisms regulate c-myc expression in HL-60 cells. *Journal of immunology (Baltimore, Md : 1950)* 145, 276-282.

Salt, I. P., and Hardie, D. G. (2017). AMP-Activated Protein Kinase: An Ubiquitous Signaling Pathway With Key Roles in the Cardiovascular System. *Circulation research* 120, 1825-1841.

Sancak, Y., Thoreen, C. C., Peterson, T. R., Lindquist, R. A., Kang, S. A., Spooner, E., Carr, S. A., and Sabatini, D. M. (2007). PRAS40 is an insulin-regulated inhibitor of the mTORC1 protein kinase. *Molecular cell* 25, 903-915.

Sanchez-Cespedes, M., Parrella, P., Esteller, M., Nomoto, S., Trink, B., Engles, J. M., Westra, W. H., Herman, J. G., and Sidransky, D. (2002). Inactivation of LKB1/STK11 is a common event in adenocarcinomas of the lung. *Cancer research* 62, 3659-3662.

Sanders, M. J., Ali, Z. S., Hegarty, B. D., Heath, R., Snowden, M. A., and Carling, D. (2007). Defining the mechanism of activation of AMP-activated protein kinase by the small molecule A-769662, a member of the thienopyridone family. *The Journal of biological chemistry* 282, 32539-32548.

Santos, E., Martin-Zanca, D., Reddy, E. P., Pierotti, M. A., Della Porta, G., and Barbacid, M. (1984). Malignant activation of a K-ras oncogene in lung carcinoma but not in normal tissue of the same patient. *Science (New York, NY)* 223, 661-664.

Santos, E., Tronick, S. R., Aaronson, S. A., Pulciani, S., and Barbacid, M. (1982). T24 human bladder carcinoma oncogene is an activated form of the normal human homologue of BALB- and Harvey-MSV transforming genes. *Nature* 298, 343-347.

Sasaki, T., Takemori, H., Yagita, Y., Terasaki, Y., Uebi, T., Horike, N., Takagi, H., Susumu, T., Teraoka, H., Kusano, K., *et al.* (2011). SIK2 is a key regulator for neuronal survival after ischemia via TORC1-CREB. *Neuron* 69, 106-119.

Sears, R., Nuckolls, F., Haura, E., Taya, Y., Tamai, K., and Nevins, J. R. (2000). Multiple Ras-dependent phosphorylation pathways regulate Myc protein stability. *Genes & development* *14*, 2501-2514.

Shackelford, D. B., Abt, E., Gerken, L., Vasquez, D. S., Seki, A., Leblanc, M., Wei, L., Fishbein, M. C., Czernin, J., Mischel, P. S., and Shaw, R. J. (2013). LKB1 inactivation dictates therapeutic response of non-small cell lung cancer to the metabolism drug phenformin. *Cancer cell* *23*, 143-158.

Shaw, R. J., Bardeesy, N., Manning, B. D., Lopez, L., Kosmatka, M., DePinho, R. A., and Cantley, L. C. (2004a). The LKB1 tumor suppressor negatively regulates mTOR signaling. *Cancer cell* *6*, 91-99.

Shaw, R. J., Kosmatka, M., Bardeesy, N., Hurley, R. L., Witters, L. A., DePinho, R. A., and Cantley, L. C. (2004b). The tumor suppressor LKB1 kinase directly activates AMP-activated kinase and regulates apoptosis in response to energy stress. *Proceedings of the National Academy of Sciences of the United States of America* *101*, 3329-3335.

Shelly, M., Cancedda, L., Heilshorn, S., Sumbre, G., and Poo, M. M. (2007). LKB1/STRAD promotes axon initiation during neuronal polarization. *Cell* *129*, 565-577.

Shen, C., Liu, Y., Shi, S., Zhang, R., Zhang, T., Xu, Q., Zhu, P., Chen, X., and Lu, F. (2017). Long-distance interaction of the integrated HPV fragment with MYC gene and 8q24.22 region upregulating the allele-specific MYC expression in HeLa cells. *International journal of cancer* *141*, 540-548.

Shi, L., Zhang, B., Sun, X., Lu, S., Liu, Z., Liu, Y., Li, H., Wang, L., Wang, X., and Zhao, C. (2014). MiR-204 inhibits human NSCLC metastasis through suppression of NUAK1. *British journal of cancer* *111*, 2316-2327.

Shibue, T., and Weinberg, R. A. (2017). EMT, CSCs, and drug resistance: the mechanistic link and clinical implications. *Nature reviews Clinical oncology*.

Shigematsu, H., Lin, L., Takahashi, T., Nomura, M., Suzuki, M., Wistuba, II, Fong, K. M., Lee, H., Toyooka, S., Shimizu, N., *et al.* (2005). Clinical and biological features associated with epidermal growth factor receptor gene mutations in lung cancers. *Journal of the National Cancer Institute* *97*, 339-346.

Singh, A., Greninger, P., Rhodes, D., Koopman, L., Violette, S., Bardeesy, N., and Settleman, J. (2009). A gene expression signature associated with "K-Ras addiction" reveals regulators of EMT and tumor cell survival. *Cancer cell* *15*, 489-500.

Sordella, R., Bell, D. W., Haber, D. A., and Settleman, J. (2004). Gefitinib-sensitizing EGFR mutations in lung cancer activate anti-apoptotic pathways. *Science (New York, NY)* *305*, 1163-1167.

Spiegel, J., Cromm, P. M., Zimmermann, G., Grossmann, T. N., and Waldmann, H. (2014). Small-molecule modulation of Ras signaling. *Nature chemical biology* *10*, 613-622.

Subramaniam, D., He, A. R., Hwang, J., Deeken, J., Pishvaian, M., Hartley, M. L., and Marshall, J. L. (2015). Irreversible multitargeted ErbB family inhibitors for therapy of lung and breast cancer. *Current cancer drug targets* 14, 775-793.

Sun, C., Hobor, S., Bertotti, A., Zecchin, D., Huang, S., Galimi, F., Cottino, F., Prahallad, A., Grenrum, W., Tzani, A., *et al.* (2014). Intrinsic resistance to MEK inhibition in KRAS mutant lung and colon cancer through transcriptional induction of ERBB3. *Cell reports* 7, 86-93.

Sun, Y., Fang, Y., Yoon, M. S., Zhang, C., Rocco, M., Zwartkruis, F. J., Armstrong, M., Brown, H. A., and Chen, J. (2008). Phospholipase D1 is an effector of Rheb in the mTOR pathway. *Proceedings of the National Academy of Sciences of the United States of America* 105, 8286-8291.

Suter, M., Riek, U., Tuerk, R., Schlattner, U., Wallimann, T., and Neumann, D. (2006). Dissecting the role of 5'-AMP for allosteric stimulation, activation, and deactivation of AMP-activated protein kinase. *The Journal of biological chemistry* 281, 32207-32216.

Sutherland, K. D., Song, J. Y., Kwon, M. C., Proost, N., Zevenhoven, J., and Berns, A. (2014). Multiple cells-of-origin of mutant K-Ras-induced mouse lung adenocarcinoma. *Proceedings of the National Academy of Sciences of the United States of America* 111, 4952-4957.

Suzuki, A., Kusakai, G., Kishimoto, A., Lu, J., Ogura, T., Lavin, M. F., and Esumi, H. (2003a). Identification of a novel protein kinase mediating Akt survival signaling to the ATM protein. *The Journal of biological chemistry* 278, 48-53.

Suzuki, A., Kusakai, G., Kishimoto, A., Minegichi, Y., Ogura, T., and Esumi, H. (2003b). Induction of cell-cell detachment during glucose starvation through F-actin conversion by SNARK, the fourth member of the AMP-activated protein kinase catalytic subunit family. *Biochemical and biophysical research communications* 311, 156-161.

Suzuki, A., Lu, J., Kusakai, G., Kishimoto, A., Ogura, T., and Esumi, H. (2004). ARK5 is a tumor invasion-associated factor downstream of Akt signaling. *Molecular and cellular biology* 24, 3526-3535.

Suzuki, A., Ogura, T., and Esumi, H. (2006). NDR2 acts as the upstream kinase of ARK5 during insulin-like growth factor-1 signaling. *The Journal of biological chemistry* 281, 13915-13921.

Takemori, H., Katoh, Y., Horike, N., Doi, J., and Okamoto, M. (2002). ACTH-induced nucleocytoplasmic translocation of salt-inducible kinase. Implication in the protein kinase A-activated gene transcription in mouse adrenocortical tumor cells. *The Journal of biological chemistry* 277, 42334-42343.

The Cancer Genome Atlas Research, N. (2014). Comprehensive molecular profiling of lung adenocarcinoma. *Nature* 511, 543-550.

Thorpe, L. M., Yuzugullu, H., and Zhao, J. J. (2015). PI3K in cancer: divergent roles of isoforms, modes of activation and therapeutic targeting. *Nature reviews Cancer* 15, 7-24.

Timm, T., Balusamy, K., Li, X., Biernat, J., Mandelkow, E., and Mandelkow, E. M. (2008). Glycogen synthase kinase (GSK) 3 β directly phosphorylates Serine 212 in the regulatory loop and inhibits microtubule affinity-regulating kinase (MARK) 2. *The Journal of biological chemistry* 283, 18873-18882.

Todorova, M. G., Fuentes, E., Soria, B., Nadal, A., and Quesada, I. (2009). Lysophosphatidic acid induces Ca²⁺ mobilization and c-Myc expression in mouse embryonic stem cells via the phospholipase C pathway. *Cellular signalling* 21, 523-528.

Townley, R., and Shapiro, L. (2007). Crystal structures of the adenylate sensor from fission yeast AMP-activated protein kinase. *Science (New York, NY)* 315, 1726-1729.

Toyama, E. Q., Herzig, S., Courchet, J., Lewis, T. L., Jr., Loson, O. C., Hellberg, K., Young, N. P., Chen, H., Polleux, F., Chan, D. C., and Shaw, R. J. (2016). Metabolism. AMP-activated protein kinase mediates mitochondrial fission in response to energy stress. *Science (New York, NY)* 351, 275-281.

Travis, W. D., Brambilla, E., Nicholson, A. G., Yatabe, Y., Austin, J. H., Beasley, M. B., Chirieac, L. R., Dacic, S., Duhig, E., Flieder, D. B., *et al.* (2015). The 2015 World Health Organization Classification of Lung Tumors: Impact of Genetic, Clinical and Radiologic Advances Since the 2004 Classification. *Journal of thoracic oncology : official publication of the International Association for the Study of Lung Cancer* 10, 1243-1260.

Turke, A. B., Zejnullahu, K., Wu, Y. L., Song, Y., Dias-Santagata, D., Lifshits, E., Toschi, L., Rogers, A., Mok, T., Sequist, L., *et al.* (2010). Preexistence and clonal selection of MET amplification in EGFR mutant NSCLC. *Cancer cell* 17, 77-88.

Turner, N., Li, J. Y., Gosby, A., To, S. W., Cheng, Z., Miyoshi, H., Taketo, M. M., Cooney, G. J., Kraegen, E. W., James, D. E., *et al.* (2008). Berberine and its more biologically available derivative, dihydroberberine, inhibit mitochondrial respiratory complex I: a mechanism for the action of berberine to activate AMP-activated protein kinase and improve insulin action. *Diabetes* 57, 1414-1418.

Unni, A. M., Lockwood, W. W., Zejnullahu, K., Lee-Lin, S. Q., and Varmus, H. (2015). Evidence that synthetic lethality underlies the mutual exclusivity of oncogenic KRAS and EGFR mutations in lung adenocarcinoma. *eLife* 4, e06907.

van Riggelen, J., Yetil, A., and Felsher, D. W. (2010). MYC as a regulator of ribosome biogenesis and protein synthesis. *Nature reviews Cancer* 10, 301-309.

Veale, D., Ashcroft, T., Marsh, C., Gibson, G. J., and Harris, A. L. (1987). Epidermal growth factor receptors in non-small cell lung cancer. *British journal of cancer* 55, 513-516.

Vetter, I. R., and Wittinghofer, A. (2001). The guanine nucleotide-binding switch in three dimensions. *Science (New York, NY)* 294, 1299-1304.

Vicent, S., Lopez-Picazo, J. M., Toledo, G., Lozano, M. D., Torre, W., Garcia-Corchon, C., Quero, C., Soria, J. C., Martin-Algarra, S., Manzano, R. G., and

- Montuenga, L. M. (2004). ERK1/2 is activated in non-small-cell lung cancer and associated with advanced tumours. *British journal of cancer* *90*, 1047-1052.
- Vicente-Manzanares, M., Ma, X., Adelstein, R. S., and Horwitz, A. R. (2009). Non-muscle myosin II takes centre stage in cell adhesion and migration. *Nature reviews Molecular cell biology* *10*, 778-790.
- Villalona-Calero, M. A., Ritch, P., Figueroa, J. A., Otterson, G. A., Belt, R., Dow, E., George, S., Leonardo, J., McCachren, S., Miller, G. L., *et al.* (2004). A phase I/II study of LY900003, an antisense inhibitor of protein kinase C-alpha, in combination with cisplatin and gemcitabine in patients with advanced non-small cell lung cancer. *Clinical cancer research : an official journal of the American Association for Cancer Research* *10*, 6086-6093.
- Vivanco, I., and Sawyers, C. L. (2002). The phosphatidylinositol 3-Kinase AKT pathway in human cancer. *Nature reviews Cancer* *2*, 489-501.
- Walz, S., Lorenzin, F., Morton, J., Wiese, K. E., von Eyss, B., Herold, S., Rycak, L., Dumay-Odelot, H., Karim, S., Bartkuhn, M., *et al.* (2014). Activation and repression by oncogenic MYC shape tumour-specific gene expression profiles. *Nature* *511*, 483-487.
- Wang, Z., Takemori, H., Halder, S. K., Nonaka, Y., and Okamoto, M. (1999). Cloning of a novel kinase (SIK) of the SNF1/AMPK family from high salt diet-treated rat adrenal. *FEBS letters* *453*, 135-139.
- Ways, D. K., Kukoly, C. A., deVente, J., Hooker, J. L., Bryant, W. O., Posekany, K. J., Fletcher, D. J., Cook, P. P., and Parker, P. J. (1995). MCF-7 breast cancer cells transfected with protein kinase C-alpha exhibit altered expression of other protein kinase C isoforms and display a more aggressive neoplastic phenotype. *The Journal of clinical investigation* *95*, 1906-1915.
- Whang, Y. M., Park, S. I., Trenary, I. A., Egnatchik, R. A., Fessel, J. P., Kaufman, J. M., Carbone, D. P., and Young, J. D. (2016). LKB1 deficiency enhances sensitivity to energetic stress induced by erlotinib treatment in non-small-cell lung cancer (NSCLC) cells. *Oncogene* *35*, 856-866.
- Wolfman, A., and Macara, I. G. (1987). Elevated levels of diacylglycerol and decreased phorbol ester sensitivity in ras-transformed fibroblasts. *Nature* *325*, 359-361.
- Woods, A., Dickerson, K., Heath, R., Hong, S. P., Momcilovic, M., Johnstone, S. R., Carlson, M., and Carling, D. (2005). Ca²⁺/calmodulin-dependent protein kinase kinase-beta acts upstream of AMP-activated protein kinase in mammalian cells. *Cell metabolism* *2*, 21-33.
- Woods, A., Johnstone, S. R., Dickerson, K., Leiper, F. C., Fryer, L. G., Neumann, D., Schlattner, U., Wallimann, T., Carlson, M., and Carling, D. (2003). LKB1 is the upstream kinase in the AMP-activated protein kinase cascade. *Current biology : CB* *13*, 2004-2008.
- Wu, N., Zheng, B., Shaywitz, A., Dagon, Y., Tower, C., Bellinger, G., Shen, C. H., Wen, J., Asara, J., McGraw, T. E., *et al.* (2013). AMPK-dependent

- degradation of TXNIP upon energy stress leads to enhanced glucose uptake via GLUT1. *Molecular cell* 49, 1167-1175.
- Wu, T. T., Hsieh, Y. H., Hsieh, Y. S., and Liu, J. Y. (2008). Reduction of PKC alpha decreases cell proliferation, migration, and invasion of human malignant hepatocellular carcinoma. *Journal of cellular biochemistry* 103, 9-20.
- Xiao, B., Heath, R., Saiu, P., Leiper, F. C., Leone, P., Jing, C., Walker, P. A., Haire, L., Eccleston, J. F., Davis, C. T., *et al.* (2007). Structural basis for AMP binding to mammalian AMP-activated protein kinase. *Nature* 449, 496-500.
- Xiao, B., Sanders, M. J., Carmena, D., Bright, N. J., Haire, L. F., Underwood, E., Patel, B. R., Heath, R. B., Walker, P. A., Hallen, S., *et al.* (2013). Structural basis of AMPK regulation by small molecule activators. *Nature communications* 4, 3017.
- Xiao, B., Sanders, M. J., Underwood, E., Heath, R., Mayer, F. V., Carmena, D., Jing, C., Walker, P. A., Eccleston, J. F., Haire, L. F., *et al.* (2011). Structure of mammalian AMPK and its regulation by ADP. *Nature* 472, 230-233.
- Xiao, P., Sun, L. L., Wang, J., Han, R. L., Ma, Q., and Zhong, D. S. (2015). LKB1 gene inactivation does not sensitize non-small cell lung cancer cells to mTOR inhibitors in vitro. *Acta pharmacologica Sinica* 36, 1107-1112.
- Xie, M., Zhang, D., Dyck, J. R., Li, Y., Zhang, H., Morishima, M., Mann, D. L., Taffet, G. E., Baldini, A., Khoury, D. S., and Schneider, M. D. (2006). A pivotal role for endogenous TGF-beta-activated kinase-1 in the LKB1/AMP-activated protein kinase energy-sensor pathway. *Proceedings of the National Academy of Sciences of the United States of America* 103, 17378-17383.
- Xu, T., Zhang, J., Chen, W., Pan, S., Zhi, X., Wen, L., Zhou, Y., Chen, B. W., Qiu, J., Zhang, Y., *et al.* (2016). ARK5 promotes doxorubicin resistance in hepatocellular carcinoma via epithelial-mesenchymal transition. *Cancer letters* 377, 140-148.
- Yamamoto, H., Takashima, S., Shintani, Y., Yamazaki, S., Seguchi, O., Nakano, A., Higo, S., Kato, H., Liao, Y., Asano, Y., *et al.* (2008). Identification of a novel substrate for TNFalpha-induced kinase NUA2. *Biochemical and biophysical research communications* 365, 541-547.
- Yang, X., Yu, K., Hao, Y., Li, D. M., Stewart, R., Insogna, K. L., and Xu, T. (2004). LATS1 tumour suppressor affects cytokinesis by inhibiting LIMK1. *Nature cell biology* 6, 609-617.
- Yarden, Y., and Sliwkowski, M. X. (2001). Untangling the ErbB signalling network. *Nature reviews Molecular cell biology* 2, 127-137.
- Ye, X. T., Guo, A. J., Yin, P. F., Cao, X. D., and Chang, J. C. (2014). Overexpression of NUA1 is associated with disease-free survival and overall survival in patients with gastric cancer. *Medical oncology (Northwood, London, England)* 31, 61.

Ylikorkala, A., Rossi, D. J., Korsisaari, N., Luukko, K., Alitalo, K., Henkemeyer, M., and Makela, T. P. (2001). Vascular abnormalities and deregulation of VEGF in Lkb1-deficient mice. *Science (New York, NY)* 293, 1323-1326.

Yonesaka, K., Zejnullahu, K., Okamoto, I., Satoh, T., Cappuzzo, F., Souglakos, J., Ercan, D., Rogers, A., Roncalli, M., Takeda, M., *et al.* (2011). Activation of ERBB2 signaling causes resistance to the EGFR-directed therapeutic antibody cetuximab. *Science translational medicine* 3, 99ra86.

Zagorska, A., Deak, M., Campbell, D. G., Banerjee, S., Hirano, M., Aizawa, S., Prescott, A. R., and Alessi, D. R. (2010). New roles for the LKB1-NUAK pathway in controlling myosin phosphatase complexes and cell adhesion. *Science signaling* 3, ra25.

Zhang, W., Ding, Y., Zhang, C., Lu, Q., Liu, Z., Coughlan, K., Okon, I., and Zou, M. H. (2017). Deletion of endothelial cell-specific liver kinase B1 increases angiogenesis and tumor growth via vascular endothelial growth factor. *Oncogene* 36, 4277-4287.

Zheng, B., Jeong, J. H., Asara, J. M., Yuan, Y. Y., Granter, S. R., Chin, L., and Cantley, L. C. (2009). Oncogenic B-RAF negatively regulates the tumor suppressor LKB1 to promote melanoma cell proliferation. *Molecular cell* 33, 237-247.

Zheng, J., and Ramirez, V. D. (2000). Inhibition of mitochondrial proton F0F1-ATPase/ATP synthase by polyphenolic phytochemicals. *British journal of pharmacology* 130, 1115-1123.

Zhou, X., Clister, T. L., Lowry, P. R., Seldin, M. M., Wong, G. W., and Zhang, J. (2015). Dynamic Visualization of mTORC1 Activity in Living Cells. *Cell reports*.

Zmijewski, J. W., Banerjee, S., Bae, H., Friggeri, A., Lazarowski, E. R., and Abraham, E. (2010). Exposure to hydrogen peroxide induces oxidation and activation of AMP-activated protein kinase. *The Journal of biological chemistry* 285, 33154-33164.